ISSN 1425-204X

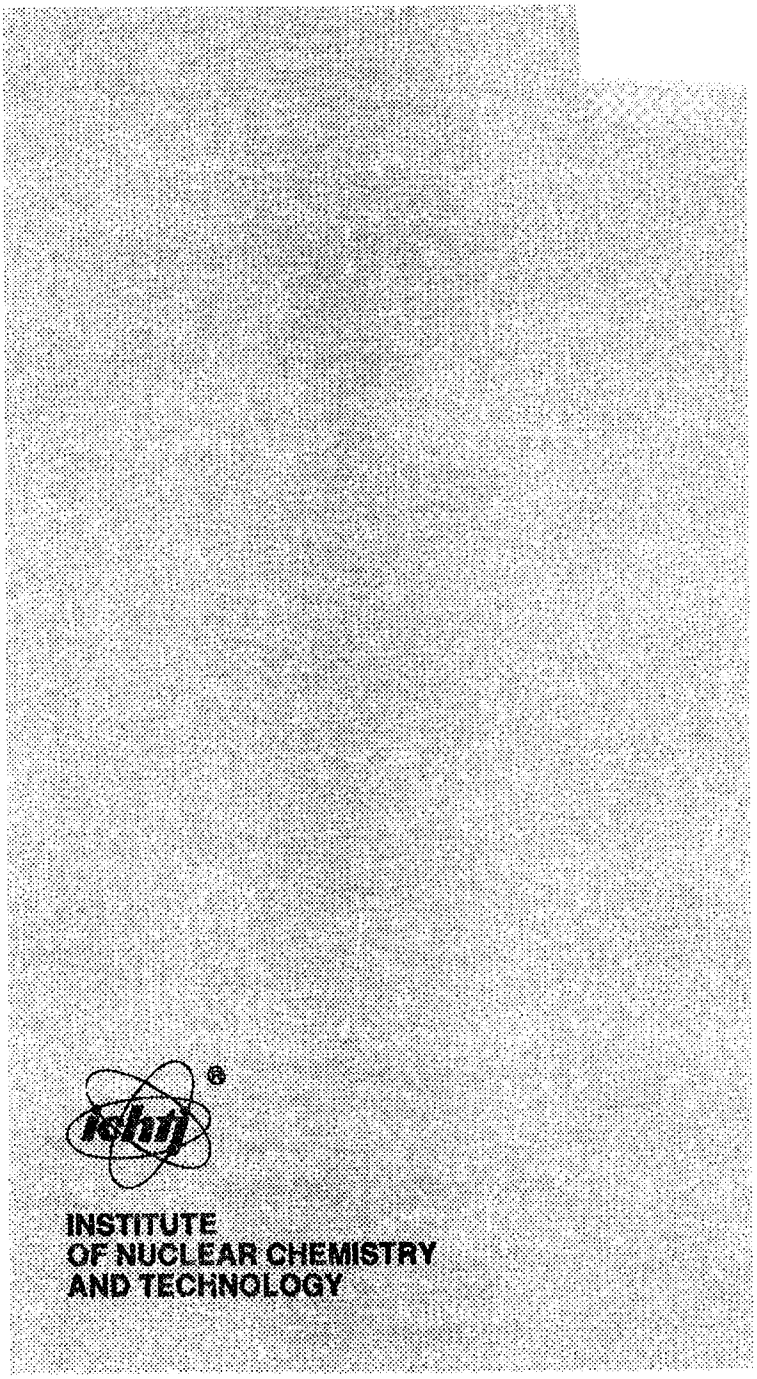

INSTITUTE
OF NUCLEAR CHEMISTRY
AND TECHNOLOGY

annual report

1995

R

CONTENTS

GENERAL INFORMATION

The Institute of Nuclear Chemistry and Technology (INCT) is one of the successors of the Institute of Nuclear Research (INR) which was established in 1955. The latter Institute, once the biggest Institute in Poland, has exerted a great influence on the scientific and intelectual life in this country.

The participation of its staff in the movement in favour of democracy in Poland has led to the dissolution of the INR in 1983. At that time the INCT, as one of the three units, was organized.

The fundamental research on radiobiology, radio- and coordination chemistry and radiation chemistry is continued. As a proof of appreciation in the field of radiation chemistry Professor Z.P. Zagórski has been awarded in 1995 with the Maria Skłodowska-Curie medal by the Society of Radiation Research.

The Institute offers didactic and research programmes for Ph.D. and D.Sc. thesis in chemistry.

Institute is one of the most advanced innovation centres working on technologies and methods in the field of:

— radiation chemistry and technology,
— application of nuclear methods in material and process engineering,
— design and production of instruments based on nuclear techniques,
— trace analysis and radioanalytical techniques,
— environmental research.

At this moment, with its nine electron accelerators in operation and with the staff experienced in the field of electron beam applications, the Institute is one of the most advanced centres of science and technology in this domain. The following activity should here be mentioned:

— experimental pilot plant for food irradiation,
— pilot plant for radiation sterilization of medical devices and transplantations,
— pilot plant for radiation modification of polymers,
— pilot plant for removal of SO_2 and NO_x from flue gases.

The last plant has been awarded with a gold medal and with a distinction by the jury at the 44th World Exhibition of Invention, Research and Industrial Innovation "Brussels Eureka'95".

In 1995 a new generation of mining radiometers RGR-40 was developed in the Institute. Based on attestation in the Experimental Mine "Barbara" and by the Central Mining Institute, president of the Higher Mining Office has approved the application of the radiometer in the mining industry.

The achievements of the Institute have been recognized by the international forum which has led to a broad cooperation with foreign institutions. The INCT scientists cooperate in reseach programmes with the leading world centres:

— sol-gel process for HTS and bioceramic materials - ENEA (Rome, Italy), Argonne National Laboratory (USA), New York University (USA);
— advanced dosimetry and detection of irradiated food - University of Gent (Belgium), University of Aix - Marseilles (France), ADMIT Group under supervision WHO, FAO and the IAEA;

- chemistry of rutherfordium (element 104) - Lawrence Berkeley Laboratory (USA), JINR (Dubna, Russia);
- complex formation of transuranes in solutions of high ionic strenght - Florida State University (Tallahasse, USA);
- sorption of radionuclides on inorganic ion exchangers - Saclay Nuclear Research Centre (France);
- technology of simultaneous removal of SO_2 and NO_x from flue gases by use of electron beam - Japan Atomic Energy Research Institute (Takasaki, Japan), Ebara Corp. (Japan), Forschungszentrum Karlsruhe (Germany), IAEA, CChEN Santiago de Chile (Chile), IPEN (Sao Paulo, Brasil), INR (Shanghai, China);
- particle track membranes - JINR (Dubna, Russia), University of Antwerp (Belgium), University of Louvain-la-Neuve (Belgium);
- membrane processes for separation of isotopes and concentration of radioactive wastes - University of Tennessee (Knoxville, USA);
- mechanisms of sensitized photooxidation of thioether compounds - University of Notre Dame (USA), Risø National Laboratory (Denmark);
- radiation-induced chemical intermediates and reactivity of silver agglomerates in zeolites - University of Houston (USA), University of Nijmegen (the Netherlands);
- smectite clays with silver - Metropolitan Leeds University (Great Britain);
- studies of nature of radiation defects generated by nuclear radiation (e^-, ions) in silicon layers and in semiconductor compounds III-V - FZR Forschungszentrum Rossendorf (Germany), Ecole Normale Superieure Paris (France), JINR (Dubna, Russia);
- radiolysis of selected liquid and solid systems by beams of accelerated ions and influence of imparting density of energy on the course of radiation processes in model liquid and solid systems - JINR (Dubna, Russia), Institute of Dyes and Intermediate Compounds (Russia), Institute of Inorganic Chemistry, Latvian Academy of Sciences (Salaspils, Latvia), Risø National Laboratory (Denmark);
- crystal chemistry of uranyl coordination compounds, chemistry of ionic intermediates in condensed phases - University of Warwick (Great Britain), University of Leicester (Great Britain), Max-Planck Institute (Germany), Hahn-Meitner Institute (Germany);
- highly accurate methods for the determination of essential or toxic elements in biological materials by NAA - National Institute of Standards and Technology (USA);
- ADP-ribosylation, cell response to radiation - Institut für Veterinarpharmakologii und Toxicologii, Universität Zürich (Switzerland), Institute of Physical Chemistry, Russian Academy of Sciences (Russia);
- repair of DNA and the structure of chromatine - New York State University Health Center at Brooklyn (USA);
- damage of DNA and mutations generated by hydrogen peroxide - MRC Cell Mutation Unit, University of Sussex (Great Britain).

The INCT participates in IAEA technical cooperation programmes and organizes training courses. The employees of the Institute undertake many expert missions for the IAEA.

In 1995 the INCT organized four scientific meetings.

Polish Section of International Nuclear Information System is situated in the INCT.

The Institute is the editor of NUKLEONIKA - world wide recognized journal for nuclear research.

MANAGEMENT OF THE INSTITUTE

MANAGING STAFF OF THE INSTITUTE

Director
Assoc.Prof. **Lech Waliś**, Ph.D.

Deputy Director for Research and Development
Prof. **Andrzej G. Chmielewski**, Ph.D., D.Sc.

Deputy Director for Administration
Edmund Freliszka, M.Sc.

Accountant General
Barbara Kaźmirska

HEADS OF THE INCT DEPARTMENTS

- Department of Nuclear Methods of Material Engineering
  Assoc.Prof. **Lech Waliś**, Ph.D.
- Department of Structural Research
  Wojciech Starosta, M.Sc.
- Department of Radioisotope Instruments and Methods
  Assoc.Prof. **Piotr Urbański**, Ph.D., D.Sc.
- Department of Radiochemistry
  Assoc.Prof. **Jerzy Narbutt**, Ph.D., D.Sc.
- Department of Nuclear Methods of Process Engineering
  Prof. **Andrzej G. Chmielewski**, Ph.D., D.Sc.
- Department of Radiation Chemistry and Technology
  Zbigniew Zimek, Ph.D.
- Department of Analytical Chemistry
  Prof. **Rajmund Dybczyński**, Ph.D., D.Sc.
- Department of Radiobiology and Health Protection
  Prof. **Irena Szumiel**, Ph.D., D.Sc.
- Pilot Plant for Food Irradiation
  Wojciech Migdał, Ph.D.
- Laboratory for Detection of Irradiated Foods
  Wacław Stachowicz, Ph.D.

PROFESSORS AND SCIENTIFIC COUNCIL

PROFESSORS

1. **Chmielewski Andrzej G.**
   chemical and process engineering, nuclear chemical engineering, isotope chemistry
2. **Dancewicz Antoni**
   biochemistry, radiobiology
3. **Dybczyński Rajmund**
   analytical chemistry
4. **Fidelis Irena**
   physical chemistry, coordination chemistry of lanthanides and actinides
5. **Leciejewicz Janusz**
   crystallography, solid state physics, material science
6. **Łukasiewicz Andrzej**
   technology of dyes
7. **Piekoszewski Jerzy**
   solid state physics
8. **Pszonicki Leon**
   analytical chemistry
9. **Rzewuski Henryk**
   solid state physics
10. **Siekierski Sławomir**
    physical chemistry, inorganic chemistry
11. **Szot Zbigniew**
    radiobiology
12. **Szumiel Irena**
    cellular radiobiology
13. **Trojanowicz Marek**
    analytical chemistry
14. **Zagórski Zbigniew**
    physical chemistry, radiation chemistry, electrochemistry

ASSOCIATE PROFESSORS

1. **Ambroż Hanna**
   physical and radiation chemistry, photochemistry
2. **Bobrowski Krzysztof**
   radiation chemistry, photochemistry, biophysics
3. **Chwastowska Jadwiga**
   analytical chemistry
4. **Grigoriew Helena**
   solid state physics, diffraction research of non-crystalline matter
5. **Michalik Jacek**
   radiation chemistry
6. **Milner Ewa**
   radiation chemistry

7. **Mioduski Tomasz**
   lanthanide and actinide chemistry
8. **Narbutt Jerzy**
   radiochemistry
9. **Parus Józef**
   analytical chemistry
10. **Urbański Piotr**
    radiometric methods, industrial measurement equipment, metrology
11. **Waliś Lech**
    physical metallurgy and heat treatment of metals
12. **Żółtowski Tadeusz**
    nuclear physics

ASSISTANT PROFESSORS (Ph.D.)

1. **Bilewicz Aleksander**
   chemistry
2. **Borkowski Marian**
   chemistry
3. **Boużyk Elżbieta**
   biology
4. **Bryl-Sandelewska Teresa**
   radiation chemistry
5. **Buczkowski Marek**
   physics
6. **Bukowski Piotr**
   mechanics
7. **Cieśla Krystyna**
   chemistry
8. **Dembiński Wojciech**
   chemistry
9. **Deptuła Andrzej**
   chemistry
10. **Dobrowolski Andrzej**
    chemistry
11. **Dźwigalski Zygmunt**
    high voltage electronics, electron injectors, gas lasers
12. **Fiderkiewicz Alfred**
    physics
13. **Fuks Leon**
    chemistry
14. **Grodkowski Jan**
    radiation chemistry
15. **Iller Edward**
    chemical and process engineering
16. **Jaworska Alicja**
    biology
17. **Kierzek Joachim**
    physics
18. **Kleczkowska Hanna**
    biology

19. **Krejzler Jadwiga**
chemistry
20. **Kruszewski Marcin**
biology
21. **Krynicki Janusz**
solid state physics
22. **Machaj Bronisław**
electricity
23. **Migdał Wojciech**
chemistry
24. **Mirkowski Jacek**
nuclear and medical electronics
25. **Nowicki Andrzej**
organic chemistry and technology, high-temperature technology
26. **Owczarczyk Andrzej**
chemistry
27. **Owczarczyk Hanna**
biology
28. **Palige Jacek**
metallurgy
29. **Panta Przemysław**
nuclear chemistry
30. **Polkowska-Motrenko Halina**
analytical chemistry
31. **Przybytniak Grażyna**
radiation chemistry
32. **Ptasiewicz-Bąk Halina**
physics
33. **Skwara Witold**
analytical chemistry
34. **Sochanowicz Barbara**
biology
35. **Stachowicz Wacław**
radiation chemistry, EPR spectroscopy
36. **Stuglik Zofia**
radiation chemistry
37. **Szpilowski Stanisław**
chemistry
38. **Tymiński Bogdan**
chemistry
39. **Urbański Tadeusz**
chemistry
40. **Walicka Małgorzata**
biology
41. **Warchoł Stanisław**
solid state physics
42. **Wasek Marek**
nuclear physics

43. **Wąsowicz Tomasz**
radiation chemistry, molecular spectroscopy

44. **Wrońska Teresa**
chemistry

45. **Zimek Zbigniew**
electronics, accelerator techniques

46. **Żmijewska Wanda**
analytical chemistry

SCIENTIFIC COUNCIL (1991-1995)

1. Assoc.Prof. **Hanna Ambroż**, Ph.D., D.Sc.
Institute of Nuclear Chemistry and Technology
physical and radiation chemistry, photochemistry

2. **Barbara Andrzejak**, M.Sc.
Institute of Nuclear Chemistry and Technology
chemistry, scientific information

3. **Barbara Bartoś**, M.Sc.
Institute of Nuclear Chemistry and Technology
radiochemistry

4. Prof. **Andrzej G. Chmielewski**, Ph.D., D.Sc.
Institute of Nuclear Chemistry and Technology
chemical and process engineering, nuclear chemical engineering, isotope chemistry

5. Assoc.Prof. **Jadwiga Chwastowska**, Ph.D., D.Sc.
Institute of Nuclear Chemistry and Technology
analytical chemistry

6. Prof. **Stefan Chwaszczewski**, Ph.D., D.Sc.
Institute of Atomic Energy
nuclear energetics

7. **Urszula Dołowska**
Institute of Nuclear Chemistry and Technology
staff representative

8. Prof. **Rajmund Dybczyński**, Ph.D., D.Sc.
Institute of Nuclear Chemistry and Technology
analytical chemistry

9. **Edward Iller**, Ph.D.
Institute of Nuclear Chemistry and Technology
chemical and process engineering

10. Assoc.Prof. **Teresa Jankowska**, Ph.D.
Institute of Nuclear Chemistry and Technology
analytical chemistry

11. **Barbara Kaźmirska**
Institute of Nuclear Chemistry and Technology
staff representative

12. Prof. **Jerzy Kroh**, Ph.D., D.Sc.
Łódź Technical University
radiation chemistry, metallurgy, physico-chemical methods

13. **Gabriel Kuc**, M.Sc.
Institute of Nuclear Chemistry and Technology
radiochemistry

14. **Wiesława Łada**, M.Sc.
Institute of Nuclear Chemistry and Technology
chemical technology

15. Assoc.Prof. **Jacek Michalik**, Ph.D., D.Sc.
Institute of Nuclear Chemistry and Technology
radiation chemistry

16. Assoc.Prof. **Ewa Milner**, Ph.D., D.Sc.
Institute of Nuclear Chemistry and Technology
radiation chemistry

17. Assoc.Prof. **Jerzy Narbutt**, Ph.D., D.Sc.
Institute of Nuclear Chemistry and Technology
radiochemistry

18. Prof. **Jerzy Niewodniczański**, Ph.D., D.Sc.
Stanisław Staszic Academy of Mining and Metallurgy
President of National Atomic Energy Agency
nuclear physics and technique

19. Prof. **Jan Przyłuski**, Ph.D., D.Sc.
Warsaw University of Technology
chemistry, solid state technology

20. Prof. **Leon Pszonicki**, Ph.D., D.Sc.
(Chairman)
Institute of Nuclear Chemistry and Technology
analytical chemistry

21. Prof. **Henryk Rzewuski**, Ph.D., D.Sc.
(Co-chairman)
Institute of Nuclear Chemistry and Technology
solid state physics

22. Prof. **Sławomir Siekierski**, Ph.D.
Institute of Nuclear Chemistry and Technology
physical chemistry, inorganic chemistry

23. **Jan Skajster**
Institute of Nuclear Chemistry and Technology
chemical technology

24. Prof. **Jerzy Sobkowski**, Ph.D., D.Sc.
University of Warsaw
physical chemistry (electrochemistry, radiochemistry)

25. **Michał Strzelecki**, M.Sc.
Institute of Nuclear Chemistry and Technology
chemical and process engineering

26. Prof. **Irena Szumiel**, Ph.D., D.Sc.
Institute of Nuclear Chemistry and Technology
cellular radiobiology

27. Prof. **Jan Tacikowski**, Ph.D.
(Co-chairman)
Institute of Precision Mechanics
physical metallurgy and heat treatment of metals

28. Assoc.Prof. **Piotr Urbański**, Ph.D., D.Sc.
(Co-chairman)
Institute of Nuclear Chemistry and Technology
radiometric methods, industrial measurement equipment, metrology

29. Assoc.Prof. **Lech Waliś**, Ph.D.
Institute of Nuclear Chemistry and Technology
physical metallurgy and heat treatment of metals

30. **Tomasz Wąsowicz**, Ph.D.
Institute of Nuclear Chemistry and Technology
radiation chemistry, molecular spectroscopy

31. Prof. **Stanisław Wroński**, Ph.D., D.Sc.
Warsaw University of Technology
chemical engineering

32. Prof. **Zbigniew Zagórski**, Ph.D., D.Sc.
Institute of Nuclear Chemistry and Technology
physical chemistry, radiation chemistry, electrochemistry

33. **Jerzy Zieliński**, M.Sc.
Institute of Nuclear Chemistry and Technology
staff representative

34. **Wiesław Zieliński**, M.Sc.
Institute of Nuclear Chemistry and Technology
staff representative

35. **Zbigniew Zimek**, Ph.D.
Institute of Nuclear Chemistry and Technology
electronics, accelerator techniques

36. **Wanda Żmijewska**, Ph.D.
Institute of Nuclear Chemistry and Technology
analytical chemistry

HONORARY MEMBERS OF THE INCT SCIENTIFIC COUNCIL (1991-1995)

1. Prof. **Jerzy Minczewski**, Ph.D.
National Atomic Agency
analytical chemistry

2. Prof. **Maria Kopeć**, Ph.D., D.Sc.
Institute of Haematology and Blood Transfusion
medicine (haematology), radiobiology

3. Prof. **Antoni Dancewicz**, Ph.D., D.Sc.
Institute of Nuclear Chemistry and Technology
biochemistry, radiobiology

SCIENTIFIC COUNCIL (1995-1999)

1. Assoc.Prof. **Hanna Ambroż**, Ph.D., D.Sc.
Institute of Nuclear Chemistry and Technology
physical and radiation chemistry, photochemistry

2. Assoc.Prof. **Krzysztof Bobrowski**, Ph.D., D.Sc.
Institute of Nuclear Chemistry and Technology
radiation chemistry, photochemistry, biophysics

3. Prof. **Andrzej G. Chmielewski**, Ph.D., D.Sc.
Institute of Nuclear Chemistry and Technology
chemical and process engineering, nuclear chemical engineering, isotope chemistry

4. Assoc.Prof. **Jadwiga Chwastowska**, Ph.D., D.Sc.
Institute of Nuclear Chemistry and Technology
analytical chemistry

5. Prof. **Rajmund Dybczyński**, Ph.D., D.Sc.
Institute of Nuclear Chemistry and Technology
analytical chemistry

6. **Zyta Głębowicz**
Institute of Nuclear Chemistry and Technology
staff representative

7. **Ewa Gniazdowska**, M.Sc.
Institute of Nuclear Chemistry and Technology
coordination chemistry

8. **Edward Iller**, Ph.D.
Institute of Nuclear Chemistry and Technology
chemical and process engineering

9. Prof. **Janusz Jurczak**, Ph.D., D.Sc.
Polish Academy of Sciences, Institute of Organic Chemistry; University of Warsaw
organic chemistry, stereochemistry

10. **Antoni Kalicki**, M.Sc.
Institute of Nuclear Chemistry and Technology
radiometric methods, industrial measurement equipment, metrology

11. **Iwona Kałuska**, M.Sc.
Institute of Nuclear Chemistry and Technology
radiation chemistry

12. **Barbara Kaźmirska**
Institute of Nuclear Chemistry and Technology
staff representative

13. Prof. **Kazimierz Korbel**, Ph.D., D.Sc.
Stanisław Staszic Academy of Mining and Metallurgy
nuclear electronics, nuclear technical physics

14. **Janusz Kraś**, M.Sc.
Institute of Nuclear Chemistry and Technology
diagnostic methods

15. **Gabriel Kuc**, M.Sc.
Institute of Nuclear Chemistry and Technology
radiochemistry

16. Prof. **Janusz Lipkowski**, Ph.D., D.Sc.
Polish Academy of Sciences, Institute of Physical Chemistry
physico-chemical methods of analysis

17. Prof. **Andrzej Łukasiewicz**, Ph.D., D.Sc.
Institute of Nuclear Chemistry and Technology
technology of dyes

18. Prof. **Józef Mayer**, Ph.D., D.Sc.
Łódź Technical University
physical and radiation chemistry

19. Assoc.Prof. **Jacek Michalik**, Ph.D., D.Sc.
(Co-chairman)
Institute of Nuclear Chemistry and Technology
radiation chemistry

20. Assoc.Prof. **Jerzy Narbutt**, Ph.D., D.Sc.
Institute of Nuclear Chemistry and Technology
radiochemistry

21. **Dariusz Pogocki**, M.Sc.
Institute of Nuclear Chemistry and Technology
pulse radiolysis

22. Prof. **Jan Przyłuski**, Ph.D., D.Sc.
Warsaw University of Technology
chemistry, solid state technology

23. Prof. **Leon Pszonicki**, Ph.D., D.Sc.
(Chairman)
Institute of Nuclear Chemistry and Technology
analytical chemistry

24. Prof. **Henryk Rzewuski**, Ph.D., D.Sc.
Institute of Nuclear Chemistry and Technology
solid state physics

25. Prof. **Sławomir Siekierski**, Ph.D.
Institute of Nuclear Chemistry and Technology
physical chemistry, inorganic chemistry

26. **Jan Skajster**
Institute of Nuclear Chemistry and Technology
chemical technology

27. **Michał Strzelecki**, M.Sc.
Institute of Nuclear Chemistry and Technology
chemical and process engineering

28. Prof. **Irena Szumiel**, Ph.D., D.Sc.
(Co-chairman)
Institute of Nuclear Chemistry and Technology
cellular radiobiology

29. Prof. **Jan Tacikowski**, Ph.D.
Insitute of Precision Mechanics
physical metallurgy and heat treatment of metals

30. Prof. **Marek Trojanowicz**, Ph.D., D.Sc.
Institute of Nuclear Chemistry and Technology
analytical chemistry

31. Assoc.Prof. **Piotr Urbański**, Ph.D., D.Sc.
Institute of Nuclear Chemistry and Technology
radiometric methods, industrial measurement equipment, metrology

32. Assoc.Prof. **Lech Waliś**, Ph.D.
Institute of Nuclear Chemistry and Technology
physical metallurgy and heat treatment of metals

33. Prof. **Stanisław Wroński**, Ph.D., D.Sc.
Warsaw University of Technology
chemical engineering

34. Prof. **Zbigniew Zagórski**, Ph.D., D.Sc.
Institute of Nuclear Chemistry and Technology
physical chemistry, radiation chemistry, electrochemistry

35. **Wiesław Zieliński**, M.Sc.
Institute of Nuclear Chemistry and Technology
staff representative

36. **Wanda Żmijewska**, Ph.D.
Institute of Nuclear Chemistry and Technology
analytical chemistry

HONORARY MEMBERS OF THE INCT SCIENTIFIC COUNCIL (1995-1999)

1. Prof. **Maria Kopeć**, Ph.D., D.Sc.
Institute of Haematology and Blood Transfusion
medicine (haematology), radiobiology

2. Prof. **Antoni Dancewicz**, Ph.D., D.Sc.
Institute of Nuclear Chemistry and Technology
biochemistry, radiobiology

RADIATION CHEMISTRY

AND

PHYSICS

RADIATION-INDUCED SILVER AGGLOMERATION IN SMECTITE CLAYS

J. Michalik, J. Sadło, H. Yamada[1/], D.R. Brown[2/], L. Kevan[3/]

[1/]National Institute for Research in Inorganic Materials, Ibaraki, Japan
[2/]Leeds Metropolitan University, Great Britain
[3/]Department of Chemistry, University of Houston, USA

PL9700797

Smectite clays are swelling clays that contain an interlayer space which can expand by the absorption of a suitable solvent. The structure of smectite clays is shown in Fig.1. The exchangeable cations in smectite clays are located in the expandable inter-

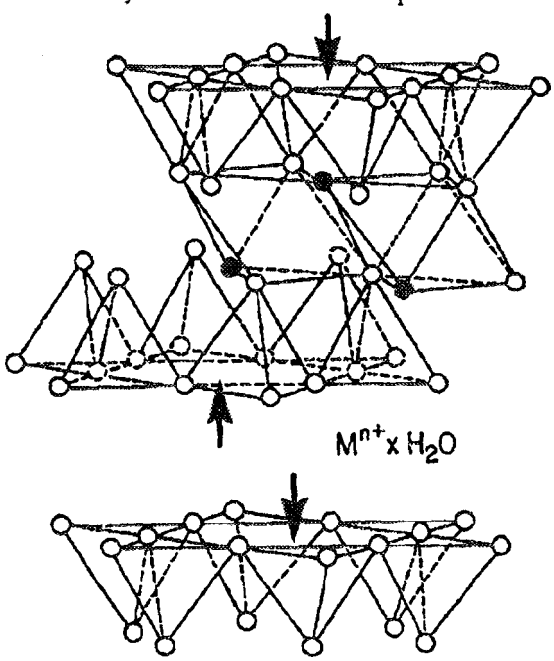

Fig.1. Schematic representation of the oxygen network in smectite clays where the open circles are oxygen and the solid circles are OH. Hydrated interlayer cations are shown, but non-exchangeable cations in the octahedral and tetrahedral lattice layers have been omitted for clarity. Si(IV) occupies the oxygen - coordinated tetrahedral lattice sites. Octahedral lattice sites are occupied predominatly by Mg(II) in hectorite and saponite (trioctahedral clays) and by Al(III) in montmorillonite (where only two thirds of the octahedral sites are filled (dioctahedral clay). Isomorphous lattice substitutions giving rise to the anionic lattice charge are in the octahedral layer for montmorillonite (Mg(II) for Al(III)) and hectorite (Li(I) for Mg(II)), and in the tetrahedral layer for saponite (Al(III) for Si(IV)). Arrows identify the hexagonal cavities in the upper and lower silicate sheets.
Half unit cell formulae:
Montmorillonite - $Na_{0.33}(Mg_{0.33}Al_{1.67})Si_4O_{10}(OH)_2$
Hectorite - $Na_{0.5}(Mg_{2.5}Li_{0.5})SiO_4O_{10}(OH)_2$
Saponite - $Na_{0.55}(Mg_{2.7}Al_{0.3})(Si_{3.15}Al_{0.85})O_{10}(OH)_2$

layers and usually show a higher mobility than the exchangeable cations in zeolites. Silver atoms have been studied as probes for the location and coordination of Ag^+ cations in hydrated montmorillonite [1] and fluorohectorite [2]. Electron spin echo modulation (ESEM) studies showed that silver is fully solvated in montmorillonite with four waters directly coordinated to the silver atom. This is the same as found in bulk solution. However for methanol and ethanol the coordination numbers are less than in frozen bulk solution. For methanol the coordination number is two, and only one for ethanol. Dehydration of montmorillonite was also studied by ESEM [2]. During dehydration distinct species with two coordinated waters and one coordinated water can be observed. The number of coordinated waters deduced from ESEM analysis correlates well with the number of waters suggested from the basal plane spacing determined by X-ray diffraction.

In fully hydrated fluorohectorite [2] also four water molecules interact with silver atom but they are not equivalent. It was postulated that silver atom solvation involves two waters and two oxygens of the basal oxygen surface in the first coordination shell with two more distant waters more weakly coordinated.

The radiation-induced silver agglomeration process has been studied in three structurally distinct, but related, smectites - montmorillonite, hectorite and saponite [3]. The clays used were synthetic and the last two of them were prepared under very high pressure. In this way high crystallinity was achieved ensuring maximum homogeneity in the sites available for exchangeable cations.

The ESR spectra of Ag-clays dehydrated at 250°C under flowing O_2 showed after γ-irradiation and thermal annealing, only doublets of Ag^0 atoms. In hectorite and saponite the Ag^0 spectra disappear on annealing above 200 K and there was no evidence for Ag cluster formation. In montmorillonite the stability of Ag^0 center with A_{iso}=549 G is remarkable; the Ag^0 signal is still detected after sample annealing to room temperature for more than an hour. It is proposed that Ag^0 atoms in montmorillonite are trapped in the so-called hexagonal cavities in the clay interlayers (Fig.1). The six-membered rings of silicon atoms with bridging oxygens in tetrahedral layers of clay lattice can strongly chelate cations of appropriate size. If Ag^+ cation, trapped in this site, captures an electron as a consequence of irradiation, the resultant Ag^0 atom, which is larger than the parent ion, would remain trapped in the cavity [3].

When the dehydrated smectite clays are exposed to methanol prior to radiolytic reduction the yield of Ag^0 increases due to hole scavanging by methanol which prevents geminate recombination. Then, subsequent thermal decay of silver atoms does lead to the formation of charged silver clusters. In addition silver hydroxymethyl radicals are formed as in the molecular sieves exposed to methanol before irradiation. In Ag-montmorillonite/CH_3OH sample Ag_3^{2+} clusters are formed after annealing at 160 K, and above 200 K they transformed into Ag_4^{3+} aggregates represented by ESR pentet with A_{iso}=133 G. In

Ag-hectorite silver tetramers appear at 180 K, whereas in Ag-saponite only at 230 K. They are not stable at temperatures higher than 250 K.

The tetrameric cluster is expected to be close to tetrahedral. Coordination by three methanol molecules could be explained if three of the four Ag

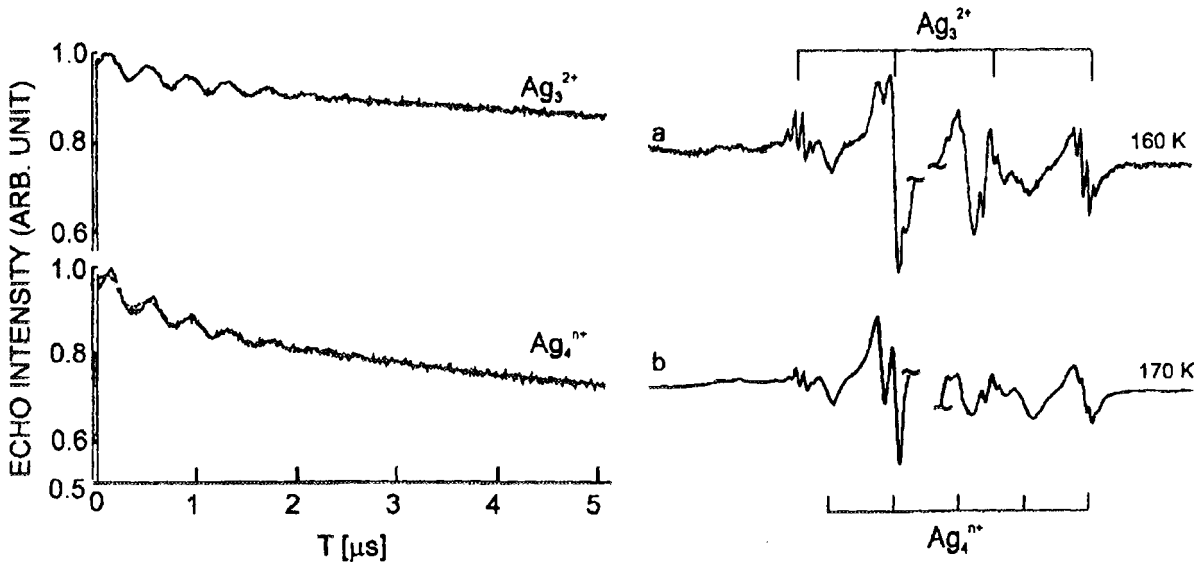

Fig.2. Experimental (-) and simulated (---) three - pulse ESEM spectra of Ag_3^{2+} and Ag_4^{3+} in Ag-montmoryllonite exposed to CH_3OD. Inserted are the ESR spectra of Ag-montmoryllonite annealed to 160 and 170 K showing (a) quartet Ag_3^{2+} and (b) quintet of Ag_4^{3+} clusters, respectively.

Fig. 2 illustrates the ESEM spectra for Ag_3^{2+} and Ag_4^{3+} in Ag-montmoryllonite exposed to CH_3OD. Modulation patterns were simulated in terms of the number of deuterium nuclei interacting with unpaired electron spin and their distance from the spin. The simulation of ESEM spectra for Ag_3^{2+} and Ag_4^{3+} showed them both to be solvated by three methanol molecules in montmoryllonite and in other types of clays.

These observations are consistent with the trimeric cluster, being trigonal planar species and lying in the plane of clay. With only one molecular layer of solvent in the interlayer, as it was concluced from X-ray diffraction, this would constrain solvation to three methanol molecules coordinating the three atoms/ions, with solvent molecules and cluster in the same plane [3].

atoms/ions lie in the plane of the clay, each of them being solvated by single methanol, and the fourth Ag is out of plane and more closely associated with the clay surface and therefore less accessible to solvent molecules. Although such a structure would not give a binominal quitet in the ESR spectrum, the experimentally observed line widths are such that some silver nucleus inequivalency could be present and still be consistent with the ESR spectrum.

References

[1]. Brown D.R., Luca V., Kevan L.: J. Chem. Soc. Faraday Trans., **87**, 2749 (1991).

[2]. Luca V., Brown D.R., Kevan L.: J. Phys. Chem., **95**, 10065 (1991).

[3]. Michalik J., Yamada H., Brown D.R., Kevan L.: J. Phys. Chem., 100, 4213 (1996).

STUDY OF INTRAMOLECULAR PROTON TRANSFER TO HYDROXY SULPHURANYL RADICAL IN METHIONINE AND ITS DERIVATIVES*

D. Pogocki, K. Bobrowski

The hydroxyl radical efficiently generates sulphur radical cation ($>S^{+\cdot}$) from organic thioethers. The latter radical subsequently associates with a non-oxidized thioether to yield three-electron-bonded intermediate, either inter- or intramolecular dimeric radical cation $(>S^{\cdot}\!\!:\!S<)^{+\cdot}$ [1]. The hydroxyl radical induced generation of these sulphur centered radical cations involves one preceding step, namely the formation of hydroxy sulphuranyl radicals, $>S^{\cdot}\text{-}OH$ [2, 3]. Therefore, in substituted organic thioethers neighbouring functional groups actively participate in the oxidation mechanism. These neighbouring groups generally act via providing electron lone pairs for the stabilization of cationic intermediates. Effects of the neighbouring groups on the OH-induced oxidation mechanism have been demonstrated in methionine and methionine-containing peptides [4, 5]. The reaction of OH radicals with these compounds does not only

*Part of this work was presented during 19-th Miller Conference Radiation Chemistry, Cervia/Milano Marittima, Italy, 16-21 September 1995.

Compounds under study

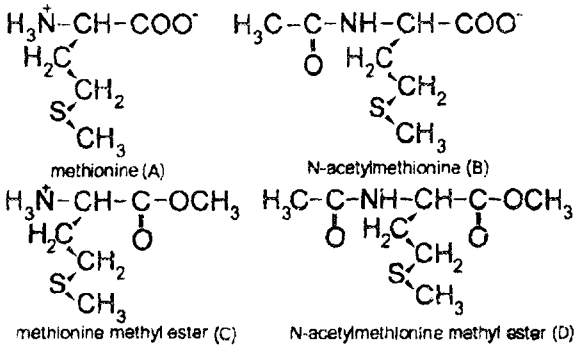

Chart 1.

lead to the expected one-electron oxidized sulphur radical cations but rather to the formation of S.∴S-bonded radical cation suggests that the decarboxylation and the S.∴S-bond formation are competitive.

The aim of the present study was to determine kinetic parameters of the intramolecular proton transfer from the protonated amino group to hydroxy sulphuranyl radical in methionine and to obtain more information on mechanistic details of the decarboxylation processes in methionine and its N-aceto derivative. Employing various methionine derivatives (Chart 1) has several advantages for this type of mechanistic study since derivatization of the amino group by acetylation inhibits formation of the S.∴N-bonded intermediate and esterification of the carboxy group prevents decarboxylation.

The reaction of hydroxyl radicals with methionine (Chart 1A) at strongly acidic pH leads to the

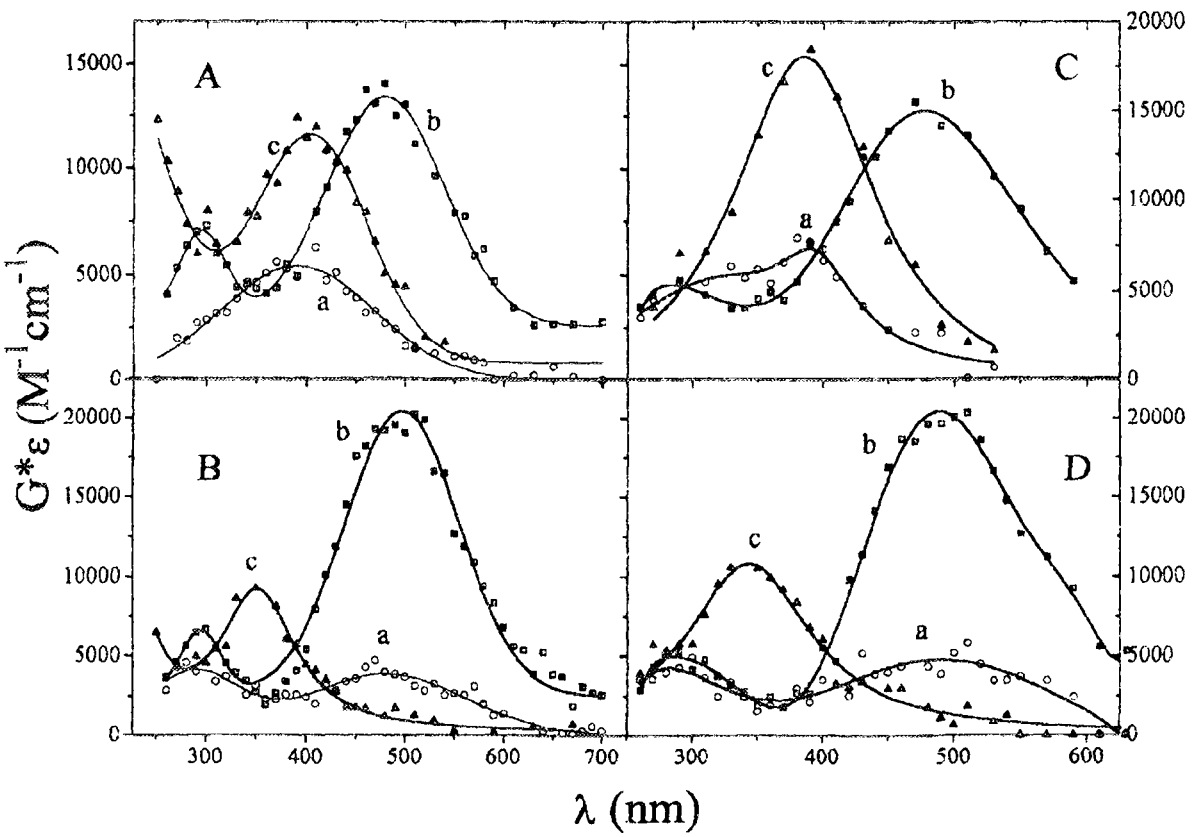

Fig.1. Transient absorption spectra observed after pulse irradiation of an N_2O-saturated aqueous solutions containing 2 mM of amino acids: L-methionine at pH 1.0 40 ns (A-a) and 1.5 μs (A-b) and at pH 6.9 40 ns (A-c) after the pulse; N-acetyl-L-methionine at pH 1.0 (B-a) and 2.0 μs (B-b) and at pH 7 40 ns (B-c) after the pulse; L-methionine methyl ester at pH 1.0 40 ns (C-a) and 2.0 μs (C-b) and at 6.7 40 ns (C-c) after the pulse; N-acetyl-L-methionine methyl ester at pH 1.0 40 ns (D-a) and 2.0 μs (D-b) and at pH 6.8 40 ns (D-c) after the pulse.

α-amino-type radicals with parallel elimination of CO_2 or side-chain fragmentation of N-terminal hydroxy amino acids into respective aldehydes [5, 6]. An S.∴N-bonded short-lived intermediate has been identified in the oxidation of methionine and its peptides and claimed to pay a key role in the OH radical induced decarboxylation of this amino acid and fragmentation of its peptides [5, 6]. The appearance of CO_2 as a stable product with a parallel decrease in the yield of the intermolecular formation of a broad spectrum in the nanosecond range with a maximum located at ca. 390 nm (Fig.1A, curve a). In the microsecond time range the transient spectrum is dominated by the spectrum with a maximum at ca. 480 nm (Fig.1A, curve b). Absorption band at longer wavelengths is due to the well known intermolecularly $(>S.\therefore S<)^+$-bonded radical cation. Since the 390 nm-band is observed in acidic solutions of methionine methyl ester (Chart 1C; Fig.1C, curve a) while is not observed in acidic solutions of

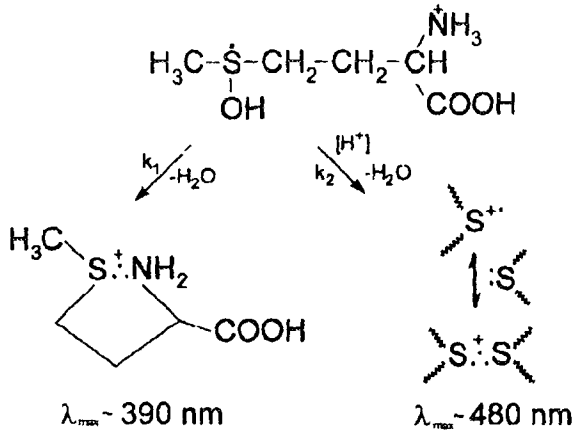

Fig.2.

yield of the S.∴N-bonded intermediate (Fig.2B, curve c) can be rationalized within similar me-

$$\frac{k_1}{k_1 + k_2[H^+]} = \frac{G(S^{\therefore}.N)}{G(S^{\therefore}.N) + G(S^{\therefore}.S)} = \Delta$$

k_1 - rate constant of intramolecular proton transfer from the protonated amino group to hydroxy sulphuranyl radical

k_2 - rate constant of external proton-catalyzed elimination of hydroxide ion from hydroxy sulphuranyl radical

$[H^+]$ - proton concentration [M]

$$\Delta = \frac{G(S^{\therefore}.S)_{N\text{-acetyl-met}} - G(S^{\therefore}.S)_{met}}{G(S^{\therefore}.S)_{N\text{-acetyl-met}}}$$

Fig.3.

N-acetylmethionine (Chart 1B; Fig.1B, curve a) and its methyl ester (Chart 1D; Fig.1D, curve a), the 390 nm-band is assigned to the intramolecularly (S.∴N)-bonded radical cation.

The overall decreased yields of intermolecularly $(>S.^{\therefore}.S<)^+$-bonded radical cations observed at pH 1 on going from N-acetylmethionine (Chart 1B; Fig.1B, curve b) to methionine (Chart 1A; Fig.1A, curve b) can be rationalized in terms of the competition between internal (k_1) and external (k_2) proton-catalyzed elimination of hydroxyl ions from the hydroxy sulphuranyl radical in methionine (Fig.2). The rate constant of intramolecular proton transfer from the protonated amino group to hydroxy sulphuranyl radical (k_1) determined from the equations presented in Fig.3 and the plot in Fig.4A is equal to $\sim 2.0 \times 10^9\ s^{-1}$.

The fact that the efficient decarboxylation occurs in N-acetylmethionine (Chart 1B; Fig.2B, curve b) may suggest a different mechanism for decarboxylation (not involving formation of the S.∴N-bonded intermediate). The higher yield of CO_2 from methionine (Fig.2B, curve a) than the chanism operating for decarboxylation in methionine.

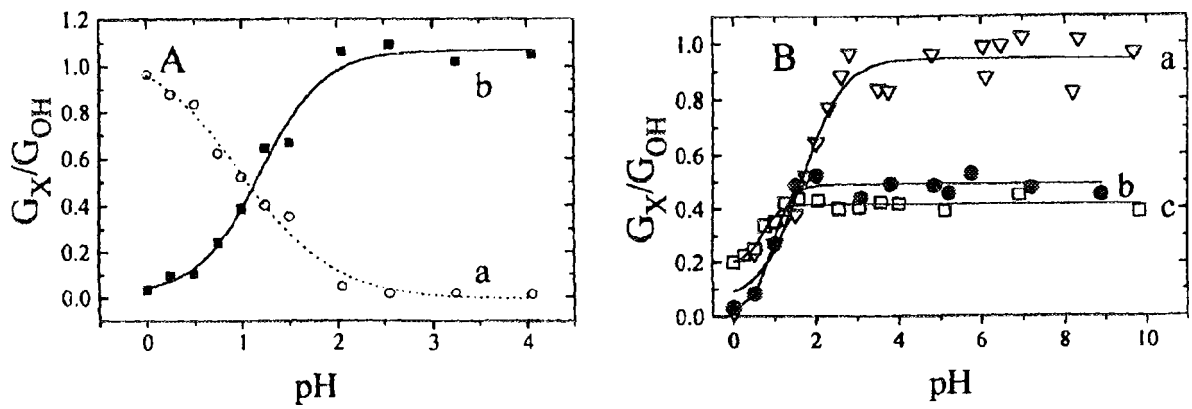

Fig.4. A: Yield of the intermolecular $(>S.^{\therefore}.S<)^+$ radical cation measured at 480 nm (A-a) and yield of intramolecular $(>S.^{\therefore}.N)^+$ radical cation measured at 390 nm (A-b) (expressed in terms of G_X/G_{OH}) as a function of pH obtained in N_2O-saturated aqueous solution of 2 mM methionine methyl ester. B: Yields of CO_2 (expressed in terms of G_X/G_{OH}) obtained in N_2O-saturated aqueous solutions of 2 mM methionine (B-a) and of 2 mM N-acetyl-L-methionine (B-b) and yield of intramolecular $(>S.^{\therefore}.N)^+$ radical cation measured at 390 nm (B-c) (expressed in terms of G_X/G_{OH}) as a function of pH obtained in N_2O-saturated aqueous solution of 2 mM methionine as a function of pH.

References

[1]. Asmus K.-D., Bahnemann D., Fischer Ch.-F., Veltwisch D.: Structure and stability of radical cations from cyclic and open-chain dithia compounds in aqueous solutions. J. Am. Chem. Soc., **101**, 5322 (1979).

[2]. Bonifačić M., Moeckel H., Bahnemann D., Asmus K.-D.: Formation of positive ions and other primary species in the oxidation of sulfides by hydroxyl radicals. J. Chem. Soc. Perkin Trans., **2**, 675 (1975).

[3]. Bobrowski K., Schoeneich Ch.: Hydroxyl radical adduct at sulfur in substituted organic sulfides stabilized by internal hydrogen bond. J. Chem. Soc. Chem. Comms., 795 (1993).

[4]. Hiller K.-O., Masloch B., Goebl M., Asmus K.-D.: Mechanism of OH radical induced oxidation of methionine in aqueous solution. J. Am. Chem. Soc., **103**, 2734 (1981).

[5]. Bobrowski K., Holcman J.: Formation and stability of intramolecular three-electron S.∴N, S.∴S and S.∴O bonds in one-electron-oxidized simple methionine peptides. Pulse radiolysis study. J. Phys. Chem., **93**, 6381 (1989).

[6]. Schoeneich Ch., Fang Zhao, Madden K.P., Bobrowski K.: Side chain fragmentation of N-terminal threonine or serine residue induced through intramolecular proton transfer to hydroxy sulfuranyl radical formed at neighbouring methionine in dipeptides. J. Am. Chem. Soc., **116**, 4641 (1994).

ON THE REACTION OF THE HYDRATED ELECTRON WITH METHIONINE-CONTAINING OLIGOPEPTIDES*

G. Strzelczak-Burlińska, K. Bobrowski, J. Holcman[1/]

[1/]Risø National Laboratory, Denmark

Electrons after their initial attachment to the carbonyl group of the peptide bond, are able to migrate in proteins to metal ions, disulphide groups or to other sites of the polypeptide backbone leading ultimately to a reductive fragmentation of protein molecules. In peptides, electron migration may result in a primary deamination due to a cleavage of the terminal N-C bond and/or in a secondary deamination due to a cleavage of the N-C bond involving nitrogen of the peptide bond [1, 2]. The first process yields ammonia and deaminated radicals while the second one yields the respective amide and secondary deaminated radicals. The rate constant of the e^-_{aq} with peptides increases linearly with the number of carbonyl groups in the peptide, suggesting that these groups are almost identical with respect to an attack by e^-_{aq} [3]. The spectral properties of some deaminated radicals, ·CH(R)-CONHR', where R is a side chain of a N-terminal amino acid residue and R' is a C-terminal either a single amino acid residue or an oligopeptide fragment, have already been investigated. Spectral properties of deaminated radicals derived from glycine- and alanine-containing homo-oligopeptides [4] suggest that the absorption maxima of deaminated radicals are sensitive to the structure of the alkyl side chain of the amino acid residue.

In this work we investigated details of the electron transfer pathways in methionine-containing oligopeptides with various numbers and the location of methionine residues with respect to the terminal functions. We have recently reported [5] relatively high yields of the deaminated radicals in the γ-irradiated polycrystalline X-Met peptides. There was no indication, however, for the presence of deaminated radicals in Met-X peptides. Since the absorption spectra of deaminated radicals derived from methionine and glycine homopeptides are different, we studied the reactions of e^-_{aq} with oligopeptides containing glycine and methionine as the amino and carboxyl terminal residues in order to detect contribution from the secondary deaminated radicals. The reaction rate constants of e^-_{aq} with methionine-containing peptides and the properties of the radicals resulting from the e^-_{aq} attack are also given.

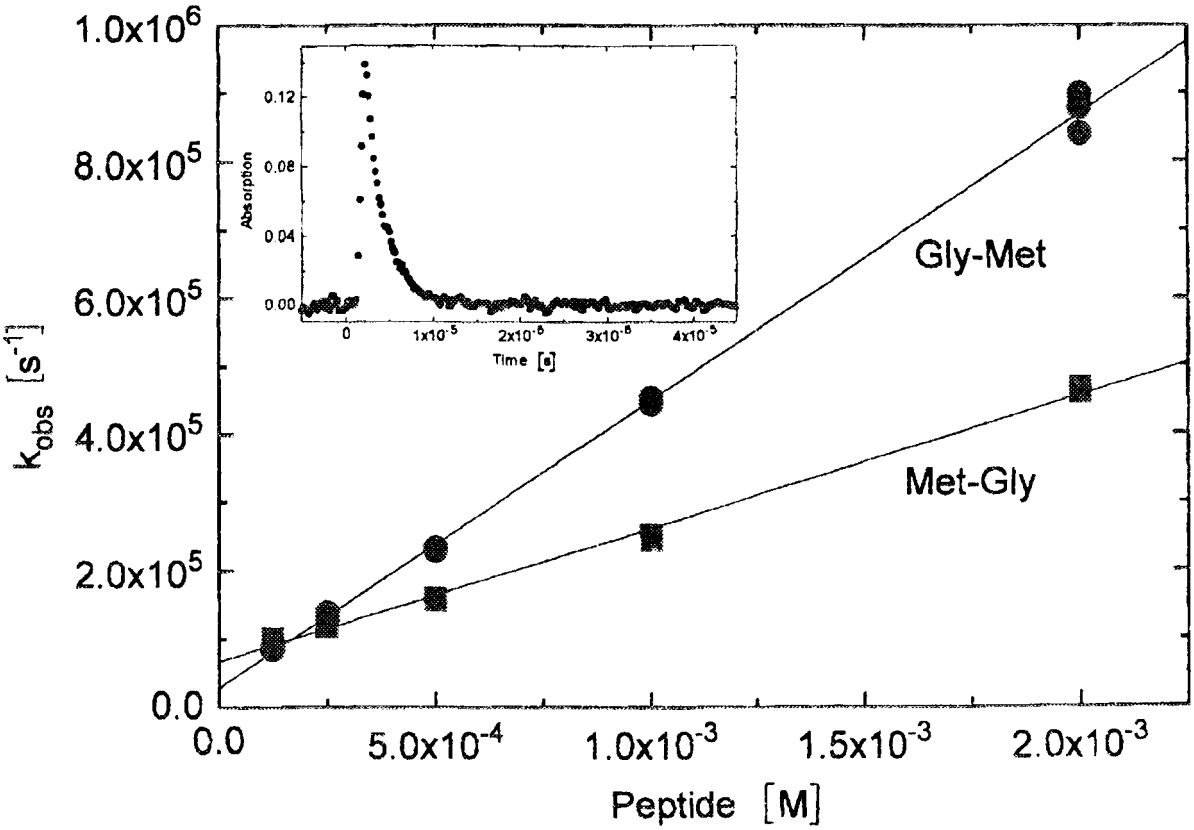

Fig.1. Peptide concentration dependence of the pseudo-first order rate constant, k_{obs}, for the decay of hydrated electron e^-_{aq} in the presence of methionyl-glycine (Met-Gly) and glycyl-methionine (Gly-Met) in Ar saturated aqueous solutions containing tert-butanol at pH 6.5. Insert: Absorption vs. time profile of the decay of e^-_{aq} (600 nm) in 2 mM solution of Met-Gly.

*Part of this work was presented during Symposium on Physical Organic Photochemistry (in honour of Professor Stefan Paszyc). Poznań, Poland, 23-27 July 1995.

Pulse radiolysis experiments were performed with 1 μs pulses of high-energy electrons from the Risø 10 MeV HRC linear accelerator. Absorbed doses were of the order of 1-2 Gy for kinetic and of 10 Gy for spectral measurements. The reactions of

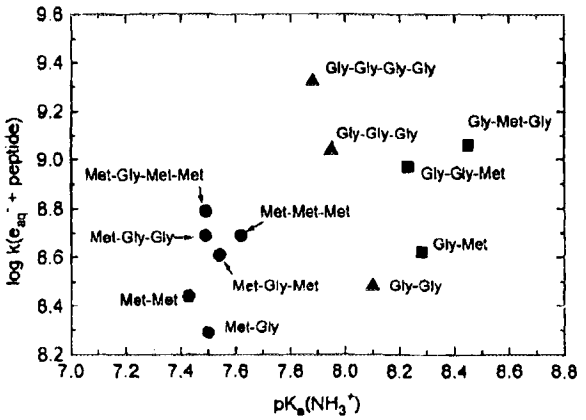

Fig.2. The rate constants for reactions between the hydrated electron and zwitterionic forms of some methionine- and glycine-containing oligopeptides plotted against the pK$_a$ of the amino group. Data for glycine-containing homooligopeptides taken after Tal and Faraggi [3].

hydrated electrons were studied in Ar-saturated solutions containing tert-butanol in order to scavenge ·OH radicals.

The peptides of L-isomeric configuration: glycyl-methionine (Gly-Met), methionyl-glycine (Met-Gly), methionyl-methionine (Met-Met), glycyl-methionyl-glycine (Gly-Met-Gly), glycyl-glycyl-methionine (Gly-Gly-Met), methionyl-glycyl-glycine (Met-Gly-Gly), methionyl-glycyl-methionine (Met-Gly-Met), methionyl-methionyl-methionine (Met-Met-Met), methionyl-glycyl-methionyl-methionine (Met-Gly-Met-Met) and cyclic methionyl-methionine (c-Met-Met) obtained from Bachem were of the purest commercially available grade and were used as received.

Bimolecular rate constants for the reaction of the hydrated electron with nine methionine-containing linear oligopeptides in zwitterionic forms and cyclic methionyl-methionine were determined by monitoring the decay of the hydrated electron at 600 nm. The concentrations of peptides were varied over a range that reduced the lifetime of the hydrated electron by factors of about 5 to 20. Some typical plots based on eq: $k_{obs}=k_o+k_s[peptide]$ are presented in Fig.1 together with the typical experimental trace for the hydrated electron decay in the presence of Met-Gly (inset of Fig.1). The rate constants, k_s, obtained from the slope of plots, for all the methionine-containing oligopeptides used at pH 5.5 and 6.5 together with those obtained for some of peptides in alkaline solutions are summarized in Table. They were found to be in the range $(0.2\text{-}2.0)\times10^9$ $M^{-1}s^{-1}$ depending on the numbers of carbonyl groups and the location of methionine residues with respect to the N-terminal of the peptide molecule. For a given homologous set of peptides, having the same number of peptide

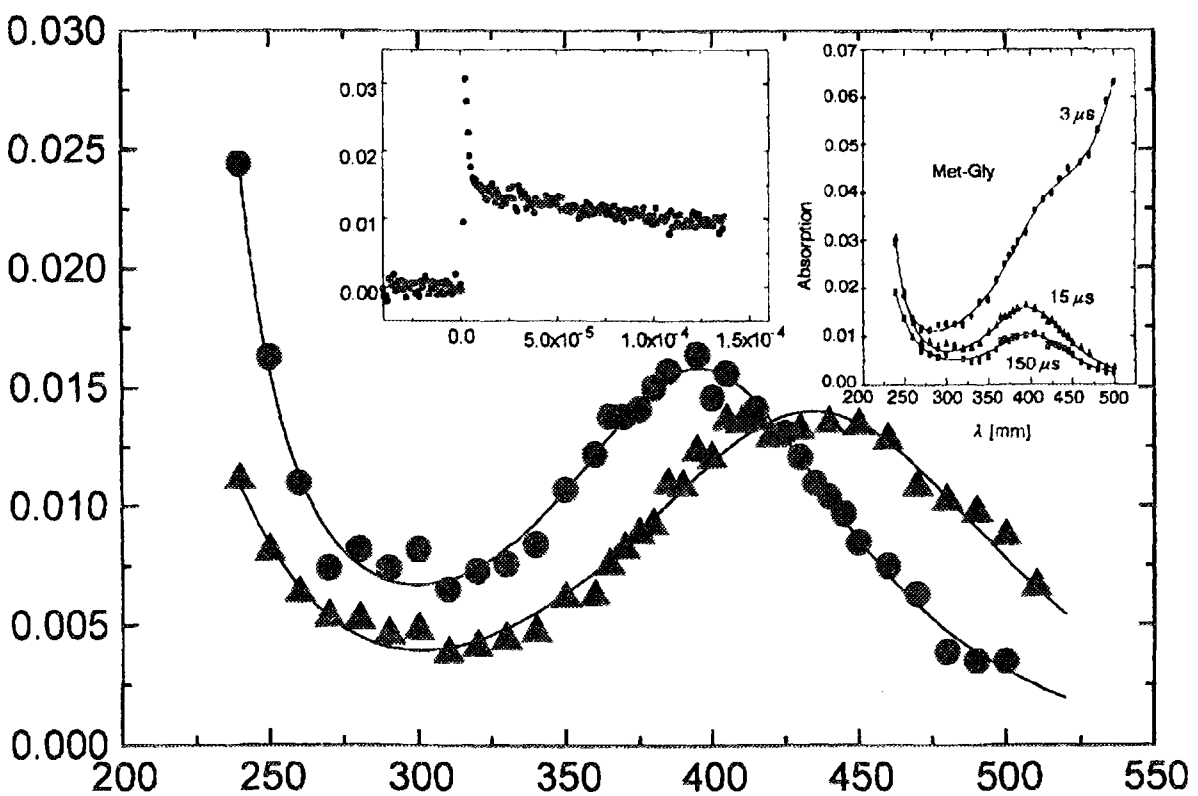

Fig.3. Absorption spectra of deaminated radicals derived from methionyl-glycine (Met-Gly) and glycyl-methionine (Gly-Met) 15 μs after the pulse: spectra obtained in the pulse radiolysis of Ar-saturated aqueous solutions of peptide (2 mM) in the presence of tert-butanol (0.2 M) at pH 6.5. Inserts: (left) Absorption vs. time profile recorded at 400 nm in 2 mM solution of Met-Gly; (right) Transient absorption spectra observed after different time delays after pulse irradiation of a 2 mM solution of Met-Gly in water saturated with Ar and added tert-butanol at pH 6.5.

bonds, the rate constant is higher when the pK_a of the amino group is higher (Fig.2). A factor that apparently influences the reactivity of the peptide is the pK_a of its amino group. The more tightly the hydrogen is bonded to the nitrogen, the higher becomes the rate constant.

Table. Rate constants of reactions of e_{aq}^- with methionine-containing oligopeptides

Peptide	k(e_{aq}^- + peptide)	
	neutral	alkaline
Gly-Met	4.20×10^8 $M^{-1}s^{-1}$a	2.22×10^7 $M^{-1}s^{-1}$c
		2.84×10^7 $M^{-1}s^{-1}$c,e
Met-Gly	1.95×10^8 $M^{-1}s^{-1}$a	1.67×10^7 $M^{-1}s^{-1}$a
	2.39×10^8 $M^{-1}s^{-1}$b	1.74×10^7 $M^{-1}s^{-1}$d,e
	2.07×10^8 $M^{-1}s^{-1}$b,e	
Met-Met	2.74×10^8 $M^{-1}s^{-1}$a	-
Met-Gly-Gly	4.90×10^8 $M^{-1}s^{-1}$a	4.74×10^7 $M^{-1}s^{-1}$d
	6.48×10^8 $M^{-1}s^{-1}$b	6.06×10^7 $M^{-1}s^{-1}$d,e
	5.57×10^8 $M^{-1}s^{-1}$b,e	
Gly-Gly-Met	9.30×10^8 $M^{-1}s^{-1}$a	8.18×10^7 $M^{-1}s^{-1}$c
		8.36×10^7 $M^{-1}s^{-1}$c,e
Gly-Met-Gly	1.15×10^9 $M^{-1}s^{-1}$a	-
Met-Gly-Met	4.10×10^8 $M^{-1}s^{-1}$a	-
Met-Met-Met	4.87×10^8 $M^{-1}s^{-1}$a	-
Met-Gly-Met-Met	6.16×10^8 $M^{-1}s^{-1}$a	-
c-(Met-Met)	1.99×10^9 $M^{-1}s^{-1}$a	-

[a] pH=6.5, [b] pH=5.5, [c] pH=10.5, [d] pH=9.5, [e] 0.1 M $NaClO_4$.

The transient optical absorption spectra of the intermediates produced in aqueous solution of Met-Gly depending on the time delay are shown in the inset of Fig.3. The optical absorption due to the deaminated radicals produced in the reaction of hydrated electrons with two different methionine-containing peptides are presented in Fig.3. The maximum of the optical absorption spectrum of deaminated radicals derived from Met-Gly is significantly blue-shifted (~30 nm) with respect to the maximum of those derived from Gly-Met.

Generally, the optical absorption spectra due to the deaminated radicals $CHR-C(=O)-NH$ derived from oligopeptides containing methionine at the N-terminus are shifted hypsochromically (~30 nm) with respect to those derived from oligopeptides containing glycine at the N-terminus. The results confirms that the absorption maxima of deaminated radicals are sensitive to the structure of the alkyl side chain (R) of the N-terminal amino acid residue, with the $R=CH_2-CH_2-S-CH_3$, absorbing at shorter wavelengths. There is no indication of the occurrence of secondary reactions other than primary deamination. Lack of deaminated radicals in the transient absorption spectrum recorded in the cyclic peptide (c-Met-Met) confirms negligible contribution of a cleavage of the N-C bond involving nitrogen of the peptide bond.

References

[1]. Simič M., Hayon E.: Reductive deamination of oligopeptides by solvated electrons in aqueous solution. Radiat. Res., **48**, 244 (1971).

[2]. Rustgi S., Riesz P.: E.s.r. and spin-trapping studies of the reactions of hydrated electrons with dipeptides. Int. J. Radiat. Biol., **34**, 127 (1978).

[3]. Tal Y., Faraggi M.: The reaction of the hydrated electron with amino acids, peptides, and proteins in aqueous solution. I. Factors affecting rate constants. Radiat. Res., **64**, 337 (1975).

[4]. Faraggi M., Tal Y.: The reaction of the hydrated electron with amino acids, peptides, and proteins in aqueous solution. II. Formation of radicals and electron transfer reactions. Radiat. Res., **64**, 347 (1975).

[5]. Burlińska G., Michalik J., Bobrowski K.: An electron spin resonance study of gamma-irradiated polycrystalline methionine-containing peptides. Radiat. Phys. Chem., **43**, 425 (1994).

4-CARBOXYBENZOPHENONE AND N-(9-METHYLPURIN-6-YL)PYRIDINIUM CATION AS PHOTOSENSITIZERS IN THE OXIDATION OF METHIONINE-CONTAINING PEPTIDES AND SULPHUR-CONTAINING AMINO ACIDS

K. Bobrowski, B. Marciniak[1/], G.L. Hug[2/]

[1/]Faculty of Chemistry, A. Mickiewicz University, Poznań, Poland

[2/]Radiation Laboratory, University of Notre Dame, USA

Excited carbonyl triplets can serve as significant oxidizing agents in biological systems and, in that capacity, can lead to enzyme inactivation and structural changes in proteins. Insight into the damage of these biological systems can be gained by analyzing simpler systems. To this end, detailed investigations of 4-carboxybenzophenone (CB)-sensitized photooxidation of aliphatic thioethers [1], sulphur-containing acids [2], amino acids [3, 4] in aqueous solutions can be consulted for insight into the oxidation mechanisms of more complex systems.

In this work [5] we investigated details of the electron-transfer pathways in the simplest amino acid residues (glycine) using peptides containing a single methionine residue. By using nanosecond flash photolysis and steady-state photolysis, it was possible to follow some of the transients (especially the three-electron-bonded species) in the CB-sensitized photooxidation of several of these peptides and to determine the extent of decarboxylation. From this information it was then possible to surmise a qualitative picture of the reaction mechanism as a function of the position of the single methionine residue in the sequence of glycines and as function of the state of ionization of the amino groups. In addition, it was possible to quantify the importance of the various reaction channels in the scheme by measuring primary photochemical quantum yields of transients from the reduction of the

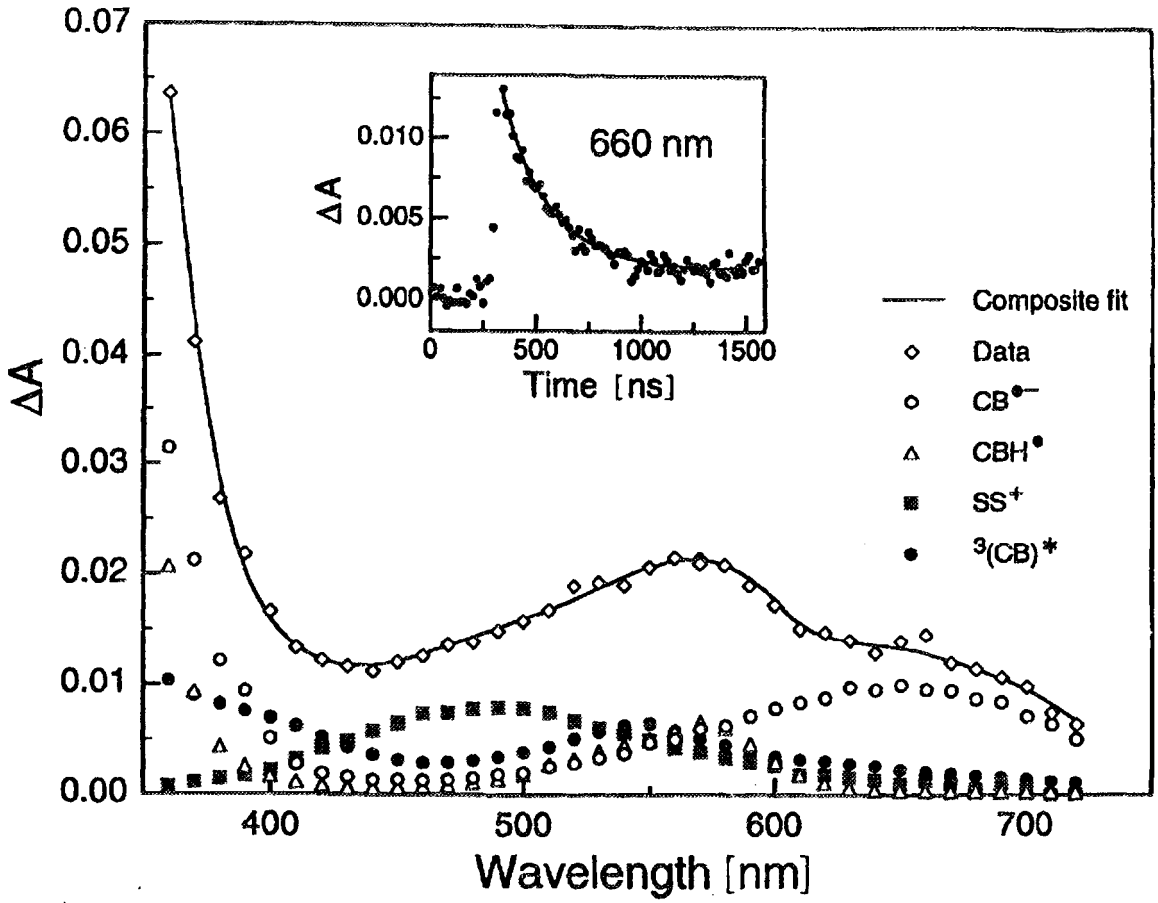

Fig.1. Resolution of the spectral components in the transient absorption spectrum following quenching of the CB triplet state in an aqueous solution of CB (2 mM) and Gly-Met (20 mM) at pH 6.0, taken at the end of the flash. Insert: kinetic trace at 660 nm (fit represents the two exponential decay for the triplet and $CB^{-\cdot}$ decays).

excited CB and rate constants for the decay of these transients.

The rate constants for quenching of the CB triplet by sulphur-containing peptides were determined

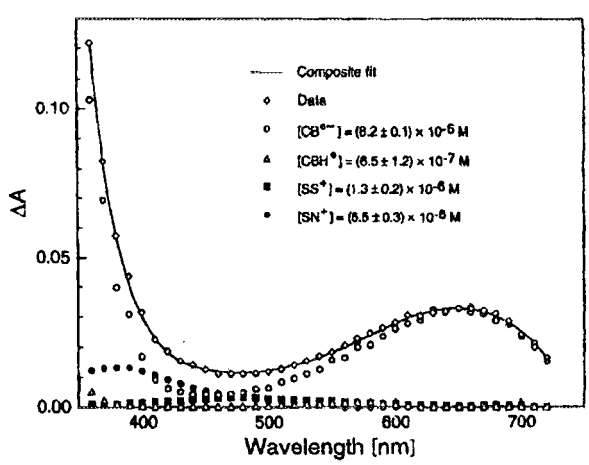

Fig.2. Resolution of the spectral components in the transient absorption spectrum following quenching of the CB triplet state in an aqueous solution of CB (2 mM) and Met-Gly (20 mM) at pH=11.1, time delay 40 ns after the triplet state has decayed.

to be in the range (1.8-2.3)x10^9 $M^{-1}s^{-1}$ for neutral and alkaline solutions. The intermediates identified were the CB ketyl radical anion, the CB ketyl radical, intermolecularly (S.:S)-bonded radical cations, and intramolecularly (S.:N)-bonded radical cations derived from peptides. The types of intermediates were found to depend on the pH of the solution and on the location of the methionine unit with respect to the terminal function (Figs 1 and 2).

According to the mechanism proposed after the formation of the charge-transfer (CT) complex, $[CB^{-\cdot}...^{+\cdot}S<]$, there are three likely fates of this complex: back electron transfer to form the reactants in their ground states, proton transfer within the complex with diffusion apart of the ketyl radical and α-alkylthioalkyl radical, or escape of the radical ions. The total quantum yields for the reduction products were near 40%, with a few exceptions. This should make the quantum yield for back electron transfer about 60%.

In contrast to quenching events with methionine [3], there was no secondary growth of $CB^{-\cdot}$ for pH>8 (or of $CBH^{\cdot}$ for pH<8) following the quenching of the CB triplet by the peptides in the current work. Within the mechanism previously proposed [3], the absence of a secondary growth of $CB^{-\cdot}$ ($CBH^{\cdot}$) could be due either to a lack of formation of α-amido-alkyl-type radicals or to their low reactivity, compared to the α-aminoalkyl-type radicals of the amino acids. The former explanation appears to be the correct one since the quantum yields are low for CO_2 formation (<0.02) in the triplet quenching of CB by the peptides.

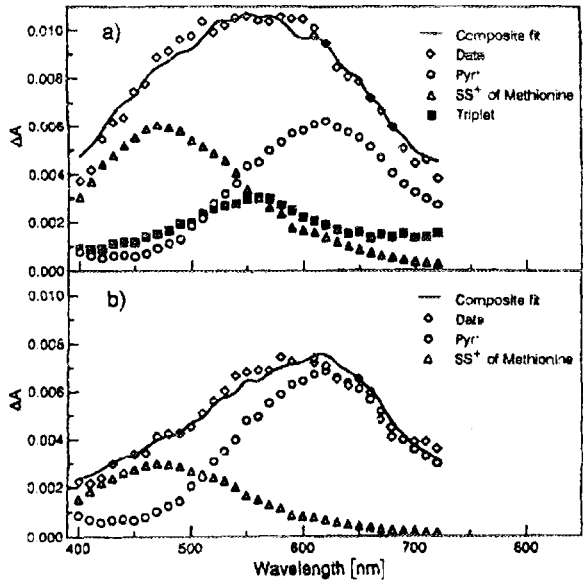

Fig.3. Resolution of the spectral components in the transient absorption spectra following the quenching of Pyr^+ ($2x10^{-4}$ M) and methionine (0.01 M) at pH=6.5 taken (a) at the end of the flash and (b) 24 μs after the flash.

The small exoergonicity of the electron-transfer process for the CB/sulphur-containing amino acids systems suggests searching for more efficient sensitizers. The triplet state of purinylpyridinium cations, e.g. N-(9-methylpurin-6-yl)pyridinium chloride, Pyr^+Cl^- should be an even better one-electron oxidant than the triplets of benzophenone derivatives in aqueous solution. In themselves, Pyr^+ cations are of biological significance as fluorescence probes in nucleic acids and other macromolecules.

In this part of work [6], we have performed a detailed mechanistic study of the photosensitized oxidation of sulphur-containing amino acids by N-(9-methylpurin-6-yl)pyridinium cation in aqueous solution. It was shown that transfer of an electron from the sulphur atom to the triplet state of Pyr^+ was a primary step in the photosensitized oxidation of sulphur-containing amino acids. This was established by the direct observation of electron transfer intermediates in the transient absorption spectra, i.e. Pyr· and the intermolecular (S.·.S)-bonded radical cation (for methionine) (Fig.3), large values of the rate constants (k_q) for quenching of the Pyr^+ triplet state by sulphur-containing amino acids (in the range of $2x10^9$ $M^{-1}s^{-1}$), and detection of Pyr-Pyr dimers in the steady state photolysis.

The slow formation of Pyr· radicals, which occurred on a microsecond time scale (Fig.4), was assigned to the one-electron reduction of the pyridinium cation ground state by the α-aminoalkyl-type radicals produced from the decarboxylation of the sulphur-centered radical cations.

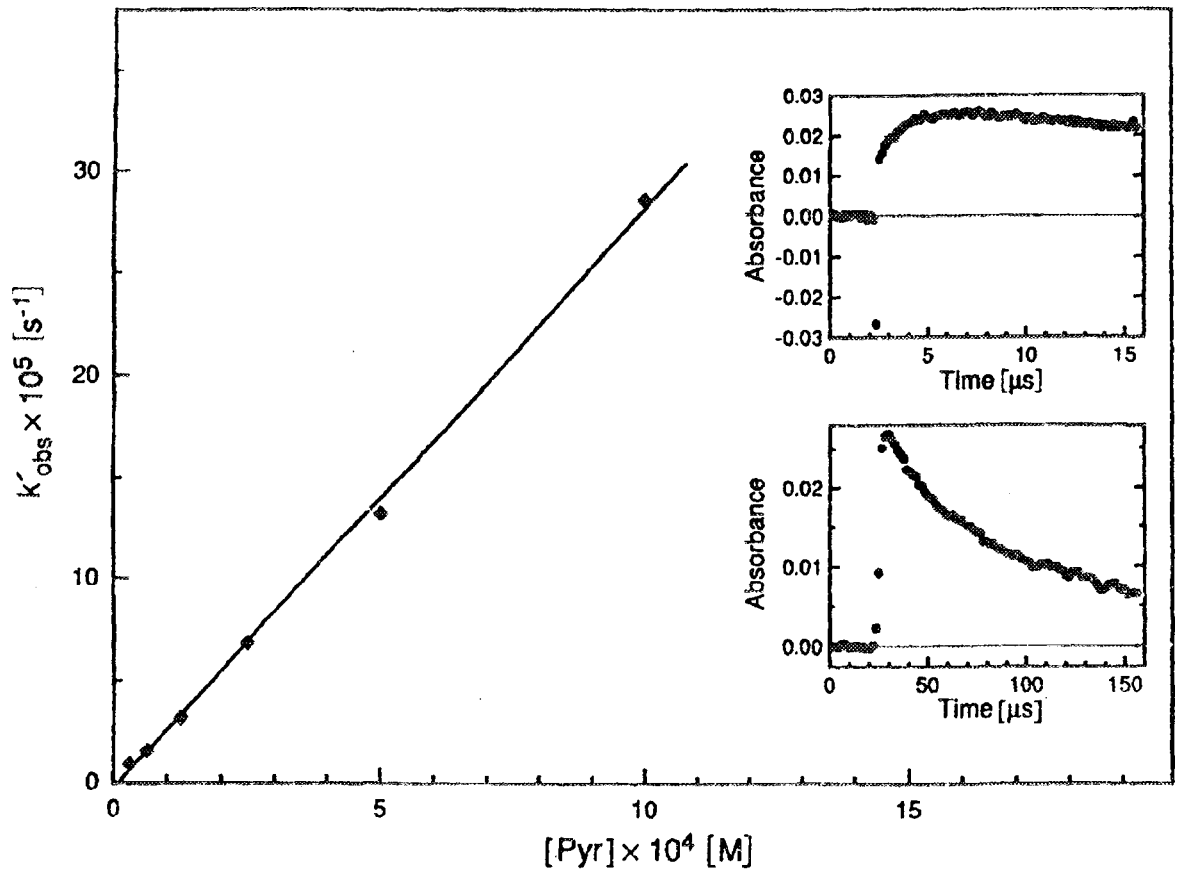

Fig.4. Pyr^+ concentration dependence of the pseudo-first order rate constant, k'_{obs}, for the reaction of Pyr^+ ground state with α-aminoalkyl radicals derived from thiaproline. Inserts: kinetic traces for growth and decay of Pyr· absorbance observed at 610 nm ([Pyr^+]=$2x10^{-4}$ M, [thiaproline]=$5x10^{-3}$ M).

References

[1]. Bobrowski K., Hug G.L., Marciniak B.: A reinvestigation of the mechanism of photoreduction of benzophenones by alkyl sulfides. J. Photochem. Photobiol. A., **81**, 159 (1994).

[2]. Marciniak B., Bobrowski K., Hug G.L., Rozwadowski J.: Photoinduced electron transfer between sulfur-containing carboxylic acids and the 4-carboxybenzophenone triplet state in aqueous solution. J. Phys. Chem., **98**, 4854 (1994).

[3]. Bobrowski K., Marciniak B., Hug G.L.: 4-carboxybenzophenone-sensitized photooxidation of sulfur-containing amino acids. Nanosecond laser flash photolysis and pulse radiolysis studies. J. Am. Chem. Soc., **114**, 10279 (1992).

[4]. Bobrowski K., Hug G.L., Marciniak B., Kozubek H.: 4-carboxybenzophenone-sensitized photooxidation of sulfur-containing amino acids in alkaline aqueous solutions. Secondary photoreactions kinetics. J. Phys. Chem., **98**, 537 (1994).

[5]. Marciniak B., Hug G.L., Bobrowski K., Kozubek H.: Mechanism of 4-carboxybenzophenone-sensitized photooxidation of methionine-containing dipeptides and tripeptides in aqueous solution. J. Phys. Chem., **99**, 13560 (1995).

[6]. Marciniak B., Hug G. L., Rozwadowski J., Bobrowski K.: Excited triplet state of N-(9-methylpurin-6-yl)pyridinium cation as an efficient photosensitizer in the oxidation of sulfur-containing amino acids. Laser flash and steady-state photolysis studies. J. Am. Chem. Soc., **117**, 127 (1995).

THE TRIPLET STATE ARYL CATION 3,5-DICHLORO-4-AMINO $^3Ar^+$

H.B. Ambroż, T.J. Kemp[1/], G.K. Przybytniak

[1/]Department of Chemistry, University of Warwick, Coventry, Great Britain

The simplest aromatic cation, the aryl cation (Ar^+) can be observed only when its electronic ground state is triplet in character, $^3Ar^+$ $(sp^2)^1(\Pi)^5$ and the only unambiguous method of detection is low temperature magnetic resonance EPR and ENDOR [1-3]. However postulated and calculated, the singlet aryl cation $^1Ar^+$ [4, 5] has never been observed and some experimental results even suggest that it is not stabilized at 77 K [6], i.e. at the temperature which allows to generate and detect over 35 amino-, oxy- and thio-substituted triplet aryl cations [1, 2] (the unsubstituted Ar^+ is supposed to render singlet ground state species [4]).

We now wish to present two species which exhibit a very strong dipolar interaction, i.e. their D parameters are of energy close or higher than the microwave energy of X-band EPR spectrometer. In the light of interpretation of these results we have to evoke previous discussions concerning several aryl cations, data of which we published earlier [1, 2] re-considering and completing our former conclusions.

We have generated two distinct triplet aryl cations 3,5-dichloro-4-amino $^3Ar^+$ (Figs 1 and 2, Table) in the matrix of parent microcrystalline dia-

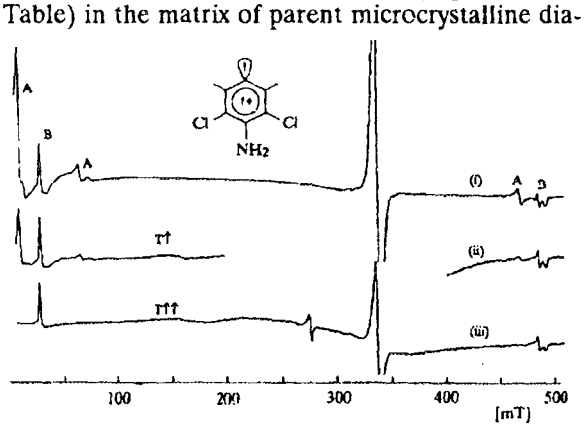

Fig.1. Triplet EPR spectrum of the 3,5-dichloro-4-amino $^3Ar^+$ species A and B. Line positions given in Table. (i) initial spectrum at 77 K, (ii) on warming and re-cooling to 77 K, (iii) on subsequent warming and re-cooling to 77 K.

zonium salt. Both the triplets provide the D parameter energy over 0.3 cm^{-1}, the highest reported so far for substituted aryl cations [1, 2]. One of the species, B, of higher value of the zero field splitting parameters (ZFS), exhibits the typical EPR spectrum without H_{min}, characteristic for the value of

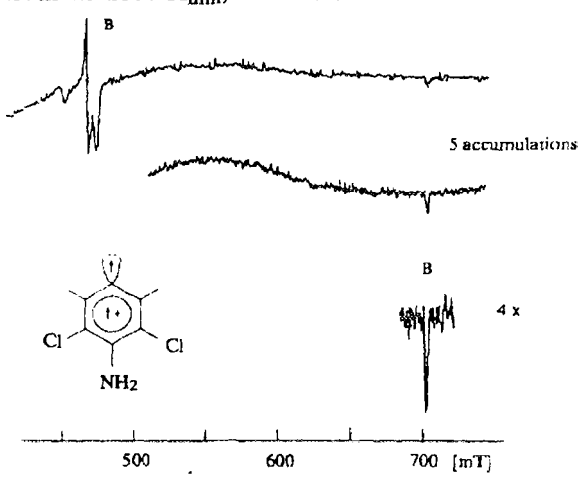

Fig.2. As in Fig.2 (i). High-field part of the spectrum in which the H_{z2} absorption of B is shown (Table).

the D parameter close to microwave energy. The other one, A, having slightly lower D, allows to observe H_{min} due to non-linear mode of energy levels when external magnetic field is approaching zero. We believe that we have observed all of the cannonical transitions allowed for the species B and not all of them for the species A, which makes its ZFS calculations imprecise (Table).

Table. Spectroscopic data of 3,5-dichloro-4-amino $^3Ar^+$, species A (δ=9.4444 GHz) and B (δ=9.4492 GHz).

		A	B
H_{min}	mT	10	-
H_{z1}	mT	-	27.4
H_{y1}	mT	65.9	-
H_{x1}	mT	73.5	-
H_{dq}	mT	-	273.5
H_{x2}	mT	467.9	482.8
H_{y2}	mT	481.8/478.8	489.2
H_{z2}	mT	-	702.1
D	cm^{-1}	0.3066	0.3152*
E	cm^{-1}	0.0029	<0.005

* As calculated from the H_{dq} position.

What is unusual in our present results?

The so called "no H_{min}" spectrum of $^3Ar^+$ has been recorded for the first time for the aryl cations. It suggests that the 3,5-dichloro-4-amino aryl cation species B exhibits the strongest electron-electron interaction found so far for these species. On the other hand the results obtained under the same conditions disclose that one chlorine substituent at meta-position of some $^3Ar^+$, e.g. 4-diethylamino and 4-morpholino $^3Ar^+$, decreases the value of the D parametr [1, 2].

The chloro-substituent having three nΠ-electron pairs is known to be a very good Π-electron donor and a very strong σ-electron acceptor. Both Π and σ effects are important for stabilizing triplet aryl cations. Electron-donor substituent always increases spin density within the ring thus stabilizes the cation, the best are Π-electron donors at p~o>m positions [5]. If one meta-chlorine lowers the value of D (the electron-withdrawing effect is overwhelming), two meta-chlorines should be more active in decreasing spin density in the ring. As it is not the case - the reason must lie in geometries of the two species, mono- and doubly-substituted 4-amino Ar^+. The latter having two bulky substituents chlorine atoms in the vicinity of the para-amino group must force a distortion (bending) of the species which helps Π-electrons interaction and prevents σ-electrons interference. Obviously the species of the not perfect Π-system (having only five Π electrons) cannot follow the rules relating to aromatic ortho-, meta- and para-positions, the planar structure of the aryl cation ring is not preserved, at least, not always. The possibility of various conformation of low energy triplet aryl cations has been noticed previously [6]. We believe that the difference in geometry of the species is the reason that one is able to observe up to four distinct triplets of different ZFS which were unambiguously identified by their different thermal stability and which reproduced their spectral parameters with high accuracy. However this is not the proof that in a glassy matrix there are all the same triplet configurations. We now believe that the glassy matrix can disperse energy levels, especially around zero field, which creates another triplet species with less precisely determinable parameters.

Our investigation of electronic absorption of Ar^+ is an additional source of information of the triplet cations. The optical spectrum of 3,5-dichloro-4-amino $^3Ar^+$ is composed of two lines (Fig.3). It is necessary to note that the EPR experiments cited above were performed in microcrystalline matrices of parent diazonium salts, whereas optical measurements - in acidic glassy media. It might evidence that the detected optical transitions are not influenced by the matrix effects or that they are not related to the different geometries of $^3Ar^+$. The

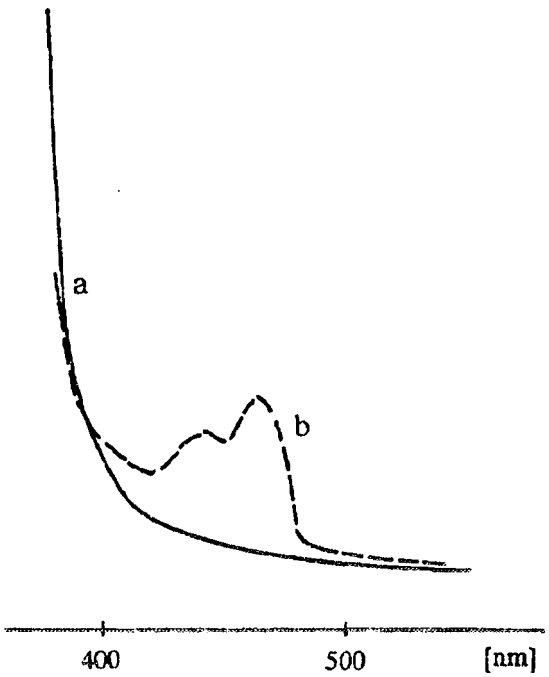

Fig.3. Electronic spectra of 3,5-dichloro-4-amino benzeno-diazonium salt (a) and aryl cation (b) λ_{max}=445 and 463 nm.

assignment of the optical absorption lines to the triplet aryl cations is unquestionable [7]. Glassy matrices, which are softer than microcrystalline media, produce another triplet EPR transitions, especially at low magnetic field, than those generated in crystals which are sharp multiplets.

References

[1]. Ambroż H.B., Kemp T.J.: J. Chem. Soc., Perkin Trans. II, 1420 (1976).

[2]. Ambroż H.B., Kemp T.J.: J. Chem. Soc., Perkin Trans. II, 768 (1980).

[3]. Scaiano J.C., Kim-Thuan N.: J. Photochem. Photobiol., **23**, 269 (1983).

[4]. Dill J.D., Schleyer P., Binkley J.S., Seeger R., Pople J.A., Haselbach E.: J. Am. Chem. Soc., **98**, 5428 (1976).

[5]. Dill J.D., Schleyer P., Pople J.A.: J. Am. Chem. Soc., **99**, 1 (1977).

[6]. Ambroż H.B., Kemp T.J.: Chem. Phys. Letters, **73**, 554 (1980).

[7]. Ambroż H.B., Kemp T.J., Przybytniak G.K.: J. Photochem. Photobiol. A: Chem., **68**, 85 (1992).

SPURS IN CRYSTALLINE L-ALANINE

Z.P. Zagórski

As it is the case in all irradiated media, dissipation of ionizing energy occurs heterogenously on the molecular level, also in a crystalline solid phase. Because of basic physics of energy deposition, new chemical entities appear in single ionization/excitation spurs and in multiionization spurs. Even with the low LET radiation, an important part (usually about 30%) of energy is deposited in multiionization spurs. The participation of multiionization spurs increases with increasing LET and the in-

creased participation is combined with the change of the structure of spurs.

It is an astonishing fact for radiation chemists, familiar with the role of spurs in aqueous solutions, that practically all publications on radiolysis of solid alanine do not use the term "spur", in spite of producing data which can and should be interpreted as spur phenomena. The only excuse is probably the justified constatation, that spur-chemistry of aqueous solutions is practically closed. Products of multiionization spur reactions are molecular hydrogen and hydrogen peroxide - both not as reactive as free radicals which dominate the single spur chemistry. The yield of molecular products in aqueous solution radiation chemistry is considered only in computer assisted simulations, but in usuall work, H_2 and H_2O_2 are neglected, except for cases where iron ions or similar ions are present, giving rise to Fenton-type reactions.

Unlike aqueous radiation chemistry, radiation chemistry of crystalline alanine, or solid state radiation chemistry in general, cannot get rid of multiionization-spur chemistry. Products of larger than one ionization spurs are by far more interesting than products of larger spurs in radiation chemistry of water and of aqueous solutions. The best example is radiolysis of tryptophan, in which multiionization spurs only may explain the different behaviour of L and DL stereoisomers, due to their different crystallographic structures [1].

Less complicated amino acid, alanine displays less spectacular effects, but still they deserve closer investigation. All three alanines, L, D and DL are widely investigated for their radiation chemistry in the solid state. The main interest is caused by the formation of the free radical $CH_3 \cdot C \cdot H \cdot COO^-$, formed inside crystals by deamination. It is stable at room temperature. It shows an easy to measure EPR spectrum, thus being the base of solid state ALA/EPR dosimetry. The same radical shows also a well defined optical electronic absorption spectrum [2, 3] which also is a foundation of different alanine dosimetry, ALA/DRS, i.e. with measurement of the optical absorption spectrum, by diffuse reflection spectrophotometry.

The energy of ionizing radiation is dissipated in alanine, as in all media, in spurs of different size. It is obvious, that the free radical mentioned above, is the result of single ionization spur, which has caused the deamination, due to the sufficient amount of deposited energy. That energy is not sufficient to destroy the molecule entirely. Moving to higher LET values, the yield of the radical diminishes, because the products of multiionization spurs in alanine do not show in the EPR spectra. These are simple chemical compounds, the debris of alanine molecule; the concentration of deposited energy is here much higher than in a single ionization spur. With higher LET values more and more energy results in formation of debris, and EPR signals from the radical are originated in less and less narrow zones outside large spurs. Therefore the shape of the signal is always the same, but the kinetics of decay are faster, because debris of the molecule, present in high concentration, diffuse to the sites of single spurs, destroying the radical.

The best investigation of EPR signal in the function of LET of radiation has been done by Hansen group [4, 5]. These authors did not use the concept of spurs in the interpretation. Our starting point has been the use of these data, plotting them in the function of LET, and combining them with textbook, classical curves for water. The results, shown in Fig. are astonishing. The yield of the free radical derived from alanine changes in the same way as the yield of free radicals in water. The analogy is not quite as good at high LET values, but the difficulties with dosimetry in that region are obvious. The curves of yield vs. LET in water have new, improved versions, but they do not reach as high LET values as presented in classical investigations.

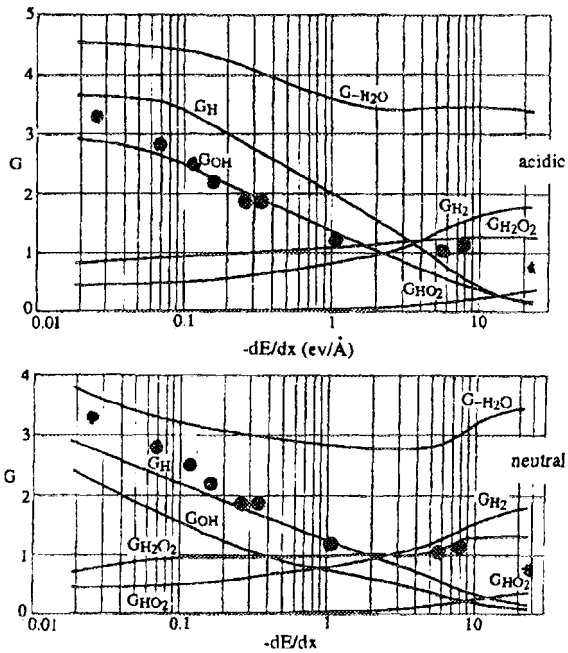

Fig. Classic dependence of yields, radical and molecular in water and aqueous solutions on LET, from [6]. Values of free radical yields of $CH_3 \cdot C \cdot H \cdot COO^-$ in the function of same LET values are introduced as filled circles, calculated from [4, 5] values.

The coincidence between radical yield in alanine and in water is astonishing, but it is worth consideration. The theoretical calculation of energy distribution between different sizes of spurs in alanine seems hopeless at the time being [7]. It would demand a knowledge of the oscillator distribution for the alanine molecule, the ionization potential in the lattice, ionization efficiency and the W-value of ionization as a function of electron energy. The experimental coincidence with water radiation chemistry shows, that either the values of listed parameters are very similar to that in water, or the differences are mutually compensated, or both.

Our experimental investigations on alanine radiation chemistry, accepted for presentation at the coming Gordon Conference "Radiation Chemistry"

will show more details supporting the basic idea on the role of energy distribution between single and large spurs in radiolysis of solid alanines.

References

[1]. Zagórski Z.P.: Radiat. Phys. Chem., 47, 385-388 (1996).

[2]. Zagórski Z.P.: J. Radioanal. Nucl. Chem., Letters, 187, 73-78 (1994).

[3]. Zagórski Z.P.: Radiat. Phys. Chem., 46, 1291-1294 (1995).

[4]. Hansen J.W., Olsen K.J., Wille M.: Radiat. Protect. Dos., 19, 43-47 (1987).

[5]. Olsen K.J., Hansen J.W.: Radiation Res., 116, 547-549 (1988).

[6]. Allen A.O.: The radiation chemistry of water and aqueous solutions. van Nostrand, Princeton 1961.

[7]. Mozumder A.: private communication.

HPLC MONITORING OF RADIOLYTIC DECOMPOSITION OF CHLOROPHENOLS IN SYNTHETIC SOLUTION AND NATURAL WATER MATRICES

A. Chudziak, T. Bryl-Sandelewska, M. Trojanowicz

Numerous studies have shown that irradiation using high energy electron beam or γ radiation from ^{60}Co sources can be efficient for the destruction of several classes of hazardous organic compounds such as halogenated alkyl hydrocarbons, aromatic hydrocarbons and chlorobenzenes [1]. The efficiency of removal of organic chemicals from contaminated water depends on radiation dose, initial concentration of contaminant, pH and turbidity. Descriptive empirical models have been developed recently for estimating the removal of selected organic compounds as a function of these factors

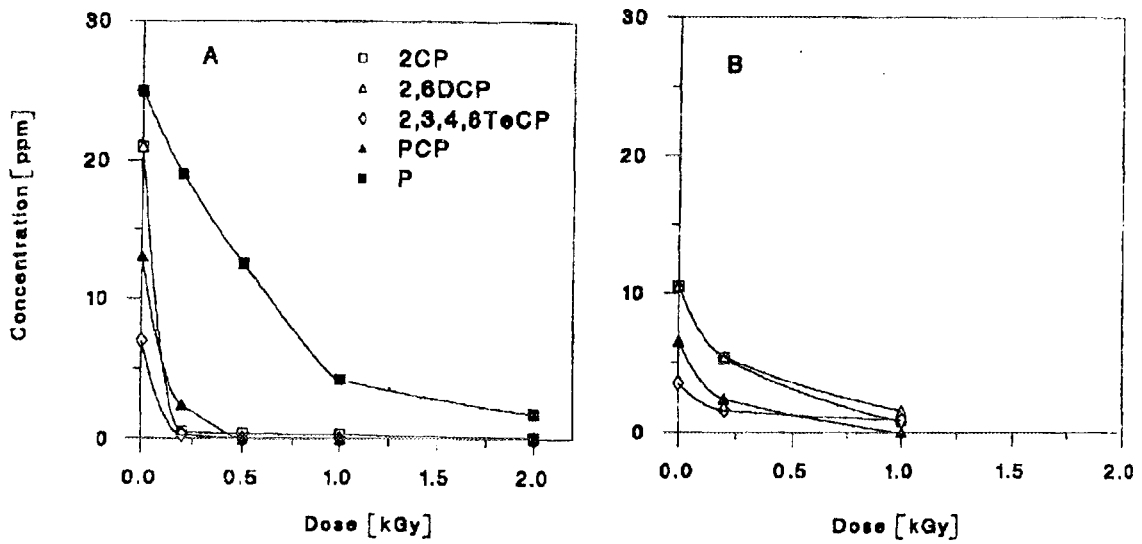

Fig.1. Effect of absorbed dose on radiolytic degradation of phenol and chlorophenols in synthetic aqueous solutions (A) and in river water (B).

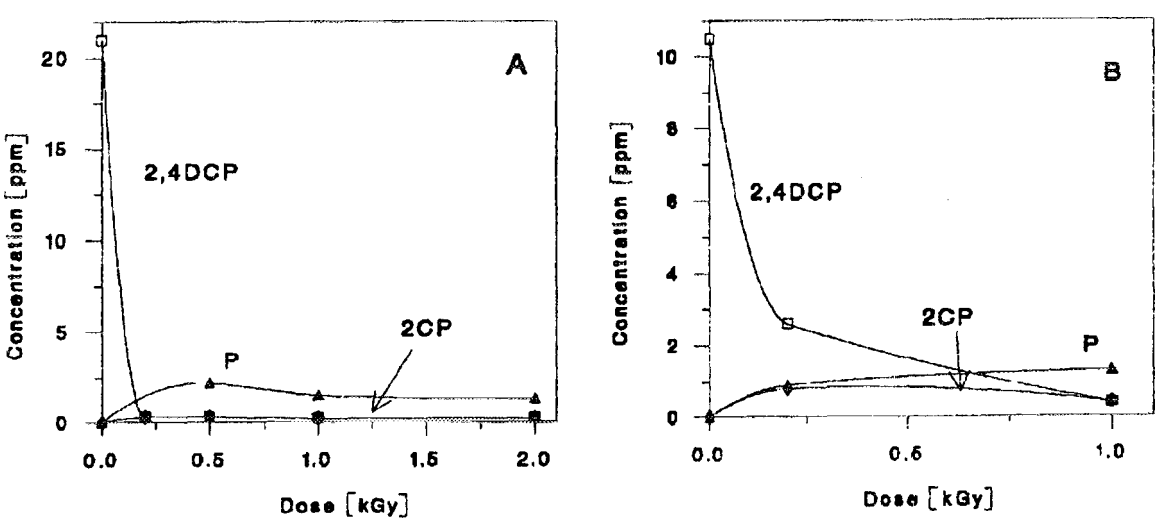

Fig.2. Effect of absorbed dose on radiolytic degradation of 2,4-dichlorophenol (2,4DCP) in synthetic aqueous solution (A) and in river water (B). Detected products: P - phenol, 2CP - 2-chlorophenol.

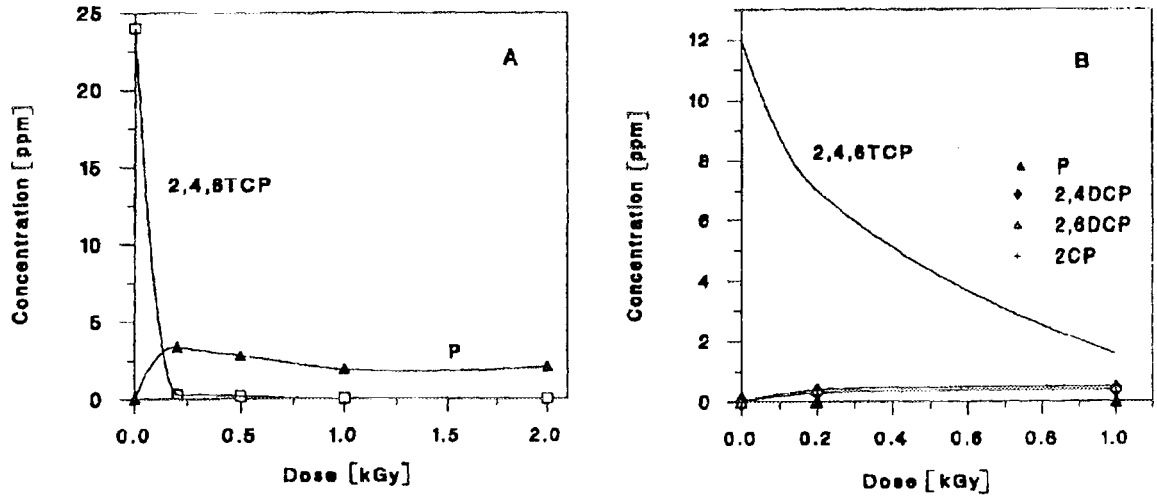

Fig.3. Effect of absorbed dose on radiolytic degradation of 2,3,6-trichlorophenol (2,4,6TCP) in synthetic aqueous solution (A) and in river water (B). Detected products: P - phenol; 2CP - 2-chlorophenol; 2,4DCP - 2,4-dichlorophenol; 2,6DCP - 2,6-dichlorophenol.

and also for estimating the dose required to meet specific treatment objectives [2]. The removal vs. dose relationship was found to be first order over the contaminant concentration range from 1 to 50 ppm. The developed model, however, can overstate the removal of compounds sensitive to a particular radicals in waters with higher concentrations of scavengers.

Phenol and chlorophenols are widely distributed at low concentrations in natural waters and have detrimental effects on water quality, being toxic for aquatic life [3].

Radiolytic degradation of phenol, and especially chlorophenols for environmental purposes has not focused so far much attention in the literature. The results of our preliminary studies have indicated the possibility of efficient removal of numerous chlorophenols at ppm level from synthetic aqueous solutions [4]. The aim of this study was to identify the products of radiolytic degradation of various chlorophenols and to determine the effect of the absorbed irradiation dose on removal. Also the influence of natural matrix of river water on the effectiveness of radiolytic degradation was studied.

The efficiency radiolytic degradation of phenol and chlorophenols was monitored by reversed-phase HPLC using earlier developed procedure, where the chromatographic retention times increase with increasing number of chlorine atoms in the solute molecule. The products of radiolytic degradation were preconcentrated using solid-phase extraction with 3 ml BAKERBOND spe phenyl columns [5].

The chromatographic measurements were carried out using HPLC setup from Perkin-Elmer, which consists of isocratic pump model LC-250, UV/VIS detector model L-95 and computing integrator LCI-100. A Spherisorb S5 ODS (0.4x25 cm) 1.5 μm column from Knauer and UV detection at 280 nm were used. Injected sample volume was 5 μl.

The irradiation was carried out using 15 ml sample solutions placed in polyethylene bags with about 10 mm layer of irradiated solution formed, which provides sufficient conditions for penetration of the beam. γ radiation from a Russian made ^{60}Co

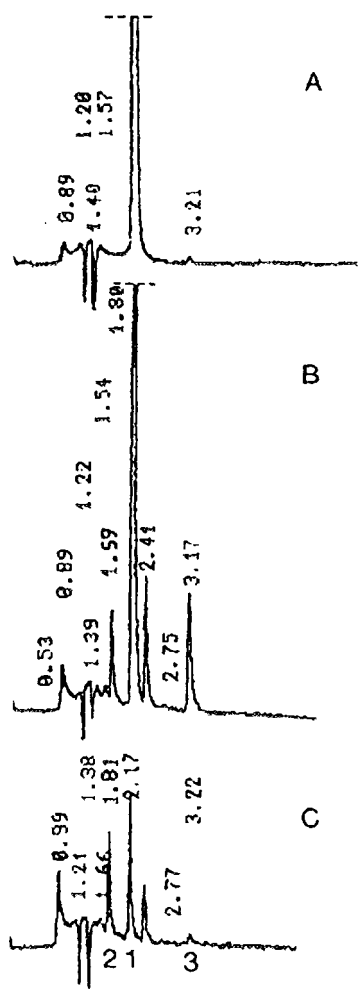

Fig.4. Examples of chromatograms obtained in monitoring of radiolytic degradation of 10.5 ppm solution of 2-chlorophenol in river water using a mixture of acetonitrile/methanol/water (30/30/40) containing 2 g/l citric acid as eluent at a flow rate of 1.5 ml/min and 10-fold preconcentration on phenyl sorbent. A - before irradiation, B - after irradiation with 0.2 kGy dose, C - after irradiation with 1.0 kGy dose. Retention times shown in min. 1 - 2-chlorophenol; 2 - phenol; 3 - 2,4-dichlorophenol.

source ISSLEDOVATEL was used. The magnitude of dose was controlled with a water calorimeter and PVC dosimeters.

Earlier it was found that in 25 ppm solutions of chlorophenols, containing 10% methonal, several chlorophenols with larger number of chloride atoms cannot be completely degraded even using a 10 kGy dose. The results obtained in this study for irradiation of aqueous solutions without scavengers demonstrate efficient removal of all the examined species by a much smaller dose (Fig.1A) The most difficult to decompose is the simple phenol, which is also a product of radiolysis of all chlorophenols except for pentachlorophenol, occurring in largest concentrations (up to several ppm). Doses up to 2.0 kGy have not decomposed it completely (Figs.2A and 3A). Degradation of chlorophenols in synthetic aqueous solutions takes place almost completely at a 0.2 kGy dose, however, for the river water matrix containing scavengers such as carbonates or oxygen it requires a larger dose (Figs.1B, 2B and 3B). For the same dose used for degradation of higher chlorophenols in river water smaller amounts of difficult to decompose phenol are produced. Fig.4 shows an example of the chromatograms obtained for 2-chlorophenol prior to and after irradiation.

Some preliminary attempts were also undertaken to identify other products of radiolytic degradation exhibiting weaker retention on the C18 column used. This was performed using 0.5 mM sulfuric acid/methanol mixture (65/35) as eluent. In radiolysis of phenol, products such as hydroquinone, resorcin and catechol were identified, as reported in the literature [6], whereas for irradiation of 2-chlorophenol only a low level of resorcin and catechol were found. Several other products separated by HPLC were not identified as yet. Even more difficult to identify were the products of such a study in a water matrix. Attempts to identify them using GC-MS technique are in progress.

References

[1]. Cooper W.J., Nickelsen M.G., Waite T.D., Kurucz C.N.: High energy electron beam irradiation: an innovative process for the treatment of aqueous based organic hazardous wastes. J. Environ. Sci. Health., A27, 219-229 (1992).

[2]. Kurucz C.N., Waite T.D., Cooper W.J., Nickelsen M.G.: Empirical models for estimating the destruction of toxic organic compounds utilizing electron beam irradiation at full scale. Radiat. Phys. Chem., 45, 805-816 (1995).

[3]. Sitting M.: Priority Toxic Pollutants, Health Impacts and Allowable Limits, Noyes Data. Park Ridge 1980.

[4]. Chudziak A., Bryl-Sandelewska T., Trojanowicz M.: Application of reversed-phase HPLC in monitoring of radiolytic decomposition of chlorophenols. Presented at 5th Polish Conference on Anatytical Chemistry, Gdańsk, 3-9 September 1995.

[5]. Chudziak A., Trojanowicz M.: Reversed-phase HPLC determination of phenols with preconcentration by solid-phase extraction. Chem. Anal., 40, 39-53 (1995).

[6]. Hashimoto S., Miyata T., Washino M., Kawakami W.: A liquid chromatographic study on the radiolysis of phenol in aqueous solution. Environ. Sci. Technol., 13, 71-75 (1979).

THERMAL DECOMPOSITION OF GAMMA IRRADIATED PROTEINS BY THERMAL ANALYSIS METHODS

K. Cieśla, E.F. Vansant[1/], M. Świderska-Kowalczyk

[1/]Department of Chemistry, University of Antwerp, Belgium

Physico-chemical changes occurring in proteins under gamma irradiation are expected to influence the course of thermal decomposition processes. The influence of gamma irradiation in water suspension on the course of thermal decomposition of proteins was studied now by differential scanning calorimetry (DSC) and thermogravimetry (TGA: TG, DTG).

The following proteins were examined: Cohn fraction IV-1 of globulins bovine (Sigma product), Cohn fraction II, III of gamma globulins bovine (Sigma product), Cohn fraction IV-1 of globulins porcine (Sigma product), gamma globulins (by Serva), casein of goat milk (by Sigma), and hemoglobin (by Serva). The 50% water suspensions of proteins were irradiated in a gamma-cell Mineyola (^{60}Co) at 24, 12, 6, 2.9, 2.5 kGy, applying a dose rate of 1.7 kGy/h. The samples were dried by lyophilization. Simultaneously, the nonirradiated reference samples were prepared. DSC and TGA measurements were carried out in an oxygen flow with a heating rate of 3°/min, applying a Perkin-Elmer heat flow DSC7 calorimeter and Mettler TA300 thermobalance.

The exothermal decomposition effects (DSC) were observed for all samples in 3 temperature

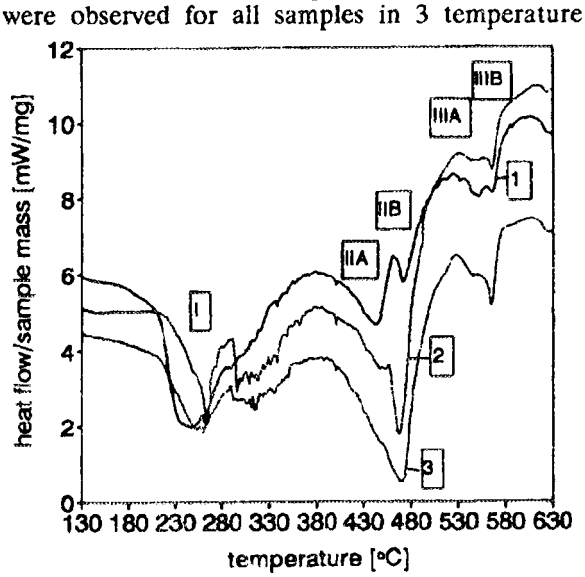

Fig.1. DSC curves recorded for fraction IV-1 of globulins bovine: reference sample (curve 1) and products irradiated at 2.5 kGy (curve 2) and 24 kGy (curve 3) applying a dose rate of 1.7 kGy/h.

ranges. The differences in thermal decomposition course were observed for all the reference and irradiated samples. The examples of DSC curves ob-

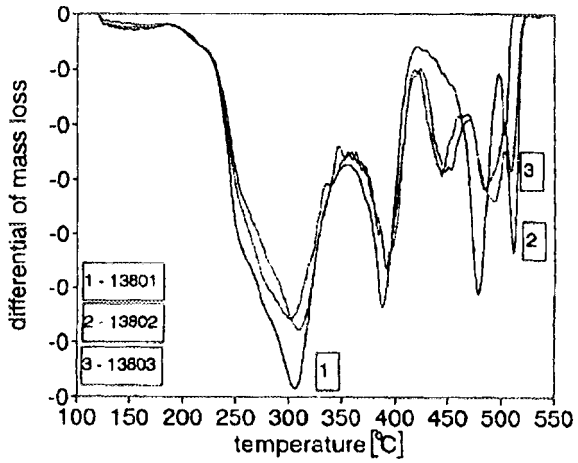

Fig.2. DTG curves recorded for hemoglobin: reference sample (curve 1), products irradiated at 25 kGy (curve 2) and 2.9 kGy (curve 3).

tained for the reference sample of globulins and the products irradiated at 2.5 and 24 kGy are presented in Fig.1. In this case in the second and third ranges two exothermal maxima were visible, indicating two decomposition processes (IIA, IIB and IIIA, IIIB). In the DSC curves of irradiated product, the first exothermal effect (I) was smaller while the second (II) was larger as compared to nonirradiated samples. Simultaneously, an additional exothermal effect appears in range I, with a maximum at higher temperatures than the maximum of the I exothermal effect. In the second and third ranges, IIA and IIIA effects become smaller, while IIB and IIIB effects appear to be relatively larger. The conclusions were confirmed by heats (J/g) calculated for the particular stages of decomposition.

The differences in the decomposition course of the irradiated and reference samples were also found by the TGA method, particularly in the last stage of the process. The examples of DTG curves recorded for the reference sample of hemoglobin and the product irradiated at 24 and 2.9 kGy are presented in Fig.2.

The work was sponsored by the KBN grant 5 S307 0511 03.

DENATURATION PROCESSES IN GAMMA IRRADIATED PROTEINS BY DIFFERENTIAL SCANNING CALORIMETRY

K. Cieśla, Y. Roos[1/]

[1/]Department of Food Technology, University of Helsinki, Finland

Gamma irradiation induces structural transformations in proteins. The changes in the tertiary and secondary structure influences the course of denaturation processes, occurring under heating of proteins in the presence of water [1].

Hemoglobin (Serva), myoglobin equine (Serva), alfa globulins of chicken egg white (Sigma) and different fractions of globulins bovine (by Loba Chemie; by Armour Pharmaceutical Company; by Sigma; by Serva; and prepared in the Department of Radiobiology in the INCT), were studied. These proteins were irradiated in solid state or in water suspension at 30, 25, 20 and 3 kGy, applying dose rates of 1.7, 1.8 and 5.1 kGy/h. The appropriate reference samples were prepared. The DSC measurements were carried out for samples sealed in steel vessels in the temperature range from 10 to 110°C with a heating rate 5°/min using a Mettler DSC-30 calorimeter with a Mettler 400 unit controlling liquid nitrogen flow.

Concentrations of water suspensions were selected permitting to observe endothermal effects connected with the denaturation: 30% for hemoglobin, 25% for myoglobin and 15-40% for different fractions of globulins. Differences in the reference and irradiated samples were observed in the temperature ranges, shapes, and denaturation heats. These differences were larger when samples suspended in water were irradiated, as compared to the irradiated solid dried proteins.

In the case of the hemoglobin reference sample an irregular endothermal effect was observed in the wide temperature range 47-100°C. In the case of products irradiated at different conditions (25 or 30 kGy), the shape of the effect is changed, due to the appearance of an additional peak at lower temperatures and also due to decrease of the main peak. The examples of DSC curves recorded for nonirradiated and irradiated hemoglobin are shown in Fig.1. In the case of myoglobin the effects with

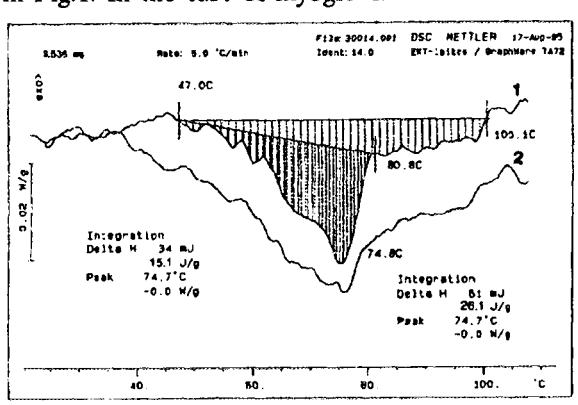

Fig.1. DSC curves recorded for the reference sample of hemoglobin (curve 1) and the solid sample irradiated with a dose 25 kGy (5.1 kGy/h) (curve 2).

regular shapes were observed for both irradiated and nonirradiated samples. The denaturation effect in the irradiated sample was observed at lower

PL9700804

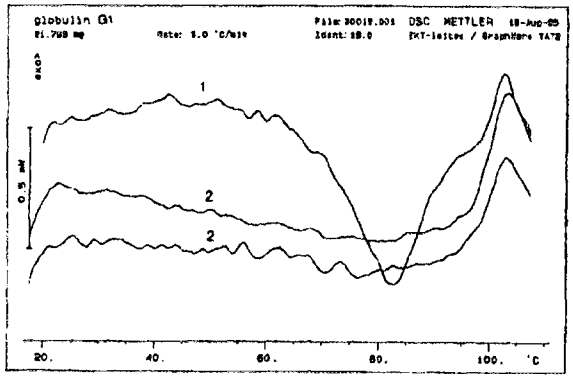

Fig.2. DSC curves recorded for gamma globulins bovine (II fraction by Loba-Chemie): 1 - reference sample, 2 - product irradiated in water suspension with 30 kGy (1.7 kGy/h).

temperatures in larger temperature range, than in the reference sample.

Denaturation effects were found to be smaller for irradiated globulins, as compared to the nonirradiated samples. Fig.2 shows a comparison of the thermal effect recorded for a suspension of the reference globulins sample (II fraction) and for the product irradiated at 30 kGy (1.8 kGy/h) in the presence of water. It was found, that the decrease in denaturation effects can be seen for gamma globulins bovine samples irradiated at a dose of 3 kGy.

The work was sponsored by KBN grant 5 S307 0511 03.

References

[1]. Relkin P.: Differential scanning calorimetry: a useful tool for studying protein denaturation. Thermochim. Acta, 243, 2, 371-386 (1994).

EXAMINATION OF IRRADIATED FLOUR AND MEAT BY AMYLOGRAPHY AND DIFFERENTIAL SCANNING CALORIMETRY

K. Cieśla, M. Świderska-Kowalczyk, W. Głuszewski

We have started to use some new physical methods, based on thermal analysis, to analyse irradiated foodstuffs. Amylography and differential scanning calorimetry (DSC) have been now applied to study irradiated flour and meat.

Amylography is the method usually applied for characterization of flours. Differential scanning calorimetry (DSC) has become in the last years a useful method for foodstuffs studies [1], however only few attempts have been reported until now to use DSC for analysis of irradiated foodstuffs [2]. In

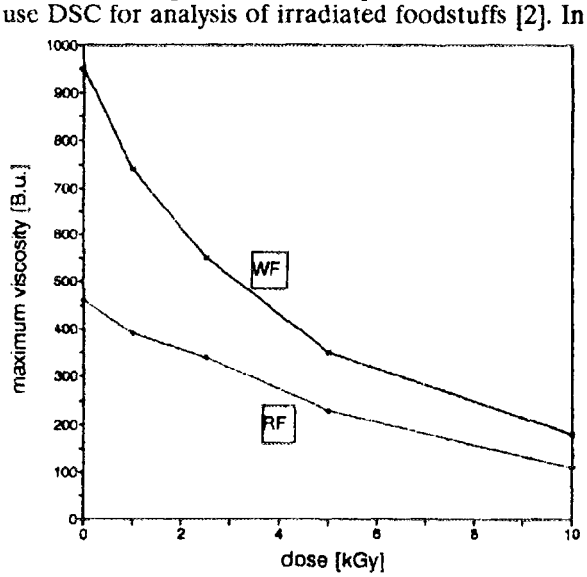

Fig.1. η_{max} (Brabender units) determined from amylograms of rye (RF) and wheat (WF) flours versus irradiation dose. The dose rate was equal to 5.5 kGy/h.

the course of starch gelatinization the viscosity of water suspension of flour grows up. The starting and final temperatures of gelatinization, maximum value of viscosity η_{max} as well as heat of gelatinization depend on the structure of starch contained in flour and can be determined by amylography and DSC methods. As the polysaccharides chains in starch are destroyed by gamma irradiation, the course of amylogram as well as the course of DSC curves are expected to differ for the irradiated and nonirradiated samples. Similarily, the denaturation of meat proteins is expected to be influenced by gamma irradiation.

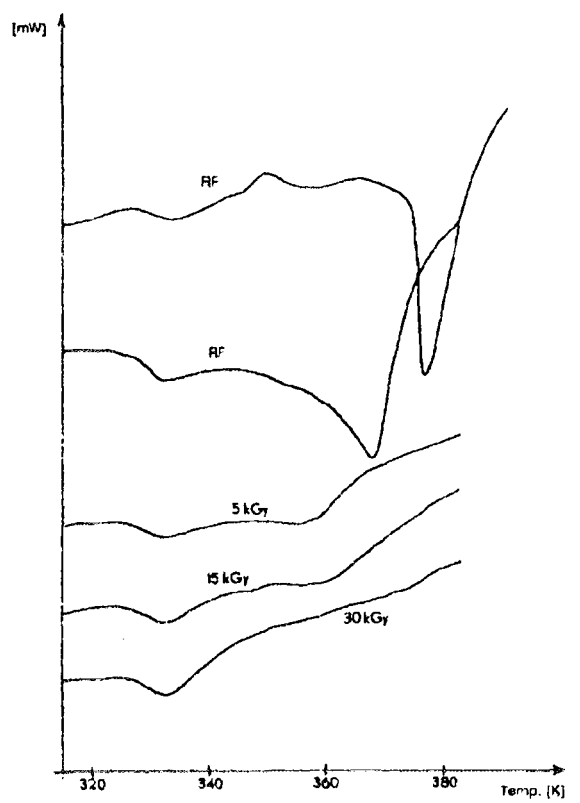

Fig.2. The DSC curves recorded with a heating rate of 2°/min for rye flour (RF) and the products irradiated at 5, 15, 30 kGy applying a dose rate of 1.7 kGy/h.

For better observation of the differences among irradiated and nonirradiated samples the irradiation doses applied in this preliminary stage of studies were considerably higher than permitted for food preservation. Such high doses can be used only for some very special kind of foodstuffs (i.e., hospital diet for immuno-compromised patients) [3].

Potato flour, two portions of wheat flour and two portions of rye flours were irradiated at 30, 15, 5, 2.5, 1 kGy, applying a dose rate of 1.7 kGy/h, and at 10, 5, 2.5, 1 kGy applying a dose rate of 5.5 kGy/h. Beef meat (grinded meat and pieces of meat) was irradiated at 24 and 12 kGy, applying a dose rate of 1.7 kGy/h. Potato starch was irradiated at 20 kGy, applying a dose rate of 1.6 kGy/h.

Viscosity measurements were performed during heating from 298 K with a rate 1.5°/min. The DSC measurements were carried out for samples kept in tightly screwed steel vessels in the temperature range up to 383 K with heating rate of 5 and 2°/min applying a Unipan 605 calorimeter with a Unipan 607 cooling system.

Significant differences were observed between η_{max} of the nonirradiated rye and wheat flours, and the irradiated products. The differences were observed when the dose 1 kGy was applied. (Fig.1). Differences were observed also in the DSC curves recorded at a heating rate of 2°/min for the nonirradiated and gamma irradiated potato starch, rye flour (30, 15, 10, 5 kGy) (Fig.2) and wheat flours (30 kGy). In the case of the nonirradiated starch, two endothermal effects have been found in the range 335.6-376.2 K with maxima at 342.8 and 360.8 K while in DSC curves of the irradiated sample the single endothermal effect was observed in the range 328.6-368.4 K with a single maximum at 337.6 K. No differences were observed in DSC curves obtained for the initial and irradiated samples of commercial potato flour.

2-3 endothermal effects were recorded on DSC curves of beef meat, probably brought about by proteins denaturation. Both effects decrease in the irradiated products, as compared with those of reference samples, stored in the same conditions. The results may be ascribed to a decrease of denaturation effects of proteins due to gamma irradiation.

The work was sponsored by KBN grant 5 S307 0511 03.

References

[1]. Application of Calorimetry and Thermal Analysis to Food Systems and Processes. Thermochimica Acta, special issue, 243, 2 (1994).

[2]. Analytical detection methods for irradiated foods; a review of current literature. Joint FAO/IAEA Division of Nuclear Techniques in Food Agriculture, IAEA, 1991. IAEA-TECDOC-587,

[3]. Review of data on high dose (10-70 kGy) irradiation of food. International Consultative Group on Food Irradiation, Karlsruhe, Germany, 29 August - 2 September 1994. WHO/FNU/FOS/95.10.

OXIDATION OF SO_2 BY SIMULTANEOUS APPLICATION OF ELECTRON BEAM AND ELECTRICAL FIELD IN HUMID AIR

H. Nichipor[1/], E. Radouk[1/], A.G. Chmielewski, Z. Zimek

[1/]Institute of Radiation Physical and Chemical Problems, Academy of Sciences, Republic of Belarus

It is well known that the SO_2 and NO_x removal from combustion flue gases by electron beam is performed with relatively high energy losses. 8-15 eV is needed to remove one molecule of SO_2 according to the literature data [1]. That is the reason why intense studies are performed to investigate more efficient processes of SO_2 oxidation at atmospheric pressure. It was found previously that the process efficiency can be significantly increased by the presence of water droplets and the application of an optimal electron beam current density [2].

Energy cost of oxidation can be also decreased by a simultaneous electron beam and microwave energy (electrical field) application. Electron dissociative attachment takes place with a high efficiency under such conditions. To investigate the kinetics of SO_2 oxidation in humid air under the influence of electron beam and electrical field a model study was undertaken. Within this model computer calculations have been made with a set of reactions important for gas phase with beam current density (0.032 mA/cm^2), different humidity and electrical field intensity level E/n=10^{-15} [Vcm^2]. The literature data were used to establish the rate constants of the processes and their dependence on electrical field intensity.

The influence of the external electrical field can be expressed by the rate constants of different processes. The chemical model includes 46 different species and 160 reactions and is based on the results obtained by Matzing [3], Busi et al. [4], Person et al. [5]. The reactions were established on the basis of radiolysis process of humid air containing SO_2. The SO_2 decomposition takes place under two chain reactions, which were initiated by electric field due to the following reaction cycle:

$$O_2 + e^- \rightarrow O^- + O \quad (1)$$

which leads to

$$O^- + O_2 + M \rightarrow O_3^- + M \quad (2)$$

$$SO_2 + O_3^- \rightarrow SO_3^- + O_2 \quad (3)$$

$$SO_3^- + H_2O \rightarrow H_2SO_4 + e^-. \quad (4)$$

The rate of chain process depends on the rate of O_3^- formation which is significantly higher when electron beam and electrical field are used simultaneously.

The second reaction chain is based on OH. The main channels of the OH formation are as follows:

$$e^- + H_2O \rightarrow H + OH + e^- \quad (5)$$

$$O^{*1}D + H_2O \rightarrow 2OH \quad (6)$$

$$O + HO_2 \rightarrow OH + O_2 \quad (7)$$

and decomposition:

$$SO_2 + OH \rightarrow HSO_3 \quad (8)$$

$$OH + HO_2 \rightarrow H_2O + O_2. \quad (9)$$

The following processes are leading to the formation of SO_3 and HO_2 which, according to reaction (7) takes back the OH radicals to the process:

$$HSO_3 + O_2 \rightarrow HSO_5 \quad (10)$$

$$HSO_3 + O_2 \rightarrow SO_3 + HO_2 \quad (11)$$

$$HSO_5 + SO_2 \rightarrow SO_3 + HSO_4 \quad (12)$$

$$SO_3 + H_2O \rightarrow H_2SO_4. \quad (13)$$

The electric field influence is expressed by the growing concentration of electrons leading to the oxygen and hydrogen atoms formation. The presence of oxygen atoms stimulate the growth of OH radicals concentration as shown by formula (7). The hydrogen atoms form HO_2 molecules according to the formula:

$$H + O_2 \rightarrow HO_2. \quad (14)$$

equal for an air humidity of 2%. The chain reactions based on the OH radicals is more effective for a higher air humidity. Energy losses of SO_2 molecule oxidation were calculated using the formula:

$$\varepsilon = \frac{[\delta + E_e n_e/\tau]}{\Delta SO_2} t \quad (15)$$

where: E_e - energy of electrons excited by electric field [eV], τ - life time of SO_3^- ions [$\tau = 1/k_5(H_2O)$], n_e - electron concentration, d - dose rate coefficient, ΔSO_2 - concentration change in time t, t - time of electron beam and electric field exposure.

The influence of water content on the energy losses is given in Table.

The rate of SO_2 oxidation initiated by the chain of reactions decreases for time $t > 10^{-4}$ s. This is due to an increase of NO_2 concentration in the air and the increasing contribution of the following processes:

$$O_3^- + NO_2 \rightarrow O_3 + NO_2^- \quad (16)$$

$$O_3^- + NO_2 \rightarrow NO_3^- + O_2. \quad (17)$$

The results of calculation showed that the SO_2 oxidation in the irradiated humid air can be intensified by the electrical field ($E/n = 10^{-15}$) applica-

Table. The influence of water content on the energy losses.

H_2O [%]	j [mA/cm^2]	n_e [1/cm^3]	δ [eV/cm^{3}s]	ΔSO_2* [molec./cm^3]	τ [s]	ε [eV/molec.]
2	0.032	10^{11}	5×10^{17}	2.44×10^{16}	10^{-7}	0.16
4	0.032	1.9×10^{11}	5×10^{17}	2.44×10^{16}	5×10^{-8}	0.57

* $t = 10^{-3}$ s.

Set of the processes was minimized to limit the calculation time. The most important reactions were taken into account to observe the investigated processes. The transient reactions were omitted. For example the process $N^+ \rightarrow N_4^+ \rightarrow O_2^+$ was written like $N_2^+ \rightarrow O_2^+$ and the primary reaction product was O_2^+ instead of N_2^+ and N_4^+. The ion recombination processes were listed according to the similar processes described by Matzing [3]. A set of programs KINETIC was applied for the complex analysis of chemical systems and kinetic study. An IBM EEC-1061 computer was used.

The simultaneous application of electron beam and electric field stimulates the effective growth of electron concentration in $t > 10^{-6}$ s which leads to the active species formation (O, HO_2, OH, SO_3^-) and SO_2 oxidation and its conversion into H_2SO_4. The influence of chain reactions (1-4) and (5-13) is

tion due to the chain reactions taking place in such conditions. The main portion of energy losses is due to the electrical field presence.

References

[1]. Tokunaga O., Suzuki N.: Radiation chemical reactions in NO_x and SO2 removal from flue gas. Radiat. Phys. Chem., 24, 145-165 (1984).

[2]. Baranchicov E.I. et al.: Investigation of SO_2 oxidation in humid air stream by high current density pulsed electron beam. Non-Thermal Plasma Techniques for Pollution Control NATO ASI Series, G34, Part B. 1993, pp. 71-76.

[3]. Matzing H.: Chemical kinetics of flue gas cleaning by electron beam. 1989. KfK Report 4494.

[4]. Busi F., D'Agelantonio M., Mulazzani Q.G., Raffaelli V., Tubertini O.: A kinetic model for radiation treatment of combustion gases. Sci. Total Environ., 64, 231 (1987).

[5]. Person J.C., Ham D.O.: Removal of SO_2 and NO_x from stack gases by electron beam irradiation. Radiat. Phys. Them., 31, 1 (1988).

RELATIVE DOSIMETERS FOR HIGH-LET RADIATIONS

Z. Stuglik

In the ion-beam radiation experiments the absolute methods of dosimetry are commonly used. They are laborious and require very precise instruments for both energy and fluence measurements. Very accurate values of the ranges and ion beam stopping power data are necessary for dose calculations. They are hardly attainable, especially for heavy projectiles which penetrate the composite, low-Z materials.

The relative dosimeters are much easier to operate but their using in the high-LET region encounters some difficulties arising from the energy-dependence of the G-values and from the post-effects, as well. Nevertheless, it seems to be

possible to find some chemical systems appropriate for high-LET dosimetry.

Dosimetric responses of three chemical systems: Fricke solution, L-α-alanine and ethanol solution of nitrile of malachite green on high-LET radiations were studied. The ion-beam irradiations were performed at the Flerov Laboratory of Nuclear Reactions, Joint Institute for Nuclear Research, Dubna using a 4-meter U-400 cyclotron. ESR-spectroscopy and UV/VIS spectrophotometry were used for the analytical control of irradiated samples. Both methods have an nondestructive character.

Results and conclusions

Fricke dosimeter:

- 0.01 M Fricke solution can be used as a secondary dosimeter for high-LET radiations provided that the $G(Fe^{3+})$-value (depending on ion type and its energy) is known from earlier experiments. For LET as high as some keV/nm $G(Fe^{3+})$-value is practically independent of LET and $\cong 3$.
- Dosimetric solutions should be stirred in time of irradiation. In the opposite case a decrease of ferrous ion oxidation is observed. Its amplitude depends on experimental conditions.
- Dosimetric solution should be very pure. Any contamination with organic compounds increases the ferrous ion oxidation yield in a similar way as in the case of low-LET radiations.
- Fricke dosimeter can be used for high fluences (higher than 10^{10} particles/cm^2).

Alanine dosimeter:

- Decrease of the sensitivity of the alanine dosimeter in high-LET area, corresponding to γ-rays, is similar to that observed for the Fricke dosimeter (about fivefold, going from γ radiation to 3.4 MeV/amu Co ions).
- The alanine could be successfully used for ion beam dosimetry but only for the fluences lower than 10^{10} particles/cm^2. For the higher ones the latent tracks overlap and saturation effects on the dose-response curve are observed.

Malachite green liquid dosimeter:

- G-value of the malachite green cation is low and concentration dependent. Both factors promoted to use the malachite green dosimeter for high dose measurement.
- Dosimetric solutions can be used without stirring (at least up to fluences of 10^{11} particles/cm^2).
- Solutions should be protected from ultraviolet (sunlight, luminescent lamps). Light from the common tungsten lamps is permissible.
- Decrease of the sensitivity of the malachite green dosimeter with LET is higher than that for Fricke and alanine dosimeters.

The work was partially supported by the State Committee for Scientific Research, Poland, under contract no. 2 2446 91 02.

A COMPARISON OF THREE MATERIALS USED FOR ESR DOSIMETRY

Z. Stuglik, J. Sadło

Any non-absolute (relative, secondary) method of radiation dosimetry grounds on a correlation between the dose and radiation effect generated in a dosimetric material. One of such effects is the creation of stable paramagnetic centers, whose nature and concentration can be analyzed by the electron spin resonance (ESR) method.

The most widely used dosimetric material for ESR dosimetry is a simple aminoacid α-alanine [1, 2]. The cheapest, racemat form of this compound is commonly used for technological purposes [3] and the chiral L-form - for transfer dosimetry and in science and medicine [4-6].

Paramagnetic signal observed in irradiated α-alanine is ascribed to the radicals CH_3-CH^*COO^- originated from the alanine after the crack of the weakest bond between the asymmetric carbon and the NH_3^+ group.

A standard bone powder was suggested as dosimetric material by Stachowicz et al. [7]. It can be used in deproteinized and non-deproteinized form. Only stable paramagnetic centers, localized in inorganic constituents of bone are useful for dosimetry. Unstable paramagnetic centers localized in organic part of non-deproteinized bone give some parasitic signals. Fortunately, they disappear completely within 7 days after irradiation and from that time also the non-deproteinized bone powder samples can be used for dose determination.

The nature of stable paramagnetic species observed in the irradiated bone is still a matter of controversy. Most probably there are few centers with the most abundant CO_2^- group occupied slightly modified phosphate sites in the hydroxyapatite lattice [8].

The aim of the work was a comparison of the sensitivity of three ESR-dosimeters: L-α-alanine, DL-α-alanine and non-deproteinized standard bone powder on ^{60}Co gamma radiation.

The sensitivity of ESR dosimeters depends on two factors:

- G-value of the paramagnetic centers created in the dosimetric material at time of irradiation,
- type of the ESR parameter which is chosen for radiation effect measurement.

Two parameters have been used to the construction of dose-response curves in ESR dosimetry:

- amplitude of ESR signal (peak-to-peak method),
- double integral.

The amplitude of the ESR signal is more frequently used, mainly because of easier measurement and lower requirements according to the class of ESR spectrometer. It is also less sensitive to the errors connected with the overlap of parasitic signals.

PL9700808

The double integral has more clear physical sense and allows to calculate the radiation yield (G-value) of paramagnetic centers if energy imparted to the sample is known from elsewhere. It is also less sensitive on some changes of the form of ESR signal (for instance line-broadening at the high dose region).

Both types of ESR parameters were mesured and analyzed for the investigated materials irradiated in ^{60}Co gamma source (ISSLIEDOVATIEL, the total dose being 0,76 kGy).

We stated that:

- Radiation yield of the radicals generated in α-alanines is the same for both L-(chiral) and DL-(racemat) forms.
- The sensitivities of the L- and DL- forms of α-alanine are the same when double integrals are used as an analytical signal but somewhat different if the amplitude of the first derivative of the ESR signal is used.
- There is confirmation that the G-value of the paramagnetic centres generated in the standard bone powder, irradiated with gamma rays, is about 50 times lower than the G-value of the paramagnetic centres in alanine.
- For all the investigated materials, but especially for the bone powder, the amplitude of the ESR signal seems to be more convenient parameter for the construction of dose-response curves than the double integral.

Table. The comparison of investigated materials from the dosimetric point of view

Material	Advantages	Disadvantages
L-α-alanine	⇒ chemical compound ⇒ stable paramagnetic centers ⇒ a little more sensitive than DL-form	⇒ low saturation level of microwave power ⇒ wide ESR signal ⇒ ~5 times more expensive than DL-form
DL-α-alanine	⇒ chemical compound ⇒ stable paramagnetic centers ⇒ cheaper than L-α-alanine	⇒ low saturation level of microwave power ⇒ wide ESR signal ⇒ a little less sensitive than L-form
Standard bone powder (non-deproteinized)	⇒ very stable paramagnetic centers ⇒ narrow ESR signal ⇒ high saturation level of microwave power	⇒ biological product ⇒ unattainable commercially ⇒ can be used as dosimeter only after decay of organic radicals

Comparison of the investigated materials from the dosimetric point of view is presented in Table.

References

[1]. Bradshaw W.W., Cadena Jr. D.B., Crawford G.W., Spetzler H.A.W.: Radiat. Res., **17**, 11-21 (1962).

[2]. Regula D.F., Defner U.: Int. J. Appl. Radiat. Isot., **33**, 1101-1114 (1982).

[3]. Kojima T., Haruyama Y., Tachibana H., Tanaka R., Okamoto J., Yagi K., Tamura N., Hara H., Kashiwazaki S.: Radiat. Phys. Chem., **42**, 757-760 (1993).

[4]. Olsen K.J., Hansen J.W., Waligórski M.P.R. Appl. Radiat. Isot., **40**, 985-987 (1989).

[5]. Regulla D., Bartolotta A., Deffner U., Onori S., Pantaloni M., Wieser A.: Appl. Radiat. Isot., **44**, 23-31 (1993).

[6]. Gobbi G., Beneventi S., Leogrande M.P., Raymondi C., Ricci S., Salvadori P., Onori S., Bartolotta A.: Phys. Med., **8**, 79-83 (1992).

[7]. Stachowicz W., Michalik J., Dziedzic-Gocławska A., Ostrowski K.: Nukleonika, **17**, 426- 431 (1972).

[8]. Vugman N.V., Rossi A.M., Rigby S.E.J.: Appl. Radiat. Isot., **46**, 311-315, (1995).

RADIATION FACILITY AT JINR U-400 CYCLOTRON CHECKED BY FRICKE DOSIMETER MEASUREMENTS

Z. Stuglik

Ion beam radiation experiments with liquids, in spite of their scientific importance, have been done rather seldom mainly because of experimental difficulties and limited access to appropriate accelerator facilities.

Some years ago one of the twelve beam lines of the 4-metre U-400 heavy ion cyclotron at Dubna was dedicated to radiochemical and radiation research (KHIPTI facility). The latter consists of two parts, dedicated to radiochemical or radiation research. Unlike most other radiation facilities, this one has been performing at a vertical ion-beam pipe which allows to irradiate liquid and powder samples in open vessels [1-3]. Above all it gives the possibility to investigate high-LET radiation processes running in thin layers of liquids exposed to the air [4].

It is well known that the ion-beam radiation experiments are not only more difficult than the low-LET ones, but also more susceptible to systematic errors. Having this in mind we decided to test our facility and techniques by repeating some experiments reported in the literature and comparing the results. Quite a few experimental data are available for acidic 0.01 M ferrous sulphate aqueous solutions saturated with air or O_2 and irradiated with ^{12}C ion beams [5-9]; this is why we chose this system for study.

Acidic, aqueous ferrous sulphate solution (Fricke dosimeter) was bombarded with the 10 MeV/amu carbon-12 ions. Dose and energy dependence of the integral yield of Fe^{3+} formation was measured and compared with the data from three other laboratories.

It was calculated using the formula:

$$G_E(Fe^{3+}) = \frac{OD_{304} \cdot v \cdot N_A \cdot 100 \cdot e^- \cdot \Delta E_{21}}{Q \cdot E_s \cdot w_{air} \cdot \varepsilon_{304}}$$

where: v is the volume of irradiated solution, N_A - the Avogadro number, e^- - the charge unit, ΔE_{2l} - the energy deposited by ^{12}C ion in the two air gaps between the electrodes of ionizing chamber, Q - the total charge collected by the electrometer during irradiation of the sample, w_{air} - the differential energy of ion pair formation in the air irradiated by 10 MeV/amu ^{12}C ion beams and ε_{304} - the molar absorption coefficient of Fe^{3+} ion at 304 nm.

The results are presented in Fig. The experimental points follow a smooth line which can be interpreted as a satisfactory result of the test.

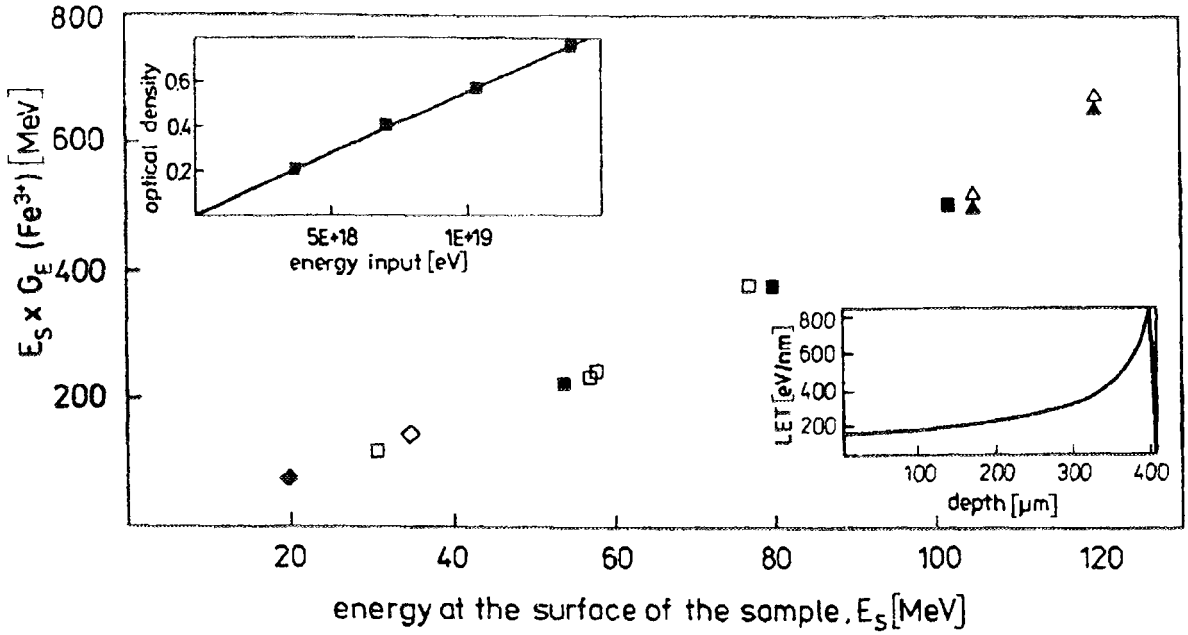

Fig. Energy dependence of $E_S * G_E(Fe^{3+})$-value for Fricke solutions irradiated with carbon ions. (■) [5], (□) [6], (◆) [8], (◇) [9], (▲) this work, w_{air}=36.1 eV; (Δ) this work, w_{air}=35 eV. Upper insert: optical density at 304 nm vs. energy input. Lower insert: LET-depth dependence for ^{12}C ion beams with initial energy of 120 MeV penetrating the Fricke solution.

Conclusions

On the basis of the results for Fricke solutions we have found that the facility functions correctly. We are aware of the difficulties and uncertainties that will increase with atomic mass of the projectiles. But it is a general problem, not only with this particular installation. More accurate stopping power data for heavy projectiles, and more numerous and accurate data of differential w-values for heavy ions in the air are needed.

The work was supported by the State Committee for Scientific Research, Poland, under contract 2 2446 91 02.

References

[1] Stuglik Z., Zvara I., Yakushev A.B., Timokhin S.N.: Radiat. Phys. Chem., **43**, 463-469 (1994).

[2] Stuglik Z., Michalik J., Stachowicz W., Ostrowski K., Zvara I., Dziedzic-Gocławska A.: Appl. Radiat. Isot., **45**, 1181-1187 (1994).

[3] Stuglik Z., Sadło J.: Radiat. Meas. (formerly Nucl. Tracks and Radiat. Meas.), **25**, 95-98 (1995).

[4] Stuglik Z.. Radiat. Res., **143**, 343-348 (1995).

[5] Schuler R.H.: J. Phys. Chem., **71**, 3712-3713 (1967).

[6] Imamura M., Matsui M., Karasawa T.: Bull. Chem. Soc. Japan, **43**, 2745-2749 (1970).

[7] Jayko M.E., Tung T.-L., Welch G.P., Garrison W.M.: Biochem. Biophys. Res. Commun., 68, 307 (1976).

[8] LaVerne J.A, Schuler R.H.: J. Phys. Chem., **87**, 4564-4049 (1983).

[9] LaVerne J.A., Schuler R.H.: J. Phys. Chem., **91**, 5770-5776 (1987).

TEMPERATURE AND DOSE RATE EFFECTS IN As IMPLANTED $GaAs_{1-x}P_x$

J. Krynicki, S. Warchoł, H. Rzewuski, R. Groetzschel[1/]

[1/]FZR Forschungszentrum Rossendorf/Dresden, Germany

The influence of temperature on damage formation in ion implanted semiconductors has been investigated intensively, mostly in Si and A_{III} B_V binary compounds such as GaAs and GaP but only very few papers have been devoted to the ternary $A_{III}B_V$ alloys. The influence of dose-rate on ion damage buildup has been observed [1] in GaAs (Si and Sn) at RT but not at LNT.

In the last paper [2] we presented results on ion damage accumulation in As implanted $GaAs_{1-x}P_x$ ternary compounds at 120 K.

In this paper we report the preliminary results on dose-rate effects in $GaAs_{1-x}P_x$ for various P compositions (x=0, 0.15, 0.39, 0.65 and 1) implanted with 150 keV As ions at 120 K and the results obtained for samples implanted at RT.

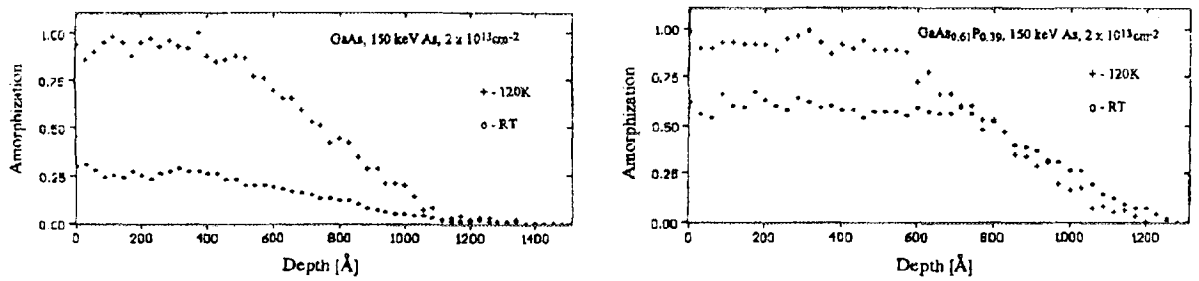

Fig.1. Amorphization (residual defects) vs. depth in binary (GaAs) and ternary (GaAsP) crystals implanted with As ions at 120 K and RT.

The postimplantation residual damage was measured using a RBS channeling technique of 2 MeV He^+ ions.

Residual defects measured for ternary crystals after implantation at 120 K and at room temperature show smaller but similar differences (Fig.1), age accumulation for lower dose rate at 120 K (Fig.2).

The results obtained indicate that the defects created during implantation in $GaAs_{1-x}P_x$ crystals have a higher temperature stability than those created in GaP and GaAs binary crystals.

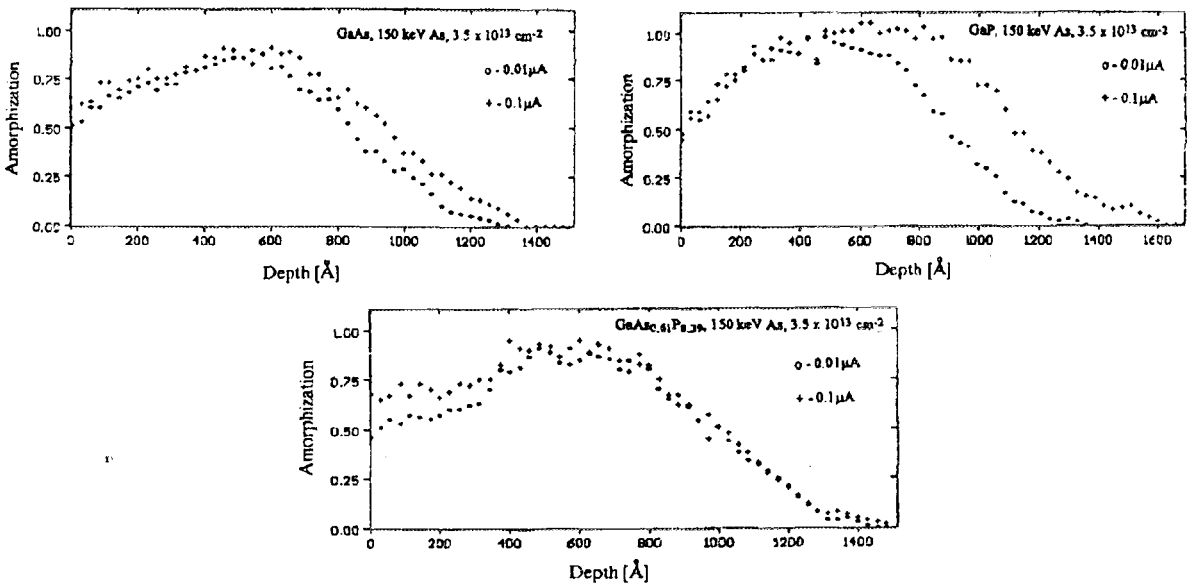

Fig.2. Amorphization (residual defects) vs. depth in binary (GaAs, GaP) and ternary (GaAsP) crystals implanted with As ions for two dose-rates at 120 K.

compared to the results obtained for GaAs under the same experimental conditions.

Residual defects in the binary (GaAs, GaP) and ternary ($GaAs_{1-x}P_x$) crystals after As implantation for both ion beam intensities (dose rate) show very similar damage profiles.

It is worth noting that for ternary crystals deeper parts of a damage profile show higher damage accumulation for lower dose rate at 120 K (Fig.2).

Further work is being carried out.

References

[1]. Haynes T.E., Holland O.W.: Nucl. Instr. and Meth., B59/60, 1028 (1991).

[2]. Krynicki J., Warchoł S., Rzewuski H., Groetzschel R.: Acta Phys. Pol., A87, 249 (1995).

RADIOCHEMISTRY

STABLE ISOTOPES

NUCLEAR ANALYTICAL METHODS

CHEMISTRY IN GENERAL

PL9700811

SOLUTION CHEMISTRY OF ELEMENT 104: SOLVENT EXTRACTION INTO TRIISOOCTYLAMINE FROM HYDROFLUORIC ACID SOLUTIONS

A. Bilewicz, C.D. Kacher[1/], D.C. Hoffman[1/]

[1/]Nuclear Science Division, Lawrence Berkeley Laboratory, USA

PL9700810

Studies performed recently on the aqueous chemistry of element 104 have provided suprising results. Differences in the adsorption of tetravalent metal ions on thin layers of cobalt ferrocyanides show that the hydrolysis tendency in the Group 4 decreases in the order Ti>104>Zr>Hf [1]. The unexpectedly strong hydrolysis of element 104, much stronger than that for Hf and Zr, has been interpreted as resulting from the relativistic effect. Due to relativistic stabilization of $7s_{1/2}$ orbitals and high expansion of $d_{5/2}$ orbitals the sp^3d^4 hybridization characteristic for coordination number (CN) 8, is unrealizable. The maximum coordination number for 104^{4+} in aqueous solution is 6 like for Ti^{4+}, while CN 8 is characteristic for Zr^{4+} and Hf^{4+}. Unexpectedly strong hydrolysis of element 104 indicates that in aqueous solution 104 is more similar to the lightest element in the Group, Ti, than for its heavier analogues, Zr and Hf.

A similar behaviour of element 104 has been found in experiments on its solvent extraction into tributylphosphate from HCl and HBr solutions [2]. In both cases the following order of extraction was observed $Zr^{4+} \approx Hf^{4+} > 104^{4+} \approx Ti^{4+}$ with increasing HCl/HBr concentration. In this case element 104 is similar rather to Ti than to Zr and Hf. The TBP extraction behaviour of the Group 4 cations results from their different tendency to hydrolysis.

To verify the idea that the coordination number of element 104 could be influenced by relativistic effects, studies on liquid-liquid extraction of fluoride complexes into triisooctylamine were performed. In hydrofluoric acid solution of concentration higher than 10^{-1} M the Group 4 cations Ti^{4+}, Zr^{4+}, Hf^{4+} form coordinatively saturated complexes of CN=6 (MF_6^{2-}) [3]. Under these conditions also the Group 14 metal cations form similar complexes SnF_6^{2-} and PbF_6^{2-} [4].

Because the interaction between the metal complexes and the amine is only electrostatic if 104^{4+} forms fluoride complexes with the same coordination number as Ti^{4+}, Zr^{4+} and Hf^{4+} (same charge of the complex anions) the extraction should be similar and should depend only on the radii of the fluoride complexes. The solvent extraction in TIOA-HF system should be convenient to study the behaviour of Group 4 cations in complexation system where all cations form complexes of the same coordination number.

The chemical properties of element 104 and its Group 4 congeners were studied by solvent extraction into 0.25 M triisooctylamine in o,m,p-xylene from hydrofluoric acid of various concentrations. The studies showed that the extraction trend for the Group 4 elements in this extraction system decreases in the order Ti>Zr≈Hf>104, in the order to inverse from the trend observed in ionic radii 104>Zr≈Hf>Ti. This order is different than that in hydrolysis, TPB-HCl and TBP-HBr extraction systems where element 104 due to the decreasing coordination number is more similar to Ti than to Zr and Hf.

References

[1]. Bilewicz, A., Kacher C.D., Siekierski S., Hoffman D.C.: Radiochimica Acta (in press).

[2]. Kacher C.D., Bilewicz A., Gregorich K.E., Hoffman D.C.: Radiochimica Acta (in press).

[3]. Wilkinson G.: Comprehensive Coordination Chemistry. Vol.3. Pergamon Press, Oxford 1987, pp.363-441.

[4]. ibid, p.200.

A CHEMICAL STUDIES OF THE ^{24}Ne CLUSTER DECAY OF ^{232}Th

Ch. Neskovic[1/], R. Delmas[1/], M. Hussonnois[2/], A. Bilewicz, B. Bartoś

[1/]Laboratoire Pierre Sue C.E.N. Saclay, France

[2/]Institut de phisique Nucleaire, Orsay, France

Spontaneous emission of neon nuclei from ^{232}Th has been already theoretically predicted [1]. Calculations show that due to the β decay of ^{24}Ne 10 kg of thorium may contain, at equilibrium, about 1000 atoms of ^{24}Na. We have devised a separation scheme of micro-amounts of sodium from large quantities of thorium and its decay products (Fig.). The separation time must be shorter than the half-life of ^{24}Na. At this stage, the experiments were made at a small scale: with only 10 g of thorium and a ^{22}Na tracer. Thorium was loaded on a column with DOWEX 50WX12 resin and about 10^6 atoms of ^{22}Na was added on the top of the column. ^{22}Na was eluted by 0.5M HNO_3 without any sodium carrier. The effluent from the DOWEX column was passed through two ion-exchange columns in the series. The first one was filled with cryptomelane-type hydrous manganese dioxide, which allows to efficiently remove the decay products of ^{232}Th, such as ^{224}Ra and ^{212}Pb. The second column was packed with crystalline hydrated antimony pentoxide, HAP, partly in sodium form, which sorbed selectively the ^{22}Na. Column containing only 0.2 g of HAP is required for 10 g of

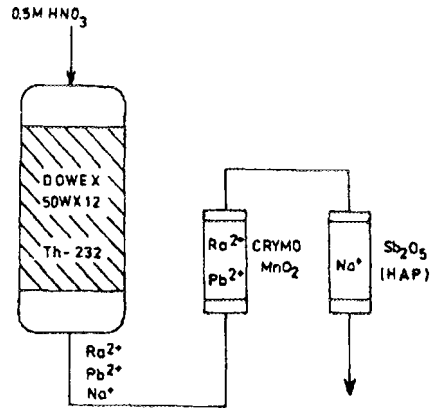

Fig. The diagram of system for the studies of isolation ^{24}Na from ^{232}Th.

thorium in order to measure γ-emission of ^{22}Na in a solid sample of a minimum volume. The separation time was 5 h, i.e. one third of ^{24}Na half-life. The yield of sodium was always greater than 95%. The decontamination factors were greater than 10^6 for thorium and 10^5 for its decay products (^{228}Ac, ^{224}Ra, ^{212}Pb, ^{212}Bi).

References

[1]. Price C.B., Moody K.J., Bonetti R., Guiglielmetti A., Chisa C., Matheoud R., Migliorino C.: Chem. Rev., C.46, 5 (1992).

MATERIALS FOR IN-SITU MONITORING OF LIGHT WATER REACTOR (LWR) WATER CHEMISTRY BY OPTICAL METHODS

L. Fuks, S. Pikus[1/]

[1/]Institute of Chemistry, Maria Curie-Skłodowska University, Lublin, Poland

It has been already shown that diffuse reflectance spectroscopy (DRS) is one of the most powerful methods for monitoring of numerous chemical reactions important in material science and in chemical technology. It appeares to be especially effective for the *in-situ* investigation of the early stages of the process. As a result, the forementioned method, discovered in the 1930'ies, successively comes back in the last 25 years as the efficacious analytical and scientific instrument [1]. General theory and practice of the DRS method has been now well documented, e.g. by Frei and MacNeil [2].

Articles, produced even from the extremely resistant stainless steel, always slowly corrode. As a result a submicroscopic layer of iron oxides is generated on their surface. Spectroscopic studies of oxidation of a stainless steel under the boiling water reactor (BWR) conditions (i.e. in 290°C and 90 barr), carried out in the Paul Scherrer Institute (PSI, Villigen, Switzerland) have shown, that:

- in the spectral region 200-3000 nm iron oxide layer absorbs strongly both the incising and the reflected light. Because absorption seems to be more pronounced than surface reflection and

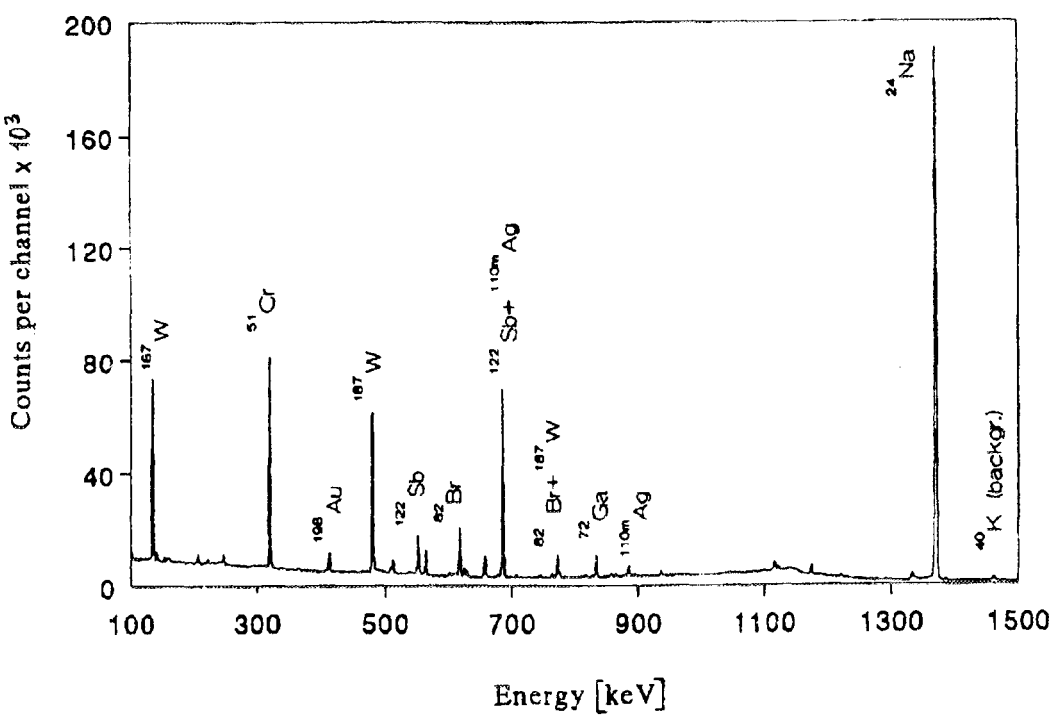

Fig.1. γ-ray spectrometry of the 65 mg sample of irradiated synthetic sapphire. Exposition time - 8 hrs, neutron flux - $6 \cdot 10^{13}$ n/(cm·sec), cooling time - 6 days, time of measurement - 66420 secs.

scattering, it should be counted as the main effect;
- aqueous solutions, containing particles of the corrosion products, exhibit strong light absorption in the spectral region of above 900 nm (i.e. the infrared light);
- because the absorption occures to be proportional to the thickness of oxide layer, when it is not too strong, DRS in the spectral region 200-900 nm can be efficaciously applied for monitoring the early stages of the corrosion process [3].

One of the most important problems for the realiable optical measurements is the proper choice of the material suitable for the production of optical windows exposed to the BWR conditions.

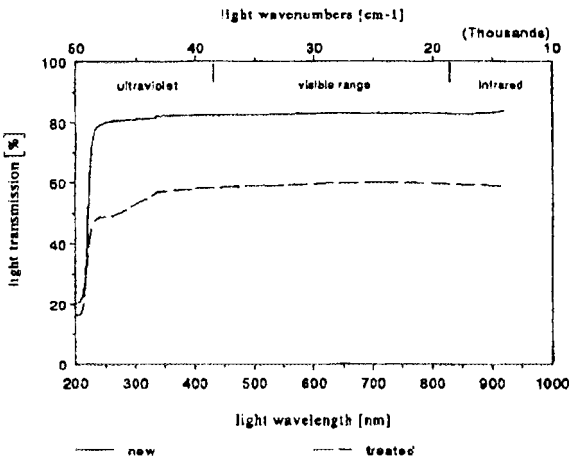

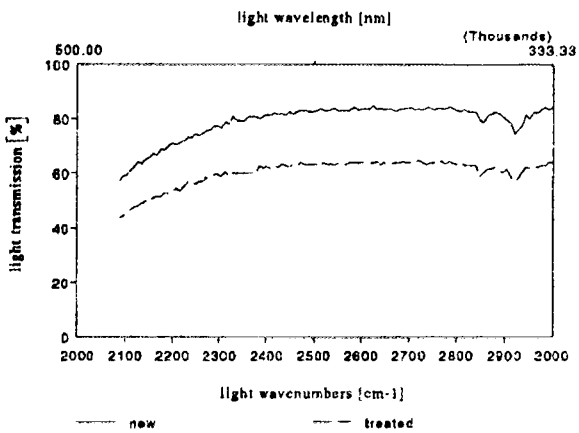

Fig.2. Transmission curves for synthetic sapphire window.

This problem at present is studied jointly in the Institute of Nuclear Chemistry and Technology (INCT, Warszawa, Poland) and in the forementioned Paul Scherrer Institute (PSI, Villigen, Switzerland) under the IAEA Research Contract 8426/RB "Materials for in-situ Monitoring of Light Water Reactor (LWR) Water Chemistry by Optical Methods".

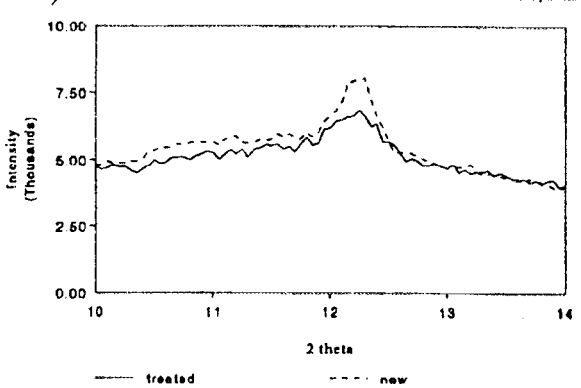

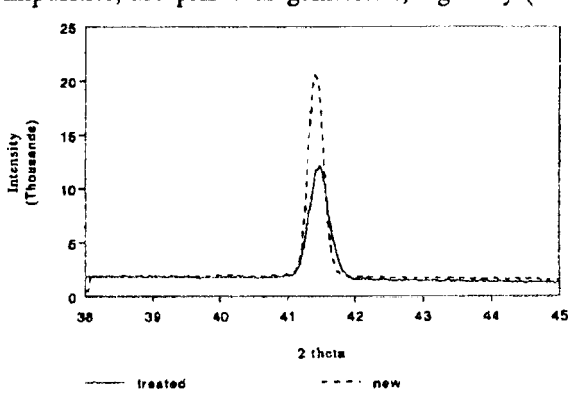

Fig.3. X-ray diffraction data for the single-crystal synthetic sapphire.

Results

Preceding experiments on the thermal stability of the potential window material, performed in the PSI, have been made using various kinds of aluminium oxide. Naturally, Al_2O_3 occurs as the mineral corundum (α-Al_2O_3; specific gravity - 3.98 g cm^{-3}) and as emery (a granular form of corundum contaminated with iron oxide and silica). At present, pure α-Al_2O_3 single-crystals are produced industrially mainly by igniting of $Al(OH)_3$ or AlO(OH) at high temperatures (~1200°C). They show rhombohedral or hexagonal crystal structures. Because of its great hardness (Mohs 9°), high melting point (2045°C), involality (10^{-6} atm at 1950°C), high specific heat and thermal conductivity (0.18 cal/g°C in 25°C, i.e. about 750 J/kg·K, and $600 \cdot 10^{-4}$ cal/(cm·sec·°C) parallel to c-axis in 260°C, respectively), low linear coefficient of thermal expansion (6.7·10-6 units/°C, parallel to c-axis, for 50°C), high chemical inertness and good electrical insulating properties [4], α-Al_2O_3 finds many applications as refractories, ceramics and abrasives (including toothpaste), in addition to its major use in the electrolytic production of Al metal. As a result of mass production, it is now relatively cheep. Larger crystals, when colored with metal-ion impurities, are prized as gemstones, e.g. ruby (Cr^{III} red), sapphire ($Fe^{II/III}$, Ti^{IV} blue), oriental emerald (?Cr^{III}/V^{III} green), oriental amethyst (Cr^{III}/Ti^{IV} violet), and oriental topaz (Fe^{III}, yellow).

Results of the detailed investigations of the synthetic sapphire window material, carried out in the INCT and in the Maria Curie-Skłodowska University, can be summarized as follows:
- Quantitative analysis of the chemical composition of the material, performed using the neutron activation analysis (NAA) has shown, that

apart of the aluminium matrix, Ag, Ga, Sb, Zn, Au, Cr, Mo, W, Ta, Na and Br can be detected as the tracers (Fig.1).

- In the spectral region 300-900 nm optical transmittance of the 5 mm layer of the synthetic sapphire remains essentially constant. The unused window material shows the transmittance on the level of 80%. Transmittance of the window hydrothermally treated in the autoclave for about 500 hrs decreases to the level of 65% (Fig.2).
- Crystalline structure, determined using X-ray diffraction, remains unchanged in the course of treatment in autoclave. However, upon the action of the BWR conditions, degree of the crystalline structure only in the surface layer decreases significantly (Fig.3).

References

[1]. Kortüm G.: Reflectance Spectroscopy. Springer Verlag, Berlin 1969.
[2]. Frei R.W., MacNeil J.D.: Diffuse Reflectance Spectroscopy in Environmental Problem Solving. CRC Press, Cleveland 1973.
[3]. Degueldre C., Dran J.C., Schenker E.: J. Nucl. Mater., 188, 255 (1992).
[4]. Malitson I.H.: J. Opt. Soc. Amer., 52, 1577 (1962).

STATE-OF-THE-ART REVIEW ON FISSION PRODUCT AEROSOL POOL SCRUBBING UNDER SEVERE ACCIDENT CONDITIONS

M. Świderska-Kowalczyk, M. Escudero Berzal[1/], M. Marcos Crespo[1/], M. Martin Espigares[1/], J. López-Jiménez[1/]
[1/]Institute of Nuclear Technology CIEMAT, Madrid, Spain

Research work performed in the framework of the specific programme "Nuclear Fission Safety 1990-1994" of the European Atomic Energy Community. Reinforced concerted action on "Reactor Safety" - Project 6: Source term (fission product behaviour).

The State-of-the-Art described in this document consists of a survey of the current fission products and aerosol pool scrubbing in water reactors under severe accident conditions.

The first chapter summarizes the general characteristics of the LWR under severe accident conditions including possible pathways in submerged beds for fission product release during an accident. Vapour and aerosol parameters, together with the main physico-chemical phenomena influencing particle removing, are defined.

In the second chapter data have been gathered from the ten experimental programmes worldwide available on vapour and aerosol pool scrubbing: ACE, EPRI, EPSI, GE, JAERI, LACE-Espana, SPARTA, UKAEA (Aerosol-Iodine), and POSEIDON. This chapter ends with the presentation of the experimental results with conclusions, uncertainties, and areas of possible future attention. A certain lack of information in both subcooled and saturated conditions has been found.

The third chapter includes a detailed description and comparison of the hydrodynamic and thermo-hydraulic processes and removal mechanisms of the pool codes SPARC, BUSCA, and SUPRA. A complementary sensitivity study has been performed with the SPARC and BUSCA codes, which is presented in the fourth chapter. Their hydrodynamic models will be checked in future experimental programmes with special attention.

The fifth chapter presents parametric studies performed using SPARC and BUSCA. They confirmed variations of decontamination factor with the main parameters: particle size, fraction noncondensable, and others.

Finally, the chapter sixth offers a discussion of the main phenomena and parameters with influence on the decontamination factor, along with the uncertainties associated.

New experimental data are requested in order to cover lack of informations. For future experimental programmes, it is recommended to link plant studies and simulating sequences selected from among the most significant contributors.

SELECTION OF ELEMENTS FOR THE STUDIES OF "EVEN-ODD" EFFECT IN CHEMICAL ISOTOPE EXCHANGE REACTIONS

W. Dembiński

The classic theory makes it known that the isotope elementary effect in chemical exchange reactions is proportional to the mass difference, Δm, of the isotopes involved. This was confirmed [1] for ^{234}U, ^{236}U, and ^{238}U. However in the same experiment, fractionation of ^{234}U and ^{235}U appeared to be much smaller than the one between ^{235}U and ^{236}U, in spite of the mass difference in either isotopic pair. This anomaly was concluded to be due to the odd mass number of ^{235}U and was called the even-odd isotope effect. A similar non classic behaviour has been also reported for another odd mass number nuclides: ^{67}Zn [2], ^{87}Sr [3], $^{135,137}Ba$ [3] and ^{157}Gd [4].

No theoretical explanation of this phenomenon has been till now presented. It may be said that more experimental data are needed to offer a reasonable interpretation of the phenomenon. It is so

because the energy value of hyper fine interactions connected with isotope nuclear spin (I), nuclear magnetic moment (μ), as well as the electric quadrupole moment (Q) are assumed to be too small to change the orbital coupling at the molecular level, the more so because, the value of I, μ and Q varied strongly with atomic numbers Z and A. Having this in mind we have selected ytterbium from the rare earth region for the first step of our fractionation studies.

Ytterbium has five even mass number isotopes: 168, 170, 172, 174, 176 and two odd mass number isotopes: 171, 173. The latter are characterized by the different spin numbers ($I_{171}=1/2$; $I_{173}=5/2$) and the different sign of the nuclear magnetic moment expressed in nuclear magnetons ($\mu_{171}=+0.49188$; $\mu_{173}=-0.67755$). Such a composition is rather unique in the periodic system and after successfull chemical fractionation may offer more information on even-odd effect than for example barium with its two odd isotopes (133 and 135) characterized by the same spin number (3/2) and nearly the same value of the magnetic moment ($\mu_{133}=+0.83291$; $\mu_{135}=+0.93107$).

The chemical properties of ytterbium enabled studies of the isotope equilibrium in the ligand exchange reactions as well as in the electron exchange reactions. The latter offer a higher value of the unit separation factor, as it is known from the literature [5], and from our studies on isotope fractionation in the liquid-liquid extraction systems containing the red-ox couples: U(III/IV) [6], Ce(III)/Ce(IV) [7, 8], Eu(II/III) [9]. However the separation of the ytterbium isotopes in a similar system was expected to be difficult because of the very high value of the standard oxidation potential $E^0_{Yb(II)/Yb(III)}=+1.15$ V and the consecutive instability of Yb(II) ions in the solutions.

To overcome these difficulties two experimental procedures have been proposed and tested:

- Fractionation of the ytterbium isotopes at the oxidation state +3 in the liquid-liquid extraction systems by means of a 16-stages extractor of the mixer-settler type (stage volume 9 ml), using di-(2-ethylhexyl) phosphoric acid (HDEHP) as the extractant and chlorides, nitrates or sulphates as anions. It was found that the value of extraction distribution coefficient should amount to 1.4-1.5 to secure the break-through (0.05%) steady state conditions. The time necessary to attain the isotope equilibrium in the whole cascade was estimated to be 15 h. The number of the theoretical stages amounted to 10-12.
- Fractionation of the ytterbium isotopes at the oxidation stage +2 and +3 by means of multistage batch precipitation. The liquid Na-amalgam has been selected as reducer of Y(III) to Y(II) in aqueous or ethyl alcohol H_2O solution. The fairly stable solutions ($t_{1/2}=1$ h) of Y(II) have been obtained provided Y(II) was stabilized by means of a acetic acid-sodium acetate buffer, citric acid or eventually sodium tetra-phenyl-boron. Studies of effective separation of Y(II) by precipitation with sulphate ions are in progress.

References

[1]. Fujii Y., Nomura M., Okomoto M.: Z. Natuforsch., **44a**, 395 (1989).

[2]. Nishizawa K., Nakamura K.: Solvent Extr. Ion Exch., **11**(3), 389 (1993).

[3]. Nishizawa K., Nakamura K.: ibid., **12**(5), 1073 (1994).

[4]. Chen J., Nomura M.: J. Nucl. Sci. Technol., **29**(11), 42 (1992).

[5]. Kakihana H., Oi T.: Proc. Int. Symp. on Separation and Chemical Exchange Uranium Enrichment. 1992, p.18.

[6]. Dembiński W., Goroncek K.: J. Radioanal. Nucl. Chem., Letters, **124**, 141 (1989).

[7]. Dembiński W., Goroncek K., Phuc N.: J. Radioanal. Nucl. Chem., Articles, **149**(1), 169-176 (1991).

[8]. Dembiński W., Goroncek K.: J. Radioanal. Nucl. Chem., Letters, **175**, 437 (1993).

[9]. Dembiński W., Mioduski T.: ibid., **199**, 159 (1995).

IS THERE ANY INFLUENCE OF "MAGIC" NUCLEI ON CHEMICAL BEHAVIOUR?

T. Mioduski

Recently, it has been discovered [1] that $^{235}_{92}U$ with odd number of neutrons behaves as $^{234.5}U$ on the ion-exchange chromatographic column while ^{234}U, ^{236}U and ^{238}U strictly hold the Bigeleisen $\Delta M/M^2$ dependence. Moreover, this small even-odd irregularity makes the CHEMEX and Asahi/ACEP chemical uranium enrichment competitive with the physical methods based on the UF_6 diffusion [2]. This even-odd isotope effect has been confirmed in other laboratories also for the isotopes of Gd, Zn, Sr and Ba with the DC18C6 crown ether as extractant [1]. The even-even isotopes: $^{84}_{38}Sr$, ^{86}Sr and ^{88}Sr display a linear increase of the isotope separation factor, $\alpha-1$, with mass number while for ^{87}Sr the $\alpha-1$ value is much lower than for ^{86}Sr. In the same extraction system, the even-even isotopes: $^{134}_{56}Ba$, ^{136}Ba and ^{138}Ba show a linear decrease of the α value. The $\alpha-1$ value decreases also from ^{135}Ba to ^{137}Ba but the isotope separation factor value for ^{137}Ba corresponds to the respective value extrapolated for the β-active ^{140}Ba. This effect of the odd nucleon number and of the nucleus spin on chemical behaviour has not found any theoretical explanation. It is difficult since e.g. in the Sr system the odd neutron isotopes behave as the even neutron isotope lighter by two neutrons while in the analogous Ba system they behave as the even neutron isotope heavier by three neutrons. Trying to elucidate the even-odd isotope effect, as a result of a slightly smaller stability of nuclei with the unpaired nucleon, the present author has predicted [2] the opposite chemical isotope effect for extra-stable

nuclides with magic nuclei (in parentheses the natural abundance is specified):
$^{148}_{60}$Nd [5.76(3)%] vs. ^{142}Nd [27.13(10)%], ^{143}Nd [12.18(5)%], ^{144}Nd [23.80(10)%], ^{145}Nd [8.30(5)%], ^{146}Nd [17.19(8)%], ^{150}Nd [5.64(3)%]
$^{54}_{26}$Fe [5.9(2)%] vs. ^{56}Fe [91.72(15)%; especially stable], ^{57}Fe [2.1(1)%], ^{58}Fe [0.28(2)%]
$^{90}_{40}$Zr [51.45(2)%] vs. ^{91}Zr [11.22(3)%], ^{92}Zr [17.15(2)%], ^{94}Zr [17.38(3)%], ^{96}Zr[2.80(1)%]
$^{98}_{42}$Mo [14.84(4)%] vs. ^{94}Mo [9.25(2)%], ^{95}Mo [15.92(4)%], ^{96}Mo [16.68(4)%], ^{97}Mo [9.55(2)%], ^{98}Mo [24.13(6)%], ^{100}Mo [9.63(2)%]
$^{52}_{24}$Cr [83.79(4)%], ^{50}Cr [4.345(5)%], ^{53}Cr [9.50(1)%], ^{54}Cr [2.365(5)%]
$^{40}_{20}$Ca [96.941(13)%; doubly magic] vs. ^{42}Ca [0.647(3)%], ^{43}Ca [0.135(3)%], ^{44}Ca [2.086(5)%], ^{46}Ca [0.004(3)%], ^{48}Ca [0.187(3)%]
$^{208}_{82}$Pb [52.46%; doubly magic] vs. ^{204}Pb [1.4(1)%], ^{206}Pb [24.1(1)%], ^{207}Pb [22.1(1)%]
$^{112}_{50}$Sn [0.97(1)%], ^{114}Sn [0.65(1)%], ^{115}Sn [0.36(1)%], ^{116}Sn [14.53(11)%], ^{117}Sn [7.68(7)%], ^{118}Sn [24.22(11)%], ^{119}Sn [8.58(4)%], ^{120}Sn [32.59(10)%], ^{122}Sn [4.63(3)%], ^{124}Sn 5.79(5)%].

In the Sn case, since all the 10 Sn isotopes (the highest number of stable isotopes) have a magic proton number, the most distinct even-odd isotope effect is expected.

The discussed study [1] was not orientated towards magic nuclei behaviour; the above mentioned magic nuclei of Ba and Sr had inconveniently high natural abundances.

The hypothesis, assuming that the magic nuclei are "more even-even" than all the others, is to be experimentally verified using the effective cascade liquid-liquid extraction system [3].

References

[1]. Nishizawa K., Nakamura K., Yamamoto T., Masuda T.: Solv. Extr. Ion Exch., 12, 1073 (1994).
[2]. Mioduski T.: Differences in chemical behaviour of isotopes as exemplified by ^{238}U and ^{235}U (in Polish). Wiad. Chem., in press (a KBN Grant no. 3TO9A 052 09 is acknowledged).
[3]. Dembiński W., Mioduski T.: Europium isotope separation in the HCl/HDEHP extraction system. J. Radioanal. Nucl. Chem., Letters, 199, 159 (1995).

PL9700816

SELECTIVITY OF ION EXCHANGE ON CRYSTALLINE ANTIMONIC ACID - RADIOTRACER STUDY IN HYDROCHLORIC ACID AND AMMONIA SOLUTIONS

A. Bilewicz, J. Narbutt

Growing interest in inorganic ion exchangers in radiochemistry and nuclear technology results from their high radiation and thermal resistance, and particularly from extremely high selectivity of certain inorganic adsorbents for various metal ions.

Crystalline antimonic(V) acid (CAA) is the well known selective adsorbent of e.g. Na^+, Sr^{2+} and some other ions [1]. Its synthesis, properties and structure have been studied by numerous authors for many years, e.g. [2]. Sorption of radionuclides of the elements belonging to the s- and f-block of the Periodic Table was studied in the Department of Radiochemistry of the Institute of Nuclear Chemistry and Technology [3], using commercial CAA of the composition determined as $Sb_2O_5.2.54H_2O$ [2], obtained from Carlo Erba, Italy. For all the metals investigated linear relationships were observed on the log-log plots of the distribution coefficient (K_d) vs. HCl concentration, the slopes being nearly equal to the valency of the exchanging ions. This indicates that the adsorption proceeded predominantly through ion exchange. The K_d values determined in the HCl solutions are consistent with those reported by Abe [1] for the CAA-HNO_3 systems. Fig.1 shows the relationships between K_d and ionic radii for the three groups of the metals studied in the system CAA - 1 M HCl. The maxima observed on the curves for mono- and divalent ions correspond with the radii in the range of about 100 to 120 pm (Na^+, Ca^{2+}, Sr^{2+}). Also the second, less distinguished maximum has been found for Rb^+ (155 pm), corroborated by an inflection on the divalent-ions curve, between Ba^{2+} (135 pm) and Ra^{2+} (142

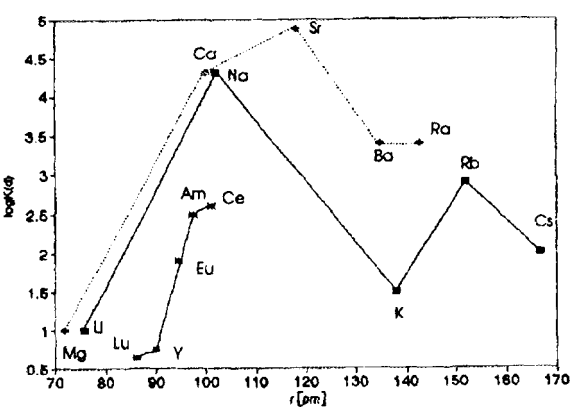

Fig.1. Dependence of the distribution coefficient of metal ions in the system CAA - 1 M HCl on their ionic radii.

pm). The appearance of such steep maxima corresponds with very high values of separation factors for certain pairs of adjacent elements in the Group. There are probably two different reasons which result in the appearance of these maxima:

- steric hindrance from the rigid, crystalline structure of the sorbent against entering too large ions;
- necessity of total dehydration of the ions before entering the sorbent structure, which causes that too small, strongly hydrated ions require too much energy for dehydration.

The results of our studies on ion exchange of some transition metal ions (Ag^+, Zn^{2+}, Cd^{2+}, Hg^{2+}) in aqueous solutions of complexing species (hydrochloric acid or ammonia) [4] are consistent with the conclusion on the ion-size recognition by CAA (the sorbent was converted into the K^+ form when alkaline ammonia solutions were studied). At not too high concentrations of the complexing species CAA very strongly adsorbs the ions whose radii fall in the range of 95-115 pm (Cd^{2+}, Hg^{2+}, Ag^+), while the small (74 pm) Zn^{2+} ion is only moderately sorbed. The slopes of the log-log plots of K_d vs. concentration of the complexing (solvating) agent correspond to the number of ligans released from the first coordination sphere of solvated ion when transferred from solution to the CAA phase [4]. Thus, assuming that the stoichiometry of the complex or solvated ion in the solution is known, we easily estimate the number of remaining ligands bonded to the ion adsorbed in the crystal lattice. In this way we conclude that the bare (as expected), large Ag^+ ions and only partly desolvated $Zn(NH_3)^{2+}$ ions are sorbed (Fig.2). Nevertheless, desolvation of both species adsorbed on CAA is more pronounced than in the case of their adsorption on not ion-size selective exchanger - hydrous

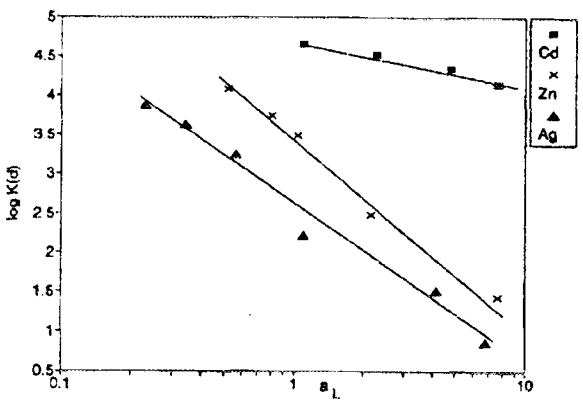

Fig.2. The distribution coefficients of Ag^+, Zn^{2+} and Cd^{2+} on CAA as a function of the activity of ammonia in the aqueous phase.

titanium oxide which adsorbs only slightly desolvated species, $Ag(NH_3)^+$ and $Zn(NH_3)_3^{2+}$ [5]. The Cd^{2+} and Hg^{2+} ions which have a very high affinity to CAA but also form very strong chloride complexes, require high HCl concentration for elution from the sorbent (Fig.3).

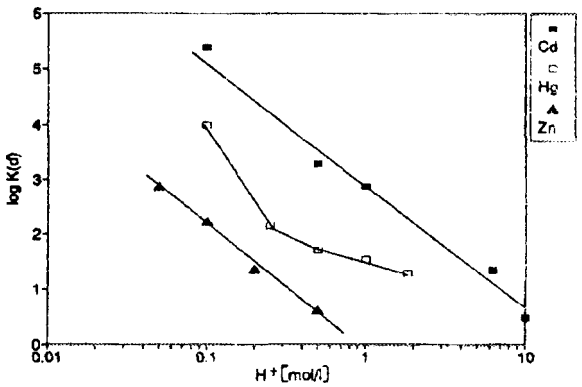

Fig.3. The distribution coefficients of Zn^{2+}, Cd^{2+} and Hg^{2+} on CAA as a function of the molar concentration of hydrochloric acid in the aqueous phase.

The ion exchange selectivity for certain ions makes CAA a useful sorbent for nuclear chemistry. Apart from its applications recently reviewed [6], CAA has been used as effective radionuclide generators. Fast procedures of milking very pure ^{90}Y from ^{90}Sr [3] and ^{115m}In from ^{115}Cd [7] with 1 M HCl solutions have been elaborated. Recently, CAA was suggested as the final sorbent for extremely small quantities of ^{24}Na in a radiochemical separation procedure designed [8] for studying the effects of expected "cluster" decay of ^{232}Th nuclei.

References

[1]. Abe M.: Sep. Sci. Technol., **15**, 23 (1980).
[2]. Zouad S., Jeanjean J., Loos-Neskovic C., Fedoroff M.: J. Solid State Chem., **98**, 1 (1992).
[3]. Bilewicz A.: Radiochim. Acta, **69**, 137 (1995).
[4]. Bilewicz A., Bazarraghaagin A., Narbutt J.: Zh. Anal. Chim. (Russ. J. Anal. Chem.), in press.
[5]. Bilewicz A., Narbutt J.: Solvent Extr. Ion Exch., **13**, 1083 (1995).
[6]. Narbutt J., Bilewicz A., Bartoś B.: J. Radioanal. Nucl. Chem., **183**, 27 (1994).
[7]. Bartoś B., Bilewicz A.: J. Radioanal. Nucl. Chem., Letters, **201**, 89 (1992).
[8]. Loos-Neskovic C., Delmas R., Hussonois M., Bartoś B., Bilewicz A.: to be published.

LANTHANIDE IONS COMPLEXATION BY URONIC ACIDS

L. Fuks

In view of the growing industrial and commercial use of toxic metals (e.g. actinides, lead, mercury, cadmium or arsenic) and their increasing release into the atmosphere, the problem of developing effective treatments for such exposure will undergo a growing importance in the future. The sheer magnitude of the problems that are faced in the reprocessing nuclear fuels and the dismantling of nuclear weapons insure that human exposures to uranium and the transuranium elements, such as plutonium or americium, will not diminish in the near future. Finally, such events as Chernobyl fallout have shown the importance of the studies leading to the development of new therapeutic methods for the removal of immobilized heavy metals.

On the other hand, a growing number of metabolic diseases are observed which are proved to be the result of the accumulation of excessive amounts of essential metals. Direct accumulation is found e.g. for copper in Wilson's Disease or for alumi-

nium in Alzheimer's Disease. Indirect accumulation, in turn, is found e.g. for iron in a great number of people with deviations in the haemoglobin synthesis, e.g. people suffering from thalassemia. It is caused by the prolonged administration of blood transfusions with an accumulation of iron to toxic or even lethal levels.

Clinical tests have shown that several natural polysaccharides, e.g. alginic acid (a straight chain, polyuronic acid comprised of anhydro α-D-mannuronic acid and L-guluronic acid) or pectines (partially methoxylated polygalacturonic acid), used as prophylactic or medication drugs in the case of heavy metal poisoning induce an increased excretion of lead [1] or mercury [2-4]. Furthermore, sodium alginate incorporated into diet of mices inducted an increase of ^{90}Sr, ^{133}Ba and ^{226}Ra radioisotopes concentration in blood as well as a decrease of their deposition in the skeleton [1]. In the marine environment, in turn, macroalgae have been used as bioindicators for fission products or transuranium elements following fallout from nuclear detonation tests and releases from nuclear facilities [5, 6].

Lanthanide ions are found in living organisms in trace amounts only, measured in ppb units [7]. Because of that they are considered not to play a sig-

Table.

Galacturonic acid	La-galacturonate	Glucuronic acid	La-glucuronate	Assignments
3447s, 3361s	about 3445s	3444sh, 3405vs	about 3340s	υ(OH) [strong hydrogen bond]
3324s, 3284sh, 2981m, 2955m		3281s, 3231sh, 3166s		υ(OH) [weak hydrogen bond]
2921m		2925s		υ(CH) [α-anomer]
2863m, 2839m		2892s, 2839m		υ(CH) [β-anomer]
2752m, 2709m		2764m, 2700, 2645m		overtones
2613m, 2547m		2593m, 2559m		overtones
1712s		1705		υ(HOCO)
1643m				$\delta(H_2O)$
	1596vs		1590vs	υ(C=H) antisymmetric
		1538sh	1510sh	
		1484sh		δ(COH) + δ(CCH)
1438m		1460m		δ(CCH) + δ(COH)
	1425s		1433m	υ(OC) symmetric
1413m	1418sh			
1367s		1366s		δ(CCH) + δ(COH)
1355m	1316sh	1348m	1349m	δ(COH) + δ(OCH)
1327m, 1302m, 1283m		1320w, 1289sh	1299m	δ(COH) + δ(OCH)
1243sh		1260s		δ(CCH) + δ(COH)
1233sh, 1215m		1226s, 1204m	1204w	δ(COH) + δ(CCH)
1154s	1149m	1158s	1150sh	υ(CC) + υ(CO)
1119sh		1126m	1111sh	υ(CO) + υ(COC)
		1103sh		υ(CO) + υ(COC) + δ(CCO)
1094vs, 1071s		1088vs, 1076sh		υ(CO) + υ(CCC)
1055s	1047s	1054m, 1025vs	1047s	υ(CO) + υ(CCO) + δ(CC)
1026s	1016sh			
		008sh	947m	υ(CO) + δ(CCH)
	970m			υ(CO) + δ(CCO)
940m		944sh		υ(CO) + υ(CCH)
908w	896w	908sh	917w, 913w	δ(CC) + υ(CO)
863w	875sh		878w	δ(CH) [β-anomer]
822s	817m, 807m			δ(CH) [α-anomer]
776m	802m	779w, 767w, 752w	767m	τ(CCO) + δ(CCO) + δ(CCH)
		715s		δ(CCO) + δ(OCO) + τ(CO)
692m				$\delta_r(H_2O)$
655m	675m	678m	672m	δ(CCO) + τ(CCO)
617m, 612m	633s	617m	629m	$\delta_w(H_2O)$
about 520m	515m	587s, about 530m	546m	τ(CO) + δ(CCO)
498m	473m	457m	474m	δ(CCO) + τ(CO)
443w,405w	427w	415w, 403w	408w	δ(CCO) + δ(CCH)

Bands: s - strong, sh - shoulder, m - medium, w - weak.

Assignments: υ - stretching, δ - bending, τ - international rotation, r - rocking, w - wagging.

nificant biological role [8, 9]. However, similarity in the ionic radii of the trivalent REEs with those of

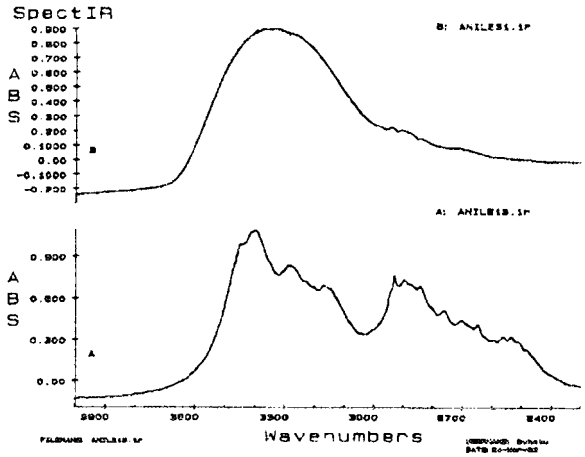

Fig.1. FT-IR spectra of the lanthanum glucuronate (upper spectrum) and glucuronic acid (lower spectrum).

calcium and sodium, in the charge-density (Z/r) with magnesium or zinc, followed by the possibility of

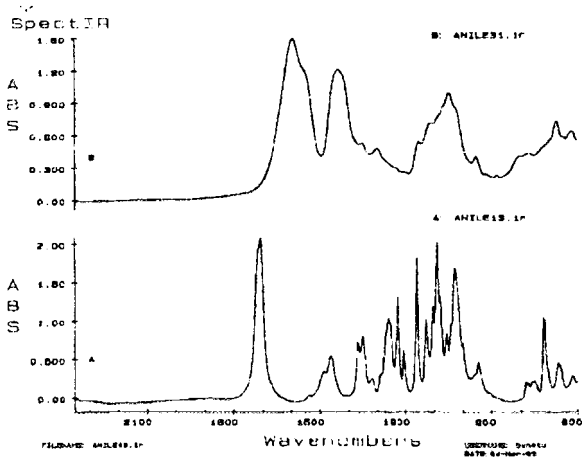

Fig.2. FT-IR spectra of the lanthanum glucuronate (upper spectrum) and glucuronic acid (lower spectrum).

mutual isomorphous replacement, combined with the unique magnetic and spectroscopic properties of the REEs make them very informative substitution

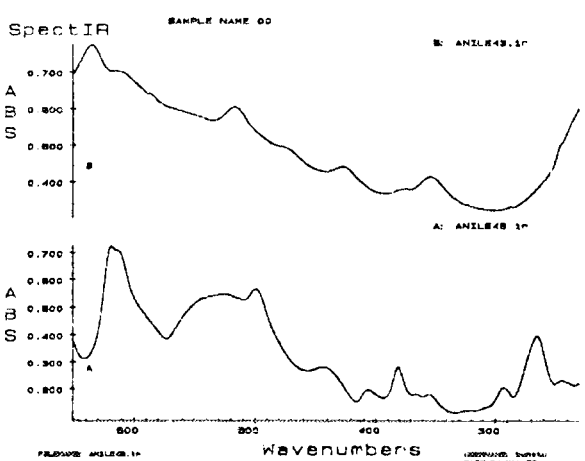

Fig.3. FT-IR spectra of the lanthanum glucuronate (upper spectrum) and glucuronic acid (lower spectrum).

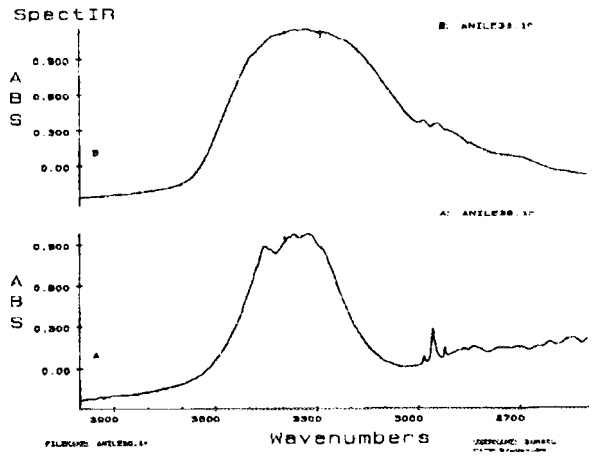

Fig.4. FT-IR spectra of the lanthanum galacturonate (upper spectrum) and galacturonic acid (lower spectrum).

probes in the various biological and medical examinations [10, 11]. Finally, because of their chemical similarity, REEs may also act as substitution probes

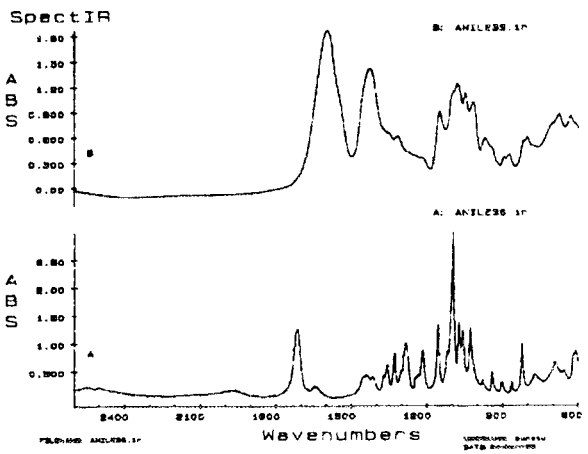

Fig.5. FT-IR spectra of the lanthanum galacturonate (upper spectrum) and galacturonic acid (lower spectrum).

for the actinides - especially for those radioactive elements available only in submicroquantities.

The study was initiated to extend the results obtained by the electronic absorption spectroscopy of the selected trivalent REE cations (ie. of La(III),

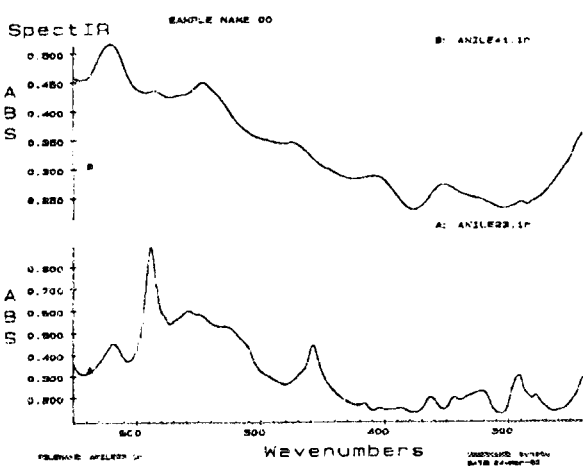

Fig.6. FT-IR spectra of the lanthanum galacturonate (upper spectrum) and galacturonic acid (lower spectrum).

Ce(III), Pr(III), Nd(III), Gd(III) and Lu(III)) complexes with mentioned above D-alduronic ligands [12]. FT-IR spectra were recorded with an IFS-113v vacuum spectrometer under the following conditions: 2 cm^{-1} bandpass, 128 scans and 4-point (trapezoidal) apodization. The solid samples were pelletized in KBr (about 1% of the acid or studied complex).

Results and discussion

The Fourier-transform infrared spectra of D-glucuronic acid, D-galacturonic acid and their lanthanum salts have been recorded in the region of 4,000-150 cm^{-1}. It can be seen, that spectra of the lanthanum-uronic acid salts are substantially different from those of the corresponding free acids. The spectra of these salts are covered by the strong and broad absorption bands related mainly to the OH, CO_2^-, CO stretching and COH bending vibrations, which overlap several other fine and sharp sugar absorption bands. The coordination involves two uronic acid anions, each binding through C(6) and C(6') carboxyl oxygen atoms and C(5) ring oxygen atom, as well as several water molecules resulting to the usual coordination geometry around the REE cation [12]. The main feature of the spectra relevant to the following discussion are given in Table and Figs 1-6.

On the basis of the comparison made for the obtained already stability constants [12] with the FT-IR spectra and literature data concerning NMR investigation of the Ln^{3+} - alduronic acid systems, the following points may be emphasized:

- The strong intermolecular sugar hydrogen bonding network is rearranged upon the complex formation.
- The 1:1 Ln^{3+}-D-galacturonate complex stability constants are greater than these for D-glucuronate. In the contrary, for 1:2 complexation only the light lanthanides (ions of the greatest radii) are favourably complexed by the D-galacturonic acid. This phenomenon was explained in terms of the steric hindrance of C(4) hydroxyl groups.
- The 1:1 complexation is effectuated simultaneously by the C(6) and C(6') carboxylic oxygen atoms as well as by ring C(5) oxygen atom. It is in certain degree supplemented by the C(4) hydroxyl groups. The 1:2 complexes, in turn, are formed only by two fully ionized acid anions through C(6) and C(6') oxygen atoms of carboxyl groups only.
- The Fourier-transform infrared spectra recorded for the both D-alduronic acids and their lanthanum(III) crystalline salts in the region of 4,000-150 cm^{-1} support the mentioned above conclusions. Furthermore, presence of a weak absorption band at about 870 cm^{-1} in the spectrum of free galacturonic acid, as well as of both investigated salts, may be related to the α-anomer conformation. Appearence of the band at 822 cm^{-1} in the spectrum of free galacturonic acid suggests, that mentioned above commercial sample of the acid must be treated as a mixture of both anomers.

References

[1]. Reprints on Prevention of Uptake on Decorporation of Radioactive Heavy Alkaline Earth Metals in Man, Mice, Swine. Ed. O. Vanderbroght. Belgian Nuclear Centre - Mol Report, 1981.

[2]. Chaika P.A.: Gig. Tr. Prof. Zabol., 10, 47 (1966).

[3]. Stanchev S., Krachanov Kh., Popova M., Kirchev N., Marchev N.: Z. Ges. Hyg., 25, 585 (1979).

[4]. Trakhtenberg I.M., Talakin Yu.N., Leskova G.E., Kakovskaya V.N., Gridneva N.V.: Gig. Tr. Prof. Zabol., 24, 33 (1980).

[5]. Pentreath V.: Impacts of Radionuclide Releases into the Marine Environment. IAEA, Vienna 1981, p. 241.

[6]. Dahlgaard H., Arkrog A., Hakkstadius L., Holm E., Rioseco J.: Rapp. P.V. Réunion Cons. Int. Expl. Mer., 186, 70 (1986).

[7]. Iyengar G.V., Kollmer W.E., Bowen H.J.: The Elemental Composition of Human Tissues and Body Fluids. Verlag Chemie, Weinheim 1978.

[8]. Krumholz L.A., Goldberg D.E., Boroughs H.: In: The Effects of Atomic Radiation on Oceanography and Fisheries. Chapter 7. Natl. Acad. of Sci. Natl. Res. Council, Publ. no. 551, 1957.

[9]. Brown P.H., Rathjen A.H., Graham R.D., Tribe D.E.: Rare Earth in Biological Systems. In: Handbook of the Physics and Chemistry of Rare Earths. Vol.13. Eds. K.A. Gschneidner, Jr, L. Eyring. Elsevier, Amsterdam 1991.

[10]. Martindale: The Extra Pharmacopoeia. Pharmaceutical Press, London 1972.

[11]. Lanthanide Probes in Life, Chemical and Earths Sciences. Eds. J.C.-G. Bünzli, G.R. Choppin. Elsevier, Amsterdam, 1989.

[12]. Fuks L., Bünzli J.C.-G.: Helv. Chim. Acta, 76, 2992 (1993).

IONIC RADII. EFFECT OF SHELL RADIUS, CATION CHARGE AND LONE ELECTRON PAIR

S. Siekierski

Radii of ions, r_i [1], were compared with radii of their outermost orbitals, $<r_{nl}>$ [2]. It has been found that for s and p block elements in the oxidation state equal to the Group valence, r_i is a linear function of $<r_{nl}>$ and for a constant value of $<r_{nl}>$ decreases with increasing formal charge of the cation (Fig.1). For p block elements in the oxidation state two below Group valence the difference r_i - $<r_{nl}>$ exhibits a saw-tooth behaviour (Fig.2), i.e. secondary periodicity, similar to that in stability of oxidation states [3]. The saw-tooth behaviour in the radii suggests that the lone pair acquires some s character between the 3-rd and 4-th Period, and becomes essentially

PL9700819

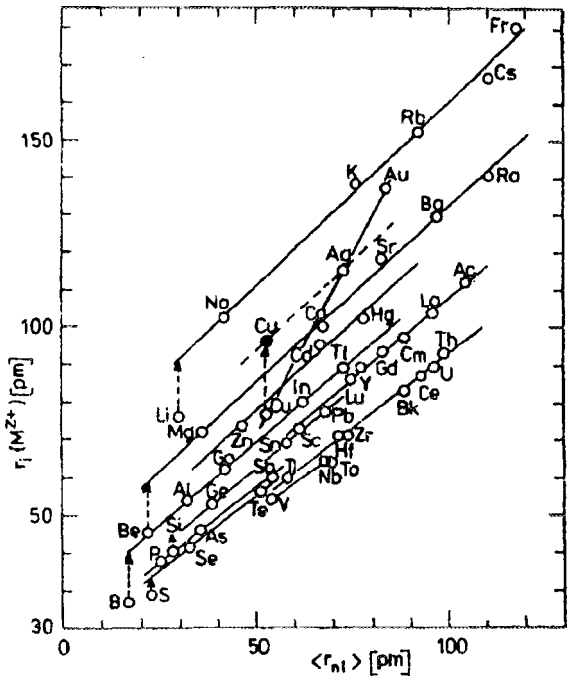

Fig.1. The ionic radius as a function of the radius of the outermost shell. The oxidation state is equal to the Group valence. The full point denotes the ionic radius of Cu(1+).

an s^2 pair in Tl(1+), Pb(2+), Bi(3+), and Po(4+). The radii of Lr(1+), 104(4+) and 105(5+) have been estimated from linear relationships between r_i and $<r_{nl}>$ and those of Al(1+), Ga(1+), In(1+) and Si(2+) from the saw-tooth pattern.

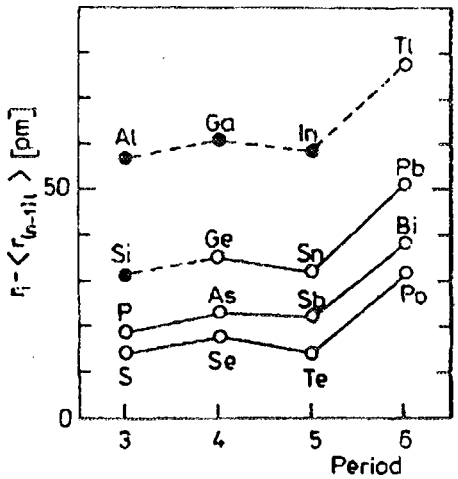

Fig.2. Variation in the difference r_i - $<r(n-1)l>$. The oxidation state is two below the Group valence. Full circles denote values estimated from the saw-tooth behaviour.

References

[1]. Shannon R D.: Acta Cryst., A32, 751 (1976).
[2]. Desclaux J.P.: Atomic Data and Nuclear Data Tables, 12, 311 (1973).
[3]. Pyykkö P.: Chem. Rev., 88, 563 (1988).

"REGULAR" AND "INVERSE" TETRAD EFFECT

T. Mioduski

The potentiometric data of Sawada et al. [1] for protonation of the lanthanide nitrilotris(methylenephosphonic) ($Ln(ntmp)^{3-}_{aq}$) are plotted in Fig., as confronted with the present author's potentiometric data [2] for protonation and hydroxo-complexation of the $Ln(dcta)^{-}_{aq}$ chelates, where dcta denotes trans-1,2-diaminocyclohexanetetraacetic acid.

The "regular" [1] and "inverse" [2] tetrad effect must be interpreted [2-4] in terms of the opposite coordination number (CN) change of the Ln(III) central ions in result of protonation. For protonation in the dcta system, the following equilibria are valid:

$$(H_2O)_mLn(dcta)^{-}_{aq} + H(OH_2)^{+}_n \quad (1)$$
$$\Leftrightarrow (H_2O)_{m+1}HLn(dcta)_{aq} + (n-1)H_2O$$

Presumably m=3 in the La-Sm range and m=2 in the Dy-Lu range of the Ln series, and the "inverse" tetrad effect is observed in the -RT Δln K vs. q variations given in Fig. For protonation in the ntmp system the following equilibria are held:

$$(H_2O)_mLn\{N[CH_2P(O)_2(O)]_3\}^{3-}_{aq} + H(OH_2)^{+}_n \quad (2)$$
$$\Leftrightarrow (H_2O)_mLn\{3[(O)(O)_2PCH_2]NH\}^{2-}_{aq} + nH_2O$$

In eq. (2) presumably m=3, at least for Y(III) and heavy lanthanides of the yttrium group. It results in the "regular" direction of the tetrad effect as presented in Fig., and the tetrad destabilization

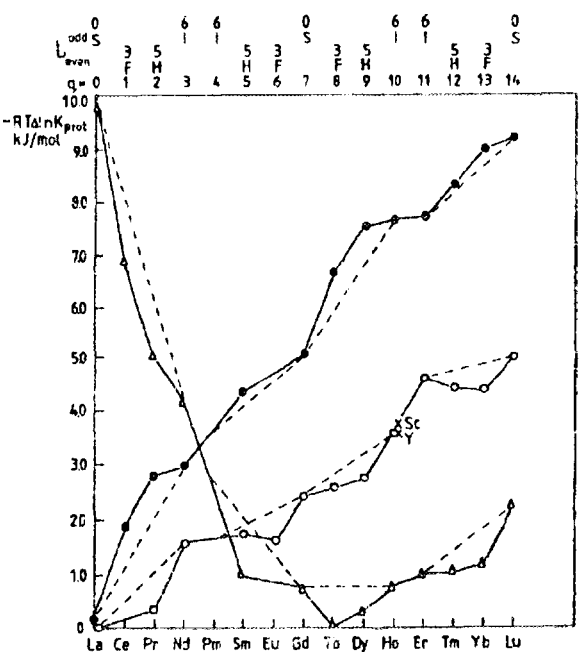

Fig. Gibbs energy variations for the $Ln(ntmp)^{3-}$ (o), $Ln(dcta)^{-}$ (upper curve; full circles) and $(HO)Ln(dcta)^{2-}$ (Δ) systems vs. number of f-electrons q, total orbital quantum number L and ground terms of lanthanides, at imprecision of ±0.17 kJ/mol.

of the protonated complexes. The destabilization is caused by a decrease in CN by 1 due to protonation of the nitrogen donor and the Ln-N bond broken. The decrease in CN is most likely from 7 to 6 for the heavy lanthanides. This decreased CN is accompanied by shortened bonds in the protonated complexes and by an increase in overlap integrals between the buried 4f-subshell with a small average radius $<r_{4f}>$ and the ligand orbitals, viz. the Ψ_{4f} and Ψ_{lig} eigenfunctions. Quasi-holmium behaviour of Sc(III) in the ntmp system must be explained [2] by an increase in CN of Sc by 1, as for lanthanides in the dcta system, in result of protonation. For scandium CN probably increases from 5 to 6 for the protonated Sc(III) complex:

$$(H_2O)_mSc\{3[(O)(O)_2PCH_2]N\}^{3-}_{aq} + H(OH_2)^+_n \quad (3)$$
$$\Leftrightarrow (H_2O)_{m+1}HSc\{3[(O)(O)_2PCH_2]N\}^{2-}_{aq} + (n-1)H_2O$$

This increase by 1 in CN of Sc is accompanied by the decrease by 1 in CN of the Ln(III) ions, as specified by eq. (2), producing quasi-holmium/yttrium behaviour of Sc(III) [2].

Correlations between the tetrad effect, CN, effective crystal radii, covalent shortenings, nephelauxetic effect, ligand field effect, spin-orbit coupling, hydration and reactivity are developed in detail in [4]. In an up-to-date look at the tetrad effect [4], it is indicated that the SO-coupling stabilization energy, although of similar absolute value to the interelectronic repulsion stabilization energy for the 5f-subshell filled in 1/4 and 3/4, is negligible as far as the resultant tetrad effect is concerned. On the other hand, the minute ligand field stabilization energy, as very sensitive to the CN changes, slightly increases the tetrad effect for the f-subshell filled in 1/4 and 3/4.

References

[1]. Sawada K., Kuribayashi M., Miyamoto H.: J. Soln. Chem., 20, 829 (1991).

[2]. Mioduski T.: Quasilanthanide(III) behaviour of scandium(III) and coordination number. Comments Inorg. Chem., 14, 263 (1993).

[3]. Mioduski T.: A lecture entitled "Tetrad effect and coordination number" given on July 21, 1994 in the Joint Institute for Nuclear Research at Dubna, Russia.

[4]. Mioduski T.: "Regular" and "inverse" tetrad effect (to be published).

SPECIATION OF CHROMIUM IN NATURAL WATERS BY SEPARATION AND PRECONCENTRATION ON A PYROLLIDINEDITHIOCARBAMATE LOADED RESIN FOLLOWED BY GRAPHITE FURNACE ATOMIC ABSORPTION SPECTROMETRY (GF AAS)

J. Chwastowska, W. Żmijewska, E. Sterlińska

In the aquatic environment dissolved chromium occurs in two oxidation states Cr(VI) and Cr(III). Since chromium (VI) is highly toxic it is of importance not only to determine the total chromium content but also the content of Cr(VI).

Speciation of chromium can be achieved by various methods, however only few of them permit its direct speciation. Generally methods of chromium speciation combine some separation and preconcentration steps (extraction, coprecipitation, ion-exchange, complexation followed by sorption) with a sensitive instrumental technique, most often GF ASS.

In this work a chelating sorbent - ammonium pyrollidinedithiocarbamate (APDC) loaded Bio Beads SM-7 resin has been proposed for the separation and preconcentration of Cr(VI) from natural waters prior to its determination by GF AAS. Contrary to sorbents containing dithiocarbamate groups obtained by synthesis, this sorbent is obtained by direct deposition of the reagent on the resin. A sorbent of this type-diethylammoniumdiethyldithiocarbamate loaded polyurethane foam was obtained by Braun and co-workers [1] and applied to the preconcentration of inorganic and organic mercury species from natural waters.

The sorbent-APDC loaded resin was prepared by shaking 100 ml of 0.01 M APDC solution in carbon tetrachloride with 4 g of Bio Beads SM-7 resin (20-50 mesh) for 1 h.

Sorption of Cr(VI) on the sorbent from solutions of various pH (1-9) was examined using the radiotracer ^{51}Cr(VI). The maximum sorption efficiency takes place in the pH range 3-4. Consequently further experiments were carried out at pH 3.5 ± 0.2.

The effects of the following parameters on the sorption efficiency of Cr(VI) were examined:
- shaking time (5 min-1 h),
- sample volume (25-200 ml),
- amount of the sorbent (0.3-1 g).

It has been found that the sorption equilibrium is attained within 15 min. The sorption efficiency decreases with increasing volume of the sample and increases with increasing amount of the sorbent.

On the basis of the above experiments the following conditions for the separation and preconcentration of Cr(VI) were established: sample volume v=100 ml, amount of the sorbent - 1 g, shaking time t_s=1 h.

Under the above conditions Cr(III) is not retained on the sorbent.

Desorption of chromium from the sorbent is carried out by decomposition of the reagent with concentrated nitric acid (the sorbent is placed in a small column and allowed to react with 2 ml of the acid for 30 min). The desorption efficiency is 97%.

The determination of chromium is carried out directly in the solution after desorption (diluted with water to 10 ml) by GF AAS.

The sorption efficiency of Cr(VI) from a synthetic water sample (of a composition similar to that of soft waters) with the additions of heavy metals was examined. EDTA was used to eliminate the effect of heavy metals. The sorption efficiency of Cr(VI) from the synthetic water solution was 65% for v=100 ml, 1 g of the sorbent and t_s=1 h. The same value of sorption efficiency was obtained for v=25 ml, 0.3 g of the sorbent and t_s=30 min.

In order to verify the elaborated method of separation and preconcentration of Cr(VI) samples of the synthetic water with additions of Cr(VI) and Cr(III) at various Cr(VI)/Cr(III) ratios (0.1-10) were analysed. The results are presented in Table 1. It follows from Table 1 that the recovery of Cr(VI) is good.

Table 1. Recovery of Cr(VI) from synthetic water containing heavy metals (h.m.) and Cr(III).

v=25 ml, 0.3 g of the sorbent, pH=3.5, 4 mg EDTA, t_s=30 min, h.m.(μg/l: Zn-100, Pb, Ni, Co, Cu-50, Cd-10.

Ratio Cr(VI)/Cr(III)	Added [μg]	Determined* [μg]	Recovery** [%]
1:1	Cr (VI) 5 Cr (III) 5	4.9 -	98
1:10	Cr (VI) 5 Cr(III) 50	5.2 -	104
10:1	Cr (VI) 10 Cr (III) 1	9.7 -	97

*By AAS with flame atomization.

**Corrected for sorption efficiency.

The sorbent was applied to the speciation of Cr(VI) in tap water. Cr(VI) was determined in samples of tap water without and with additions of known amounts of Cr(VI). The determination was carried out by GF AAS. The content of total chromium was determined as well (after 10-fold preconcentration by evaporation). The results are given in Table 2. It follows from Table 2 that the amounts of Cr(VI) recovered from the samples, to which known amounts Cr(VI) had been added, agree well with the amounts added (after subtraction of the original content in the examined water), which indicates no systematic error.

Table 2. Results of analysis of tap water.

Cr total [μg/l]	Cr(VI) [μg/l]			
Determined	Determined A	Added B	Determined A+B	Calculated (A+B)-A
0.45	0.40 0.40 0.27 0.37			
	$\bar{x}$ =0.36 ±0.062			
		0.80 0.80 0.80	1.21 1.26 1.11	0.41 0.46 0.31
			$\bar{x}$ =1.19 ±0.076	$\bar{x}$ =0.39 ±0.076

The obtained content of total Cr in the examined tap water (0.36 μg/l) is much lower than the admissible value for drinking water (50 μg/l). About 80% of the chromium exists as Cr(VI).

References

[1]. Braun T., Abbas M.N., Bakos L., Elek A., Anal. Chim. Acta, 131, 311 (1981).

A STUDY ON THE EFFECT OF COLUMN OVERLOADING AND ITS INFLUENCE ON THE QUALITY OF ANALYTICAL RESULTS WHEN DETERMINING SIMPLE ANIONS BY ION CHROMATOGRAPHY

K. Kulisa, R. Dybczyński, H. Polkowska-Motrenko

Ion chromatography is known as a modern, fast and selective method of simultaneous determination of many ionic species in aqueous solutions on ppm (mg/l) and even ppb (μg/l) level [1]. In analytical practice, the necessity of determination of trace quantities of ionic species in the presence of macro-quantities of other ions frequently occurs. The presence of high concentrations of certain ions may be the reason of column overloading, leading to deformation of the results of analyses. There are no data concerning this problem in the available literature. Determination of concentration limits for all ions and column types is a very important factor influencing the accuracy of analyses. A commercially available ion chromatograph Dionex 2000i/SP and several analytical anion-exchange columns Ion Pac AS4A, AS5, AS9SC and Fast Anion-1 were used in this study. Analytical columns AS4A, AS5 and AS9SC were connected with guard columns (AG4A, AG5 and AG9SC, respectively). All the columns were filled with new type "agglomerated" ion exchange resins of low ion-exchange capacity and the structure enabling high velocity of ion exchange reaction, so that the chromatograms of complicated ionic mixtures could be obtained in several minutes. The chromatograph was equipped with anion micromembrane suppressor AMMS-1 regenerated with solution of 0.025 M H_2SO_4, a Dionex conductivity detector CDM-II and an UV/VIS variable wavelength Detector VDM II. The signals from the detectors were processed using a computer program Labtech Chrom. A sodium carbonate - bicarbonate solutions $NaHCO_3/Na_2CO_3$ of different concentrations for each column (AS4A - 0.5 mM $NaHCO_3$/1.3 mM Na_2CO_3, AS5, AS9SC - 1.7 mM $NaHCO_3$/1.8 mM Na_2CO_3, Fast Anion-1 - 0.15 mM $NaHCO_3$/2.0 mM Na_2CO_3) were used as a mobile phase.

The chromatograms were obtained for each of the investigated columns as a function of an anion being a macro-constituent. 3 series of solutions each consisting of 3 anions, where two were of fixed

concentrations (trace level) and the concentration of the third one was changeable in a rather broad range, were studied.
Series 1 - Cl^- - 5 mg/l, NO_3^- - 10 mg/l, SO_4^{2-} changing concentration 10, 30, 50, 100, 150, 200, 300 and 500 mg/l.
Series 2 - Cl^- - 5 mg/l, SO_4^{2-} - 15 mg/l, NO_3^- changing concentration 10, 20, 40, 100, 150, 200, 300 and 500 mg/l.
Series 3 - NO_3^- - 10 mg/l, SO_4^{2-} - 15 mg/l, Cl^- changing concentration 5, 10, 15, 20, 50, 100, 300 and 500 mg/l.

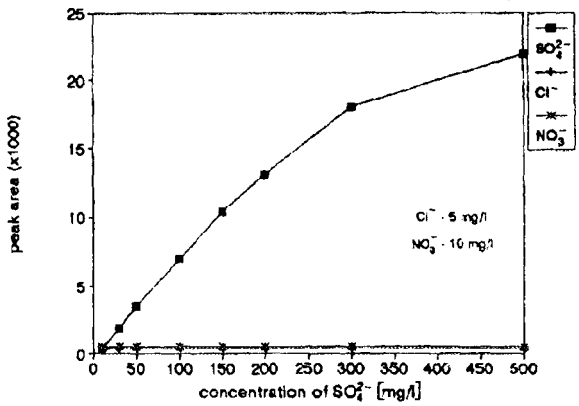

Fig.1. Peak area - column AS9SC.

On the basis of this study the basic characteristics of chromatographic process as: peak area, retention time, column efficiency and peak shape parameters

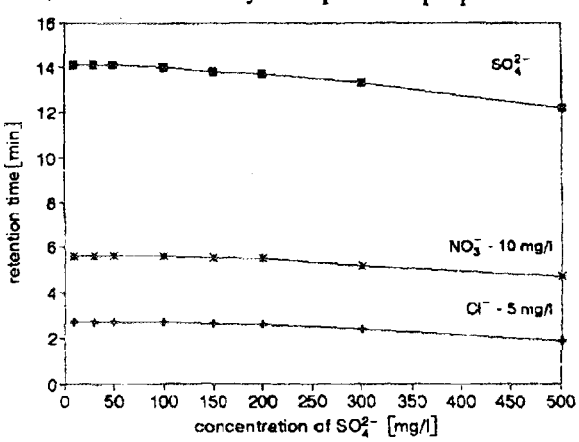

Fig.2. Retention time (min) - column AS9SC.

were calculated as a function of macro-constituent concentration in the analyzed solution for each column and for each of the investigated anions. Examples of typical changes of peak area and retention time as a function of macro-constituent concentration are shown in Figs 1 and 2. It follows from these results that for all the investigated columns, limits of concentration values where the linearity of calibration curves and the stability of retention times for macro-constituent were maintained are: for Cl^- - 0.84 meq./l (30 mg/l), for NO_3^- - 0.64 meq./l (40 mg/l) and for SO_4^{2-} - 1.04 meq./l (50 mg/l). The influence of macro-constituent concentration on peak areas and retention times of trace ions was observed only above the macro-constituent concentration values of ca. 150 mg/l (4.2 meq./l for Cl^-, 2.4 meq./l for NO_3^- and 3.12 meq./l for SO_4^{2-} respectively). Above these values of concentration one can observe changes of retention times of all anions which in the case of analyses of real samples may cause difficulties in identification of the species. Non-linearity of characteristics of peak areas

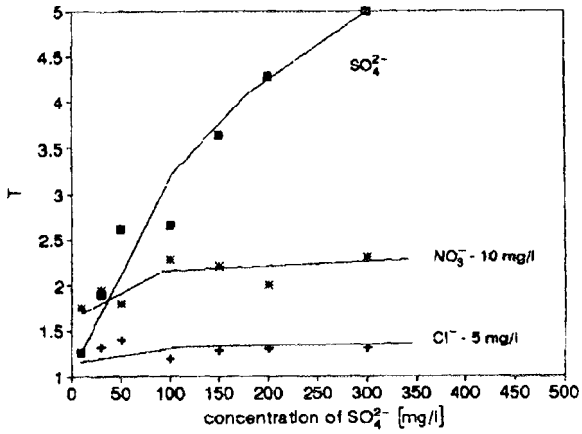

Fig.3. Tailing factor - column AS9SC.

as a function of anion concentration is a source of errors in quantitative determinations. When analyzing real samples, their dilution to the above mentioned anion concentration values is necessary.

The shape of peak may also have influence on precision and accuracy of the determinations. An

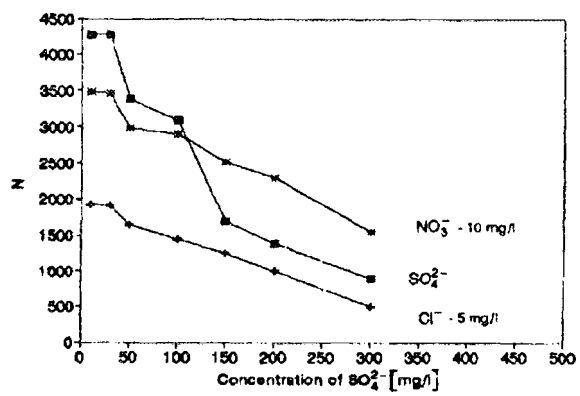

Fig.4. Number of theoretical plates - column AS9SC.

example of the changes of tailing factors of chromatographic peaks as a function of macro-anion concentration is shown in Fig.3. The characteristics of theoretical plate number of the column as a function of anion concentration is shown in Fig.4 [2]. These parameters strongly depend on the concentration of macro-constituent both for macro- and trace anions. The symmetry of the peaks is the best and column efficiency is the highest when the concentration of macro-constituent is low and decrease along with increasing concentration. Decreasing of column efficiency values is slow at the beginning and becomes very pronounced above the limits of concentrations of macro-constituents mentioned previously.

To summarize: the admissible values of concentrations of anions determined in this study are the limiting values from the point of view of column efficiency parameters as well as characteristics of chromatographic peaks. When analyzing the real samples care must be taken not to exceed the limiting concentration values of the most abundant constituent. It is one of the main conditions to obtain precise and accurate results of analysis.

References

[1]. Haddad P.R.: Ion Chromatography. Principles and Applications. Elsevier, Amsterdam 1990, p. 776.

[2]. Weiss J.: Handbuch der Ionenchromatographie. VCH Verlagsgesellschaft mbH, Weinheim 1985, p. 288.

PL9700820

DEVISING OF THE METHOD FOR THE DETERMINATION OF SMALL AND VERY SMALL AMOUNTS OF CADMIUM IN BIOLOGICAL MATERIALS BY RADIOCHEMICAL VERSION OF NEUTRON ACTIVATION ANALYSIS

Z. Samczyński, R. Dybczyński

Accurate determination of cadmium in biological materials is of great importance due to its toxic properties, still growing concentration level of this metal in biosphere, and its tendency to accumulation in human body mainly in kidneys [1]. Neutron activation analysis because of its favourable detection limits as well as minimization of the problem of blank, seems to be a logical method of choice for the determination of trace amounts of Cd. The method for cadmium determination by radiochemical NAA using amphoteric ion exchange resin Retardion 11A8 intended especially for biomaterials of very low cadmium content has been devised.

Retardion 11A8 belongs to the class of amphoteric ion exchangers. It contains both anionic strongly basic benzyltrimethylammonium groups and an equivalent amount of weakly acidic carboxylate groups [2]. Depending on the composition of the external solution, elements existing as anions or anionic complexes can be taken up by the anion exchange groups, as well as those existing as cations or cationic complexes can be retained by the cation exchange groups. It seemed possible, that cadmium forming anionic chloride complexes in HCl solutions and cationic amine complexes in NH_3 solutions [3] should be taken up both by cation and anion exchange groups exploiting cation and anion exchange functions of Retardion 11A8.

Ion exchange behaviour of cadmium and other elements in a wide range of concentrations of HCl and NH_3 was investigated by means of the batch equilibration technique. The results revealed, that in both systems there exist quite pronounced ranges of concentrations where cadmium shows high affinity towards the ion exchanger. The above conclusions were verified by column experiments using radioactive tracers. Cadmium is selectively retained on the column while passing 2 mol l^{-1} HCl and 1 mol l^{-1} NH_3 + 0.1 mol l^{-1} NH_4Cl solutions (Fig.), whereas the accompanying elements are practically completely eluted. Zinc showing similar properties like cadmium is also kept by the ion exchanger in the course of elution with the above eluents. For this reason, separation of both these elements is necessary. It was found that Zn can be effectively washed out with the solution of the composition: 0.05 mol l^{-1} NH_3 + 2.0 mol l^{-1} NH_4Cl, while Cd is still bound by the resin. The final stripping of cadmium was performed with 8 mol l^{-1} NH_3 + 1.0 mol l^{-1} NH_4Cl solution.

Determination of cadmium in biological materials by neutron activation analysis using Retardion 11A8 for the selective separation of cadmium was already described previously [4]. Separation of Cd from other radionuclides present in neutron irradiated biological materials as well as accuracy of analytical results were satisfactory. During long γ-ray spectrometric measurements, however, trace amounts of several radionuclides were still ob-

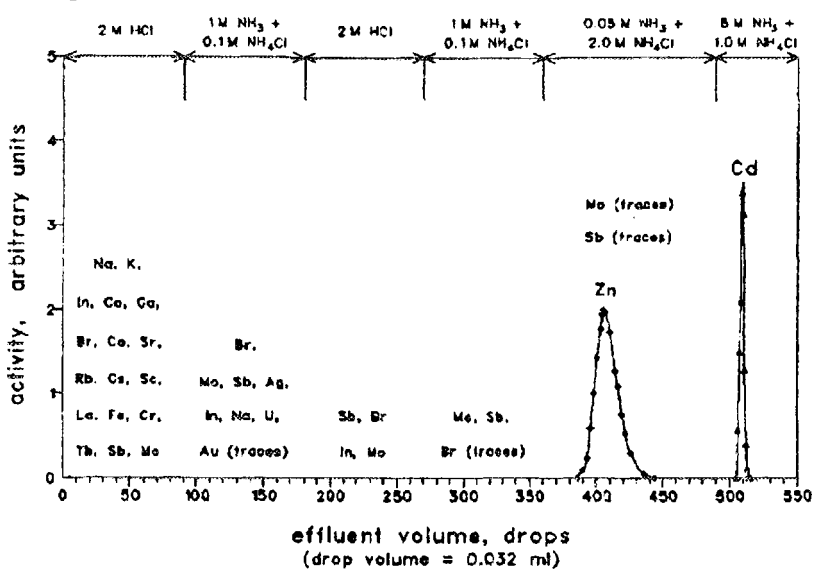

Fig. Ion exchange separation of cadmium from other elements by a stepwise elution. Column: 12.0 cm x 0.0707 cm^2; Retardion 11A8 ($23 \leq \phi \leq 46\,\mu m$).

Table. Results of cadmium determination in the certified reference materials.

Material	Certified value for Cd and its confidence limits [mg/kg]	Results of individual determinations [mg/kg]	Arithmetic mean* and its confidence limits [mg/kg]	Relative standard deviation [%]
IAEA H-8 Horse Kidney	189 ±6 (183-195)	186.4 191.6 191.2 187.2 182.7	187.8 ±4.6**	2.0
IAEA MA-M-2 Mussel Tissue	1.32 (1.16-1.54)	1.45 1.48 1.54 1.54 1.60	1.52 ±0.07**	3.8
CTA-OTL-1 Oriental Tobacco Leaves	1.12 ±0.12 (1.00-1.24)	1.19 1.14 1.17 1.08 1.25	1.17 ±0.08***	5.4
IAEA H-9 Human Diet	0.0315 ±0.0045 (0.0270-0.0360)	0.0343 0.0354 0.0314 0.0304	0.0329 ±0.0038**	7.2
IAEA H-4 Animal Muscle	0.0049 ±0.0010 (0.0039-0.0059)	0.00521 0.00492 0.00566 0.00517 0.00460	0.00511 ±0.00049***	7.7

* Results are presented as $\bar{x} \pm t_{0.05} \cdot \frac{s}{\sqrt{n}}$, where: $\bar{x}$ - arithmetic mean, s - standard deviation, $t_{0.05}$ - parameter of Student's distribution for significance level of $\alpha=0.05$ and n-1 degrees of freedom, n - number of determinations.

** Analytical results obtained using the former version of the method [4].

*** Analytical results obtained using the improved version of the method.

served in the γ-ray spectrum of the cadmium fraction. In the improved version of the method, presented in this paper the main effort was directed towards the demonstration of possibilities of interference free cadmium determination in biological materials of low level Cd content.

Samples of biological materials and Cd standards were irradiated in the EWA nuclear reactor (neutron flux - $8 \cdot 10^{13}$ n $cm^{-1}s^{-1}$, activation time - 16-48 hrs). After 3-5 days of cooling the materials were mineralized with HNO_3+$HClO_4$ mixture (1+1). The next step was the removing of SiO_2 by means of HF and evaporation to dryness. The residue was afterwards dissolved in 2 mol l^{-1} HCl and transferred quantitatively onto the top of Retardion 11A8 column (15 cm x 0.126 cm^2, particle size - 23-46 μm). Then the ion exchange procedure was performed in the way described above (Fig.). The elaborated method was used for the determination of Cd in two biological certified reference materials i.e. IAEA H-4 Animal Muscle [5] and CTA-OTL-1 Oriental Tobacco Leaves [6]. Because of low Cd content in first of the two materials, long γ-ray counting times of 60000 s and more had to be employed. The modification of the ion exchange separation scheme raised the selectivity of Cd isolation still keeping intact the 100% yield of the analyte (average 99.8% ±0.4% recovery in the cadmium fraction as determined in tracer experiments). Decontamination factors established for several selected elements were as follows: Na and Sc>10^6, Co and Sb>10^5, Mo≈10^4, Zn≈10^3. Gamma-ray spectrum of the cadmium fraction was practically free from other activities. The detection limit calculated according to Rogers [7] amounted to 0.5 μg/kg (sample weight - 100 mg, neutron flux - $8 \cdot 10^{13}$ n $cm^{-1}s^{-1}$, activation time - 48 hrs, cooling time - 7 days, measurement time - 72000 s). The residual blank resulting from the canning material was practically zero. The analytical results of cadmium determination in the above mentioned materials together with those obtained in the previous work [4] are listed in Table.

One can easily note a very good accuracy and precision of the method demonstrated over the concentration range from single ppbs up to hundreds of ppms. It is worth stressing, that the observed increase of relative standard deviation from 2% in Horse Kidney to 7.7% in Animal Muscle is surprisingly small considering, that the corresponding decrease in the concentration of the analyte amounts nearly five orders of magnitude.

References

[1]. Metals and Their Components in the Environment. Ed. E. Merian. VCH, Weinheim 1991, 1438 p.

[2]. Hatch M.J., Dillon J.A., Smith H.B.: Ind. Eng. Chem., **49**, 1812-1819 (1957).

[3]. Martell R.M., Smith A.E.: Critical Stability Constants. Vol. 4. Plenum Press, New York 1976, 257 p.

[4]. Dybczyński R., Samczyński Z.: J. Radioanal. Nucl. Chem., Articles, **150**, 143-153 (1991).

[5]. Byrne A.R., Camara-Rica C., Cornelis R., de Goeij J.J.M., Iyengar G.V., Kirkbright G., Knapp G., Parr R.M., Stoeppler M.: Fresenius Z. Anal. Chem., **326**, 723-729 (1987).

[6]. Dybczyński R., Polkowska-Motrenko H., Samczyński Z., Szopa Z.: Fresenius J. Anal. Chem., **345**, 99-103 (1993).

[7]. Rogers V.C.: Anal. Chem., **42**, 807-809 (1970).

PL9700821

MECHANISM OF THE CHLORIDE ION EFFECTS ON THE ANALYTICAL SIGNAL OF SELENIUM MODIFIED BY PALLADIUM IN GRAPHITE FURNACE ATOMIC ABSORPTION SPECTROMETRY

L. Pszonicki, W. Skwara

Selenium is an important element in humans and its determination at trace levels in various matrices, such as environmental materials and biological fluids, is of significance. However, it belongs to the troublesome trace elements to analyse owing to the volatility of its compounds. One of the methods most commonly used for its determination is the electrothermal atomic absorption spectrometry (ET AAS). In this method the losses of analyte in the early stages of the analytical process, such as drying and pyrolysing of the sample, can be avoided by the use of proper chemical modifiers. The modifiers most frequently used in the determination of selenium are nitrates of nickel, copper and palladium [1]. The last one found application in the determination of many elements [2]. Therefore it is considered as a very versatile and becomes more and more popular.

The palladium modifier is used in the selenium determination either alone or in a mixture with various additions [3], particularly, with magnesium [1, 2]. These additions are used mainly for the elimination of the interference effect of the chloride ion as reported by many authors [4-6]. Although the processes in the graphite tube during atomization are rather complex some propositions of the mechanism responsible for the chloride interferences may be found [4, 5]. However, they do not explain all the observed phenomena and the problem requires further investigations.

Up to now the effect of the thermally stable chlorides, particularly of sodium and potassium chlorides, was investigated as a common effect of chloride ions and associated metal ions. In our investigations the chloride ions were introduced to the sample in the form of hydrochloric acid. It was found that for the samples dissolved directly in hydrochloric acid the analytical signals obtained in the presence of palladium chloride is equal to that measured for samples in nitric acid when palladium is also in the nitrate form. This indicates that there is no direct effect of chloride ions. The situation changes dramatically when even a small amount of hydrochloric acid is added to the sample in nitric acid. The selenium signal is suppressed to about 20%, sometimes to about 0%, of its value. A similar effect is observed when some amount of nitric acid is added to the sample in hydrochloric acid. Such a very strong suppression may be caused only by the losses of analyte in the presence of the mixture of nitric and chloride ions in the acidic medium. The detailed examination of this phenomenon indicates that the losses occur already during the drying at the early stage of the pyrolysis phase. It may be explained by the activity of the free chlorine atoms evolved from the mixture of nitric and hydrochloric acids. Chlorine can form with selenium some compounds which are not formed in the presence of hydrochloric acid and which are volatile in the temperature range 100-200°C, e.g. $SeOCl_2$ or Se_2Cl_2.

A similar suppression effect is observed when ferric chloride is added to a sample dissolved in hydrochloric acid. However in this case the losses of selenium occur during pyrolysis phase above 300°C. It corresponds to the decomposition temperature of $FeCl_3$ (315°C). Chlorides decomposing in higher temperatures do not give such suppression effects. This confirms the hypothesis that the suppression of selenium signal in the presence of the palladium modifier is caused not by the chloride ions in the direct way but by the evolved free chlorine atoms which can be produced during drying and pyrolysis of the mixture of nitrites and chlorides in the acidic medium or by pyrolysis of the easy decomposing chlorides.

The discussed suppression effect may be eliminated by the addition to the sample easy decomposing nitrates of alkali or alkaline earth metals since their oxides neutralize the evolved chlorine. Magnesium nitrate is particularly suitable because of its very low decomposition temperature.

References

[1]. Johannessen J.K., Gammelgaard B., Jons O., Hansen S.H.: J. Anal. At. Spectrom., **8**, 999-1004 (1993).

[2]. Welz B., Schlemmer G., Mukadavit J.R.: ibid., **7**, 1256-1271 (1992).

[3]. Matsumoto K.: Anal. Sci., **9**, 447-453 (1993).

[4]. Byrne J.P., Chakrabarti C.L., Gregoire D.C., Lamoureux M., Ly T.: J. Anal. At. Spectrom., **7**, 371-381 (1992).

[5]. Javier Aller A., Garcia-Olalla C.: ibid., **7**, 753-760 (1992).

[6]. Radziuk B., Thomassen Y.: ibid., **7**, 397-403 (1992).

SOL-GEL FOR PREPARATION OF $YBa_2Cu_4O_8$ PRECURSORS FROM BY COMPLEX SOL-GEL PROCESS (CSGP)

A. Deptuła, W. Łada, T. Olczak, K.C. Goretta[1/]

[1/]Energy Technology Division, Argonne National Laboratory, USA

Numerous papers have covered preparation of the $YBa_2Cu_3O_x$ (123) phase by sol-gel processes; only a few have been devoted to synthesis of the $YBa_2Cu_4O_8$ (124) phase by this method. For

example, S. Sakka et al. [1] modified their ammonia-acetate by addition of tartaric acid. In the present work a modified acetate-ammonia sol-gel process, used by the present authors for 123 preparation [2], to prepare 124 precursors. The modification, which we called CSGP, consists in introducing a strong complexing agent - ascorbic acid (ASC) - which exhibits additionally a strong reducing character to the acetate sol. In our previous studies [3, 4] we have proved that during synthesis of $(Bi,Pb)_2Sr_2Ca_2Cu_3O_x$ precursors, this additive promotes formation of homogeneous gels that can be calcined in air directly, without melting to carbonate-free ceramics.

A schematic diagram of the preparation of acetate (AC) and acetate-ascorbate (ASC) sols is shown in Fig.1.

Addition of a strong reducer as ascorbic acid to blue AC sols changes the colour to black, characteristic of the presence of Cu^{1+}. Also the shard and coatings obtained by evaporation of volatiles retained the colours.

The thermal analyses of ground AC and ASC gels are shown in Fig.2.

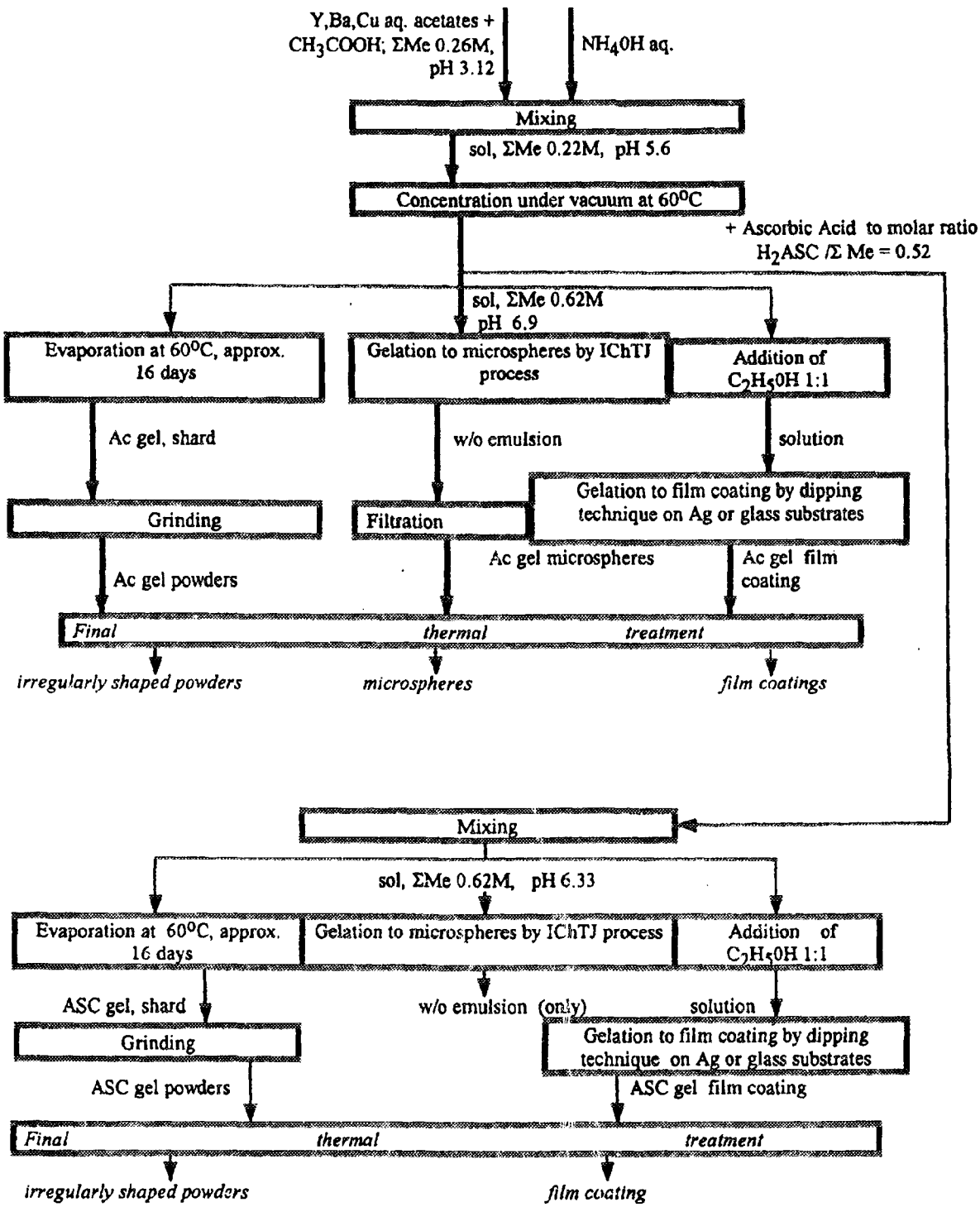

Fig.1. Method for preparation of YBCO 124 precursors.

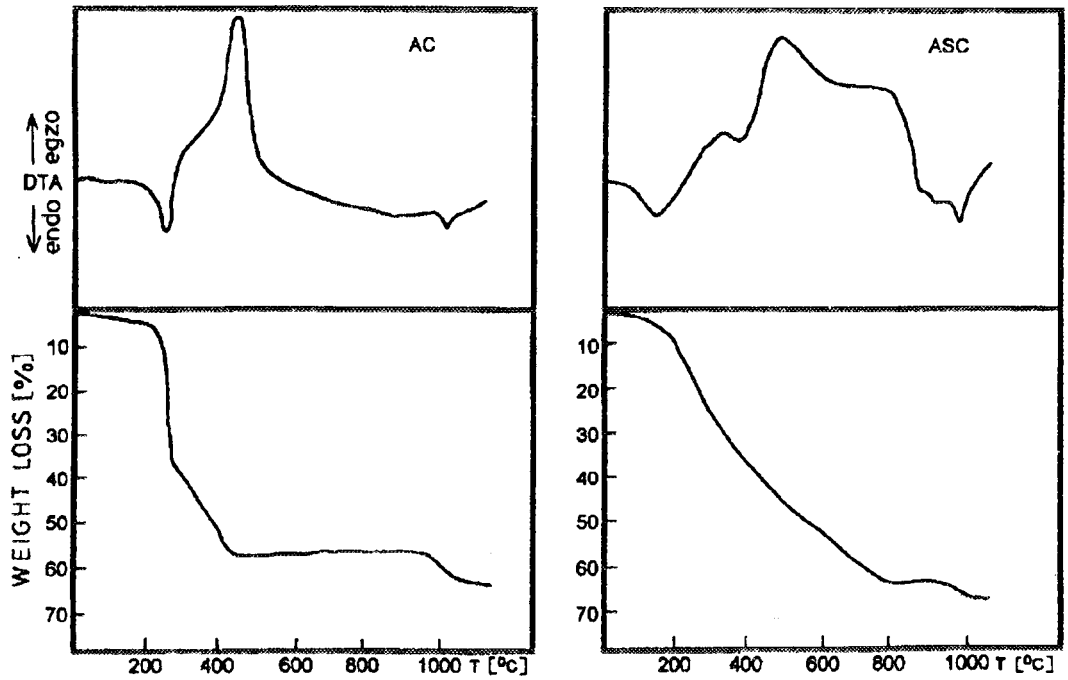

Fig.2. Thermal analysis of YBCO 124 AC and ASC gels dried at 100°C for 12 days.

In the AC gels, the thermal transformations are very distinct. The first endotherm at approximately 300°C, is accompanied by drastic mass loss, presumably from volatiles and chemically combined water. The last sharp exotherm connected with oxidation of organics, has a maximum at approximately 500°C. The mass of the AC sample is constant from 500 to 930°C. Thermal decomposition of ASC gels is more complex. After a broad endotherm at approximately 150°C, which is associated with a relatively small mass loss, several broad exotherms accompanied by continuous mass losses are observed. The total mass loss for ASC gels was 10% higher than for the AC gels because of higher organic content. At high temperatures, small drops in the TGA indicate reduction of Cu species, and loss of oxygen. The differences between the AC and ASC gels appear to be connected with the extent to which they are amorphous (Fig.3).

After drying at 100°C the ASC gel is perfectly amorphous, in contrast to the AC gel in which crystalline acetates are observed. The amorphous nature of the ASC gels, in which a strong bidentate network of ascorbic anions is present, seems to be responsible for the strong bonding of volatiles and the concomitant prolonged thermal decomposition. The amorphous character of the ASC gels appears to be responsible for better quality of coatings prepared by a dipping technique [4] on glass and silver substrates (Fig.4).

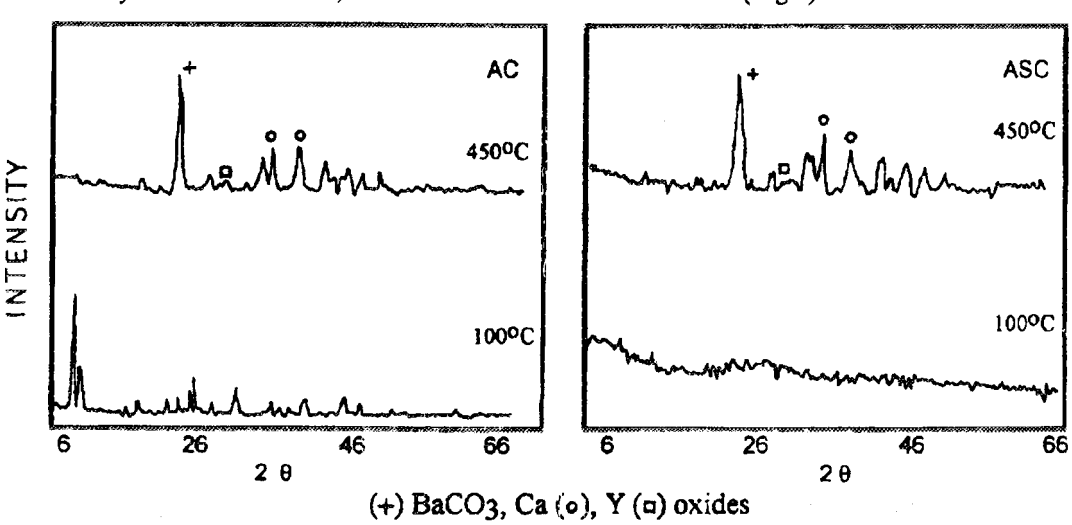

Fig.3. XRD patterns of YBCO 124 AC and ASC gels dried at 100°C 12 days and calcined at 450°C for 4 h.

The thickness of the 124 coatings varied from 40 to 20 μm and decreases with the amount of ethanol added to the sols and with increased withdrawal rate. In all the cases, it has been confirmed [4] that the addition of ethanol to sols facilitates the formation of uniform coatings.

In contrast to the AC system, gelation of ASC sol emulsions in 2-ethylhexanol-1 by extraction of

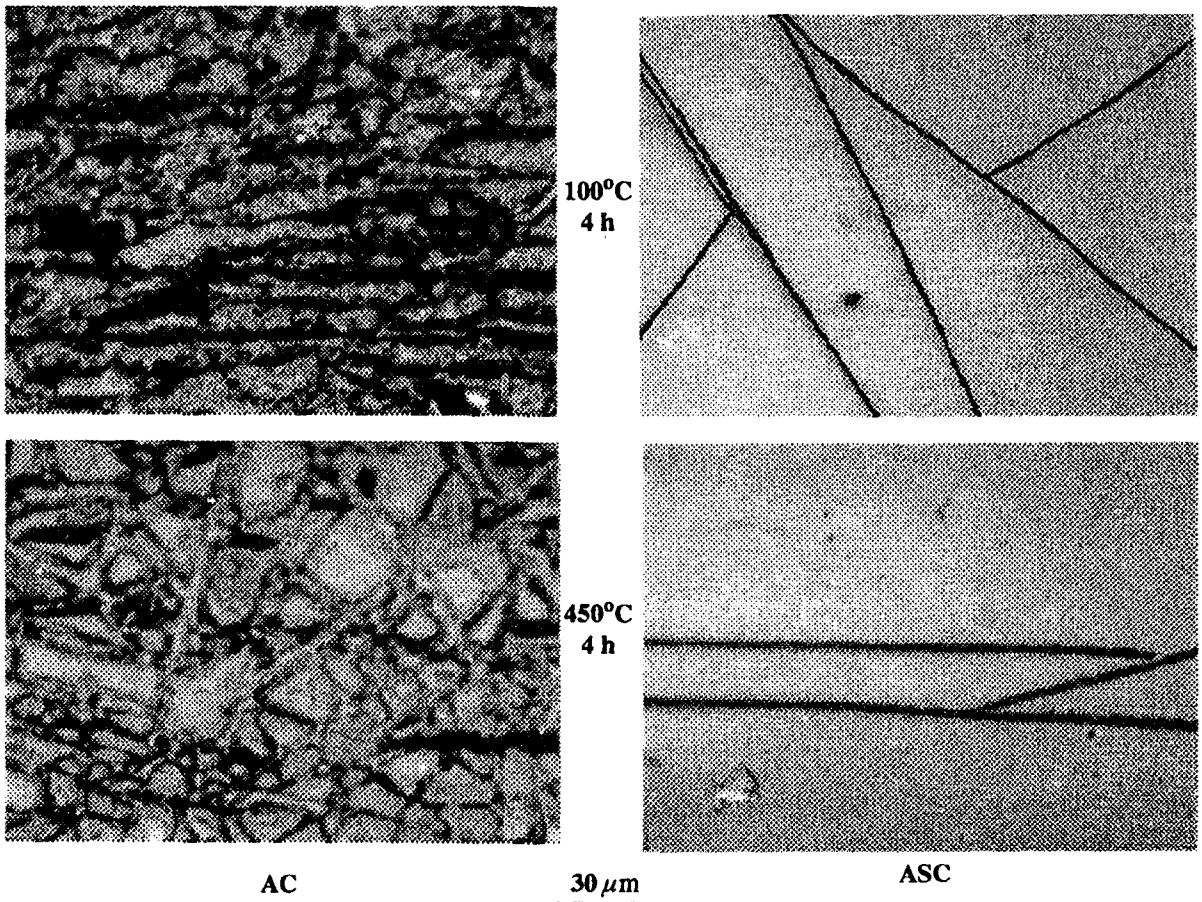

Fig.4. Photomicrographs of coatings of YBCO 124 AC and ASC gels on glass or Ag substrates.

water (IChTJ process) to spherical particles, proved to be unsuccessful (Fig.1). A possible reason for this is the strong bonding of water to the ASC gel, as reported above.

After calcination of both gels at 450°C for 4 h the CO_3 contents were 22 and 19.5% for AC and ASC, respectively. This suggests that some of the carbonates are combined with copper, also because if all of the barium were combined as $BaCO_3$, the CO_3 content should be 14.3%. Lack of the XRD patterns corresponding to copper carbonates (Fig.3) indicates that they are still in amorphous state.

In contrast to $Bi_2Sr_2CaCu_2O_x$ and $(Bi,Pb)_2Sr_2Ca_2Cu_3O_x$ ascorbate gels [2, 3] only small reduction of CO_3 content is observed for ascorbate gel as compared to acetate gels. However, addition of ascorbic acid results in the formation of more homogeneous and amorphous gels, which confirms the observation of S. Sakka et al. [1] who noted a similar effect in the presence of tartaric acid.

References

[1]. Fujihara S., Zhuang H., Yoko T., Kozuka H., Sakka S.: J. Mat. Res., 7, 2355 (1992).

[2]. Deptuła A., Łada W., Olczak T., Lanagan M.T., Dorris S.E., Goretta K.C., Poeppel R.B.: Formation of Phase-Pure, Carbonate-Free, Superconducting Ceramics From Organic Precursors. Polish Patent pending no. P. 300 557 (October 1993).

[3]. Deptuła A., Łada W., Olczak T.: Sol-Gel Process for Preparation of High Temperature Superconductors Precursors from Acidic Acetate - Ammonia - Ascorbic Acid - Systems. Annual Report 1993, IChTJ, Warszawa 1994, p.73.

[4]. Łada W., Deptuła A., Olczak T., Torbicz W., Pijanowska D., Di Bartolomeo A.: Preparation of Thin SnO_2 Layers by Inorganic Sol-Gel Process. J. Sol-Gel Sci. Technol., 2, 551 (1994).

RETENTION OF SODIUM ON HYDRATED ANTIMONY PENTOXIDE MICROSPHERES (DIAMETER <20 μm) PREPARED BY SOL-GEL PROCESS

A. Deptuła, W. Żmijewska, W. Łada, T. Olczak

E. Girardi and E. Sabbioni [1] have found that hydrated antimony pentoxide (HAP) can be used as a sorbent for the retention of sodium with excellent selectivity. They prepared irregularly shaped powders by hydrolysis of $SbCl_5$ with water. After calcination at 270°C they used selected fraction of 100-300 μm. The objective of the present work was the preparation (HAP) in the form of microspheres, using the

IChTJ sol-gel process [2]. We believed that the spherical shape of HAP particles will improve the mechanical resistance, decrease of the hydraulic resistance and consequently facilitate practical use of HAP as a sorbent for retention of sodium.

Antimony pentoxide sol was prepared by peptization at 95°C of fresh precipitate obtained by hydrolysis of $SbCl_5$ with water. The conditions of the precipitation of hydrated antimony pentoxide, its peptization as well as properties of the sols are shown in Table 1. The peptization was carried out using only a small addition of water (<5%).

Table 1. Precipitation of hydrated antimony pentoxide and its peptization at 95°C.

No. of sol	Precipitation conditions		Sol properties			
	temperature [°C]	antimony losses [%]	concentration [M]	Cl/Sb molar ratio	viscosity [cSt]	pH
1	3	65	0.7	0.45	1.8	1.8
2	20	40	0.9	0.04	12.0	1.5
3	30	55	0.7	0.34	6.0	1.6

Then the sol emulsion in 2-ethylhexanol-1(EH) was formed. The emulsion drops by extraction of water with partially dehydrated EH according [2] to the nearly perfect microspheres (Fig.1).

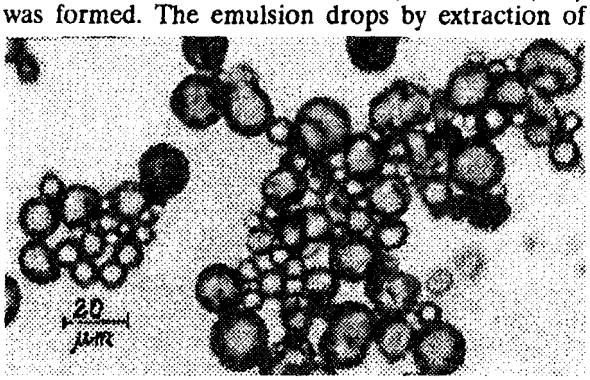

Fig.1. Microspheres of HAP.

Table 2. Retention capacity of HAP for sodium.

Sample	Treatment	mg Na/g $Sb_2O_5 \cdot 4\,H_2O$	Retention conditions
0	no	12	static
1	3M HNO_3, 3 days, 20°C	16	static
2	3M HNO_3, 15 min, boil p	18	static
3	NH_4OH aq, 15 min, boil p	19 23	static dynamic
4	water, 15 min, boil p	18	static

The obtained gels, after washing with acetone, were leached with water, concentrated NH_4OH or 3M HNO_3, washed from NH_4^+, NO_3^- ions and dried in the ambient conditions to constant weight. These operations were carried out on the basis of [3] where their positive effect on catalysts activity was observed. After washing with acetone the powders were leached. The conditions of the treatment as well as the retention (studied under static and dynamic conditions using the radionuclide ^{24}Na in 6M HCl) capacity of the HAP samples are shown in Table 2.

The untreated gel had a maximum capacity of 12 mg Na/g $Sb_2O_5 \cdot 4\,H_2O$. After treatment the capacity increased to 16 or even >18 mg Na/g for boiling procedures. In dynamic conditions the retention capacity is even higher - 23 mg Na/g. In order to elucidate the differences in the sorption capacity of the samples from Table 1 physicochemical studies were carried out.

The thermal analysis and XRD patterns of the samples are very similar, corresponding to the composition $Sb_2O_5 \cdot 4\,H_2O$. Also the IR spectra (Fig.2) of all the samples are similar, except for sample no. 3 where the band δ as NH_4^+ 1405 cm^{-1}, characteristic of ammonia adsorbed on e.g. Sb_6O_{13} [4], is observed.

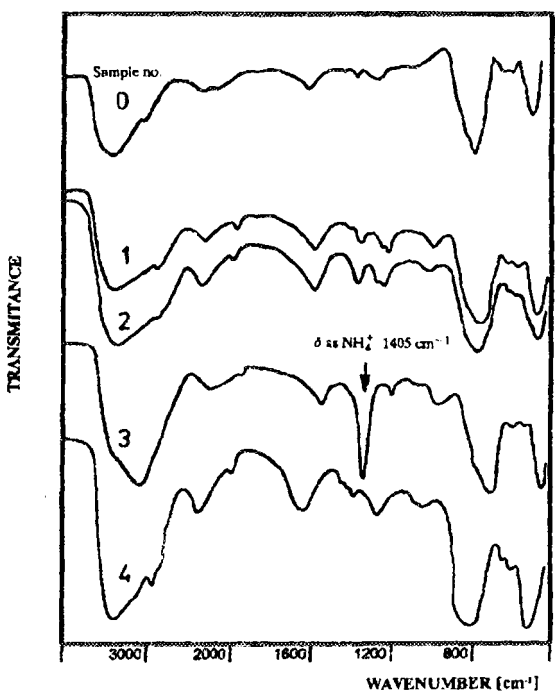

Fig.2. Infrared spectra of HAP samples.

Because this sample shows the best sorption properties it seems that the presence of ammonia is a positive factor for the sodium retention.

The untreated sample (no. 0) has worse retention capacity. The results of the physico-chemical studies have not shown essential differences in the structure and composition (except for HAP no. 3). Consequently the positive effect of leaching can be interpreted as changes of physical properties of the grains (e.g. surface). Another possible reason can be the presence of traces (non detectable by the employed methods) of organics in the untreated sample, originating from the solvent used in the process.

The obtained microspheres have two principal advantages over a similar fraction of irregularly shaped powders:
- lower hydraulic resistance,
- higher stability - no repeptization phenomena were observed.

References

[1]. Girardi E., Sabbioni E.: J. Radioanal. Chem., 1, 169 (1968).
[2]. Deptuła A., Rebandel J., Drozda W., Łada W., Olczak T.: Production of Spherical Powders of Inorganic Compounds by Water Extraction Variant of Sol-Gel Process. In: Better Ceramic Through Chemistry V. Eds. M.J. Hampden-Smith, W.G. Klemperer, C.J. Brinker. p. 277 (Mat. Res. Soc. Symp. Proc. 270, Pittsburgh, PA, 1992).
[3]. Deptuła A., Łada W., Olczak T., Di Bartolomeo A.: Preparation of Pt/Al_2O_3 Catalysts by Sol-Gel Process and its Application to Uranyl Ion Reduction. In: Better Ceramic Through Chemistry VI. Eds. M.J. Hampden-Smith, W.G. Klemperer , C.J.Brinker. 1994, p.661 (Mat. Res. Soc. Symp. Proc. 346, Pittsburgh, PA, 1994).
[4]. Davidov A.A.: IK - Spectroscopiya i Khimia Povierkhnosti Okislov (in Russian). Nauka, 42 (1984).

SINTERING OF ZrO_2-CaO, ZrO_2-Y_2O_3 AND ZrO_2-CeO_2 SPHERICAL POWDERS PREPARED BY IChTJ SOL-GEL PROCESS

A. Deptuła, M. Carewska[1/], T. Olczak, W. Łada
[1/]C.R.E. Casaccia, ENEA, Rome, Italy

PL9700822

Calcia, yttria or ceria stabilized ZrO_2 solid solutions are one of the most extensively studied systems due to many practical applications. One of the most promising methods of their preparation is the sol-gel processing. These powders were fabricated by the continuous IChTJ sol-gel process (Fig.1) described in detail in [1, 2] mainly for preparation of coatings by plasma spraying technique.

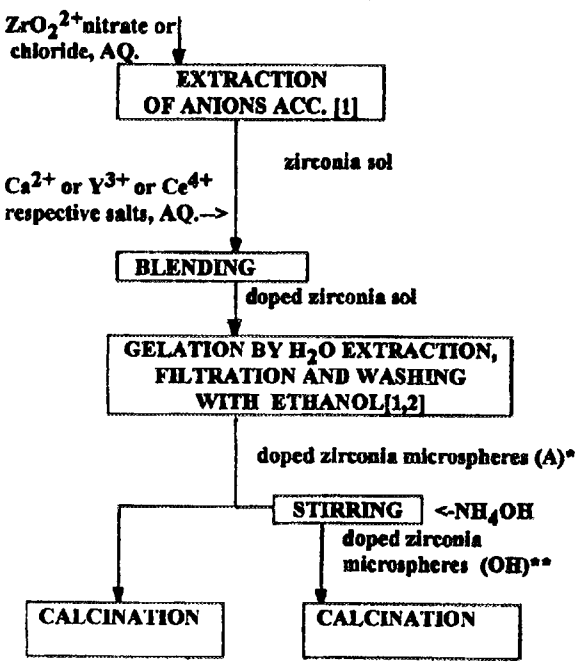

SPHERICAL POWDERS OF ZrO_2-CaO, ZrO_2-Y_2O_3 AND ZrO_2-CeO_2 (DIAMETERS 1-100μm)

Fig.1. Flow-sheet of the sol-gel process for preparation of doped zirconia microspheres. * - (A) powders derived from anion-containing gels, ** - (OH) powders derived from OH^--containing gels.

However in this paper, we describe systematic studies on sinterability at 1700°C of the green compacts pressed under 3000 kg/cm^2 from spherical powders (Fig.2) of doped zirconia microspheres.

The chemical composition of the gels, dried at 150°C, is shown in Table 1.

Table 1. Chemical composition of doped zirconia gels, dried at 150°C.

No.	Dopant-anion*	Dopant** m/o	Anion/$\sum$ Me molar ratio	% C
1	CaO-NO_3	7.7	0.7	1.1
2	CaO-OH (NO_3)	8.0	-	
3	CaO-Cl	18.6	1.0	0.6
4	CaO-OH (Cl)	19.0	0.8	
5	Y_2O_3-NO_3	4.1	0.8	1.5
6	Y_2O_3-OH (NO_3)	4.0	-	1.3
7	Y_2O_3-Cl	6.0	1.2	
8	Y_2O_3-OH (Cl)	5.9	-	
9	CeO_2-NO_3	13.3	0.5	1.9
10	CeO_2-OH (NO_3)	14.0	-	1.7
11	CeO_2-Cl	17.0	1.1	2.0
12	CeO_2-OH (Cl)	17.5	-	1.5

* in parenthesis the anionic form of the parents gel is given.
** ZrO_2+dopant=100 m/o.

On the basis of the results of thermal analysis of these gels, calcination of powders before pressing was carried out at 400, 600 and 800°C, respectively.

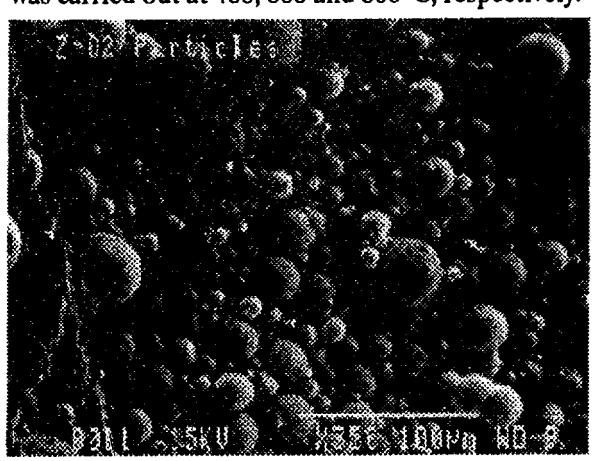

Fig.2. Representative spherical powders of doped zirconia microspheres.

The bulk densities of ZrO_2-CaO and ZrO_2-Y_2O_3 materials after sintering are relatively low (<85% TD), however slightly higher (several % TD) for the latter ones. In the case of ZrO_2-CeO_2 system the bulk densities are considerable higher (generally 90% TD). Those pellets have also high apparent densities, very close to the theoretical ones. It means

that sintered pellets of ceria doped zirconia have very low closed porosity in contrast to the pellets of ZrO_2-CaO (Y_2O_3). As the preparation and physico-chemical properties of the powders are the same or very similar, the above results point to the importance of CeO_2 as dopant. The sequence of sinterability of the studied systems is given in Table 2.

Table 2. Sequence of sinterability of gels.

Dopant	The order of sinterability
CaO	Cl > OH (Cl) > NO_3 > OH (NO_3)
Y_2O_3	Cl > OH (Cl) > NO_3 > OH (NO_3)
CeO_2	OH(NO_3) > NO_3 > OH (Cl) > Cl

One of the most significant differences between the dopants used, namely CaO, Y_2O_3 and CeO_2, is the ability of cerium to change its valency state. As was suggested in [3] this property could be responsible for better densification of the ZrO_2-CeO_2 system. In the first step Ce^{4+} accelerates the oxidation of the residual carbon impurities in gels and subsequently the formed Ce^{3+} is reoxidated by atmospheric oxygen. This reduction/reoxidation process could modify the microspheres morphology leading to formation of the so called soft aggregates, which can easily be broken during compaction increasing final sintering density.

Conclusions

- The ceria - doped zirconia sintered pellets (prepared from spherical powders fabricated by the IChTJ sol-gel process) exhibit much higher bulk densities than those of ZrO_2-CaO (Y_2O_3) samples, presumably due to cerium reduction/reoxidation.
- In contrast to ZrO_2-CaO, ZrO_2-Y_2O_3 powders the ZrO_2-CeO_2 hydroxide gels derived powders show better sinterability than those derived from anionic forms of these gels. In the latter systems nitrate gels sinter better than chloride ones.

References

[1]. Deptuła A., Rebandel J., Drozda W., Łada W., Olczak T.: Production of Spherical Powders of Inorganic Compounds by Water Extraction Variant of Sol-Gel Process. In: Better Ceramic Through Chemistry V. Eds. M.J. Hampden-Smith, W.G. Klemperer, C.J. Brinker. p. 277 (Mat. Res. Soc. Symp. Proc. 270, Pittsburgh, PA, 1992).

[2]. Deptuła A., Łada W., Olczak T., Chmielewski A.G.: Some Comments on the Production of Medium Sized Spherical Particles by Anion and Water Extraction Variant of Sol-Gel Process. In: Hollow and Solid Spheres and Microspheres-Science and Technology Associated with Their Fabrication and Application. Eds. M. Berg, T. Bernat, D.L. Wilcox Sr., J.K. Cochran Jr., D. Kellerman. p. 83 (Mat. Res. Soc. Symp. Proc. 372, Pittsburgh PA, 1995).

[3]. Deptuła A., Carewska M., Olczak T., Łada W.: J. Electrochem. Soc., 140, 2294 (1993).

LOCATION OF THE PROTON IN THE VERY STRONG O-H...O HYDROGEN BONDS IN 2-(N,N-DITHYLAMINO-N-OXYMETHYL)-4,6-DICHLOROPHENOL. A NEUTRON DIFFRACTION STUDY*

H. Ptasiewicz-Bąk, R. Tellgren[1/], I. Olovsson[1/], A. Koll[2/]

[1/]Institute of Chemistry, University of Uppsala, Sweden
[2/]Institute of Chemistry, University of Wrocław, Poland

The title compound has one especially interesting feature from the hydrogen bond point of view: it contains two crystallographically independent molecules A and B, both with a very strong intramolecular hydrogen bond O--H--O. Often in the case of such strong hydrogen bonds there is some crystallographic symmetry at the centre of the O--O bond (mirror plane or twofold axis perpendicular to the O--O bond or centre of symmetry). It is very difficult to determine with certainty whether the proton is precisely at the centre or slightly off-centred, even with neutron diffraction. Unless special technique is applied, the least-squares refinement will in the latter case give rise to two half-occupied positions. It is therefore impossible to decide whether there is actual disorder in the structure or just one off-centred proton.

The present compound is one of the rather few examples of potentially symmetric hydrogen bonds with no crystallographic symmetry in the bond. From a chemical point of view the oxygen bridging atoms in both molecules A and B have different character: one of the oxygens is bonded to carbon and the other to nitrogen (Fig.). Usually in such a situation asymmetric hydrogen bonds are formed.

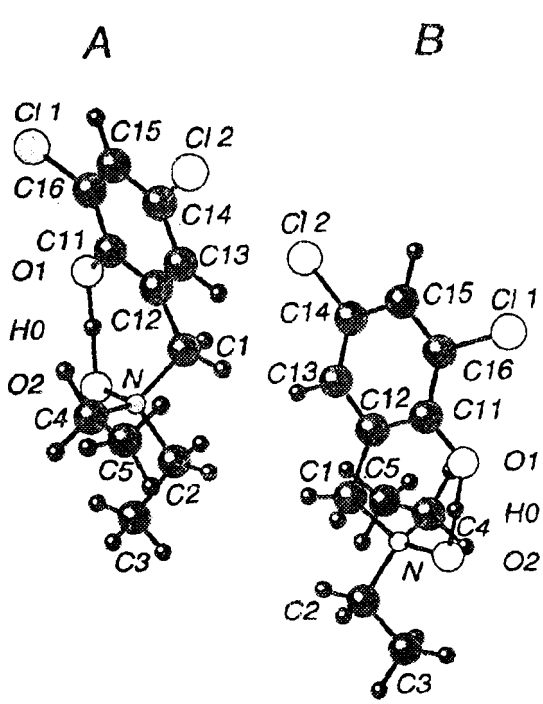

Fig.

*Submitted to Acta Crystallographica.

Due to the large uncertainty in the location of the proton in the X-ray study [1] a neutron diffraction investigation has now been performed to resolve this question.

The neutron data were collected at room temperature at the Neutron Research Laboratory in Studsvik on a Huber-Aracor four-circle diffractometer with a Cu(220) double monochromator. Crystal data: space group $P2_1/c$, a=11.729(3)A, b=16.232(4)A, c=13.689(3)A, β=107.37(3), V=2487.3A^3. Molecular formula $C_{11}H_{15}NO_2Cl_2$, M_r=264.2, Z=8.

The structure contains two different molecules A and B, with intramolecular hydrogen bonds O---O distances 2.423(4)A and 2.400(5)A, respectively, and with no crystallographic symmetry. The single crystal neutron diffraction study shows quite unambigously that the proton in both cases is located slightly off-centred. In the A molecule O1-H=1.167(6)A, H-O2=1.258(6)A and the angle O-H-O=175.8(5); in the B molecule O1-H=1.186(7)A, H-O2= =1.214(7)A and the angle O-H-O=176.5(5). As expected, the proton is closer to the centre in the slightly shorter hydrogen bond.

References

[1]. Koll A., Rospenk M., Sobczyk L., Głowiak T.: Can. J. Chem., 64, 1850-1854 (1986).

CRYSTAL CHEMISTRY OF COORDINATION COMPOUNDS WITH HETEROCYCLIC CARBOXYLIC ACIDS. PART VII: THE CRYSTAL AND MOLECULAR STRUCTURES OF CALCIUM COMPLEXES WITH 2-PYRAZINECARBOXYLIC AND 2,3-PYRAZINEDICARBOXYLIC ACIDS*

J. Leciejewicz, H. Ptasiewicz-Bąk

As a part of our research programme related to the crystal chemistry of metal coordination compounds with heterocyclic carboxylic acids [1-6], an X-ray diffraction study has been undertaken with the aim to determine the crystal structures of calcium complexes with 2-pyrazinecarboxylic and 2,3-pyrazinedicarboxylic acids. Pyrazine acids are known as effective chelating agents exhibiting donor sites represented by the carboxylic group (or groups) and two heteroring nitrogens. In the 3-d transition metal dipyrazinates [3] and the uranyl dipyrazinate [6] only nitrogen atom located in the neighbourhood of the carboxylic group has been found to be chelating the central ion, jointly with one oxygen of this carboxylic group.

The crystal structure of calcum dipyrazinate tetrahydrate (title compound I) confirms this tendency. Monomeric molecules consist of a calcium atom linked to four oxygens of water molecules (d_{Ca-O}=2.369-2.517 Å), to two nitrogens (d_{Ca-N}=2.617 Å) and two carboxylate oxygens of two pyrazinic acid molecules (d_{Ca-O}=2.465 Å). Fig.1 shows the molecule of the title compound I. The molecules are held together by a system of fairly strong hydrogen bonds as indicated by their lengths 2.68-2.89 Å.

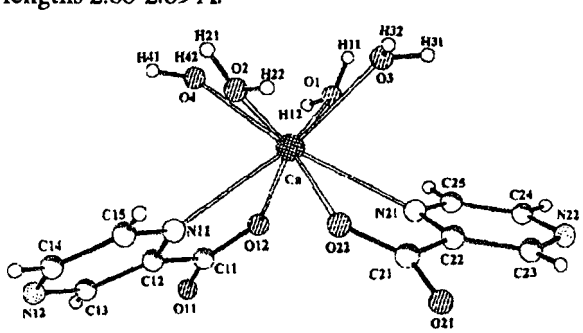

Fig.1. The molecule of title compound I.

One might expect that addition of another carboxylic group to the pyrazine ring will enhance its second nitrogen to act as a ligand. Calcium complex with pzdc - 2,3-pyrazinedicarboxylic acid (title compound II) was obtained and single crystals grown. In the structure of this compound molecular sheets have been found piled up in the direction of the c axis. The sheet is formed by calcium atoms linked to four pzdc molecules: one of them donates a nitrogen (d_{Ca-N}=2.675 Å) and an oxygen atom (d_{Ca-O}=2.426 Å), two oxygens are donated by a bidentate carboxylic group (d_{Ca-O}=2.574 Å) of another pzdc molecule. A chain -pzdc-Ca-pzdc - could be visualized. The oxygens of the above bidentate carboxylic group are also linked to calcium atoms in chains above and below (d_{Ca-O}=2.309 and 2.332 Å). Fig.2 displays a fragment of the sheet. In addition, two water molecules (d_{Ca-O}=2.432 Å) are attached to each calcium ion completing eightfold

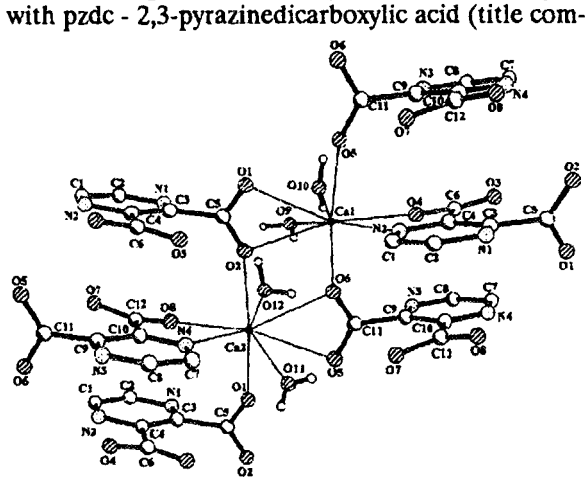

Fig.2. A fragment of the molecular sheet in the structure of title compound II.

*Submitted to Journal of Coordination Chemistry.

coordination. The molecular alignment within a sheet is shown in Fig.3. Two solvation water molecules were identified between the sheets. They link the sheets via hydrogen bonds in the way shown in Fig.4.

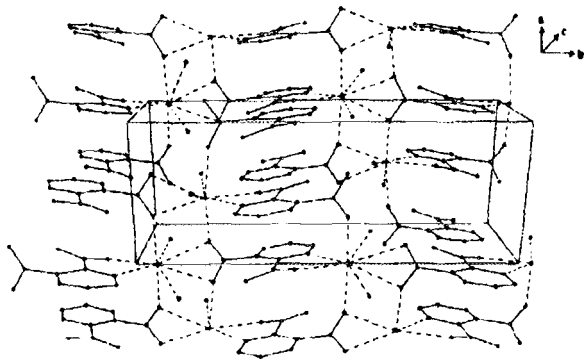

Fig.3. The packing diagram of the structure of title compound II viewed along the c axis.

Unlike in the pzdc complexes with 3-d transition metals, the second carboxylic group in the title compound II does not initiate the nearest to it heteroring nitrogen atom to chelate the central ion. This effect might be connected with the steric restrictions imposed by the calcium atom which usually coordinates eight ligands.

X-ray data collection was carried out using the KUMA KM4 four circle diffractometer at the Institute of Nuclear Chemistry and Technology. CuK_α radiation. Data processing and refinement was performed with SHELXL 93 programme package.

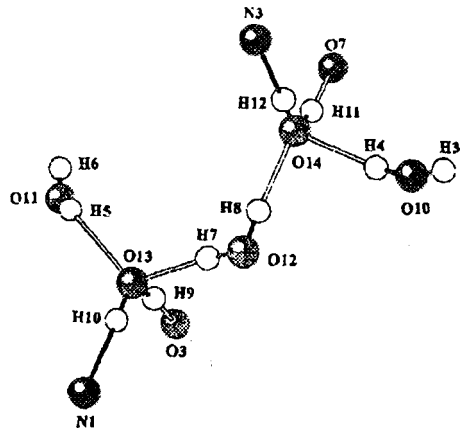

Fig.4. Hydrogen bonds operating via solvate water molecules located between molecular sheets in title compound II.

References

[1]. Alcock N.W., Kemp T.J., Leciejewicz J.: Inorg. Chim. Acta, 1884, 208 (1991).
[2]. Paluchowska B., Lis T., Leciejewicz J.: Acta Crystallogr., C50, 683 (1994).
[3]. Ptasiewicz-Bąk H., Leciejewicz J., Zachara J.: J. Coordin. Chem., 36, 317 (1995).
[4]. Paluchowska B., Maurin J.K., Leciejewicz J.: Acta Crystallogr., C52, 342 (1996).
[5]. Paluchowska B., Maurin J.K., Leciejewicz J.: Acta Crystallogr., C52, 347 (1996).
[6]. Alcock N.W., Kemp T.J., Roe M.S., Leciejewicz J.: Inorg. Chim. Acta (in press).

CRYSTAL CHEMISTRY OF COORDINATION COMPOUNDS WITH HETEROCYCLIC CARBOXYLIC ACIDS. PART VIII: THE CRYSTAL AND MOLECULAR STRUCTURES OF MAGNESIUM COMPLEXES WITH 2-FURANCARBOXYLIC AND 3-FURANCARBOXYLIC ACIDS

B. Paluchowska[1/], J.K. Maurin[1/], J. Leciejewicz

[1/]Institute of Atomic Energy, Otwock-Świerk, Poland

Magnesium complex with 2-furancarboxylic acid (title compound (1)) forms dimeric molecules in which two Mg atoms are bridged by one water molecule and the oxygen atoms donated by bidentate carboxylic groups of two furoate molecules. A distorted coordination octahedron around one of the Mg^{2+} cations consists of two oxygen atoms, each donated by monodentate carboxylic group, an oxygen of a water molecule, an oxygen from the bridging water molecule and two oxygens from the bridging bidentate carboxylic groups (Fig.1). The Mg-O bond lengths range from 2.006 to 2.162 Å. The second Mg^{2+} ion exhibits also a distorted octahedral coordination composed, apart from the above three bridging oxygens, by three water molecules. The corresponding Mg-O bond distances amount to 2.027-2.097 Å; the Mg-Mg distance is 3.575 Å. Extensive hydrogen bonding scheme is operating between the unbonded oxygen atoms of the monodentate carboxylic groups and the dimer molecules via the coordinated waters, supplemented by the solvate water molecules.

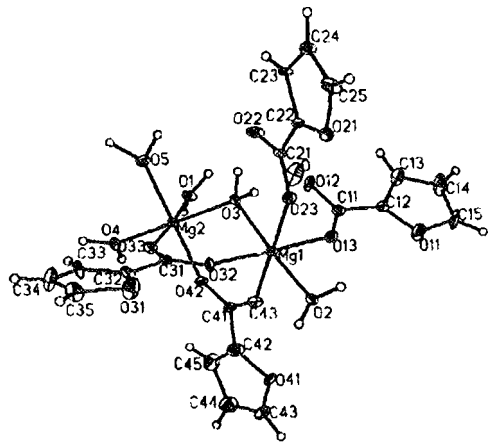

Fig.1.

Polimeric chain structure was detected in the Mg^{2+} complex with 3-furancarboxylic (title compound (2)). Magnesium atoms are linked by bidentate carboxylic groups. With three water oxygens and an oxygen from a monodentate carboxylic group an octahedral coordination around Mg atom is completed. Fig.2 shows a fragment of the chain, which is propagating along the c direction. In the picture, the bridging oxygens are denoted as 021n and 021a. The Mg-O bonds range from 2.029 to 2.147 Å. There is also one solvent water molecule, which takes part in the hydrogen bond system.

In both structures the Mg atom does not exhibit any preference for the bonding to the heteroring oxygen atom.

X-ray data collection was carried out using the KUMA KM4 four circle diffractometer at the Institute of Nuclear Chemistry and Technology. CuK_α radiation. Data processing and refinement was performed with SHELXL 93 programme package.

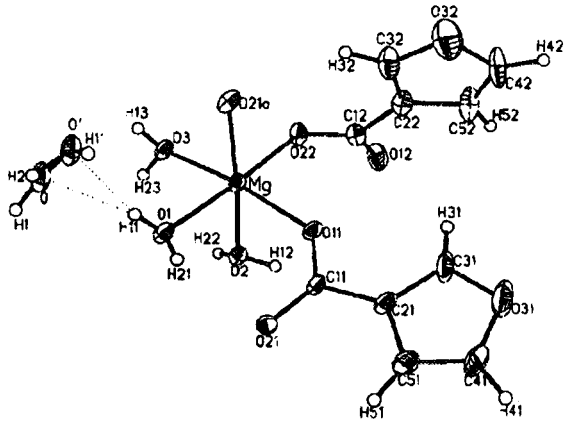

Fig.2.

CRYSTAL CHEMISTRY OF COORDINATION COMPOUNDS WITH HETEROCYCLIC CARBOXYLIC ACIDS. PART IX: THE CRYSTAL AND MOLECULAR STRUCTURES OF DINUCLEAR COPPER (II) COMPLEXES WITH 3-FURANCARBOXYLIC ACID AND 2-THIOPEPHENCARBOXYLIC ACID*

B. Paluchowska[1/], J.K. Maurin[1/], J. Leciejewicz

[1/]Institute of Atomic Energy, Otwock-Świerk, Poland

The crystals of copper (II) di(2-furoate) dihydrate (title compound (1)) and copper (II) dithiophenate dihydrate (title compound (2)) contain dimeric units composed by two copper atoms bridged by four bidentate carboxylic groups donated by the title acids. The molecule of compound (1) is displayed in Fig. The coordination about the Cu atom is square pyramidal: four oxygens from the carboxylic groups make a plane, an oxygen of a water molecule is above it. In the case of title compound (1) the copper atom is situated 0.209 Å above this plane. All Cu-O bond distances fall in the normal range of values (1.93-1.97 Å) encountered in copper carboxylate complexes, the Cu-Cu distance being 2.612 and 2.605 Å in title compounds (1) and (2) respectively The common feature of both compounds is the absence of any direct bonding between the heteroring atom (oxygen or sulfur) and the copper cation, however, the heteroatoms participate in a network of intermolecular hydrogen bonds.

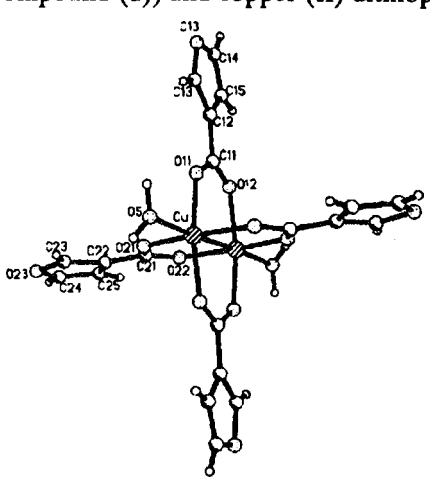

Fig. The molecule of title compound (1).

X-ray data collection was carried out using the KUMA KM4 four circle diffractometer at the Institute of Nuclear Chemistry and Technology. CuK_α radiation. Data processing and refinement was performed with SHELXL 93 programme package.

*Journal of Coordination Chemistry (in press).

MAGNETIC ORDERING IN LANTHANIDE INTERMETALLIC PHASES

J. Leciejewicz, A. Szytuła[1/]

[1/]Institute of Physics, Jagiellonian University, Kraków, Poland

A large number of ternary lanthanide stannides with 1:1:1 stoichiometry exhibits the hexagonal LiGaGe type of crystal structure. Some of them have been studied by neutron diffraction, supplemented by magnetometric methods.

Magnetic ordering in RAgSn (R=Pr,Nd,Tb,Dy,Ho,Er)

Some RAgSn compounds were reported to show at 4 K simple colinear antiferromagnetic ordering, however, these results were obtained basing on low resolution neutron diffraction patterns. New sets of data have been collected at 1.5-1.9 K and at a number of temperatures below the respective Neel points not only for NdAgSn, TbAgSn and HoAgSn which were studied earlier [1, 2] but also for three other phases belonging to the RAgSn series: PrAgSn, DyAgSn and ErAgSn. Neutron diffractograms of all the six compounds were obtained using the E6 instrument at the BER II reactor at Hahn-Meitner Institute in Berlin, Germany. The

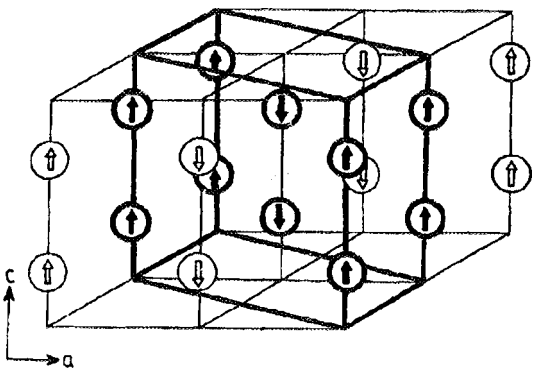

Fig.1. The antiferromagnetic unit cell of NdAgSn, TbAgSn, (above 11 K) DyAgSn, HoAgSn (below 10 K) and ErAgSn (below 4.5 K).

neutron wavelength was 2.426 Å. The data are currently processed and evaluated.

PrAgSn - neutron patterns show that below the Neel point at 9 K long range magnetic order has been set up. The magnetic peaks positions indicate an incommensurate magnetic structure.

NdAgSn - neutron data collected at 1.5 K confirm the existance of the previously reported collinear antiferromagnetic structure with Nd^{3+} moments aligned along the hexagonal axis [2]. This structure is shown in Fig.1.

TbAgSn - excellent resolution of neutron diffraction patterns made it possible to detect at 1.5 K satellite peaks close to the main antiferromagnetic peak M010 connected with the magnetic structure displayed in Fig.1. The satelite peaks vanish at 11 K leaving the main magnetic peak. M010 associated

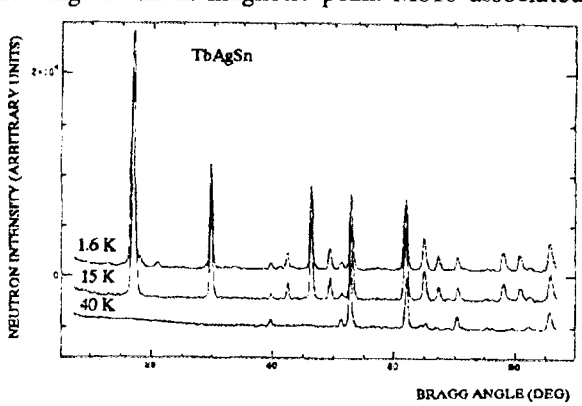

Fig.2. Neutron diffraction patterns of TbAgSn recorded at 1.6, 15.0, 40.0 K.

with the magnetic structure displayed in Fig.1. It falls to zero at 35 K - the Neel point (Fig.2).

DyAgSn - the collinear antiferromagnetic structure (Fig.1) has been detected at 1.6 K. It is stable to 9 K - the Neel point.

HoAgSn - the earlier reported [1] collinear antiferromagnetic structure (Fig.1) was found to be stable at 1.6 K, however, at 10 K two satellite peaks are observed indicating that the transition to the paramagnetic state proceeds via a noncollinear

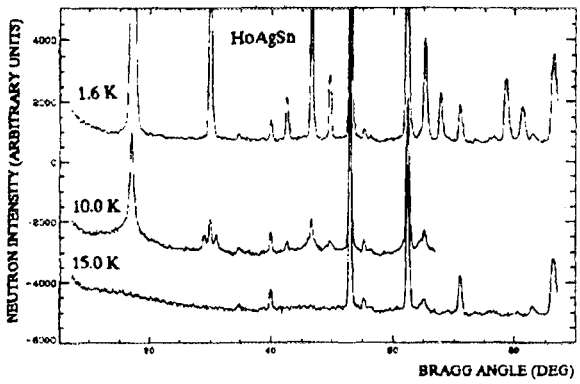

Fig.3. Neutron diffraction patterns of HoAgSn.

magnetic phase. The Neel point has been confirmed to be at 11 K (Fig.3).

ErAgSn - neutron diffractograms recorded between 1.7 and 6 K show the colinear antiferromagnetic structure (Fig.1) transforms itselt at 4.5 K into a noncolinear order, as reflected by appearence of satellite magnetic peaks close to the strong M010 magnetic reflection (Fig.4). The intensities of all

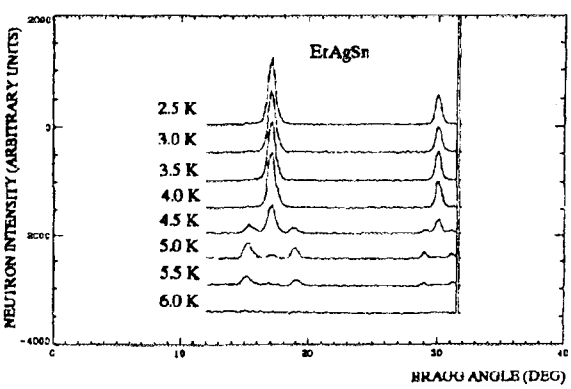

Fig.4. Neutron diffractograms of ErAgSn.

magnetic peaks fall to zero at 6 K - the Neel point of ErAgSn.

Magnetic structure of TbCuSn

RCuSn phases also show the hexagonal LiGaGe - type crystal structure. Neutron diffraction data have been up to now collected for CeCuSn and TbCuSn. As previously, the neutron data have been obtained at the E6 diffractometer, Hahn-Meitner Institute.

CeCuSn - neutron diffractograms recorded between 1.5 and 10 K indicate the presence of long range magnetic order of a complicated type stable below 6 K.

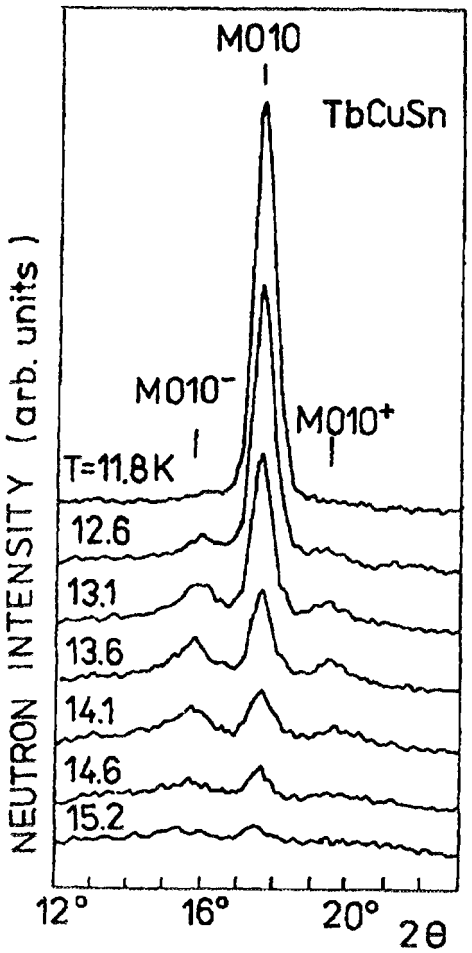

Fig.5. Neutron diffractograms of TbCuSn.

TbCuSn - Fig.5 shows neutron diffractograms obtained at temperatures between 1.5 and 15 K. A colinear, antiferromagnetic structure with magnetic moments localized on Tb^{3+} ions was deduced from the data obtained at 1.5 K. The moments are aligned normal to the hexagonal axis (Fig.6). A magnetic

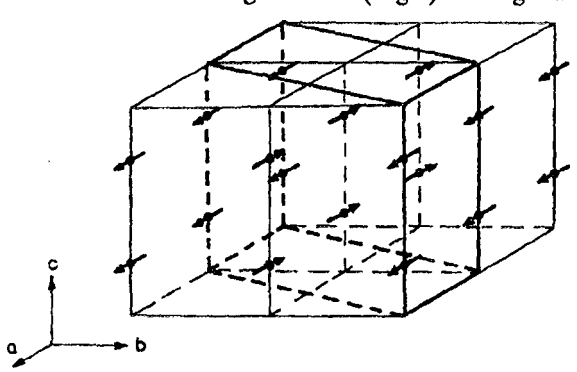

Fig.6. The collinear antiferromagnetic structure of TbCuSn at 1.5 K.

phase transition to an incommesurate structure described by the wave vector **k**=[0, 0.11, 0] takes place at 12 K. This structure is shown schematically in Fig.7. The moments are in the (001) plane and make angles from -39 to +39 deg. with the [100] axis. The magnetic moment localized on the Tb^{3+} ion amounts to 7.40(5) μ_B at 1.5 K. The Neel point is at 15.3 K [3].

Antiferromagnetic ordering in the hexagonal phase of TbPtSn

TbPtSn is known to have two polymorphic modifications: orthorhombic (TiNiSi - type of crystal structure) and hexagonal (ZrNiAl - type structure). The orthorhombic phase exhibits at 1.5 K a sine modulated antiferromagnetic ordering which transforms itself at 10 K into another incommensurate structure which is stable up to the Neel point at 13.8 K [4-6].

Recently, the hexagonal modification was obtained in a quanity large enough te perform a neutron diffraction experiment. E6 diffractometer

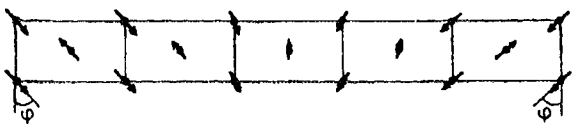

Fig.7. Schematic representation of the incommensurate magnetic structure of TbCuSn.

at BER II reactor (Hahn-Meitner Institute) was used to collect the data. Fig.8 displays neutron

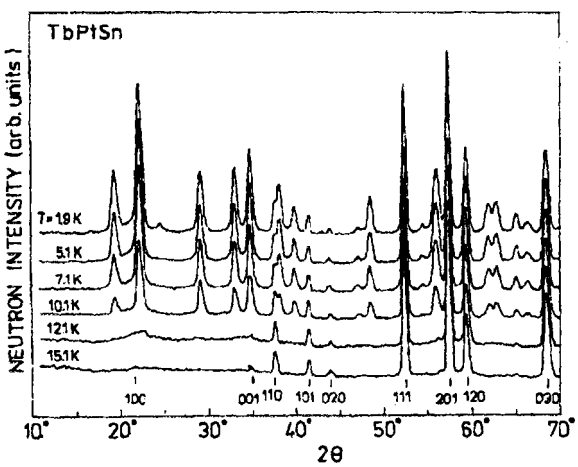

Fig.8. Neutron diffractograms of hexagonal TbPtSn.

patterns recorded at temperatures between 1.9 and 15 K. The magnetic structure which remains unchanged from 1.9 to 11 K (the Neel point) is defined by the wave vector **k**=[0.726, 0.766, $^1/_2$]. The magnetic moment on Tb^{3+} ion is 8.8 (10) μ_B at

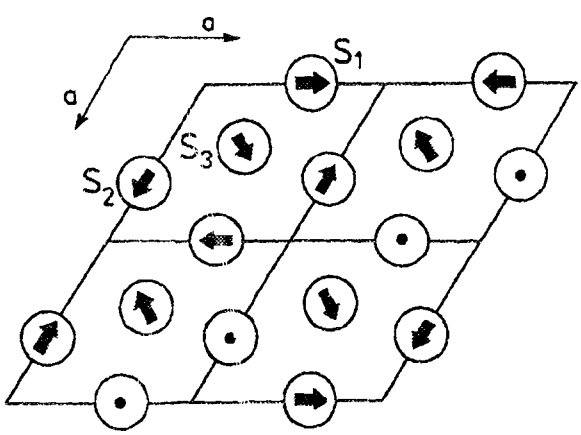

Fig.9. Magnetic moment alignment in the (001) plane in hexagonal TbPtSn.

1.9 K. The alignment of magnetic moments in the (001) plane is schematically shown in Fig.9. The magnetic cell is doubled in the c - direction, so that the moments in the adjacent plane are directed reversibly [7].

References

[1]. Bażela W., Leciejewicz J., Małetka K., Szytuła A.: Magnetic structure of TbAgSn and HoAgSn. J. Magn. Magn. Mat., 117, L1 (1992).

[2]. Bażela W., Guillot M., Leciejewicz J., Małetka K., Szytuła A., Tomkowicz Z.: Magnetic properties of RAgSn (R=Nd,Tb,Ho) compounds. J. Magn. Magn. Mat., 140-144, 1137 (1995).

[3]. Baran S., Leciejewicz J., Stuesser N., Szytuła A., Tomkowicz Z.: A magnetic phase transition in TbCuSn. Solid St. Commun. (in press).

[4]. Bażela W., Kolenda M., Leciejewicz J., Stuesser N., Szytuła A., Zygmunt A.: Magnetic structure of RPtSn (R=Ce,Tb,Ho). J. Magn. Magn. Mat., 140-144, 881 (1995).

[5]. Kolenda M., Leciejewicz J., Stuesser N., Szytuła A., Zygmunt A.: Incommensurate magnetic ordering in CePtSn and TbPtSn. J. Magn. Magn. Mat., 145, 85 (1995).

[6]. Szytuła A., Penc B., Kolenda M., Leciejewicz J., Stuesser N., Zygmunt A.: Antiferromagnetic ordering in RPtSn (R=Dy,Ho,Er) compounds. J. Magn. Magn. Mat., 153, 273 (1996).

[7]. Szytuła A., Kolenda M., Leciejewicz J., Stuesser N.: Non-colinear antiferromagnetic structure of hexagonal TbPtSn. J. Magn. Magn. Mat. (in press).

THE IINS SPECTROSCOPY OF AMINOACIDS III*: L-ISOLEUCINE

A. Pawlukojć, J. Leciejewicz, I. Natkaniec[1/]

[1/]Joint Institute of Nuclear Research, Frank Neutron Physics Laboratory, Dubna, Russia

Continuing our investigations of hydrogen bond vibrations in crystals of aminoacids by incoherent and inelastic neutron scattering (IINS), a study of normal (protonated) and deuterized isoleucine (L-2 amino-3-methylpentancarboxylic acid) has been completed.

NERA-PR inverted geometry time-of-flight spectrometer operating at the pulsed reactor IBR-2 at Dubna was used to collect neutron scattering data at 80 K. The incident neutron energy was determined by the reactor-sample flight path of 109.05 m, the energy of scattered neutrons - by pyrolytic graphite analysers (E=4.7 MeV) located behind a berylium filter. The spectra were recorded at ten scattering angles (mean 90 deg.) and summed up after subtractting the background due to the sample holder and cryostat.

Polycrystalline, commercial grade L-isoleucine was used for data recording. The deuterized sample had its aminogroup hydrogens substituted up to 95% by deuterium.

Sharp peaks were observed on IINS spectra recorded at 80 K. Therefore, the vibrations were treated as harmonic and the phonon density of states function $G(\omega)$ was calculated assuming one phonon mechanism.

This function, obtained for the protonated and deuterized samples is shown in Fig. The modes observed at 505 and 518 cm^{-1} on the $G(\omega)$ pattern and marked by arrows in Fig. were identified as due to

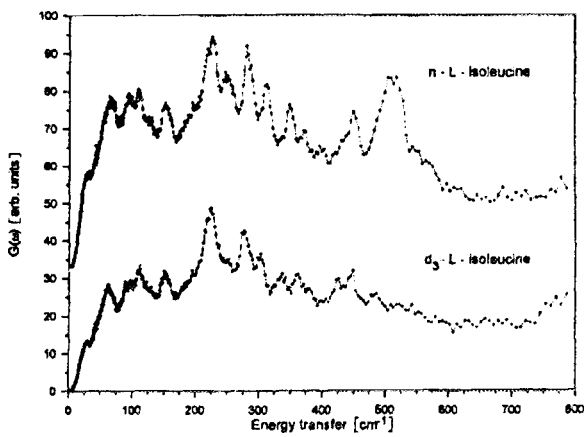

Fig. Phonon density of states function against energy transfer for n-L-isoleucine and d3-L-isoleucine.

the vibrations of strong hydrogen bonds operating between the nitrogen atom of an aminogroup and the nearest oxygen atom of the carboxylic group belonging to the adjacent molecule. The mode at 250 cm^{-1} was ascribed to weak hydrogen bonds with the N-H...O distance longer than 3.0 Å.

*Part I. Pawlukojć A, Bobrowicz L., Natkaniec I., Leciejewicz J.: Neutron spectroscopy study of L- and DL-valine. Spectrochim. Acta, 51A, 303 (1995).
Part II. Pawlukojć A., Leciejewicz J., Natkaniec I.: The IINS spectroscopy of aminoacids: L-leucine. Spectrochim. Acta (in press).

RADIOBIOLOGY

PL9700825

DNA REPAIR IN ADAPTED HUMAN LYMPHOCYTES

PL9700824

M. Wojewódzka , I. Szumiel

In our previous work [1] we demonstrated that the development of adaptive response in human lymphocytes requires the presence of calcium ions in the medium at the time of applying the adapting dose. This result was interpreted in terms of alarm signal hypothesis [2]. It could be expected that adaptation to the challenge dose is accompanied by a higher DNA repair rate and that intervention at the level of intracellular signal transduction would abolish the development of the adaptive response both at the cellular level (revealed by micronuclei frequency) and at the level of DNA repair.

To examine this assumption, the following experiments were carried out. Lymphocytes from 4 human (non-smoker) donors received an adapting dose of 0.01 Gy of X rays 6 h after stimulation with phytohaemagglutinin and a challenge dose of 1.5 Gy 10 h later. The adaptive response in three donors and its lack in the fourth donor was identified by the micronuclei frequency estimated after cytochalasin B treatment and cell harvest at 72 h (Fig.1).

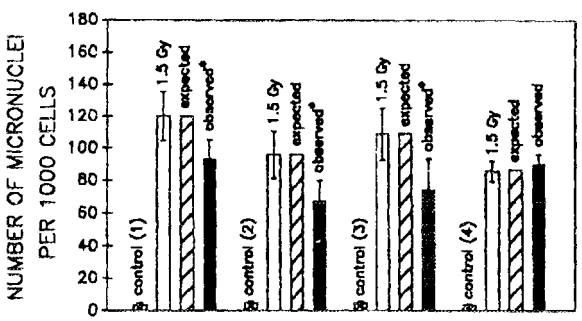

Fig.1. Comparison of the adaptive response induced in human lymphocytes with 1 cGy X-rays. The end-point analyzed was the frequency of micronuclei (5000 cells scored per experimental point). The first 3 donors show a statistically significant (Student's t-test, $P<0.001$) difference from the expected micronuclei frequency. Donor 4 has shown a lack of adaptive response.

Initial DNA damage and its repair rate were measured with the "comet" assay immediately after giving the challenge dose (on ice). Although in some experiments lower initial DNA damage and higher repair rate were observed in adapted, as compared to non-adapted lymphocytes (Fig.2), this was not a rule. On the other hand, lymphocytes from the donor lacking adaptive response (as estimated by the micronuclei test) repaired DNA damage at the same rate, irrespectively of irradiation with the adapting dose or sham-irradiation. These results are consistent with those of Wójcik et al. (in press), who observed a discrepancy between adaptation estimated from chromosomal aberration frequency and from DNA repair rate measured by the "comet" assay. Moreover, inhibitors of signal transduction, such as staurosporine, TMB-8, and anti-CD38 antibody, applied together with the adapting dose, prevent the development of the adaptive response, as identified by the micronuclei test. Nevertheless, these inhibitors do not significantly affect the rate of DNA repair in lymphocytes subjected to such combined (inhibitor+adapting dose) treatment. So, there is a discrepancy in the manifestation of the adaptive response at the cellular and molecular level. The higher rate of DNA repair, sometimes observed in the adapted cells, as compared to the non-adapted ones, does not seem to be a constant feature of adaptation.

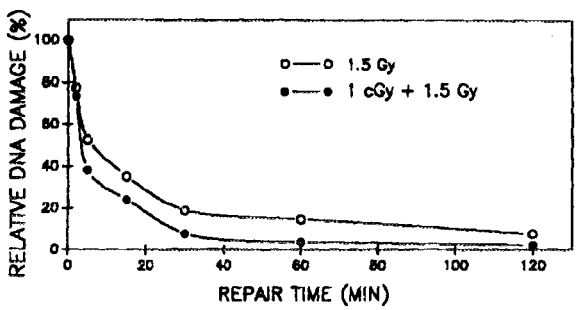

Fig.2. DNA repair rate (per cent damage remaining) in human lymphocytes after 1.5 Gy X-irradiation with or without 1 cGy pre-exposure.

References

[1]. Wojewódzka M.,Walicka M., Sochanowicz B., Szumiel I.: Int. J. Radiat. Biol., **66**, 99-109 (1994).

[2]. Weichselbaum R.R., Hallahan D.E., Sukhatme V., Dritschilo A., Sherman M.L., Kufe D.W.: J. Nat. Cancer Inst., **83**, 480-484 (1991).

INTERDEPENDENCE OF INITIAL DNA DAMAGE, ITS REPAIR AND SENSITIVITY TO TOPOISOMERASE I POISON, CAMPTOTHECIN

I. Grądzka, I. Szumiel

Two L5178Y (LY) murine lymphoma cell sublines, LY-R, resistant, and LY-S, sensitive to X-radiation, display inverse cross-sensitivity to camptothecin (CPT): LY-R cells are more susceptible to this specific topoisomerase I inhibitor than LY-S cells. After 1 h incubation with CPT, the doses that inhibit growth by 50% (ID_{50}) at 48 hrs incubation are 0.54 μM for LY-R cells and 1.25 μM for LY-S cells. Initial numbers of DNA-protein crosslinks (DPCs), measured at this level of growth inhibition, are two-fold higher in LY-R (5.6 Gray-equivalents) than in LY-S cells (3.1 Gray-equivalents), which corresponds well with the greater in vitro sensitivity of Topo I from LY-R cells to CPT [1, 2]. Converse-

ly, the initial levels of single-strand DNA breaks (SSBs) and double-strand DNA breaks (DSBs) are

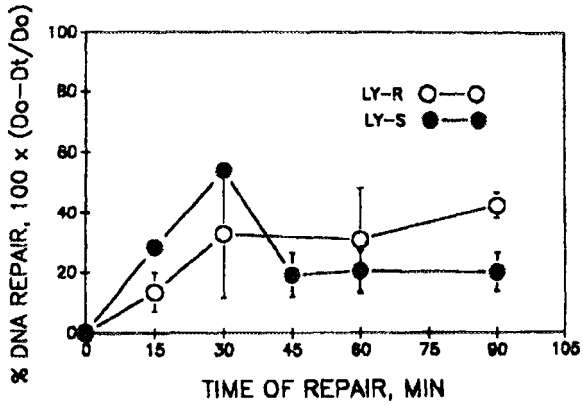

Fig. DNA double strand breaks (DSBs) measured by field inversion gel electrophoresis (FIGE), after 1 h incubation of LY cells with CPT and subsequent incubation in a fresh medium. DSBs values are given in Gray equivalents. Points are the means of 3-5 experiments ±SE.

lower in LY-R cells (4.2 Gray-equivalent SSBs and 5.8 Gray-equivalent DSBs) than in LY-S cells (8.0 Gray-equivalent SSBs and 12.0 Gray-equivalent DSBs). Dissimilarity in the replication-dependent DNA damage observed after 1 h treatment with CPT is not due to the difference in DNA synthesis rates between the two cell lines; this factor should be considered, because DSBs arise in consequence of collision of replication forks with the cleavable complex (DNA-CPT-topoisomerase I). The difference between LY sublines in this respect may arise from a substantially slower repair of DNA breaks in LY-S cells than in LY-R cells [3]. After a period of faster repair, there is a considerable slowing down of the process, with a resulting high level of the residual damage, as shown in Fig.

References

[1]. Kowalska-Loth B., Staroń K., Buraczewska I., Szumiel I., Kapiszewska M., Lange C.S.: Biochem. Biophys. Acta, **1172**, 17-123 (1993).

[2]. Staroń K., Kowalska-Loth B., Ząbek J., Czerwiński R.M., Nieznański K., Szumiel I.: Biochim. Biophys. Acta, **1260**, 35-42 (1995).

[3]. Włodek D., Hittelman W.N.: Radiat. Res., **112**, 146-155 (1987).

TOPOISOMERASE I IS NOT DOWN-REGULATED BY X-IRRADIATION IN L5178Y-R SUBLINE

I. Grądzka, I. Szumiel

A number of reports show a more than additive effect of combined treatment of mammalian cells with camptothecin (CPT) or other modulators of topoisomerase I and X-rays (reviewed in [1]). The molecular mechanism of this effect is unclear. Recently, a hypothesis has been put forward by Boothman et al. [1], which explains the potentiating of post-irradiation lethality by CPT treatment. The authors report downregulation of topoisomerase I activity after X-irradiation, due to an ADP-ribosylation mediated inactivation without diminished topoisomerase I gene expression. They propose that the downregulation is required for undisturbed DNA repair; otherwise, topoisomerase I would increase the number of double-strand breaks (DSBs) and contribute to the lethal effect of irradiation.

We have previously examined the response of two sublines of L5178Y (LY) murine lymphoma to combined X-ray+CPT treament [2]. We found that the radiosensitive subline LY-S is radiosensitized by CPT and this is reflected in an increased formation of the DNA-topoisomerase "cleavable complex", as judged from the amount of DNA-protein crosslinks (DPCs). In contrast, the other subline, LY-R, is not radiosensitized by CPT and the level of DPC remains unaltered. The result for LY-S cells is compatible with the hypothesis of Boothman et al. [1], which predicts an increased formation of the "cleavable complex" at the sites of X-ray-generated SSBs. To further explore the relevance of the hypothesis in the examined cellular model, we subjected LY sublines to pre-treatment with benzamide (BZ), an inhibitor of poly ADP-ribosylation), followed by X-irradiation. Then, we determined the activity of topoisomerase I in extracts from X-irradiated (5 Gy) cells 10 min after irradiation. As illustrated in Fig., activity of the extractable enzyme was diminished in X-irradiated LY-S cells, but not in LY-R cells. This result is

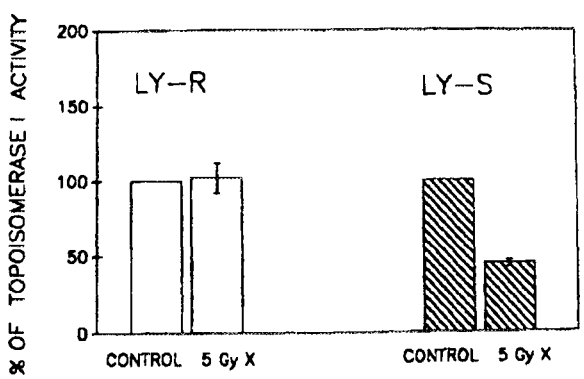

Fig. Downregulation of topoisomerase I in LY sublines after irradiation with 5 Gy X-rays. At 10 min interval after irradiation nuclear extracts were prepared, their protein concentrations were determined and plasmid DNA unwinding assays were performed as described in [1]. An equal amount of total protein was used for each reaction. Form I supercoiled substrate was separated from reaction intermediates and form II open circular plasmid DNA by agarose gel electrophoresis. The per cent loss of supercoiled substrate was determined after densitometry of the recorded separation pattern. The mean results are from 4 (LY-R) or 3 (LY-S) experiments ±SE.

consistent with the 5 times higher poly (ADP-ribose) polymerase activity in LY-S than in LY-R cells (unpublished results).

References

[1]. Boothman D.A., Fukunaga N., Wang M.: Cancer Res., 54, 618-4626 (1994).

[2]. Szumiel I., Buraczewska I., Grądzka I., Gasińska A.: Int. J. Radiat. Biol., 67, 41-448 (1995).

ANTIOXIDANT DEFENSE IN L5178Y SUBLINES: GLUTATHIONE

B. Sochanowicz

In an attempt to characterize cellular features that determine the sensitivity to hydrogen peroxide of two sublines of murine lymphoma L5178Y we estimated the reduced glutathione (GSH) fluorimetrically with monobromobimane (MBB) in cell suspensions containing $4x10^5$ cells in 1.5 ml PBS; the mean fluorescence was 198 (±29) for LY-R cells and 305 (±49) for LY-S cells, indicating a 54% higher GSH content in the latter subline. The measurement, however, is dependent on the intrinsic GSH transferase activity and the total thiol content [1]; so, the content calculated from the fluorescence does not necessarily agree with that obtained by an enzymatic assay or chromatographic determination.

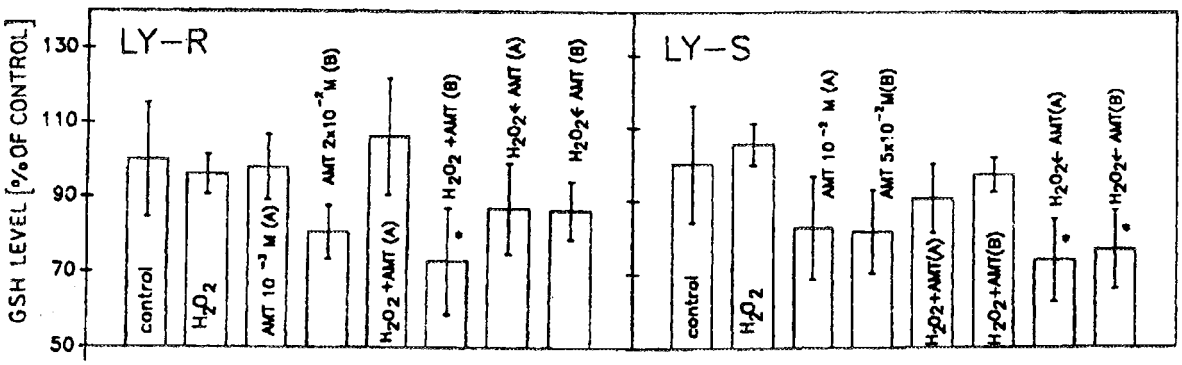

Fig. GSH levels in LY-R and LY-S cells following exposure to hydrogen peroxide 50 μM or AMT. H_2O_2+AMT denotes simultaneous 1 h exposure (at two AMT concentrations: LY-R, 1 mM (A) and 20 mM (B); LY-S 10 mM (A) and 50 mM (B). AMT → H_2O_2 denotes 1 h AMT treatment preceding 1 h hydrogen peroxide treatment. Fluorimetric determinations with MBB were repeated in duplicates 6 times; mean results ± standard deviation are shown. Significant differences from the control (Student's t-test, $P<0.05$) are marked by asterisks.

Hydrogen peroxide treatment (50 μM, 1 h, 37°C) did not change the GSH content of LY cells, whereas catalase inhibitor, AMT (aminotriazole), applied at 2 concentrations, lowered it slightly (Fig.). Supralethal hydrogen peroxide concentration, 1 mM, decreased the GSH content to 60.9 (±6.7) in LY-R cells and to 68.7 (±9.5) in LY-S cells (standard deviation in parantheses). Combined simultaneous treatment with hydrogen peroxide and AMT did not significantly decrease the GSH content. Sequential treatment (1 h AMT followed by medium change and 1 h hydrogen peroxide treatment) at both AMT concentrations significantly decreased the GSH content in the LY-S cells and only slightly - in the LY-R cells. These results, shown in Fig., may be taken as an indication of a relatively greater importance of catalase than GSH peroxidase (G-Px) in the antioxidant defense system of the LY cells. This especially was seen in LY-R cells, where upon inhibiting catalase the defense apparently was not taken over by G-Px, as judged from the relatively small decrease in the GSH content. The result did not comply with the about 2 times higher total activity of the enzyme in the LY-R than in the LY-S cells, but was consistent with the lower GSH content in the LY-R cells.

References

[1]. Shrieve D.C., Bump E.A., Rice G.C.: J. Biol. Chem., 263, 14107-14114 (1988).

ANTIOXIDANT DEFENSE IN L5178Y SUBLINES: CATALASE

E. Bouzyk, M. Kruszewski, N. Jarocewicz

We undertook an attempt to characterize cellular features that determine the sensitivity to hydrogen peroxide of two sublines of murine lymphoma L5178Y [1, 2]. These sublines are inversely cross-sensitive to hydrogen peroxide and X-rays. We found that the amount of initial DNA damage [1] and iron content [3] contribute to the sensitivity difference. Here, we report a diminished total activity of catalase and an enhanced susceptibility to catalase inhibitor, AMT (aminotriazole) in the sensitive subline.

Catalase activity in LY sublines differed about 2 times: it was 14085 (±2068) units per mg of the

PL9700829

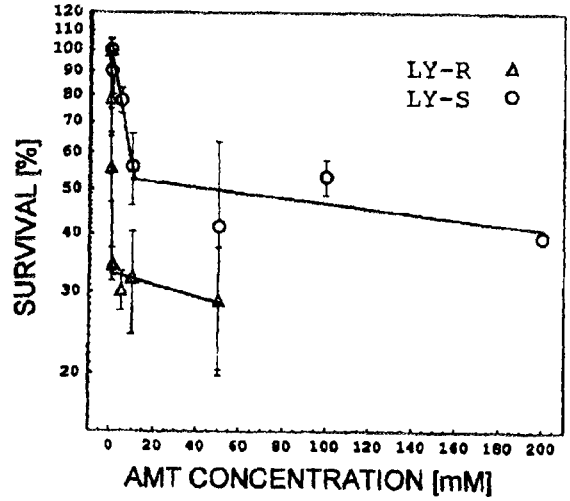

Fig.1. Sensitivity of L5178Y to AMT (3-amino-1,2,4-triazole, inhibitor of catalase). Cells were treated with AMT (1 h, 37°C). Surviving fractions were estimated by cloning and mean results shown from 3 experiments ±SD (standard deviation).

total cellular protein in LY-R cells and 26700 (±2682) - in LY-S cells (standard deviation in parantheses). Sensitivity of LY sublines to AMT was determined by cloning. As shown in Fig.1, the dose-survival curves were biphasic, with an exponential part and a plateau, probably reflecting the effect of a complete inhibition of catalase; when this was achieved, further increments in AMT concentration did not much affect the cells. The slopes of the steep exponential parts differed about tenfold for LY-R and LY-S cells (values -48.1 and -4.07, respectively), indicating a marked sensitivity difference. Also the plateau level was lower for LY-R cells (32.9% versus 53.3% for LY-S cells).

Accordingly, the decrease in catalase activity in extracts from AMT treated cells (1 h, 37°C) was greater in LY-R than in LY-S cells. Such a difference could be the result of differential AMT penetration into the intact cell or its compartments. Therefore, AMT treatment was applied in vitro, i.e. the inhibitor added directly to cell extracts for 20 min and catalase activity was estimated. Then, however, the decrease in activity percentage also was more pronounced in LY-R than in LY-S cells (Fig.2). These results showed that catalase from LY-R cells was more susceptible to AMT and that the effect measured in AMT-treated cells was not influenced by the inhibitor's accessibility inside the

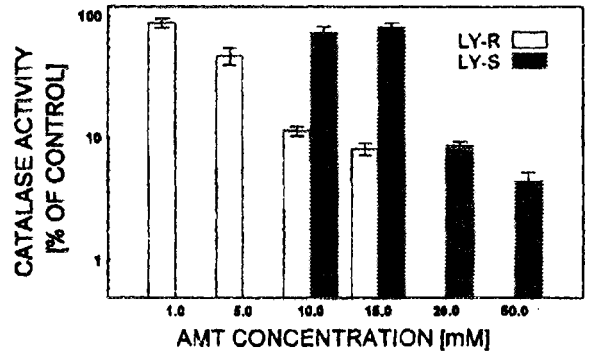

Fig.2. Catalase activity in AMT-treated LY cell homogenates. Enzymatic activity was determined in 3-4 experiments and related to the amount of protein (mg). Bars indicate SEM.

cell. The cytotoxicity of AMT alone was only roughly related to the degree of catalase inhibition; there was no statistically significant direct correlation (at α=0.05) in the AMT concentration range corresponding to the steep decrease in survival (results not shown). Hence, the cytotoxic effect of AMT might depend on another, unspecified target, different from catalase; alternatively, lack of defense by catalase against endogenous oxidants had a more pronounced effect in LY-R cells than in LY-S cells, in agreement with the higher sensitivity of the former cells, due to higher iron content [3] and in consequence, higher danger of damage by the products of Fenton reaction.

References

[1]. Kruszewski M., Green M.H.L., Lowe J.E., Szumiel I.: Mutat. Res., 308, 233-241 (1994).

[2]. Kruszewski M., Green M.H.L., Lowe J.E., Szumiel I.: Mutat. Res., 326, 155-163 (1995).

[3]. Szumiel I., Kapiszewska M., Kruszewski M., Iwaneńko T., Lange C.S.: Radiat. Environ. Biophys., 34, 113-119 (1995).

"PROTECTIVE ENZYMES" IN L5178Y SUBLINES AND DNA DAMAGE

M. Kruszewski, T. Iwaneńko

A more precise information about the role of selenium-induced glutathione peroxidase (G-Px) in the response of LY sublines to hydrogen peroxide is provided by experiments carried out with the "comet" assay. This assay (also called single cell gel electrophoresis) allows to detect DNA strand breaks in nucleoids from single cells (review in [1]). Nucleoid DNA is arranged as supercoiled loops protruding from the nuclear matrix. Damaged loops become released from the supercoiling status (1 single strand break per loop is enough to produce the effect) and - upon subsequent electrophoresis and staining - are seen in the fluorescence microscope as a "tail" of the comet, the head of which is the nucleoid core. The measure of damage is the "tail moment", i.e. the length of tail multiplied by the amount of DNA in the tail [2].

As shown in Fig., the level of DNA damage was the same in LY-R and LY-S cells after completing 1 h incubation with hydrogen peroxide, irrespective of the presence of AMT, inhibitor of catalase. Since DNA repair took place during exposure to the damaging agent, there are 2 possible interpretations of this observation: (1) catalase inhibition did not increase the damage, because reparable DNA damage was completely repaired; (2) catalase did

PL9700830

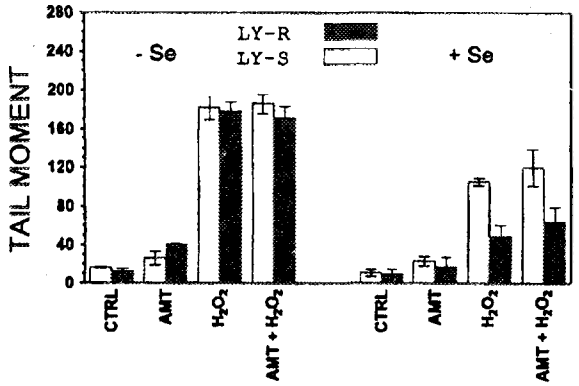

Fig. DNA damage expressed as tail moments (see text) in LY-R and LY-S cells following 1 h exposure at 37°C to hydrogen peroxide 50 μM, AMT (catalase inhibitor), and to combined simultaneous treatment with these agents. CTRL - control; AMT concentrations: LY-R cells - 5 mM, LY-S cells - 10 mM. These concentrations reduced the catalase activity by 80%.

not protect the nucleus and DNA damage was unaffected by catalase inhibition. In contrast, after induction of G-Px by selenium, DNA damage was considerably lowered. The decrease was relatively larger in LY-R than in LY-S cells, in spite of the higher increase in G-Px activity in the latter cells (LY-R cells: increase from 5.2 to 79.8 units x 10^3; LY-S cells: increase from 2.5 to 126.6 units x 10^3). This indicates a difference in the relative importance of catalase and G-Px for DNA protection in the LY sublines. It also may indicate differences in the intracellular distribution of both protective enzymes in relation to critical targets.

References

[1]. McKelvey-Martin V.J., Green M.H.L., Schmezer P., Pool-Zobel B.L., De Meo M.P., Collins A.: Mutat. Res., **288**, 47-63 (1993).

[2]. Olive P.L., Włodek D., Banath J.P.: Cancer Res., **51**, 4671-4676 (1991).

THE INFLUENCE OF COPPER (II) ON RADIATION-INDUCED DAMAGES TO DNA

H.B. Ambroż, I. Grądzka, T.J. Kemp[1/], M. Kruszewski, G.K. Przybytniak, T. Wrońska

[1/]Department of Chemistry, University of Warwick, Coventry, Great Britain

Primary products of radiation-induced, direct damages to DNA can be studied by EPR spectroscopy. According to molecular ab initio calculations [1] as well as experimental evidences [2, 3] the favoured site of electron localization is thymine ($T^{\cdot -}$) and cytosine ($C^{\cdot -}$) while the holes are mainly localized on guanine ($G^{\cdot +}$). Also our results indicate that at 77 K these transients exhibit a spectrum which is superposition of all of them (Fig.1a). It is known that if the temperature is raised up above 77

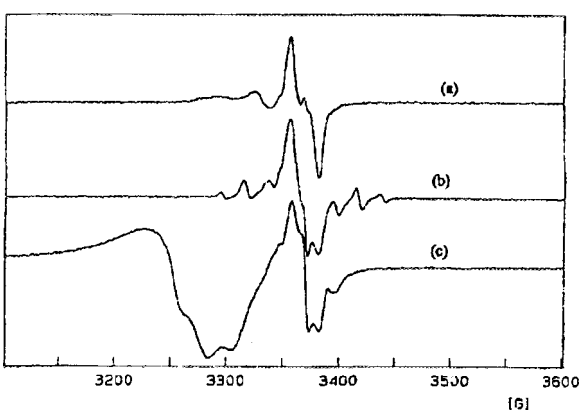

Fig.1. EPR spectra of DNA (calf thymus) 100 mg/ml, 77 K: (a) after gamma irradiation with dose 4.8 kGy; (b) after annealing, recorded at 77 K; (c) as (b) with 10 mM Cu(II).

K the radical anion of thymine $T^{\cdot -}$ reacts with a proton [2] giving the radical $TH^{\cdot}$ which could be followed by observation of very characteristic octet (Fig.1b). The addition of copper ion Cu(II) at a concentration higher than 10 mM distinctly decreases line intensities (Fig.1c). If the concentration reaches 20 mM they disappear completely.

The simplest explanation is scavenging of electrons or one electron oxidation of $T^{\cdot -}$ by Cu(II). In that case however the reduction of Cu(II)-DNA complex signal should be observed. But contrary, in our experiments, after annealing the intensity of these lines is higher. The reason could be that part of the added Cu(II) is binded to DNA in the form of a dimer structure $Cu^{2+} \cdots Cu^{2+}$, and then undetectable by EPR [4]. After one-electron reduction the dimer decomposes to Cu(II) and Cu(I) and the recorded amount of Cu(II) complexes increases almost twice. It seems that at that range of concentration the majority of all Cu(II) exsists in an aggregated, dimagnetic form. Such effect can be explained if the dimers are more favourably situated

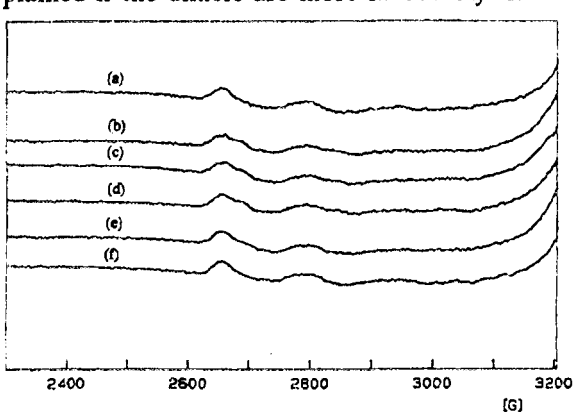

Fig.2. EPR spectra of the parallel lines of Cu(II) (2 mM) in Cu(II)-DNA complex, 77 K: (a) before irradiation; (b) after gamma irradiation with dose 4.8 kGy; (c-f) after gradual annealing, recorded at 77 K.

than the monomers (probably guanine and cytosine are involved) and then more easily accept electrons.

According to our results their role is less significant in capture electrons in ionization events and more evident in secondary redox processes.

The Cu(II)-DNA complexes have well defined EPR spectral parameters. Almost the same signal is obtained under various conditions. The only noticed change is a small additional spectrum (A=152 mT, g=2.28) induced by gamma irradiation observed for the low concentration of Cu(II) (2 mM) which disappears on sample warming (Fig.2). Some of complexing fragments of DNA after irradiation can entirely change their properties i.e. by oxidation ($G^{\cdot+}$). Obviously Cu(II) is not in dynamic equilibrium with other complexing sites at cryogenic temperatures. For that reason the structure of the intermediate (which disappears after warming) could be observed.

Other reason of this detection could be the $Cu^{2+} \cdots Cu^{1+}$ dimer in which exchange between the two copper ions is recorded as a new signal. It does not imply that the only one $Cu^{2+} \cdots Cu^{2+}$ dimer structure is possible in DNA chain. The first dimer is much more populated at higher concentrations and after one electron reduction disintegrates. The second dimer concerns only a small fraction of all Cu(II) ions, is more easily accomodated and better complexed if reduced to the $Cu^{2+} \cdots Cu^{1+}$ dimer. These sites are saturated at a Cu:base-pair ratio of 1:40, as was postulated by Symons [5].

The role of Cu(II) in direct and indirect damages of pBR322 plasmid DNA have been estimated by gel electrophoresis. Although conclusions from EPR spectroscopy indicate that in direct damages the ion Cu(II) (or its dimer) accepting electrons acts as a protection agent the total effect, when direct and indirect damages are taken into account, is different. At the concentration of 10 mM Cu(II), plasmid (0.2 mg/ml) after gamma irradiation with a dose of 200 Gy occurs only in an open circular nicked form (II) (single strand-break) or a linear form (III) (double strand-break). The same degree of damages is caused without participation of Cu(II) by a dose of 500 Gy. The strand-breakage is accelerated by copper (II) via indirect way. For lower concentrations (1 mM Cu(II)), at 200 Gy, the fraction of undamaged superhelical form is lower than for the pure plasmid. Hydrated Cu(II) ions catalyse the decomposition of H_2O_2 forming ·OH radicals which attack DNA and in this way sensitize DNA cleavage. The mechanism of this reaction is still discussed.

References

[1]. Colson A.O., Sevilla M.D.: Int. J. Radiat. Biol., **67**, 6, 627 (1995).

[2]. Symons M.C.R.: J. Chem. Soc., Faraday Trans. 1, **83**, 1 (1987).

[3]. Wang W., Yan M., Becker D., Sevilla M.D.: Rad. Res., **137**, 2 (1994).

[4]. Pezzano H., Podo F.: Chem. Rev., **80**, 5, 366 (1980).

[5]. Cullis P.M., McClymont J., Bartlett M.N.O., Symons M.C.R.: J. Chem. Soc., Chem. Commun., **18**, 599 (1987).

NUCLEAR TECHNOLOGIES

AND

METHODS

PL9700831
PL9700832

PROCESS ENGINEERING

MULTISTAGE PROCESS OF DEUTERIUM AND HEAVY OXYGEN ENRICHMENT BY MEMBRANE DISTILLATION

A.G. Chmielewski, G. Zakrzewska-Trznadel, N.R. Miljević[1/], A. Van Hook[2/]
[1/]Institute of Nuclear Science, Vinca, Belgrade, Yugoslavia
[2/]Chemistry Department, University of Tennessee, Knoxville, USA

Membrane processes have been employed in nuclear technology for many years. The application of membrane permeation for natural isotope enrichment was discussed previously [1, 2]. It was shown that permeation coupled with phase transition is characterized by a high H/D and $^{16}O/^{18}O$ separation factor [3, 4]. An economic analysis of the process of separation of hydrogen and oxygen isotopes in a system of two countercurrent cascades combined in a series showed many advantages and suggested that it could compete with other methods of isotope enrichment [5]. One stage experiments demonstrated many advantages of membrane distillation, which can be driven with waste heat. Therefore energy demand can be significantly reduced.

A new experimental setup for investigation of a multistage process of membrane distillation was constructed. Four permeation cells connected in a series simulated a 4-stage countercurrent cascade.

Two configurations of membrane distillation (MD) employing PTFE flat-sheet membranes were investigated, including direct contact MD and an air gap MD:

a) Direct contact membrane distillation (DCMD). The membrane directly contacts warm and cold solutions. The permeate condenses in the cold stream. The counterflow principle can be applied for both stream and high heat transfer coefficients accompanying the heat transport through the membrane. It is easy to recover part of the heat in this configuration by emploing additional heat exchangers.
b) Air-gap membrane distillation (AGMD). An additional air gap is involved. The permeate condenses on a separate surface cooled by a cold stream flowing counter-current to the warm stream. The heat lost in this configuration is lower than in a) arrangement, but heat recovery is more difficult.

The first, direct contact MD is more efficient. It is characterized by a high distillate flow rate. The temperature polarisation coefficients, were higher for direct contact MD.

The experimental setup was equipped with a data acquisition system composed of a 486/256 kB computer (CPU 486DX/66MHz) and a PCL 813, 32-channel A/D converter card. All temperatures and increments of permeate weight were recorded with the computer. The measuring signals were collected by a system of 13 thermocouples, 12 resistance thermometers and 4 electronic balances.

The vapour pressure difference across the membrane, which results from the temperature difference, causes the evaporation of water and its diffusion from the warm to the cold side. The distillate condensing on the cold side is depleted in heavy isotopes of hydrogen and oxygen, while the worm stream is enriched. The H/D and $^{16}O/^{18}O$ separation factors were determined for the 4-stage cascade.

References

[1]. Sun-Tak Hwang, Kammermeyer K.: Membranes in Separation, Techniques of Chemistry. Vol.VII. A. Wiley-Interscience Publication, New York-London-Sydney-Toronto 1975.
[2]. Chmielewski A.G., Zakrzewska-Trznadel G., Miljević N.R., Van Hook W.A.: Sposób wzbogacania wody naturalnej w tlen-18. Patent 168 152.
[3]. Chmielewski A.G., Zakrzewska-Trznadel G., Miljević N.R., Van Hook W.A.: Sep. Sci. Technol., 30 (7-9), 1653-1667 (1995).
[4]. Chmielewski A.G., Zakrzewska-Trznadel G.: Efekty izotopowe wodoru i tlenu w procesie permeacji wody przez membrany polimerowe. Prace Wydziału Inżynierii Chemicznej i Procesowej PW, XXII, 1-2, 23 (1995).
[5]. Chmielewski A.G., Matuszak A., Zakrzewska-Trznadel G., Van Hook W.A., Miljević N.R.: Sep. Sci. Technol., 28 (1-3), 909-927 (1993).

RADIOTRACER INVESTIGATIONS OF FLUE GAS FLOW DYNAMICS IN TWO STAGE IRRADIATION PILOT PLANT FOR NO_x AND SO_2 REMOVAL IN POWER STATION IN KAWĘCZYN

A.G. Chmielewski, A. Owczarczyk, J. Palige, A. Dobrowolski, E. Iller

Using radiotracers two series of experiments were carried out on flue gas flow dynamics in a two stage irradiation pilot plant at Kawęczyn for the removal of NO_x and SO_2.

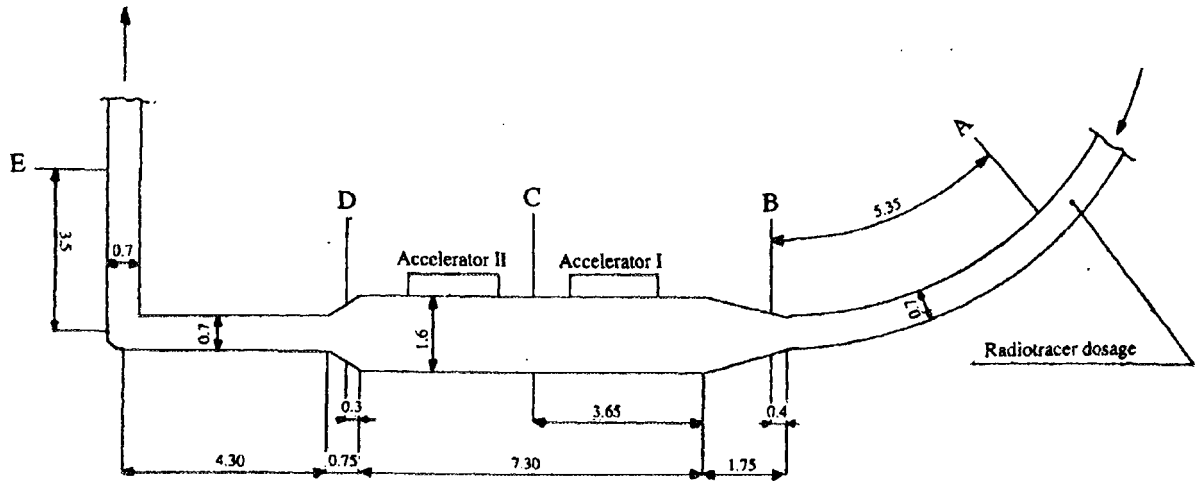

Fig.1. Location of scintillation probes during radiotracer investigations of flue gas flow dynamic in process vessel in EPS Kawęczyn.

The two accelerators were switched off during the first series of experiments and switched on during the second series of experiments. In both the series flue gas flow rates were similar and were maintained in the range 5000 to 15000 Nm^3/h. Br-82 in the form of methyl bromide of activity 2-5 mCi was used as radiotracer. Measurement of changes in radioactivity of the gas stream after tracer injection were made using scintillation probes connected to an electronic data acquiring and recording system. Location of the scintillation probes is presented in Fig.1 (series 1 - A,B,C,D; series 2 - A,E).

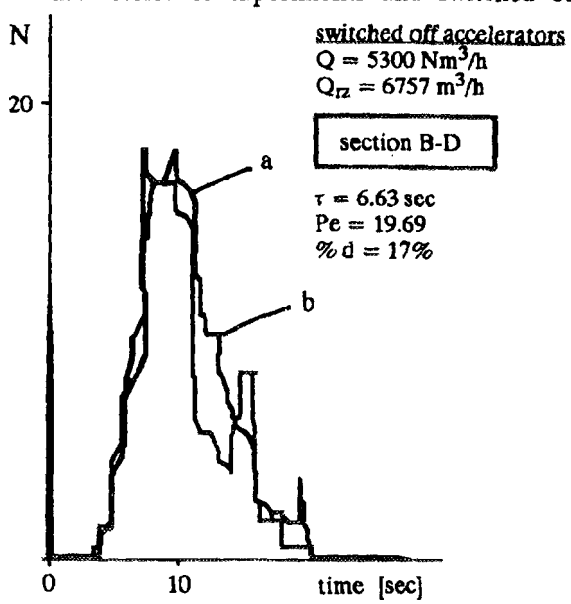

Fig.2. Comparison output signal (a) with model output signal (b) for investigated B-D section by switched off accelerators.

The results obtained have shown good gas mixing conditions and a longer mean residence time in the case of the switched on accelerators because of the heat streams convention caused by temperature gradient. In this case the zone of flow stagnation has been close to zero while in the case of the switched off accelerators the 17% contribution of the flow stagnation zone has been observed. The most adequate description of the dynamic behaviour of flue gas appeared to be the model of plug flow with turbulent diffusion. The model parameters values: mean residence time (τ) and Peclet number (Pe) were established by using experimental data with the help of an optimization method. Results of calculations have shown good agreement of the model with experimental data. An example is presented in Fig.2.

The very low contribution of the dead volume in the process vessel under operational conditions as well as lack of such unfavourable phenomena as back flow, channeling, recycling etc. allow us to state that the reactor construction is close to optimal.

INFLUENCE OF DOSE DISTRIBUTION AND FLOW PATTERN BETWEEN IRRADIATION STAGES ON REMOVAL OF NO_x

A.G. Chmielewski, B. Tymiński, A. Dobrowolski

The efficiency of NO_x removal for single and double stage irradiation processes with regard of dose distribution in the cross section of process vessel and flow pattern of flue gas between the stages has been calculated on the basis of Wittig's experimental equation [1].

This equation has the following form:

$$\alpha=\frac{[NO_x]_0-[NO_x]}{[NO_x]_0}=k_1[1-\exp(-k_2D/[NO_x]_0)] \quad (1)$$

where: α - conversion degree of NO_x (efficiency of NO_x removal); $[NO_x]_0$ - concentration of NO_x in the inlet gas of irradiation stage [ppm]; $[NO_x]$ - concentration of NO_x in the outlet gas of irradiation stage [ppm]; D - mean irradiation dose [kGy]; k_1, k_2 - model constants.

The formula (1) describes the single-step process of the NO_x removal. This formula has been used as

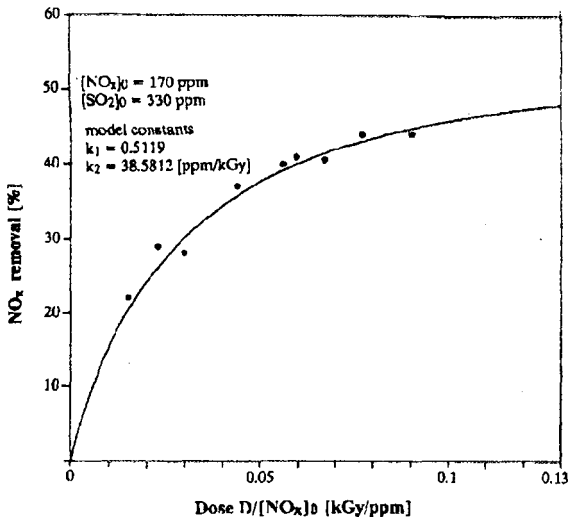

Fig.1. Approximation of data from EPS Kawęczyn for one stage irradiation with regard of dose distribution.

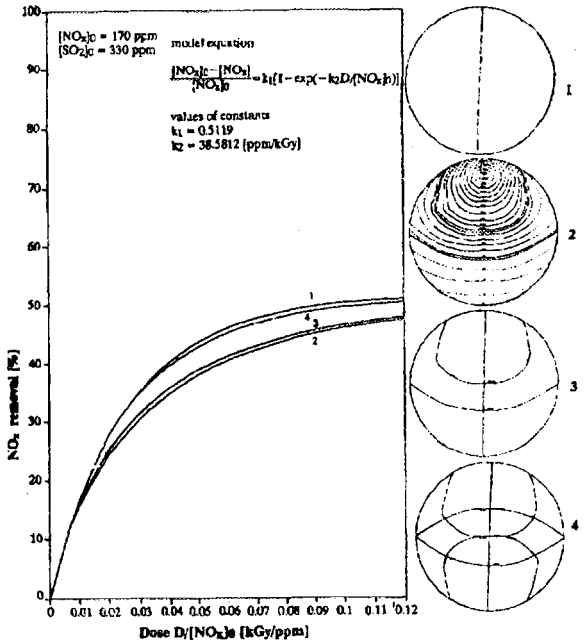

Fig.2. Estimation NO_X removal for single stage irradiation: 1 - uniform dose distribution, 2 - with regard of dose distribution in cross section of reactor (24 zones), 3 - with regard of dose distribution in cross section of reactor (3 zones), 4 - irradiation from both sides (3 zones).

a balance equation for the single and double stage processes.

The formula of NO_X concentration in the outlet gas of the k-irradiation stage for the i-zone of dose distribution has the following form:

$$[NO_X]_k^i=[NO_X]_{0k}^i[1-k_1(1-\exp(-k_2y_iz_kD/[NO_X]_{0k}^i))] \quad (2)$$

where: $[NO_X]_k^i$ - NO_X concentration in the outlet of k-irradiation stage for i-zone of dose distribution [ppm], $[NO_X]_{0k}^i$ - NO_X concentration in the inlet of k-irradiation stage for i-zone of dose distribution, z_k - dose delivery ratio for k-stage, z_kD - dose absorbed in the k-stage, y_i - ratio of dose absorbed in

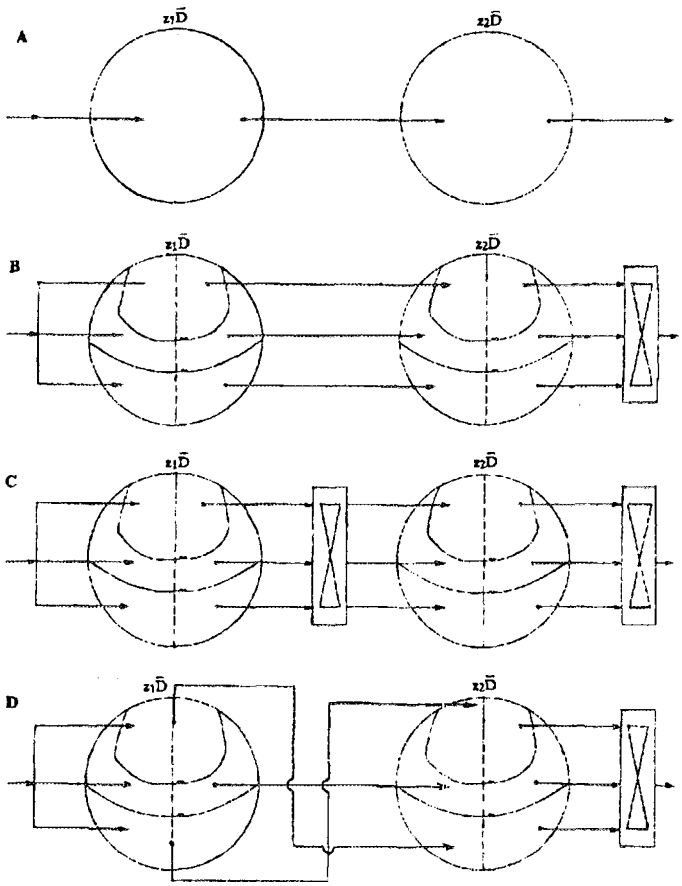

Fig.3. Models of NO_X removal for two stage irradiation: A - without regard of dose distribution in the process vessel, B - with regard of dose distribution in the process vessel and segregation flow pattern between stages, C - with regard of dose distribution in the process vessel and ideal mixing between stages, D - with regard of dose distribution in the process vessel and crossing the oposite gas streams.

the i-zone to dose absorbed in the cross section of process vessel.

The formula (2) has been used for approximation of the experimental data for a single stage irradiation in the power station in Kawęczyn as well as for the NO_x removal model estimation for a double stages irradiation. The model constants k_1, k_2 were established by using experimental data for the single-step irradiation with the help of optimization method on the basis of 24 zones of dose distribution. The results are presented in Fig.1. The determined values k_1, k_2 were used for model curves for the single and double irradiation systems. The NO_x removal models for the single step irradiation are presented in Fig.2. The four models are considered:

1 - uniform dose distribution model,
2 - model with regard of dose distribution in the cross section of reactor (24 zones),
3 - model with regard of dose distribution in the cross section of reactor (3 zones),
4 - model of irradiation from both sides by half the dose rate.

The NO_x removal in the case of irradiation from both sides by half the dose rate (model 4) is very close to the NO_x removal at uniform dose distribution (model 1).

The NO_x removal efficiency at one side irradiation for 3 and 24 zones of the dose distribution (models 3 and 2) is very similar. For that reason, the two-stage one side irradiation models have been calculated by taking into consideration 3 zones of the dose distribution.

The schemes of two-stage irradiation models are presented in Fig.3. The models are considered as follows:

- without regard of dose distribution in the process vessel model,
- with regard of dose distribution in the process vessel and segregation flow pattern between the stages model,
- with regard of dose distribution in the process vessel and ideal mixing between the stages model,
- with regard of dose distribution in the process vessel and crossing the opposite gas streams model.

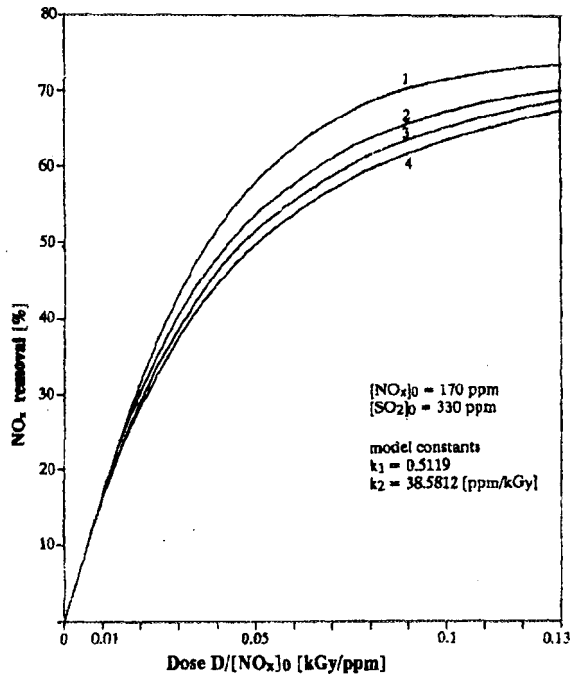

Fig.4. Estimation NOx removal for double irradiation (equal dose delivery): 1 - without regard of dose distribution in the process vessel, 2 - with regard of dose distribution in the process vessel and crossing the opposite gas streams, 3 - with regard of dose distribution in the process vessel and ideal mixing between stages, 4 - with regard of dose distribution in the process vessel and segregation flow pattern between stages.

The calculations for the above models were made at an equal dose delivery ratio at each stage ($z_1=z_2=0.5$). The results obtained are presented in Fig.4. The NO_x removal in the case of crossing the opposite gas streams is close to the NO_x removal at uniform dose distribution. The technical realization of that two-stages model with crossing and the opposite gas streams seems to be the optimal solution for the two-stages NO_x removal system.

References

[1]. Wittig S., Spiegel G., Platzer K.H., Willibald U.: Projekt Europaisches fur Massnahmen zur Luftreinhaltung Simultane Rauchgasreinigung durch Elektronenstrahl kfk, Karlsruhe. 1988.

APPLICATION OF SelRO MEMBRANES TO THE TREATMENT OF AGGRESSIVE WASTES CONTAINING THE ABSORBENT GENOSORB

A.G. Chmielewski, M. Harasimowicz, J. Palige

The subject of our interest were wastes originated in the production of H_2SO_4 containing an organic absorbent GENOSORB (Hoechst) - tetraethylene glycol dimethyl ether (a homogeneous mixture of $H_3CO(CH_3CH_2O)_nCH_3$; n=3÷5; average molar mass - about 200). Up to now the wastes were directed to a general waste utilization collector and then neutralized. Because in this waste treatment process any GENOSORB recovery cycle was not applied, the loss of it calculated only as the cost of this component was about 1 million PLN/year. This loss could be reduced by such a charge in the waste streams treatment, which allows recovery of GENOSORB.

The experiments were carried out with the waste having the GENOSORB concentration from 1 to 10 g/dm^3. The GENOSORB solution useful to the H_2SO_4 purification process should have the concentration from 10 to 200 g/dm^3, then the waste must be concentrated by ten-twenty times. To this aim the following kinds of the semipermeable membranes were applied:

PL9700834

- NTR-739 HF (hyperfiltration) and NTR-7197 (nanofiltration) made by NITTO,
- UTC-60 (hyperfiltration) and UTC-70 (nanofiltration) made by TORAY,
- SelRO type: MPT-32 and MPT-34 (KIRYAT WEIZMANN Ltd.).

All the membranes mentioned above are resistant to the GENOSORB interaction on their polymeric ultra-thin separating layer, but only the SelRO membranes can work continuously in the solutions at pH=0÷14. This condition prefers this kind of the membranes for concentration of acid waste (pH=0.8÷2.5) containing GENOSORB because the NTR (NITTO) and UTC (TORAY) membranes need an initial treatment resulting in an increase of pH value up to 4÷5.

The best results of the GENOSORB recovery were obtained in the experiments with MPT-34 membrane, which was applied for the concentration of the waste at pH=2 and the following concentration of the main components [mg/dm^3]: GENOSORB - 490; SO_4^{2-} - 312; Na^+ - 1.0; Cl^- - 5.5; F^- - 2.1.

The initial waste volume was reduced by a factor of 10, i.e. it was separated on the retentate and permeate in the proportion 1:9. Concentrations of GENOSORB and other components in the retentate were the following: GENOSORB - 4780; SO_4^{2-} - 655; Na^+ - 8.3; Cl^- - 22.6; F^- - 10.2.

In this manner more than 97% of GENOSORB was concentrated in the retentate; a volume reduction by twenty times causes a small decrease of the GENOSORB recovery factor, which reaches 96.3%. The concentration of GENOSORB was measured using a Perkin Elmer-5000 gas chromatograph; for concentration measurements of the other components a liquid spectrophotometer HACH DR-2000 was used.

The results obtained on a laboratory scale with the MPT-43 membrane were a basis for preparing a pilot-plant project and technical conditions for a full scale unit project. This unit should be constructed from twenty parallel connected industrial size 4"x40" MPS-34-A1 KIRYAT WEIZMANN membrane modules (average efficiency of each: 0.3 m^3/h at the operating pressure 3 MPa). The minimal GENOSORB recovery should not be below 95%, at its concentration in the waste of about 2 g/dm^3 and the volume reduction coefficient VRC=10÷20.

A total cost of this plant including the project, construction, and the exploitation costs through the first 3 years was calculated to be 0.9 million of PLN.

SELECTION OF A NEW OUTFALL POINT LOCALIZATION FOR SEWAGES DISCHARGED FROM "CELLULOSE AND PAPER FACTORY ŚWIECIE" (CPFS) INTO THE VISTULA RIVER

A. Owczarczyk, R. Wierzchnicki, M. Strzelecki, B. Więcław

Investigations concerning different aspects of the pollution transport in natural water receivers are related directly to the natural environment protection. Diminishing amount of the water resources due to human activity as well as progressing degree of the natural water contamination oblige us to undertake intensive investigations with the purpose to learn the actual situation, predict endangering and decide which means are adequate to improve the water quality.

The pollutants discharged disperse under mixing conditions persisting in surrounding water. This process results in diminishing and gradual homogenization of the pollutants concentration within the stream cross-section.

From the point of view of environment protection it is highly desirable to provide a possible high rate of transverse mixing. An optimal choice of location of the outfall significantly improves the pattern of initial stage of mixing which, in consequence, causes a rapid decrease of pollutants. A low concentration of the latter promotes biological activity of the receiver leading to gradual elimination of the impurities from water environment.

The investment plan of CPFS has assumed the transition of the sewage discharge point 900 m downstream and pass the outfall from the bank to the selected point at the bottom in the river stream. The goal of this work was to select a new optimal localization of sewage outfall.

Actually the discharge point is located at the river bank. The experimental work consists in a series of radiotracer experiments in the Vistula river in order to obtain the transverse distribution of dilution of the discharged effluent in the various distances from the outfall. Similar experiments were carried out after injection of the tracer in the selected points located along the river width.

Respective distributions of the dilution values, corresponding to certain locations of the outfall on the river width axis were calculated, on the basis of the measured distributions of the instantaneuosly injected tracer, by space integration techniques. Rhodamine was used as the tracer.

Table. Coefficient of mixing improvement ΔSM/SM (ΔSM - difference of mixing factors between points in "new" and "old" cross-sections).

Distance from the left bank [m]	Profile		
	1	2	3
26	0.41	0.15	0.10
48	0.61	0.20	0.10
90	0.10	0.23	0.13

The measuring reach of the length of 8,000 m was tested. The distribution of the effluent dilution was calculated for three transverse profiles. The

injection points were localized at 26.48 and 90 m from the left bank of the river.

The data obtained allowed to select the water region optimal for the new location of the discharge point. Placing the outfall in the optimal position should result in certain improving the mixing pattern.

The obtained results have been compared with the actual effluent dilution measured by the tracer injection to the "old" bank outfall. The point at the distance of 48 m from the bank has been recognized as an optimal localization.

DETERMINATION OF WATER LEAKAGES IN HEAT-GENERATING PLANTS

A. Owczarczyk, H. Burliński, B. Więcław, M. Srzelecki, R. Wierzchnicki

Circulating water systems, similary as other piping systems, are liable to lose their water tightness which leads to water losses. If there are two or more such closed water circuits adjacent to each other it is clear that leakages between them are likely to occur. The situation of that kind are encoutered at district heating plants between the municipal circulating water and cooling systems of heat and power generating plants. It is obvious that the occurrence of leakages between systems is disadvantageous for both technological and economical reasons and therefore they have to be localized and eliminated as soon as possible.

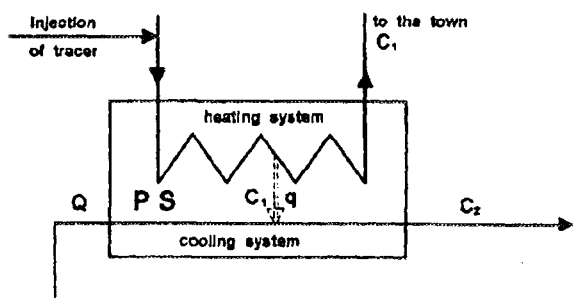

Fig. Principle of the method.

The practical solution of this problem consists in injection of a tracer (Br-82 or rhodamine B) into the water coming back from the heating system and looking for its occurrence in the plant cooling system. The principle of the method is shown in Fig.

The tracer balance equation has the following form:

$$q\int_{t_1}^{t_2} c_1(t)dt=(Q+q)\int_{t_2}^{t_3} c_2(t)dt. \quad (1)$$

Since usually $Q>>q$ equation (1) will be sympli-fied and the leakage flow-rate q can be calculated as follows:

$$q=Q\frac{\int_{t_2}^{t_3} c_2(t)dt}{\int_{t_1}^{t_2} c_1(t)dt} \quad (2)$$

where: q - leakage flow rate; Q - flow rate in cooling system; c_1 - tracer concentration in heated water system; c_2 - tracer concentration in cooling system; t_1, t_2 - period of sample collection from heated system; t_2, t_3 - period of sample collection from cooling system.

The measurements of leakages were conducted in the Warsaw Heat-Generated Plant Siekierki at the beginning of the heating season 1995. The results are shown in Table.

Table. Leakages in heating system Siekierki.

Date	q [m^3/h]
28.09.95	113
24.10.95	-

The big leakage 113 m^3/h recognized in the first measurement was successfully removed, so that during the second measurement, a month later, we did not find any leakage.

PL9700836

MATERIAL ENGINEERING, STRUCTURAL STUDIES, DIAGNOSTICS

ALLOYING OF AUSTENITIC STAINLESS STEEL WITH NITROGEN USING HIGH-INTENSITY PULSED BEAMS OF NITROGEN PLASMA

J. Piekoszewski, L. Waliś, Z. Werner[1/], J. Białoskórski[1/], L. Nowicki[1/], M. Kopcewicz[2/], A. Grabias[2/]

[1/]Sołtan Institute for Nuclear Studies, Otwock-Świerk, Poland

[2/]Institute of Electronic Materials Technology, Warszawa, Poland

In our previous papers [1, 2] we reported the feasibility of introduction of nitrogen atoms into metals using high-intensity pulsed ion beams (HIPIB). The characteristic features of this process are:

- the doping occurs by diffusion in the pulse-delivered foreign (N) atoms in the surface layer melted by the heat supplied by the same ion pulse, the retained doses being 10^{16}-10^{17} N/cm^2 per pulse, for energy densities ranging between 5.8 and 9.8 J/cm^2;
- the bulk material remains at a practically unchanged temperature since the process has a transient character and occurs in the microsecond time scale. The materials studied in [1, 2] were: pure iron (ARMCO), low-carbon 18H2N4W and high-carbon N9 steels. The most striking finding was that regardless of the initial composition of the processed material, at the doses higher than about 4x10^{17}N/cm^2 the predominant phase in the near - surface layer (of at least as thick as 0.1 μm) is fcc austenite.

The major purpose of the present work was twofold:

- to extend the variety of the processed steels by studying the case of austenitic stainless steels of 18-9 type,
- to check the possibility of controlling the N dose by varying the number of pulses at a constant energy density rather than their magnitude.

The samples were prepared of: 1H18N9T austenitic stainless steel (equivalent to AISI 321 type); also some additional samples of ARMCO iron were irradiated. Each sample was irradiated separately with a varying number of nitrogen plasma pulses, generated in the IBIS rod plasma injector described elsewhere [2]. The energy density of pulses was kept constant at 7 J/cm^2.

The samples were characterized by the following methods: the ^{57}Fe Conversion Electron Mössbauer Spectroscopy (CEMS), Nuclear Reaction Analysis (NRA) using the ^{14}N(d,α)^{12}C reaction, microhardness HV_{001} and surface roughness R_a measurements. The main results obtained can be summarized as follows:

- The retained dose of N increases linearly with the number of pulses for both materials in the range from 0 to 20 pulses. Each pulse introduces about 0.4x10^{17} N/cm^2.

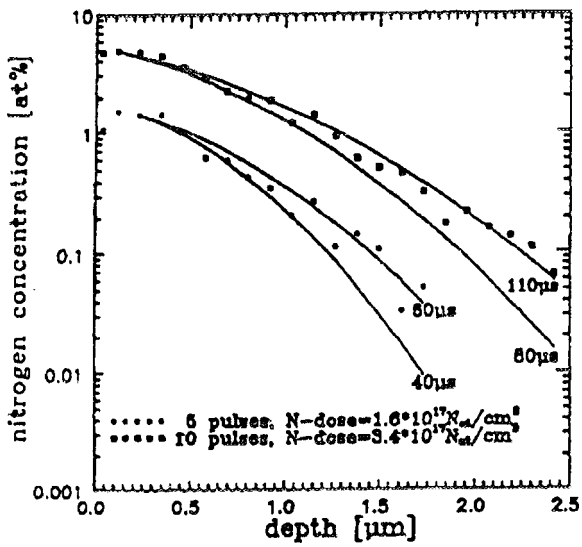

Fig.1. NRA depth profiles in nitrogen plasma pulse processed 1H18N9T steel. Number of pulses. N-dose and ranges of diffusion time of nitrogen in molten steel are indicated.

- The single pulse is sufficient to remove the polishing - induced martensitic phase, observed in CEMS spectra of unprocessed 1H18N9T sam-

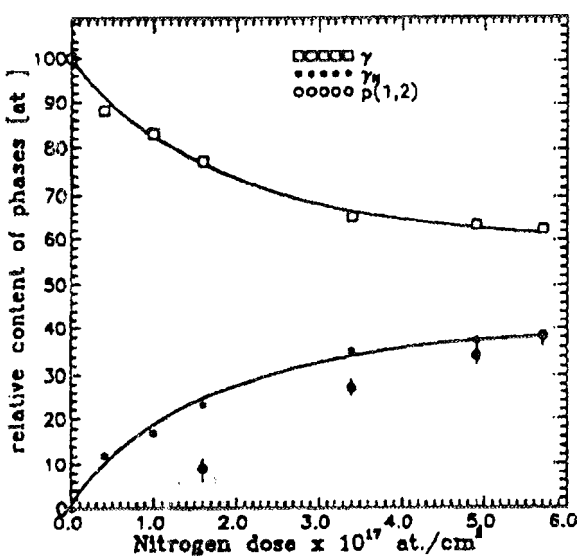

Fig.2. Evolution of γ and γN phases as a function of N-dose in nitrogen plasma pulse processed 1H18N9T steel. Some computed values of γN fraction p(1,2) are also depicted.

ples. This confirms the tendency for the pulse induced austenitic transformation observed in [1, 2].

- The analysis of NRA nitrogen in-depth profiles like those shown in Fig.1 indicates that:
  - melting depth of the top layer extends to a depth of at least 2.5 μm,
  - the effective diffusion time τ of nitrogen in the molten layer is roughly proportional to the number of pulses and ranges from 30 to 160 μs.
- The numerical analysis of CEMS spectra shows that nitrogen dissolves in austenitic lattice forming a new phase - γ_N. In the γ_N phase Fe atoms have nitrogen atoms as the nearest neighbours at the interstitial lattice sites. The dependencies of the experimental (derived from CEMS data) γ and γ_N and computed fraction of γ_N denoted as p(1,2) are shown in Fig.2.
- The microhardness HV_{001} of martensite free 1H18N9T increases linearly with N. This fact is interpreted as a result of the interstitial solid solution hardening mechanism in accordance with data given in Fig.2. The grain size hardening mechanism is excluded from considerations, since each successive pulse erases the memory of the former grain structure and hence cannot exhibit a cumulative character, in contrast to the observed results.

References

[1]. Piekoszewski J., Langner J.,Nowicki L., Turos A., Waliś L., Ciurapiński A.: Mater. Lett., **14**, 131 (1992).

[2]. Piekoszewski J., Langner J., Białoskórski J., Kozłowska B., Wernwer Z., Kopcewicz M., Waliś L., Ciurapiński A.: Nucl. Instr. Meth., **B80/81**, 344 (1993).

PL9700837

SURFACE MORPHOLOGY OF NITROGEN-ALLOYED STEELS USING HIGH INTENSITY PULSED PLASMA BEAMS

J. Piekoszewski, L. Waliś, J. Langner[1/]

[1/]Sołtan Institute for Nuclear Studies, Otwock-Świerk, Poland

In our preceding abstract of the "Annual Report" it was shown that it is possible to introduce high doses of nitrogen into various kinds of steels and thereby to alter their near-surface properties, using high intensity pulsed nitrogen plasma beams. However, even if the desirable structural characteristics are attained in this way, the range of the potential applications of this technique will depend, to a considerable extent, on the final roughness of the processed surface. On the other hand, it is known [1] that the transient processing in which melting near surface occurs always results in some alteration of the surface morphology. Until now, the available information concerning this issue are rather poor. In this work we report the result of a study of the surface morphology of two kind of steel samples subjected to nitrogen alloying with the use of high intensity pulsed plasma beams. Emphasis has been placed upon the influence of the initial constituents of the substrate, i.e. whether it consists of a single phase or of a heterogeneous mixture of more than one phase, and on the initial roughness of the surface.

The samples were prepared of:

- medium carbon steel 45,
- stainless steel 1H18N9T (AISI 321).

The first consists of two constituents, i.e. ferrite and perlite in approximately equal proportions and the second consists of a single phase, i.e austenite.

Each sample was irradiated with pulsed nitrogen plasma pulses generated in an IBIS accelerator described elsewhere [2]. As far as the first aspect of this work is concerned the main results are as follows. In the case of 1H18N9T of initial roughness 0.05 R_a, the main changes in R_a occur after the first pulse. Subsequent pulses practically do not affect the mean values of R_a, although the nonuniformity ($\sigma R_a/R_a$) increases with the number of pulses n. By contrast, the pulses have cumulative

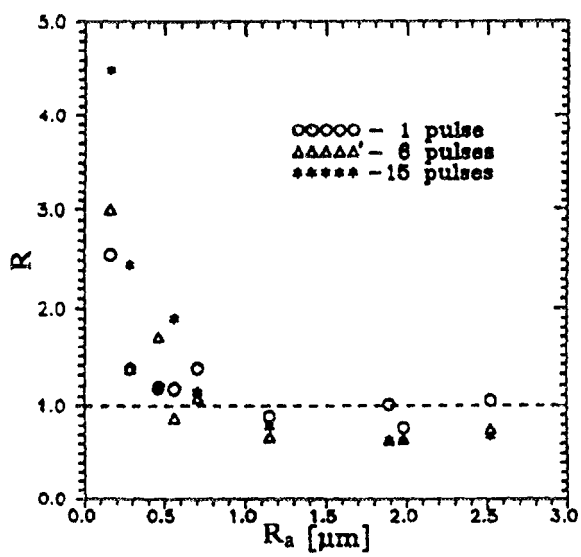

Fig. Dependence of the normalized roughness R of 45 steel processed with 1, 6 and 15 pulses on the value of its initial R.

effect in the case of 45 steel. Here, both R_a and nonuniformity increases significantly with n. The difference in behaviour of these two materials is accounted for by the following facts. 1H18N9T remains a homogeneous single phase after each subsequent pulse, therefore there is no cumulation in the morphology alteration. In 45 steel, perlite and ferrite exhibit a different ablation efficiency, therefore since they cannot be mixed during the melting, the difference in morphology of these constituents is greater after each pulse, resulting in

the rise of R_a. Another aspect explored here, was the relation between the initial and final state of the surface morphology of the processed material. Fig. shows the dependence of the normalized roughness R, after processing, on the initial R_a for 45 steel irradiated with 1, 6 and 15 pulses. When an initial surface is fairly smooth, then the pulse processing deteriorates its smoothness. In contrast, when an initial surface is very rough, then the pulse processing smooths this surface. The demarcation region between deterioration and improvement lies in our case somewhere about 0.5 μm R_a of the initial roughness. The evolution of the morphology mentioned above is confirmed by Scanning Electron Microscopy (not shown here). In all cases the microhardness HV_{001} increases by a factor of 1.9, 2.1 and 2.3 after 1, 6 and 15 pulses respectively.

Practical conclusion: if for some reason, it would be beneficial to increase the microhardness of a given work piece and its R_a can be larger than 0.5 μm, then a single pulse is sufficient to achieve this modification. If in another case, it would be desirable to improve both HV and R_a of initially rough material, then several pulses should be applied.

References

[1]. Anthony T.R., Cline H.E.: J. Appl. Phys., **48**, 3888 (1997).
[2]. Piekoszewski J., Langner J.: Nucl. Instr. Meth., **B53**, 148 (1991).

EXAMINATION OF HIGH-TEMPERATURE RESISTANCE OF ISOTOPE SMOKE DETECTORS

A. Nowicki, L. Rowińska, E. Pańczyk

PL9700838

Smoke detectors used in fire protection systems can be hazardous if during the fire they are damaged to such an extent that the radioactive nuclide contained in the detector is released to the environment. Therefore results of the examination of their resistance to high temperature play an important role in granting permissions for their use in alarm systems.

In the Department of Nuclear Methods of Material Engineering of this Institute a high-temperature resistance of isotope smoke detectors, manufactured by Hekatron GmbH (Germany), has been examined.

The examination was carried out at temperatures 500 and 1200°C, according to [1-3].

Subject of the examinations

Two types of the smoke detectors IRM 136 and IRM 141 were examined. The detectors were supplied by ALIMPEX Company Ltd.

The smoke detector, type IRM 136, is designed for fire control of large cubature compartments such as rooms in factories, sport halls, shops, store houses etc. Owing to the application of two ionization chambers an exceptionally high sensitivity to smoke detection has been archieved. The radionuclide ^{241}Am of activity 2x14.8 kBq=29.6 kBq deposited on an IAM Pd 4 foil was used as a sourece of α-radiation.

The smoke detector, type IRM 141, is designed for fire control of compartments of small and medium cubature including habitable rooms. Owing to the electronic systems specially elaborated for that purpose a high sensivity to smoke detection has been achieved despite of the application of low activity (3.6 kBq) α-radiation source ^{241}Am, deposited on AMMQ 1181 foil.

Examination procedure

The examination of high-temperature resistance of the smoke detectors was carried out using an apparatus shown in Fig. The principal part of the

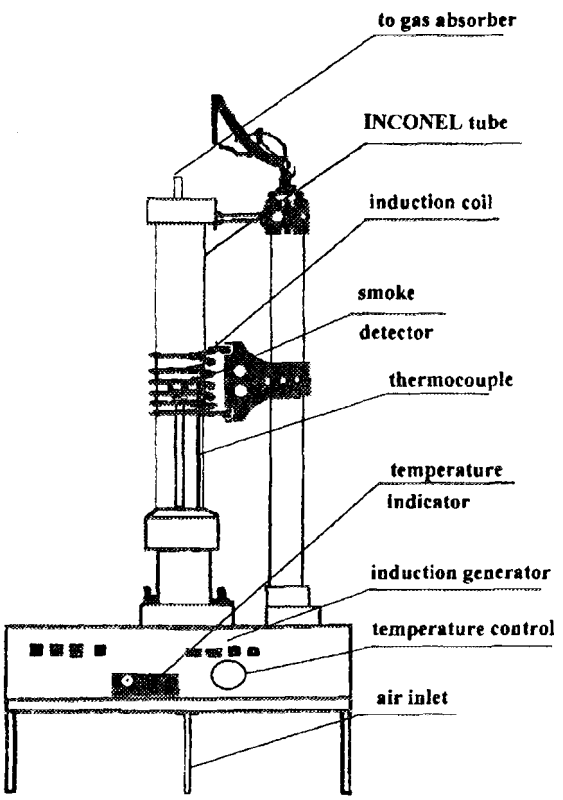

Fig. Apparatus for testing to the smoke detectors.

apparatus is a tube 950 mm long and of 90 mm internal diameter made of the fire resistant alloy INCONEL, mounted perpendicularly, with a weld on the bottom, with an air inlet and a fixed thermocouple. The tube is closed with a tight PTFE stopper with a gas outlet. The tube is heated (induction heating) over a lenght of 200 mm (the total volume of the heating zone is 1200 cm^3).

A complete smoke detector was placed in the middle of the heating zone on a quartz support (contacts up). The temperature was mantained at the desired level with an accuracy of 1.5% (approx.

10°C) and measured by means of a Ni-CrNi thermocouple placed close to the smoke detector.

The upper outlet of the furnace was successively connected to a cold finger type tube cooled with liquid nitrogen, a washer with 1M HCl solution and a dust filter made of porous glass. The air flow was 1.5-2 l/min. The time necessary to reach the temperature 600 and 1200°C was 15 and 45 min, respectively. The burning time at both temperature was 60 min.

Radiometric measurements

The content of the absorbers was extracted with a hot 18% aq. HCl solution and the washings were prepared for scintillation counting. The metal parts of the smoke detector were washed with few drops of a HCl solution and the washings prepared for scintillation counting. The ashes after burning of the smoke detector, the quartz support and some parts of the detector were examined using γ-ray spectrometry.

Preliminary measurements of the ^{241}Am activity released from the detector source were carried out with the aid of a scintillation head, type SSA-1PW, coupled to a RUST-3 radiometer. Precise measurements of the ^{241}Am activity released during the examination were carried out with the aid of liquid scintillators. The measurements were performed using a Beckman Model LS 6000LL spectrometer in the energy range corresponding to the energy of α-particles of ^{241}Am (E_α=5.4 MeV). The contamination of the selected surface areas was measured by γ-ray spectrometry using an HPGe detector (Ortec) and a multichannel analyser Canberra S-100 controlled by a PC IBM/PS2. γ-rays of ^{242}Am of energy 59.5 keV were measured.

Examination of the smoke detector type IRM 136 at 600°C

The smoke detector undergoes significant destruction. The plastic casing is burnt. The detector breaks up into several parts. The laminate of the printed board is burnt. In both ionization chambers the foil strips with the radionuclide ^{241}Am are intact. The activity released during the burning of the detector at 600°C is less than 3 Bq.

Examination of the smoke detector type IRM 136 at 1200°C

The detector undergoes complete destruction. The plastic casing is burnt. The contact pins are fused, the detector breaks up into several pieces. In both ionization chambers the foil strips with the radionuclide ^{241}Am undergo melting and dispersion.

The activity released during the ashing at 1200°C is 1380 Bq, of which 280 Bq is released to the environment. The latter value exceeds the permissible level [1, 3].

Examination of the smoke detector type IRM 141 at 1200°C

The detector undergoes significant destruction. The plastic casing is burnt. The contact pins are fused. The detector breaks up into the printed board and the ionization chamber sub-assembly. However owing to the very strong casing of the ionization chamber and high quality laminate used for the manufacturing of the printed board the sub-assembly of the ionization chamber does not break up into individual elements. This part was taken as a whole when performing contamination measurements. The foil with the radionuclide ^{241}Am undergoes melting, however the radioactive material is not released to the enviroment. The activity released during the ashing of the detector at 1200°C is less than 2 Bq.

Conclusions

The smoke detector type IRM 141 meets the requirements as to the high-temperature resistance at 1200°C. The smoke detector, type IRM 136, meets these requirements at 600°C but not at 1200°C. Particularly the ^{241}Am sources used in detectors made by various manufacturers are not resistant to the temperature 1200°C.

It should, however, be noted that the examination of high-temperature resistance at 1200°C is not included in the Polish Standard [1, 2], but only in recommendations [3]. Only examination at 800°C is recommended in the Polish Standard [2] similarly as in the ISO Standard [4].

References

[1]. Sealed radiation sources. Resistance classes. Requirements and examinations. Polish Standard PN-86/J-202000.

[2]. Sealed radiation sources. Methods of leak proof control. Polish Standard PN-89/J-02001.

[3]. National Inspectorate for Nuclear Safety and Radiological Protection. Requirements no. DJ/06.001.01./1207/3521/59 of July 14, 1989.

[4]. Sealed radioactive sources. Classification. ISO Standard 2919-1980.

WELDING ELECTRODES DOPED WITH THORIUM DIOXIDE

A. Nowicki

In the Metalurgical Works for High Melting Metals (MWHMM) in cooperation with the Institute of Nuclear Chemistry and Technology (INCT) a technology for manufacturing of tungsten welding electrodes doped with thorium dioxide has been developed.

High-melting weldings electrodes made of tungsten are used in automatic welding machines for works carried out in a protective atmosphere. Addition of ThO_2 to tungsten has a double effect [1]. Firstly, ThO_2 as an oxide with high melting point inhibits recrystallization processes of tungs-

ten at high working temperatures of the electrodes, which extends the durability of the electrodes. Secondly, being a radioactive material ThO_2 causes ionization of the gas surrounding of the electrode, which facilitates ignition of the electric arc. This is particularly desirable in the automatic welding machines.

In the INCT a procedure has been developed for the preparation of tungsten-ThO_2. mixtures containing 1.5% (by weight) of ThO_2. Following the permission of the National Inspectorate for Nuclear Safety and Radiological Protection [2], 20 kg of the mixture was prepared. The mixture was a subject to pressing and sintering processes used in MWHMM for manufacturing of tungsten rods doped with other oxides.

These works were controlled by the INCT to ensure radiological safety. During the control even minimal radioactive contaminations arising during pressing, sintering and mechanical working of the tungsten rods were removed without delay. All the radioactive wastes were transported to the radioactive waste store at the Institute.

The obtained batch of tungsten electrodes doped with ThO_2 in the form of rods, 1.6 mm in diameter, was handed over to the customers, e.g. the Institute of Welding Technology, for examination of the usability of the electrodes in automatic welding machines.

The results of this examination will permit to undertake the decision whether or not to implement the elaborated technology.

References

[1]. Korsunov B.G.: Metallurgiya redkich metallov. Poroskovaya metallurgiya. Matallurgiya, Moskwa 1987, 134p.

[2]. National Inspectorate for Nuclear Safety and Radiological Protection. Licence D-7155 of June 15, 1995.

NEW MAGNETIC MATERIALS OBTAINED FROM AMINOTRIAZOLE COMPLEXES WITH TRANSITION METALS

A. Łukasiewicz, L. Waliś, H. Grigoriew

In an earlier publication [1] ferromagnetic materials have been obtained by thermal decomposition in the air of aminotriazole complexes with transition metals of general formula $MAnX_2$ (M - transition metal or two different transition metals; A - anion present in the complex; n = 1 or 2; X - 3-amino-1,2,4 triazole), denoted as MAX. The oxide material FP, containing iron and cobalt, obtained by decomposition of the $(FeCo)SO_3$ complex has strong ferromagnetic properties [2]. In the course of further studies on MAX complexes their compounds with metal oxalates (M'ox) were synthesized. It has been found that MAX.M'ox compounds undergo in the air exothermic decomposition to oxide materials, similarly to MAX. The thermal decomposition of MAX.M'ox to carbide materials (M,M')C in an oxygen-free atmosphere was then examined.

Table 1. Saturation magnetization of (M,M')C materials.

No.	Metal M and M'		Density [mGm^{-3}]	Saturation magnetization J(T)
	M	M'		
1	Co	2Co	6.85	1.27
2	Co	2Ni	6.21	1.22
3	Ni	2Co	5.82	1.11
4	Ni	2Fe	5.44	1.13
5	NiCo	2NiCo	6.06	0.97
6	Mn	2Co	5.22	0.53
7	Co	2Mn	3.75	0.29
8	Ni	2Ni	3.80	0.13
9	$(FeCo)SO_3$ FP		4.95	0.45

Using X-ray diffraction analysis it has been shown that the (M,M')C materials contain metal carbides and free metals phases, these materials being ferromagnetic. As metal carbides do not exhibit ferromagnetic properties this indicates mutual solubilization of the phases.

Properties of (M,M')C materials

The results of measurements of saturation magnetization of (M,M')C materials, carried out in the Institute of Material Engineering of the Warsaw Technical University are presented in Table 1. These properties have been compared with those of the FP material described previously [2]. The phase composition of some (M,M')C materials is given in Table 2.

Table 2. Phase composition of (M,M')C materials.

Sample no.	Metal		Phase	
	M	M'	certain	probable
2	Co	2Ni	Co, NiC	Ni
3	Ni	2Co	Co, NiC	Ni
4	Ni	2Fe	Ni, $Fe_{2.5}C$	Fe_5C_2, Fe_3C, FeC, Fe
5	NiCo	2NiCo	Co, NiC	Ni

Since the reflections of various phases of iron carbides overlap (according to ASTM charts) it is difficult to explicitly determine which phases are present in sample no. 4.

Discussion and results

In most cases (samples 1-6) the examined (M,M')C materials exhibit stronger ferromagnetic properties than the FP material (sample 9) described previously. Materials with magnetization above 1T can be considered as candidates for permanent magnets. Four of the examined (M,M')C materials (half of the samples) show such properties. Formation of the metal carbide phase during oxygen-free decomposition of MAX.M'ox follows from the previously described [1] properties of MAX complexes.

Oxalates of some metals (Co) are thermally decomposed to free metals. It should be noted that the formation of the free metal does not depend on

the position of the respective cation, in MAX or in M'ox. In sample no. 4 free nickel occurs and iron carbide predominates despite of the fact that Ni^{2+} and Fe^{2+} are contained in MAX and in M'ox, respectively. The oxygen-free thermal decomposition of the MAX.M'ox complex is of interest from the point of view of research as well as of applications (new materials for manufacturing permanent magnets). This work is a subject to publication and a patent claim.

References

[1]. Łukasiewicz A., Michalik J., Mikoś J., Waliś L., I. Woźniak I..: Mater. Lett., 14, 127 (1992).

[2]. Kaszuwara W., Leonowicz M., Łukasiewicz A.: Mater. Lett., 12, 429 (1992).

NEW ENVIRONMENT-FRIENDLY PREPARATIONS FOR IMPREGNATING AND DYEING OF WOOD

A. Łukasiewicz, L. Rowińska, L. Waliś

Preparations for impregnating wood, based on the complexes of aminotriazole with transition metals, denoted as MAX, have been described previously [1]. MAX preparations are obtained and applied as aqueous solutions. They exhibit fungicidal properties and form water insoluble salts with acid dyes. They can be used for dyeing of wood using two aqueous solutions [2].

Extensive studies on the properties of MAX complexes were carried out. As a result new preparations have been obtained, which can be used for impregnating and dyeing of wood using one solution. The new preparations are common complexes of MAX with basic dye-Bismarck Brown (BB). Bismarck Brown has free amine groups, which together with ligand X form a complex with metal M. The MAX-BB complex is soluble in water. Its aqueous solutions are stable and can be used as commercial products. After evaporation of water an insoluble MAX-BB layer is formed on wood.

It follows from the literature data that the BB dyes are used for dyeing of wood despite of their leachability with water and low resistance to light. A brown-red colour of wood is obtained. Preliminary tests have shown that after binding to MAX the BB dye is not leachable with water and its resistance against light increases significantly.

Samples of pine wood dyed with BB alone and with the MAX-BB preparation were exposed simultaneously to light (UV lamp). After 50 h of irradiation the colour of the wood dyed with BB significantly faded while no changes in the colour of wood dyed with MAX-BB were observed.

MAX-BB preparations are being subjected to various tests before offering them for sale. Preparations in various shades of the brown colour are being developed. The MAX-BB preparations will be a subject to a patent claim.

References

[1]. Łukasiewicz A., Michalik J., Waliś L.: Obtaining of protective and colour layers on wood and other materials. P-298206 (1993).

[2]. Łukasiewicz A., Michalik J., Waliś L.: Obtaining new protective layers on wood. P-303875 (1994).

APPLICATION OF FOLLOW-UP DETECTORS TO LEAKPROOF CONTROL OF UNDERGROUND PIPELINES

J. Kraś, W. Kielak, S. Myczkowski

The detectors, developed in the last years, for leakproof control and localization of leaks in underground pipings, using the radioisotope method, were used for routine control in 1995.

A pipeline of Φ=260 mm, 150 km long (Koluszki-Boronów) as well as a pipeline of Φ=210 mm, 70 km long (Czemczeszur-Teheran, Iran) were controlled. Both pipeline were found to be leakproof.

An ABSR-3 detector was modernized to increase the capacity of its batteries. The modernization permitted to extend the working time of the detector in the pipeline from 35 to 75 h. Owing to the extension of the working time it is possible to control twice longer pipelines with diameters 200-300 mm in a single pass, which permits to considerably reduce the cost of control.

Studies have been undertaken in order to develop a detector with continuous recording of its position in the controlled pipeline (hodometer).

A detector for control of pipelines with diameters in the range 200-600 mm and external dimensions similar to those of ABSR-3 detector has been designed.

In 1995 leakproof control of 140 technological objects was carried out.

PL9700841

DETERMINATION OF TRACE ELEMENTS IN FILLINGS OF SARCOPHAGI OF EGYPTIAN MUMMIES FROM THE ARCHEOLOGICAL MUSEUM IN KRAKÓW

E. Pańczyk, M. Ligęza[1/], J. Kierzek, K. Cieśla, L. Waliś

[1/] Academy of Fine Arts, Kraków, Poland

Introduction

The Archeological Museum in Kraków in co-operation with the Academy of Fine Arts in Kraków has begun complex renovation and examination of the collection of Egyptian sarcophagi and mummies from the period of XXIth Dynasty, as well as the Ptolomean and Roman periods. In the Ancient Egypt sarcophagi were made of sycamore trunks and all leaks were filled with a mixture of clay and sawdust [1, 2].

Analysis of the elemental compositions and crystalline structure of those fillings is an important source of information about the origin and age of the sarcophagi. The content of trace elements is a "finger print" of a clay deposit and is characteristic of a mineral and its geological history [3].

Two methods, X-ray fluorescence and instrumental neutron activation analysis, are particularly suitable for such studies. On the other hand examination of crystalline structure by X-ray diffraction will permit to identify the minerals present in the fillings material.

The purpose of the present work was to accumulate information necessary for supplying documentary evidence for the Egyptian Sarcophagi from the collection of the Archeological Museum in Kraków. The obtained results will constitute a bank of data, enabling a comparison of materials used in the Ancient Egypt.

Characteristics of objects

Preliminary examinations comprised the fillings originating from the following objects:

- a sarcophagus, XXIth Dynasty, containing the Nesychonsu mummy of the wife of Amon priest from Luxor, dated from 1085-941 B.C. (samples no. 3 and 5);
- two sarcophagi from the Ptolemean period, dated from 332 B.C.-31 A.D. excavated in El Gamhud; the exploration was carried out by Tadeusz Smoleński under the auspices of the Kraków Academy of Sciences and Austro-Hungary in 1907; the excavations were financially supported by Philip Back (samples no. 1, 2, 4 and 7);
- a sarcophagus from the Roman period, dated from 4th century A.D. (sample no. 6).

Seven representative samples were taken from the above four sarcophagi.

Research methods

X-ray fluorescence analysis

Preliminary analysis of the elemental composition of the fillings was carried out with the aid of energy dispersive X-ray fluorescence. In this method charcteristic X-radiation of elements is excited by means of a radioisotope source or an X-ray tube. The spectrum of the characteristic radiation was measured by means of a spectrometer with a Si(Li) detector for energy range 2-25 keV and with a planar HP-Ge detector for energies above 25 keV. The excitation of X-rays in the objects examined was carried out by means of the radioisotope sources Fe-55, Cd-109 and Am-241. The first source was used for the determination of light elements: K, Ca, Ti, the Cd-109 source was used for Mn, Fe, Ni, Cu, Zn, Ga, Rb, Sr, Zr, Nb and Pb, the Am-241 source was used for Sn, Ba, La, Ce, Pr and Nd. The analysis of X-ray spectra and processing of the results was carried out using a set of AXIL-QXAS programs elaborated and disseminated by the International Atomic Energy Agency in Vienna.

Table 1. Photopeak area ratios [%]. Excitation source Cd-109.

Element	Sample no.						
	1	2	3	4	5	6	7
Cl	0.07	0.54	0.1	0.17	0.14	0.034	0.15
Ar	0.94	0.57	1.0	0.93	0.95	0.28	1.93
K	1.64	1.96	1.56	1.17	1.15	0.19	1.55
Ca	5.77	18.77	4.76	7.51	6.3	30.16	6.98
Ti	2.35	1.42	1.74	1.6	2.42	0.30	1.71
Cr	0.081	0.14	0.074	0.33	0.15	0.06	0.21
Mn	0.27	0.44	0.36	0.38	0.41	0.1	0.42
Fe	28.44	29.51	28.15	30.24	29.75	18.81	34.03
Ni	0.08	0.011	0.05	0.02	0.06	0.014	0.087
Cu	0.74	0.68	0.80	1.82	0.72	0.26	1.75
Zn	0.51	1.27	1.14	1.61	0.75	0.26	1.12
As	-	-	-	-	-	1.4	0.41
Br	0.19	0.33	0.08	0.22	0.07	0.084	0.29
Rb	1.27	1.26	1.22	1.4	1.45	0.45	1.64
Sr	14.16	24.26	13.74	15.64	15.12	41.6	17.88
Y	1.29	0.73	1.38	1.45	1.61	0.40	2.13
Zr	40.00	16.83	41.33	32.78	36.36	4.95	24.72
Nb	1.35	0.63	1.47	1.35	1.74	0.43	1.91
Au	0.46	0.21	0.38	0.48	0.5	0.08	0.71
Pb	0.36	0.43	0.67	0.89	0.38	0.14	0.39

Twenty one measurements of X-ray spectra excited in the examined objects were carried out. After processing with the aid of the AXIL-QXAS program the intensities of X-ray lines of 27 ele-

Table 2. Photopeak area ratios [%]. Excitation source Fe-55.

Element	Sample no.						
	1	2	3	4	5	6	7
Al	0.19	0.12	0.25	0.14	0.2	0.07	0.17
Si	4.3	0.75	3.8	3.11	3.77	0.06	6.51
S	0.41	1.08	0.69	0.57	0.47	0.36	0.71
Cl	1.26	2.78	1.37	2.06	1.9	0.6	1.47
Ar	4.46	3.89	6.0	3.81	4.14	1.19	6.39
K	29.57	12.7	24.01	13.57	14.83	2.52	14.49
Ca	59.07	76.23	54.70	68.28	63.95	94.08	62.82
Ti	9.75	2.47	9.19	8.47	10.75	1.13	7.44

ments and of the scattered radiation were obtained. The obtained results bear a qualitative character and

are presented in Tables 1, 2 and 3 as photopeak area ratios for individual excitation sources. The observed distribution patterns of trace elements for three objects (XXIth Dynasty, sarcophagi from the Ptolomean period) are similar, while the Roman sarcophagus exhibits distinst differences particularly in the content of Cl, Ti, Ba, Sr, Y, Zr and Au.

Table 3. Photopeak area ratios [%]. Excitation source Am-241.

Element	Sample no.						
	1	2	3	4	5	6	7
Sb	5.32	5.92	5.61	4.15	4.59	7.07	8.88
Ba	83.39	85.31	78.87	83.51	81.91	63.15	86.2
La	4.24	-	4.34	0.48	2.88	8.44	2.45
Ce	6.25	-	7.64	9.28	4.86	17.46	1.0
Nd	0.81	8.77	3.54	2.59	5.77	3.88	1.47

Instrumental neutron activation analysis

Instrumental activation analysis was chosen as the second method for determining the history and origin of the examined sarcophagi on the basis of elemental analysis. It is an ideal method for solving the problem because owing to its high sensitivity it permits to determine extremely low concentration levels of trace elements. In addition major components of clay such as O, Si, Al, Ca, K, Mg either do not react with thermal neutrons or form short-lived radioinuclides [4]. The analysis was carried out using standards. A set of standards was prepared on the basis of the results of X-ray fluorescence analysis. Attention was paid to choosing optimum conditions of irradiation in a nuclear reactor. Samples of weight of 100 mg, sealed in quartz ampoules, were irradiated together with appropriate standards, in the nuclear reactor at a thermal neutron flux of $5x10^{13}$ n/cm^{2}s for 12 h and cooled for 24 h. The activity of the samples was then measured by means of an HP-Ge detector (ORTEC) coupled to a Canberra-System S 100 spectrometer controlled by an IBM/PS2 computer. The obtained spectra were processed a using micro-SAMPO program [5]. Twenty seven elements were identified in the samples examined. Preliminary results of the analyses are presented in Table 4. The analysis of the obtained concentrations of elements confirms the dependences observed previously - the samples taken from the Roman sarcophagus (sample no. 6) clearly differs from the other samples in respect to the content of Fe, As, Co, Ni, Tb, Hf and Au.

X-ray phase analysis

X-ray phase analysis based on the powder method is widely used in mineralogy and petrography. Preliminary examination, without separation of minerals, comprised three samples representing the sarcophagi from the periods of XXIth Dynasty (sample no. 5) and the Ptolemean (sample no. 1) and Roman (sample no. 6) periods. All analyses were performed using the characteristic X-radiation $K_\alpha Cu$ (K_α ~0.1542 nm). The diffractograms were processed using an XRAYAN program. The results are shown in Fig.

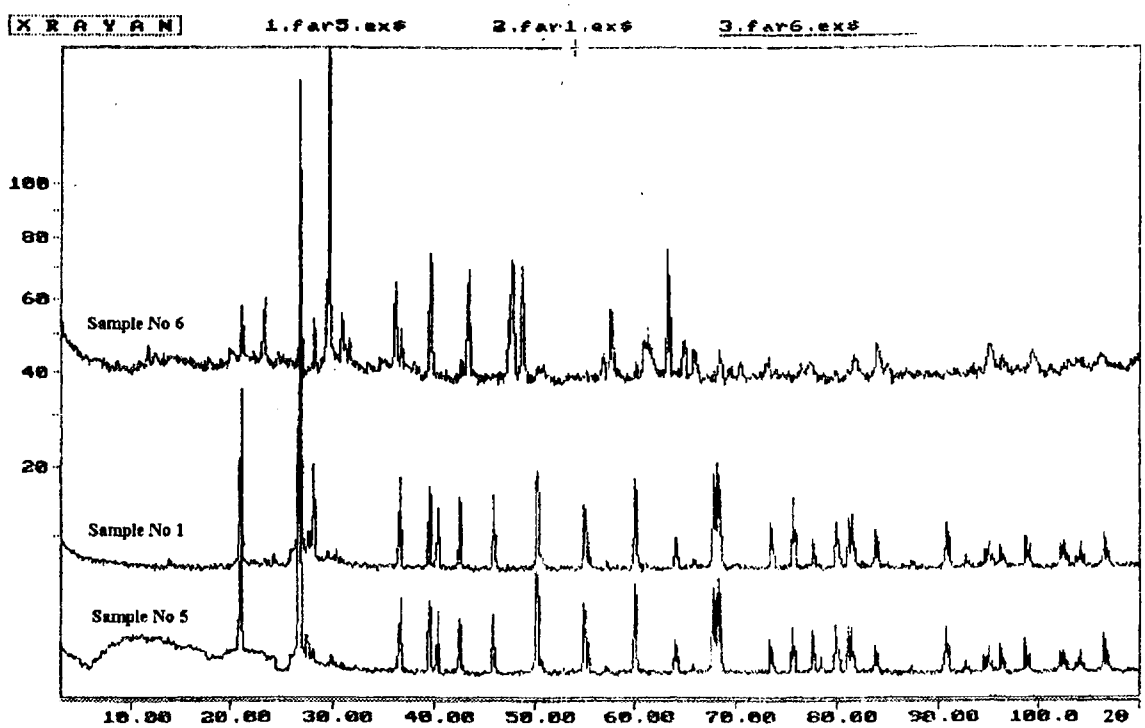

Fig. Phase composition of mummies fillings.

In addition to quartz, calcite and dolomite a great number of feldspars and pyroxenes were identified. In sample no. 6, originating from a Roman sarcophagus, which significantly differed from the other samples in respect to the concentration of elements determined also vital differences in the crystalline structure were observed. The sample contains, in addition to aragonite and magnesite,

PL9700842

huntite a mineral used in the Acient Egypt as white pigment for decorative ceramics. This preliminary analysis needs a more thorough study. The detectability of minerals in a mixture varies in a wide range (generally from 0.5-30%) depending on such factors as crystallization degree, mineral symmetry, scattering and absorption coefficients of X-rays, angle range at which the smallest reflections appear, dimensions and shape of crystallities. In practice the number of components of a mixture that can be identified is limited.

Table 4. Concentration of trace elements in mummies fillings [ppm].

Element	Sample no.						
	1	2	3	4	5	6	7
Na	4860	7350	3370	4600	4420	1020	2600
K	50300	77700	55000	50000	40000	-	-
Sc	43.8	6.9	4.9	5.9	5.4	2.9	3.2
Cr	11	31.7	17.6	18.0	14.0	16.0	9.0
Fe	2120	2270	1600	1900	1650	870	1170
Co	134	177	74.7	110	88	39	85
Ni	-	470	320	-	-	1300	-
Zn	3.1	7.7	5.2	5.1	1.2	2	4.1
Ga	-	-	93.5	-	-	100	-
As	1.8	0.22	8.0	3.1	1.6	140	2.9
Br	30.5	60.2	25.7	23	35	17.3	7.0
Mo	0.5	0.54	0.33	0.43	0.46	1.9	0.3
Cd	3.37	2.8	-	-	-	-	-
Sb	16.0	24.2	26.0	26	27.4	30	34
Cs	0.35	0.22	0.35	0.39	0.31	0.05	0.02
Ba	29.4	37	41.0	42	48	14	2.3
La	7.4	5.2	5.5	6.3	6.3	2.4	8.6
Ce	7.2	5.2	6.1	6.0	6.9	3.5	9.2
Nd	2.4	12.3	8.6	7.5	16.4	2.45	19.7
Eu	0.3	0.24	0.21	0.25	0.25	0.04	0.04
Yb	0.7	0.38	0.65	0.31	0.33	0.28	0.5
Tb	0.4	0.17	0.28	0.49	0.17	0.03	0.12
Hf	3.9	3.3	4.5	4.1	2.5	0.31	0.6
Ta	41.8	41.2	36.0	44	32.4	13.0	42
W	4.1	4.32	7.2	4.5	4.1	7.4	0.4
Au	0.004	0.03	0.19	0.03	0.009	1.1	0.005
Th	0.23	0.1	0.24	0.22	0.2	0.11	0.7
^{238}U	0.41	0.46	0.37	0.32	0.4	0.54	0.5

Summary

The preliminary examinations of the fillings of Egyptian sarcophagi have confirmed the suitability of the applied complementary methods. However in order to obtain reliable data further investigation of the elemental composition with the aid of the X-ray fluorescence method as well as the activation method it is necessary to use suitable geological standards. This will enable us to compare the obtained results with the data avaiable in other centers [6]. On the other hand in order to determine the crystalline structure of the examined fillings petrogarphic studies should be performed or separation of the minerals characteristic for the fillings should be carried out.

At the final stage of the studies multivariate statistical analysis of the results will be applied e.g. analysis of principal components and cluster analysis.

References

[1]. Lucas A., Harris J.R.: Ancient Egyptian materials and industries. London 1962.

[2]. Riederer J.: Studies in Conservation, **21** (1976).

[3]. Cejka J., Frydrych J., Kapralova M., Urbanec E.: Z. Agyptische Sprache, **103** (1976).

[4]. Peisach M. et al.: J. of Radioanal. Chem., **69** (1989).

[5]. Koskelo M.J., Aarnio P.A., Routti J.T.: Computer Thys. Commun., **24** (1981).

[6]. Ismail S.S., Grass F.: Chem. Erde, **49**, 3 (1989).

STUDY OF CHINESE PORCELAINS BY X-RAY FLUORESCENCE ANALYSIS

J. Kierzek, B. Małożewska-Bućko

Introduction

An often problem important to museum workers is to determine the authenticity (age) of Chinese porcelains, because in many cases imitations are indistinguishable from the originals. There are many methods to determine the period in which a given object was manufactured. These methods often base on subjective opinions of experts, who take into consideration colour, glaze, shape, paintings, etc.

Quantitative and more objective methods for the determination of porcelaine age have been elaborated. They consist in the determination of elemental composition of the studied objects. The age of blue-and-white porcelains often is determined basing on the manganese-to-cobalt ratio [1, 2]. For this purpose also the kalium-to-iron ratio may be used [3]. The other methods are based on zinc-rubidium ratio, content of zinc and arsenic [4], content of barium [5, 6], zirconium and niobium content [7], and relative content of rubidium, strontium, zirconium, and niobium [8]. In all the works quoted, for the determination of age X-ray fluorescence analysis was applied. Recently, for the determination of porcelain age X-ray fluorescence analysis has been used for more elements, than previously mentioned. In work [9] 15 elements were analyzed, and the multivariate data analysis was applied for the age determination.

The aim of this work was the determination of age of a Chinese urn for grain, dating back, probably, to the XIII century. For this purpose X-ray fluorescence analysis and cluster analysis for objects classification were applied.

Studied objects

Four objects from the National Museum in Warszawa were studied:

1. an urn for grain no. 1, China, XIII (?) century;
2. an urn for grain no. 2, topped with a figure of a dog and a wriggling dragon, China, XIX (?) century;
3. a fragment of ceramics, China, about 1250 year;

4. a bowl for a ring, decorated inside by two appliqued fishes, China, XIII century.

Urns 1 and 2 have lids which were treated in this study as independent objects. There are doubts concerning the age of the urn for grain no. 1.

Methodology

The determination of elemental analysis was performed using the energy-dispersive X-ray fluorescence technique. This is a nondestructive assay and due to the measurement technique can be successfully applied for the elemental content determination of the studied objects. This method is based on exciting of the characteristic radiation of elements by radionuclide sources or an X-ray tube. Recording of the characteristic radiation spectrum was performed using a spectrometric set with a semiconductor detector Si(Li) in the energy range 2-25 keV, and with a planar detector HPGe in the energy range above 25 keV. For excitation of X-ray radiation in the studied objects the following radionuclide sources were used: ^{55}Fe, ^{109}Cd, and ^{241}Am. The first ^{55}Fe source was applied for light elements K, Ca, Ti analysis; the source ^{109}Cd - for Mn, Fe, Ni, Cu, Zn, Ga, Rb, Sr, Y, Zr, Nb, and Pb; the source ^{241}Am for elements Sn, Ba, La, Ce, Pr, and Nd. The portable fluorescent analyzers enable studying of museum objects without the necessity of their transport to a laboratory.

above, lids of two urns were treated as independent objects in order to demonstrate that in the case of two identical objects (a pair urn-lid) the obtained results are similar. With such an approach 6 objects were measured (urn no.1 and its lid (XIII century), urn no. 2 and its lid, bowl (XIII century), and fragment of ceramics (XIII century). 18 measurements for areas covered with glaze were carried out (6 with the use of ^{55}Fe source, 6 with ^{109}Cd source, and 6 using ^{241}Am source). After analysis by the AXIL-QXAS program, intensities of X-ray radiation lines and scattered radiation of 21 elements (K, Ca, Ti, Mn, Fe, Ni, Cu, Zn, Ga, Rb, Sr, Y, Zr, Nb, Sn, Ba, La, Ce, Pr, Nd, and Pb) were obtained.

Similar objects (similar features) have the same spectra (heights of peaks and mutual relations between heights of peaks). An example of the spectrum of the characteristic radiation excited by the ^{109}Cd source is shown in Fig.1.

Fig.2 represents the results of cluster analysis for 6 objects, each described by 14 features, which corresponded to contents of 14 elements (K, Ca, Ti, Mn, Fe, Rb, Sr, Y, Zr, Nb, Sn, Ba, La, and Ce). These elements are present in all the objects at medium concentrations. Each feature is a number equal to the ratio of the intensity of characteristic line to the intensity of incoherent scattered radiation. Scattered radiation significantly corrects the differences due to the measurement geometry for

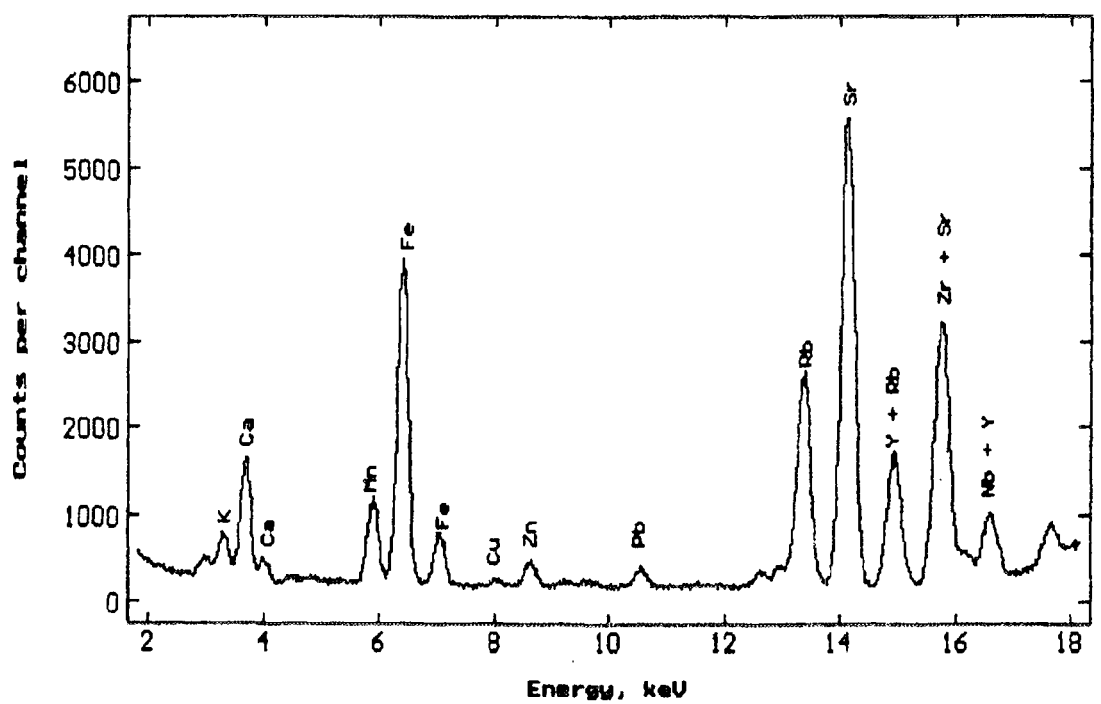

Fig.1. An example of fluorescence spectrum of a bowl for a ring (XIII century).

The X-ray spectra analysis and processing of the results were performed by the AXIL-QXAS programmes set, elaborated and distributed by the IAEA in Vienna.

Results

30 measurements of X-ray radiation excited in the studied objects were done. As was mentioned

particular objects. On the basis of the cluster analysis shown in Fig.2 it can be stated, that there is a significant similarity between the urn no. 1 and its lid, and the urn no. 2 and its lid, respectively. The objects of each pair are the same. Similarity of the objects (urn-lid) confirms correctness of the applied method. Quite a high degree of similarity (ca 0.6) exists between the bowl (XIII century) and the

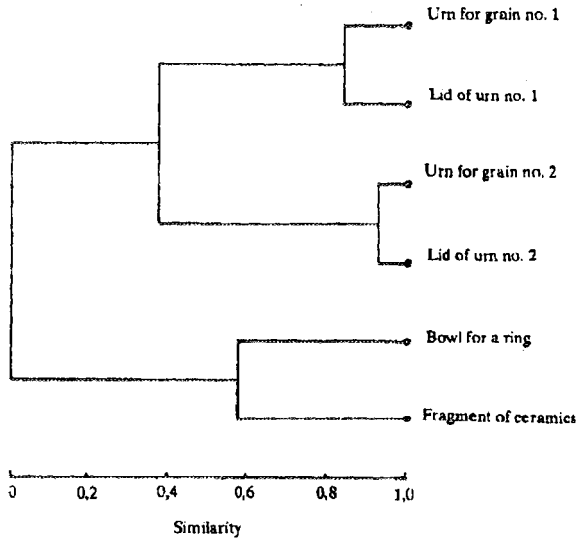

Fig.2. Dendrogram based on hierarchical clustering for 6 objects of Chinese porcelain.

fragment of ceramics (also XIII century). The urn from the XIII century is more "similar" to the urn from XIX century, than the pairs of the objects: bowl - fragment of ceramics. Of course, this degree of similarity is obtained on the basis of only 14 features.

A number of the examined objects is also a very important factor. Only for four objects of the present study it was rather difficult to draw explicit conclusions.

Conclusions

Due to the small number of the studied objects (four) the exact age determination of the urn for grain was not possible. On the basis of the measured spectra of excited X-ray radiation and performed cluster analysis of the objects described by 14 features the only thing possible to say is that dating this urn back to the XIII's century seems to be rather doubtful. With the features analyzed, the urn is more similar to the urn from XIX century, than to the bowl and the fragment of ceramics coming from the XIII century.

References

[1]. Yap C.T., Tang S.M.: X-ray fluorescence analysis of modern and recent Chinese porcelains. Archaeometry, **26**, 78-81 (1984).

[2]. Yap C.T.: X-ray fluorescence studies on low-Z elements of straits Chinese porcelains using Fe-55 and Cd-109 annular sources. X-Ray Spectrometry, **16**, 55-56 (1987).

[3]. Yap C.T., Tang S.M.: ZnK_{α}/RbK_{β} ratio of Ch'ing, Republic and Modern Chinese porcelains. X-Ray Spectrometry, **14**, 157-158 (1985).

[4]. Yap C.T.: X-ray fluorescence determination of trace element concentrations of zinc and arsenic and their relation to ceramic attribution. X-Ray Spectrometry, **16**, 229-231 (1987).

[5]. Yap C.T., Tang S.M.: Quantitative XRF analysis of trace barium in porcelains by source excitation. Appl. Spectrosc., **39**, 1040-1042 (1985).

[6]. Yap C.T., Tang S.M.: Energy-dispersive X-ray fluorescence analysis of Chinese porcelains using Am-241. Archaeometry, **27**, 61-63 (1985).

[7]. Yap C.T.: EDXRF analysis of straits Chinese porcelains for zirconium and niobium using a Cadmium-109 source. Appl. Spectrosc., **40**, 839-840 (1986).

[8]. Yap C.T., Tang S.M.: X-ray fluorescence analysis of Chinese porcelains from K'ang Hsi to modern times using Cd-109 source. Appl. Spectrosc., **38**, 527-529 (1984).

[9]. Swerts J., Aerts A., De Bicop N., Adams F., Van Epsen P.: Age determination of Chinese porcelain by X-ray fluorescence and multivariate analysis. Chemometrics and Intelligent Laboratory Systems, **22**, 97-105 (1994).

AUTOMATIC INDEXING TEST OF e-BN

K. Godwod[1/], H. Grigoriew, W. Starosta

[1/]Institute of Physics, Polish Academy of Science, Warszawa, Poland

The effect of shock-wave on crystallization of BN was first discovered by Batsanov et al. [1]. After shock pressure they found increasing degree of crystallinity of BN powder, and crystals of dimensions up to parts of mm. The X-ray diffraction pattern of these crystals was different from those of known forms of BN, such as hexagonal (h-BN), wurzite-type (w-BN) and zinc-blende type (z-BN).

Also Batsanov measured the density, ir-spectrum and refractive index of the crystals, all different from those in known phases of BN.

Batsanow named this unknown phase e-BN (explosive). On the basis of his diffraction data, the ASTM card, no. 18-251 was generated, marked O as an unknown structure.

In spite of the interest in BN structures and possibilities of many applications of this material, the e-BN structure has remained quite unknown for 30 years. The only attempt to find related structure was made by Akashi et al. [2]. Using a slightly different method of preparation they obtained a new modification of e-BN with a bit of other interlayer distances, in comparison with data from no. 18 251 card. Akashi stated that this form has a cubic symmetry fcc and the lattice parameter a=8.405 Å.

However, we have been informed by other authors [3], that using the impulse plasma method under reduced pressure they obtained small quantities of e-BN with exactly the same interlayer distances as those in ASTM no. 18 251. Because Batsanov's data are more thorough, we decided to use his data, from ASTM card, in our test. We used two sets of diffraction lines from the card: the first one, contained all 26 lines and the second one, contained 20 lines, excluding the weakest ones which could originate from additions.

Automatic indexing tests were made using computer programs by W. Paszkowicz (Institute of Physics, Polish Academy of Science).

We obtained the following results:

1. For entire set of ASTM 18-251 lines:
   symmetry: monoclinic

Table 1.

No.	a	b	c	γ	vol.	merit
1	4.2826	5.6628	18.8302	91.355	456.534	0.1093
2	4.8384	9.1631	25.2877	91.377	1120.801	0.09923
3	7.0817	6.1028	27.3667	91.394	1182.394	0.0993

where: a, b, c - dimensions of unit cell in Å; γ - angle; merit - the coefficient of fitting (should be at the most about 0.1).

The 3 possible unit cells (Table 1) of big volumes (456-1182) have rod-like shapes and angle γ in the range 91.35-91.4°.

2. For 20-lines set of ASTM 18-251 lines:
   symmetry: orthorombic

Table 2.

No.	a	b	c	vol.	merit
1	3.7699	10.6411	24.7474	992.7638	0.1076
2	3.7781	19.4624	23.9299	1759.5869	0.1041
3	3.9204	23.0697	25.0569	2266.2075	0.1009
4	4.1899	19.3252	27.1297	2196.7096	0.0953
5	4.8890	6.4613	7.9681	251.7067	0.1064
6	5.0416	18.3360	27.1586	2510.6164	0.1051
7	5.7398	21.2819	27.0205	3300.6581	1.1078

The volumes of these cells change from 250 to 3300 $Å^3$ and their shapes are mainly slice-like (except for cells no. 1 and no. 5).

The results, especially the number of possible unit cells of various structures, parameters, volumes and shapes are difficult to understand assuming that the ASTM card no. 18-251 presents interlayer lines originating in one crystal phase. Also polytypes are excluded because of the lack of hexagonal or cubic symmetry.

More likely the card presents lines originating from two phases, formed together in the nonequilibrium process.

The problem of finding of e-BN structure seems complicated and requires a sample of sufficient degree of crystallinity of e-BN phase, and precise diffraction measurements, because the analysis of the card data does not lead to positive synonymous conclusions.

Also using the ASTM card no. 18-251 data in phase analysis can lead to incorrect results.

References

[1]. Batsanov S.S., Blochina G.E., Deribas A.A.: J. Struct. Chem., 6, 227 (1965) (in Russian).

[2]. Akashi T., Pak H.R., Sawaoka A.B.: J. Mater. Sci., 21, 4060 (1986).

[3]. Sokołowska A., Olszyna A.: J. Cryst. Growth, 116, 507 (1992).

[4]. Paszkowicz W.: J. Appl. Cryst., 20, 166 (1987).

PL9700843

RADIATION TECHNOLOGIES

TOWARDS STANDARDIZATION OF THERMOLUMINESCENCE ANALYSIS APPLIED FOR DETECTION OF IRRADIATED FOODSTUFFS

K. Malec-Czechowska, A.M. Dancewicz, Z. Szot

There are several methods applied for detection of irradiated foodstuffs [1]. None of them is universal and none allows to determine the dose absorbed. However, two methods have a good chance to be implemented in the practice of detection of irradiated foodstuffs. These are: electron spin resonance spectroscopy, which allows a direct detection of free radicals and paramagnetic centers [2], and thermoluminescence (Tl) analysis [3]. The latter was studied extensively during the last decade in order to make its application universal [4]. However, in spite of the essential progress made in the method of Tl analysis, its standardization met virtual difficulties. At present, the most reliable procedure which allows comparison of the results of Tl analyses performed in various laboratories is based on:

- using Tl analysis of minerals separated from the sample,
- normalizing Tl intensity by relating it to the Tl intensity of the same sample exposed to a defined saturating dose of gamma radiation (coefficient K_{Tl}),
- using a defined temperature interval for comparison Tl intensities.

Sanderson et al. [5] have shown that the main source of Tl are minerals present in the sample. Their separation followed by Tl measurement has been made since a standard procedure in Tl analysis of irradiated dry foodstuffs. Normalization of Tl intensity has been introduced in order to eliminate the Tl dependence on mineral composition and its energy storing property. Using for Tl intensity measurement a defined temperature interval, instead of the whole diapason of heating temperature, minimizes uncertainty of Tl values caused by quick fading of Tl in the area of low temperatures (40-140°C).

Experiments carried out in this Laboratory during 1995 were directed towards further extention and standardization of Tl analysis of irradiated foodstuffs. The method of mineral separation, Tl measurements, and normalization as well as the home made Tl reader used were described earlier [6]. At present, the list of foodstuffs analyzed was enlarged and the results obtained are published elsewhere [7]. The main goal of the present studies was to compare values of K_{Tl} obtained for the whole glow curve, and for the part of it, considered as the most optimal. In the procedure of Tl analysis put forward by the European Community laboratories the optimal interval of heating temperature is defined as that between the temperature of the peak V of glow curve of a TLD-100 dosimeter and the lower temperature obtained by deducting from the peak V temperature the interval between the peak V and VI temperatures. Because of the differences in the perfomance of Tl readers, calibration of the instrument is needed by measuring the glow curve of the TLD-100 dosimeter and finding the adequate temperature interval. For this purpose we

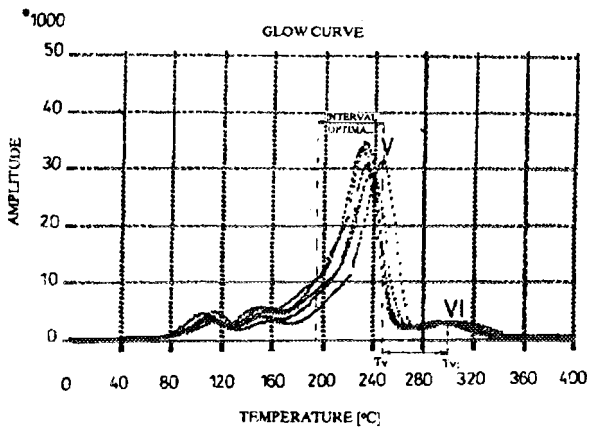

Fig. Glow curves of thermoluminescence dosimeter type MTS-N irradiated with a 220 mGy dose of X-rays. The curves were recorded at the heating rate 10°C/s. V and VI thermoluminescence peaks used for calculating temperature interval optimal for K_{Tl} coefficient calculation.

were using Tl dosimeters designed as MTS-N and produced in the Institute of Nuclear Physics in Kraków. The Tl glow curve of MTS-N dosimeter is similar to that of TLD-100. Glow curves for few MTS-N dosimeters irradiated with a 220 mGy dose of X-rays are shown in Fig. The mean temperature interval for optimal measurement of Tl coefficient calculated for 10 curves was between 189 ±4°C and 246 ±10°C.

Table shows that the K_{Tl} coefficient calculated for the optimal temperature interval of the glow curve in all cases gave a positive answer whether sample has been irradiated or not within the last 16 months, while the same coefficient calculated for the whole glow curve temperature interval (40-395°C) led to few erroneous identifications when the treshold values of K_{Tl} was set as 0.5 below which the sample should be declared as unirradiated. The results obtained are in good agreement with the European Community draft of standardized procedure for Tl measurement of irradiated foodstuffs which proposes

PL9700844

Table. The mean values of thermoluminescence coefficient K_{TI} calculated from the whole glow curve (40-395°C) and from the optimal part of the glow curve heating interval (189-246°C) for minerals of non-irradiated and irradiated herbs and spices examined at different time after exposure. The coefficient K_{TI} is given as the ratio of the thermoluminescence intensity of a given sample to the thermoluminescence intensity of the same sample exposed to normalizing dose of 1 kGy γ-rays.

Herbs and spices	Unirradiated (control)		Time after exposure to 5 kGy of ^{60}Co γ-rays							
			3 months		6 months		8,5 months		16 months	
	whole	opt.	whole*	opt.**	whole*	opt.**	whole*	opt.**	whole*	opt.**
Marjoram	0.002	0.003	0.825	2.870	0.529	1.814	0.621	4.492	0.387***	0.974
Thyme	0.003	0.007	0.942	4.492	0.611	2.034	0.658	2.338	0.394***	1.188
Basil	0.005	0.018	0.743	2.041	0.642	1.785	0.653	3.608	0.716	1.257
Oregano	0.005	0.034	0.859	1.628	0.596	1.128	0.728	4.365	0.605	1.214
Sage	0.003	0.008	0.845	1.919	0.672	1.778	0.820	7.842	1.064	2.486
Black pepper	0.010	0.020	1.590	3.374	1.229	4.890	0.645	3.876	1.208	3.783
Hot paprika	0.004	0.010	0.840	1.490	0.482***	0.992	0.680	4.650	0.706	2.334
Ginger	0.007	0.031	0.954	1.003	1.250	1.389	1.320	5.109	-	-
Dill seeds	0.020	0.020	0.901	2.201	0.462***	1.091	0.608	1.342	0.818	1.863
Caraway seeds	0.013	0.112	0.973	1.617	0.378***	0.704	0.134***	4.451	0.789	1.549

* - whole - K_{TI} calculated for the whole glow curve.
** - opt. - calculated for the optimal heating temperature interval (189-246°C).
*** - considered as non-irradiated.

the calculation of K_{TI} coefficient for the optimal temperature interval defined as described above [8].

One can conclude that the present standardization of the TI analysis procedure applied to the identification of irradiated foodstuffs is at the stage where it can be recommended as an official method for usage in laboratories called to test irradiated foodstuffs.

The work reported here was sponsored by the State Scientific Research Committee grant no. 5S 30705103.

References

[1]. Bogl K.W.: Radiat. Phys. Chem., 35, 301-310 (1990).
[2]. Stachowicz W.: J. Sci. Food Agric., 58, 407-415 (1992).
[3]. Heide L., Bogl K.W.: Inst. Strahlehygiene Hefte, 53 (1984).
[4]. Schreiber G.A., Helle N., Bogl K.W.: Int. J. Radiat. Biol., 63, 105-130 (1993).
[5]. Sanderson D.C.W., Slater C., Kairns K.J.: Radiat. Phys. Chem., 34, 915-924 (1989).
[6]. Malec-Czechowska K., Dancewicz A.M., Szot Z.: Thermoluminescene method in identification of irradiated foodstuffs (in Polish). Nuclear Technics in Industry, Medicine, Agriculture and Environment Protection, Warszawa, 24-27 April 1995, pp. 131-136.
[7]. Malec-Czechowska K., Dancewicz A.M., Szot Z.: Nukleonika (in press).
[8]. Foodstuffs. Detection of irradiated food from which silicate minerals can be isolated. Method by thermoluminescence CEN/TC 275/WG 8 N 50-1995.

EFFECT OF IONIZING RADIATION ON PROPERTIES OF ACRYLIC PRESSURE SENSITIVE ADHESIVES

E. Wojtyńska[1/], W. Głuszewski, J. Bojarski, P.P. Panta

[1/]Institute of Industrial Chemistry, Warszawa, Poland

Pressure sensitive adhesives for medical applications (sticking plasters) should be resistant to sterilization, particularly to radiation sterilization. Both the self adhesive glue and its base would be unaffected by sterilization doses of fast electrons. There are the following glues utilized in medical products:

- based on natural rubber,
- hot melt adhesives,
- copolymers of acrylic acid and 2-ethylhexyl acrylate.

Rubber cements and hot melt adhesives are both sensitive to processing temperatures and to ultraviolet (UV) radiation. They are degraded and loose their starting useful properties. Hence, they are not suitable for use, e.g. for preparating sutures and sanitary napkins. Contrary to that acrylic copolymers are more heat resistant and do not change their colour after exposure to UV. Thus, one might expect that acrylic copolymers should be resistant to ionizing radiation. A development of radiation resistant glue was the most important aim of works devoted to the technology of acrylic self adhesives, prepared in the form of water emulsion. The radiation resistant glue should not be degradable, and should also hold its adhesive properties, such as: adhesion tack and cohesion. These properties depend on fine polymer structure.

The glue parameters are examined as follows:

- adhesion - by measuring of force needed to failure the glue joint between smoothed chromium steel plate and adhesive plaster of 25 mm width. Adhesive plasters for medical applications should have the adhesion within the range 3 to 7 N/25 mm - peel adhesion;
- cohesion - by measurement of the time of deglutination of the adhesive plaster (glued to glass inside a thermostat at 70°C, and 0.5 kg loading). The cohesion of medical use of adhesive plaster should be greater than one hour.
- tack - by measurement of the path length of roll of the steell ball accelerated from the inclined

plane with a slope of 45°. The steel ball should roll from 3 to 15 cm - along the glue surface of adhesive plaster - the tack rolling ball method.

Above the mentioned properties of the self adhesive glues depend on many various factors. The adhesion and tack are connected with the diffusion of free polymer chains, Van der Waals interaction and an electrostatic attraction (of functional groups generated at the surface of glue layer). The cohesion depends on the molecular mass of the polymer. Assuming normalized measurements and the application of identical recipes for manufacturing of glues, it is reasonable to expect, that the obtained parameters are a function of the averaged molecular mass of its statistical distribution. The adhesion and tack are larger at lower masses, and the cohesion is higher at larger masses.

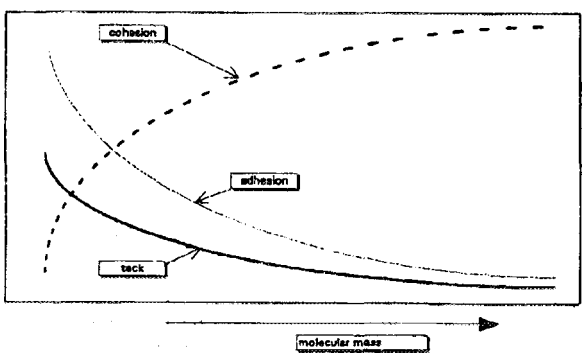

Fig.1. The main properties of pressure sensitive adhesive vs. molecular mass of used polymer, after [1].

Data in Fig.1 suggest that the glue having good properties should be characterized by a certain optimum molecular mass and its statistical distribution. The similar dependencies of glue properties as a function of molecular masses with more detailed data are presented in Fig.2.

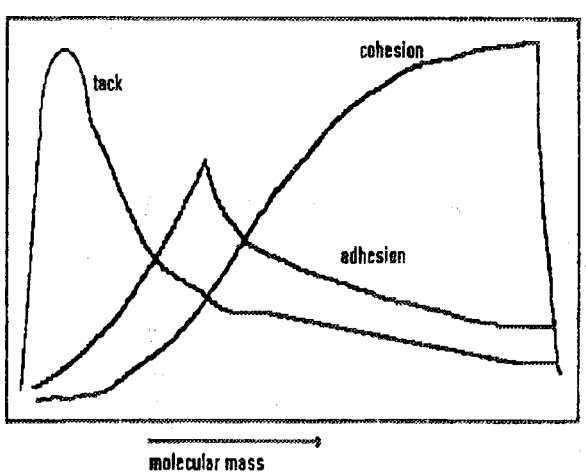

Fig.2. Relationship between the properties of self adhesive glue and the polymer molecular mass for wide range of change of molecular masses.

One can observe, that a polymer after irradiation should not be degraded and not cross-linked, because too large change of the molecular mass influence the change of glue properties.

Samples preparation

The glue coats were prepared of various values of adhesion from 1 to 15 N/25 mm, and the cohesion test results within the range of 2 min up to above 1 hour. The variety of substrates: polyester foils, cloths and unwoven fabrics were coated. These samples were irradiated with a recommended dose of 25 kGy. Firstly the sample with worse properties was used for preparation of coat on the surface of polyester foil. Then the samples obtained by this way were irradiated with various doses from 20 to 40 kGy. All samples before and after irradiation were examined for the determination of: adhesion, cohesion and tack.

Irradiation procedure

The irradiations were conducted in a new electron beam facility for radiation sterilization of medical devices for single use (installed in the INCT), applying an electron linac: UELV-10-10-S-70-1 (Table 1).

Table 1. Main technical characteristics of the UELV-10-10-S-70-1 electron linear accelerator, produced by the Research Production Association, TORIY, Russia.

Electron energy	10 MeV
Energy instability	5%
EB current instability	5%
Average beam power	up to 10 kW
Pulse duration	4.5 μs
Repetition rate	25 to 400 Hz
Scan frequency	1, 2, 5 Hz
Scan line length	65 cm

The samples were irradiated with the recommended dose of 25 kGy. Some samples were irradiated with increasing doses: 20, 25, 30 and 35 kGy at conveyor velocites of: 53, 42, 36 and 30 cm/min. The values of dose were determined using

Table 2. Properties of glued coats for various samples of the glue, irradiated with dose of 25 kGy.

Run no.	Before irradiated		After irradiated	
	adhesion N/2.5 cm	cohesion (time)	adhesion N/2.5 cm	cohesion (time)
1	3.5-10	2 min	3.5-6.5	> 1 h
2	3.0-5.8	3 h	3.6-4.8	3 h
3	3.3-6.2	1 h	3.6-4.8	1 h
4	7.0-10	3 h	7.3-9.0	3 h
5	3.0-5.8	7 min	3.0-4.7	> 12 h

a quasi-adiabatic water calorimeter with an accuracy better than 10%. The spatial distribution of dose inside the irradiated samples was measured employing a routine dosimetric PVC film. The radia-

Table 3. Properties of glued coats manufactured with a choosen glue batch after the absorption of various doses.

Dose [kGy]	Adhesion N/2.5 cm	Cohesion (time)
0	3.5	33 min
22.9	3.5-6.2	> 1 h
26.1	3.5-5.7	> 1 h
31.1	5.0-7.2	> 1 h
38.5	3.0-4.5	> 1 h

tion-induced change of PVC optical absorbance was determined spectrophotometrically at 395 nm. Obtained results are shown in Tables 2 and 3.

Conclusions

- sticking plasters for medical applications prepared on the basis of the acrylic emulsion self adhesive glues are radiation resistant up to a dose level of 40 kGy;
- properties of the irradiated glue are improved, the adhesive dose is not changing and the cohesion increases. The elaborated glue is suitable for sticking plasters or self adhesive tapes contacting with living human tissue.

Reference

[1]. Krenceski M, Johnson J.J, Temin S.C.: Macromol. Chem. Phys., C26(1) (1986).

PARTICLE TRACK MEMBRANES IN A CORONA DISCHARGE FIELD

M. Buczkowski, W. Starosta, D. Wawszczak, A. Fiderkiewicz

Particle track membranes (PTMs) are advanced technology products manufactured by cyclotron technique. Thin polymeric film is bombarded by accelerated heavy ions beam and then processed with a photochemical treatment (UV sensitization and chemical etching). The result is a thin microporous membrane with geometrically perfect cylindrical pores and a smooth, flat surface. A typical polymeric material for PTMs is a polyethylene terephtalate (PETP) film, 10-15 μm in thickness. Another features of PTMs made of PETP film are: good mechanical strength, good chemical, thermal

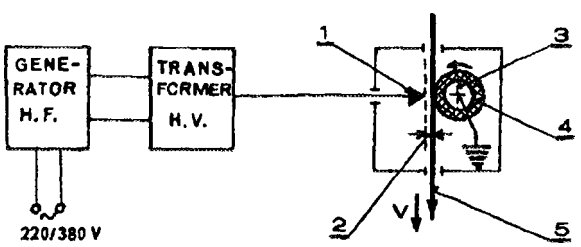

Fig.1. The device for corona discharge activation of polymer films: 1 - a multi-edge electrode, 2 - the air gap, 3 - a cylindrical electrode, 4 - an isolator, 5 - the moving strip of a membrane.

resistance and very high radiation resistance. The characteristic values of PTMs are: pore size in the range from 3.0 to 0.2 μm and surface pore density, respectively from 10^6 to 10^9 pores/cm^2.

PTMs can be used for microfiltration including microbiological cleaning in: biochemistry, micro-

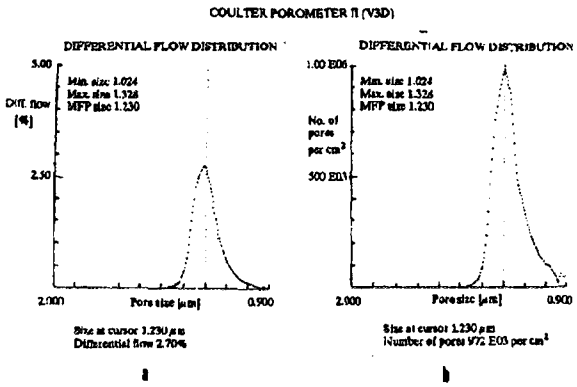

Fig.2. Parameters of the PETP particle track membrane from Coulter Porometer II instrument: a - differential flow distribution, b - differential pore number distribution.

biology, medicine, pharmacy, biotechnologies, environmental monitoring [1, 2].

Because of the wide range of possible applications it is a need for the modification of surface properties of PTMs, among others for preparing multilayer devices. One method for such a modification is the corona discharge activation. PTMs samples have been treated with a corona discharge using an industrial type activator in METALCHEM Centre, Toruń, Poland (Fig.1). The high voltage was 10-20 kV with a frequency of 10-40 kHz [3].

A sample of a particle track membrane was taken for experiments. The main filtrating parameters of the PTM, obtained with a Coulter Porometer II

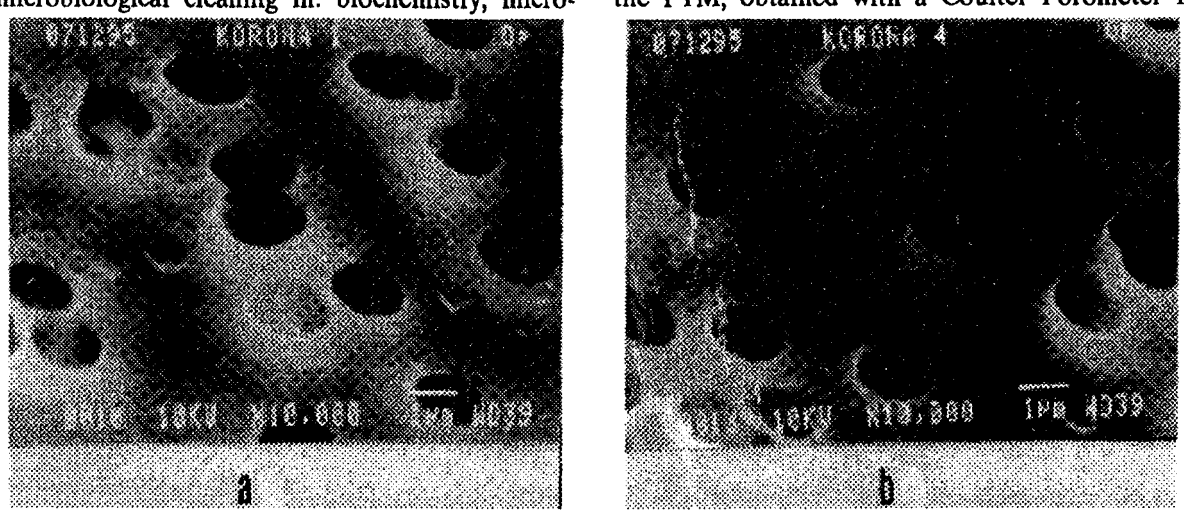

Fig.3. SEM photograph of PTM surface after the corona discharge: a - high velocity of membrane moving, b - small velocity of membrane moving (near region of spark discharge).

PL9700846

instrument, were the following: mean value of pore size - 1.23 μm, surface pore density - $1.3*10^7$ cm^{-2}, permeability - 54 litre*min^{-1}*cm^{-2} (Fig.2). A strip of such PTM was moved between the electrodes during the corona discharge with a fluent change of velocity (Fig.1).

Unitary energy of activation depends on the velocity of the moving membrane strip between the electrodes. In the case of too small velocity the corona discharge changes into the spark discharge which causes the local destruction of the membrane. When the velocity is higher one cannot observe changes on the surface of the membrane by SEM photography (Fig.3), and also it is no change in filtration parameters.

In conclusion one can say that the corona discharge activation is a good method for changing of the surface energy of the particle track membranes. Before such treatment it is necessary to choose proper parameters of activation such as high voltage and velocity of the moving membrane strip.

References

[1]. Proc. of the 2rd Meeting on Particle Track Membranes and Their Applications, Szczyrk, Poland, 2-6 December 1991. INCT, Warszawa 1992, pp. 90.

[2]. Proc. of the 3rd Conf. on Particle Track Membranes and Their Applications, Jachranka, Poland, 26-29 October 1993. INCT, Warszawa 1995, pp.123.

[3]. Ratajczak Z.: Aktywowanie folii z PE i PP. Poradnik. OB-RMiUCh, METALCHEM, Toruń 1995, 17p.

EB POLLUTANTS REMOVAL PROCESS FROM MODEL GASES WITH HIGH SO_2 CONCENTRATION

A.G. Chmielewski, Z. Zimek, S. Bułka, J. Licki[1/], L.Z. Villanueva[2/], L.S. Ahumada[2/]

[1/]Institute of Nuclear Energy, Otwock-Świerk, Poland,

[2/]Chilan Commission of Nuclear Energy, Chile

The emission of noxious pollutants (SO_2 among them) into the atmosphere from the heavy industry activity is of growing concern and this has generated an interest in finding viable and cost-effective solutions to SO_2 pollution control. By-products produced in such a technology are also of great importance. In the case of SO_2 removal in principle they are: concentrated SO_2, sulfuric acid, elemental sulfur or ammonia sulfate.

In the recent years for the removal of SO_2 and NO_x from flue gases an electron beam process has been developed. Up to now the technology has been applied for the flue gas treatment with SO_2 concentrations up to 3000 ppm. The goal of this work is to check the possibility of applying the process for industrial gases with a high SO_2 concentration (up to 15% vol.). This range of SO_2 concentration is encountered in industrial off-gases released in processes applied in the copper industry. Because it is well known that SO_2 in the eb process is removed mostly by a thermochemical reaction and partly by a radiation induced reaction only, the energy transfer (G factors) for SO_2 transformation being limited, therefore other modifications of the process are studied to improve the reaction efficiency.

The laboratory unit in the Institute of Nuclear Chemistry and Technology [1, 2] has been used for

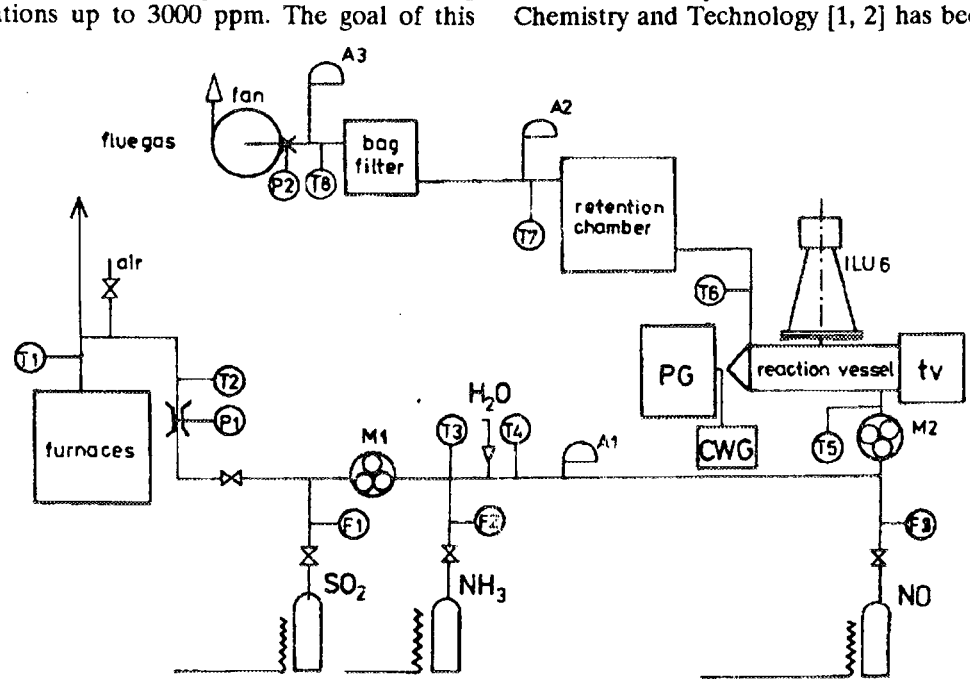

Fig. Process flow diagram: T1-T8 - temperature sensors, P1-P2 - pressure sensors, F1-F3 - flow meters, M1-M2 - gas mixers, A1-A3 - gas sampling points, PG - microwave pulse generator, CWG - microwave c.w. generator, tv - tv camera, ILU6 - electron acelerator.

investigation of the SO_2 removal efficiency from flue gases with high SO_2 concentration. The process flow diagram is shown in Fig. A heating device with a water-tube boiler with 100 kW thermal power was applied to produce the combustion gas. The proper composition of flue gas has been obtained by introducing SO_2 and NH_3 into the gas stream. Natural gas is burned in a house heating furnace whose construction, from the technical point of view, is similar to the water-tube boiler. The produced combustion gas flows to an irradiation chamber. On the transportation way of the gas some controls and gauges are located. The orifice is used for the determination of flow rate of the combustion gas, by measuring drop pressure of the gas flowing through the orifice. Along the pathway between the boiler and irradiation chamber the probes are located for the analysis of flue gases and for the dosage of SO_2, NH_3, H_2O.

A steam generator was designed, built and installed to increase the water content in flue gas. The amount of steam is controlled by adjustable AC voltage which is used for water evaporation. The temperature along the transportation way of the gas from the furnace to the irradiation and retention chamber is kept by 6 separate adjusted heaters to stabilize the temperature on the required level. Each has changeable electrical power up to 1 kW.

The reaction vessel is constructed as a cylinder with a diameter 200 mm. The electron beam introduces the reaction volume perpendicularly to the axis of the vessel. It passes though a titanium window 25 mm thick. The inlet and outlet of the flue gas are mounted on the wall side of the vessel. The stream of the gas can flow exactly with a flow rate of 5 m^3/h.

Measurements of the gas composition before and after irradiation were performed to determine the efficiency of SO_2 removal from gases. At the inlet to the installation high concentrations of SO_2 up to 15% (V) are measured. The gas leaving the irradiation chamber contains: a lower concentration of SO_2, the unreacted NH_3 and aerosols of sulfuric and nitric acids and solid particles of ammonium sulfate and nitrate (final product). The solid particles of the final products are of submicron size and hygroscopic. They may clog and incrust the gas sample line or a capillary at the gas analyzers. To separate them, a set of gas filters were inserted at the beginning of the gas sampling line. The dilution technique was used for the measurement of this high SO_2 concentration. Due to the high concentration of SO_2, up to 15% (V), and water, up to 20% (V), used for this application, the dilution ratio of 100 to 1 was selected. Both the gas conditioning and the dilution units were equipped with suitable sets of capillaries. The Nessler method was used to determine the ammonia content at the outlet of the installation; standard solution of NH_4Cl and water free of ammonia were used. Water content in the flue gas was measured by the moisture absorption tube method (EPA Method 4, JIS Z 8808-1977). ILU 6 accelerator was used to accelerate the electron beam [2, 3]. The dose deposited in the flue gas was changed by using a different repetition rate of the electron pulses. The electron beam passing through the accelerator window, layer of air, reactor chamber window, loses its energy. Only 13.2% of the total energy of the electron beam at the entrance of the reaction vessel is deposited in the gas phase.

Table. The matrix of experimental results of SO_2 removal efficiency.

	SO_2 [%]	NH_3	DOSE [kGy]	H_2O [%]
SO_2	5; 10; 15	0.9	6.8	15
NH_3	10	0.7; 0.9; 1.1	6.8	15
DOSE	10	0.9	3.4; 6.8; 10.2	15
H_2O	10	0.9	6.8	10; 15; 20
ΔSO_2	85; 85; 82	66; 85; 95	75; 85; 88	66; 85; 92

To conclude the flue gas with high SO_2 content can be effectively cleaned by the NH_3 and electron beam simultaneous treatment. The efficiency 90-95% of the SO_2 removal was obtained in specific conditions (SO_2 content 10-15%). The ammonia stoichiometry, humidity and dose have a sharp influence on the SO_2 removal efficiency. The product formed in the process is ammonia sulfate which is a commercial fertilizer especially useful in arid zone where the soil deficit of sulfur is observed. The experimental results are given in Table.

References

[1]. Chmielewski A.G., Iller E., Zimek Z., Licki J.: Laboratory and Industrial Installation for Electron Beam Flue Gas Treatment. Proceedings of an International Symposium on Application of Isotopes and Radiation in Conservation Environment, Karlsruhe, 9-13 March 1992. IAEA-JM-325/124, p. 81, 19.

[2]. Zimek Z., Stachowicz W.: Multipurpose electron accelerator facility in INCT. 4th Conference on Radioisotope Application and Radiation Processing in Industry, Leipzig, 19-23 September 1988.

[3]. Chmielewski A.G., Zimek Z., Panta P.P.: Electron beam system and dose distribution in the process vessel in pilot plant for flue gases treatment. Report INCT-2117, Warszawa 1991.

REMOVAL OF SO_2 FROM HIGH HUMIDIFIED FLUE GAS BY USE OF E-B METHOD

A.G. Chmielewski, B. Tymiński, J. Licki[1/], E. Iller, Z. Zimek

[1/]Institute of Nuclear Energy, Otwock-Świerk, Poland

Water vapour concentration in irradiated flue gas is a very important parameter affecting SO_2 removal. It was found that the humidity 10 to 12% vol. is satisfactory. Usually in raw flue gas the humidity is

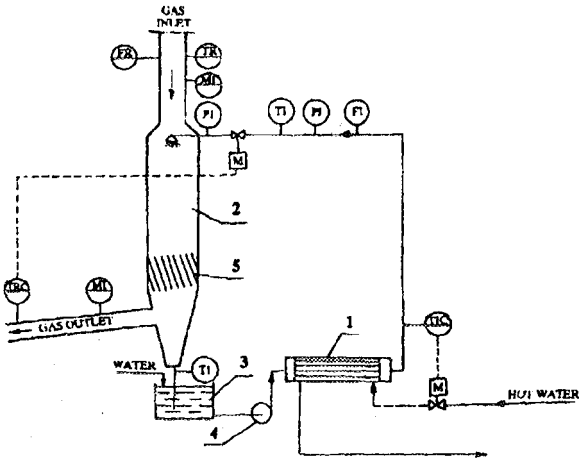

Fig.1.

4 to 6% vol. however the temperature is too high for an efficient removal of SO_2. Reduction of temperature and an increase of humidity usually is done by direct evaporation of fine sprayed water droplets. Such a method of flue gas conditioning is good if the temperature of raw flue gas is 150-160°C. In the case of lower temperature, which is usually at EPS Kawęczyn, the entalphy of flue gas is too low for the evaporation of a satisfactory amount of water. Some improvement was achieved by spraying hot water. In the case when the temperature of inlet flue gas is lower than 110°C the real method of efficient humidification of flue gas is partial evaporation of hot water. The scheme of such a system of conditioning of flue gas is presented in Fig.1. Circulating of water is forced by a pump 4 through a heat exchanger 1 a control valve and a spraying nozzle system. The sprayed water evaporates in a spray cooler 2 and its temperature decreases to about 50°C. At the bottom of the spray cooler is a layer of packing 5 where water droplets are separated from gas phase and water flows to a tank 3. In the process of humidification it is possible to change the temperature of sprayed water and its amount which allows to control temperature and humidity of the conditioned flue gas. Fig.2 presents the results of experiments in which a high efficiency removal of SO_2 was achieved.

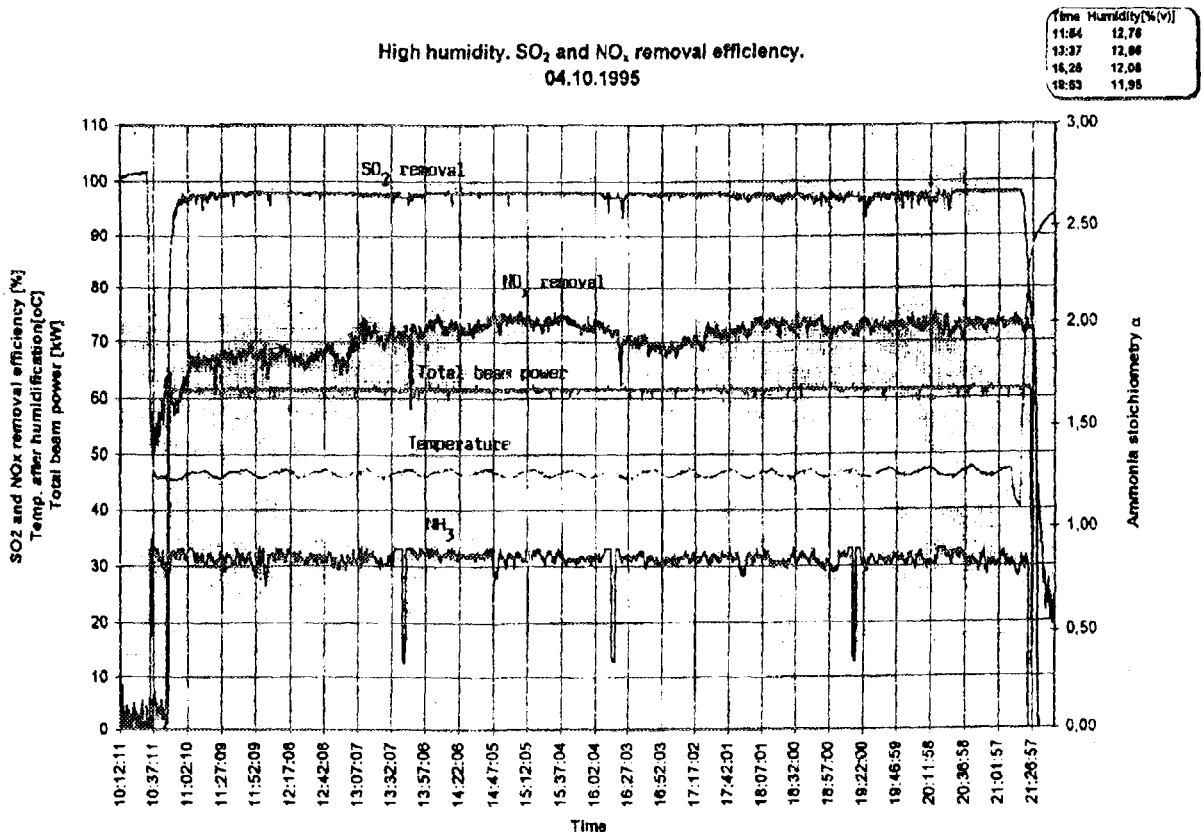

Fig.2.

PL9700848

NUCLEONIC CONTROL SYSTEMS

RADON MONITORS

B. Machaj

This research aimed to compare and verify numerous methods [1-8] of registration of alpha activity of radon short lived daughters deposited on a filter and to establish the best processing algorithm of the signal including multidimensional methods of regression (Partial Least Square). This work includes: elaboration of a computer program for computing the activity of radon and its decay products against time, elaboration of a program for multidimensional regression, and a comparison of the obtained results. Construction of a radon chamber for practical verification of the computations is foreseen. A gauge for continuous measurement of radon concentration in the mine air is under consideration.

A computer program based on known relations for activity variations [9, 10] simulating activity variation of radon and its short lived decay products in a measuring chamber was elaborated and verified. The program computes activity variation for different radiation equilibrium degree between radon and its decay products. It has some additional facilities such as: computation of total alpha activity produced by $^{222}Rn+^{218}Po+^{214}Po$ against time, and total registered activity (number of alpha decays) from time t=0 to current time. The results of computations every 1 min. in the range 0-255 min are stored on a computer disk and transformed into

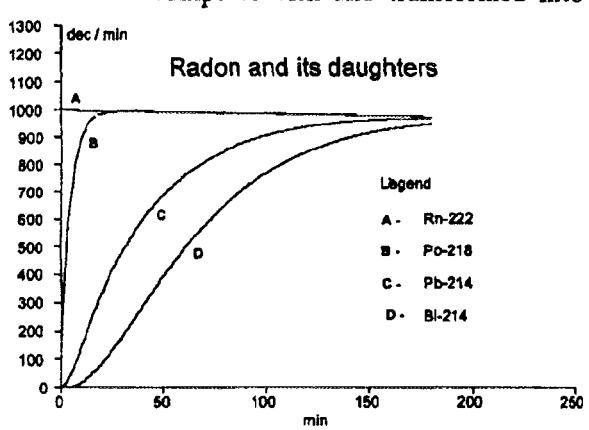

Fig.1. Activity variations of radon and its short lived decay product against time in a measuring chamber. Radon activity at t=0 equals 1000 dec/min, activity of ^{218}Po, ^{214}Pb and ^{214}Bi equals 0.

ASCII format that can be used by ready made computer programs for drawing diagrams (e.g. WordPerfect), Figs 1 and 2. The second part of the program concerning variation of activity of decay products deposited on the filter during sampling period is under development now. The program will compute activity variation every 1 min starting from the moment t=0 when deposition of the sample

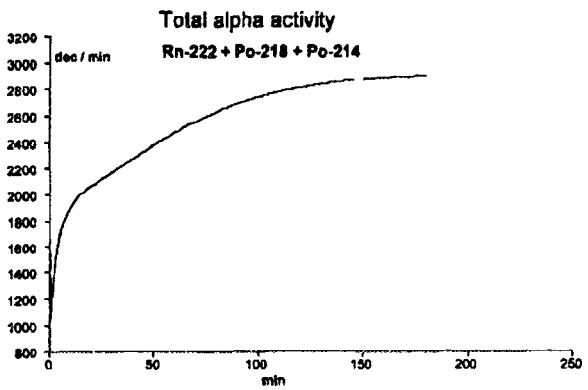

Fig.2. Total alpha activity of $^{222}Rn+^{218}Po+^{214}Po$ against time in a measuring chamber at t=0 radon activity equals 1000 dec/min, activity of ^{218}Po, ^{214}Pb and ^{214}Bi equals 0.

begins until 100 min. Again the computations are done for the different radiation equilibrium degrees with similar facilities as in the previous program.

The constructed radon measuring stand consists of two parts: a small (5 l) reference radon source chamber with a 200 kBq ^{226}Ra open source giving a radon concentration of approx. 40 Bq/cm^3, and the proper radon chamber approx. 1 m^3 in volume. The air from the source chamber with high radon concentration is injected into the radon chamber to get the required radon concentration. The radon chamber was constructed, while the source radon chamber is still under construction.

Continuous radon monitor of radon concentration in air

Registration of alpha activity produced by ^{222}Rn, ^{218}Po and ^{214}Po follows immediately after the measuring chamber is filled with filtered air, within the period 15-120 min. Two ways of alpha activity registration are considered: by the Lucas chamber with a ZnS(Ag) scintillator and a semiconductor detector of scintillation light and by a semiconductor alpha detector. It results from the analysis that for the registration of alpha activity more efficient is the Lucas chamber. The estimated number of registered pulses from the Lucas cell at a ^{222}Rn concentration of 250 Bq/m^3 is 11 pulses/15 min ±43% and 124 pulses/120 min ±13%, whereas for the semiconductor detector with an active area of 1200 mm^2 it is 7 pulses/15 min 50% and 96 pulses/120 min ±16%. To speed up the exchange of the air in the measuring chamber, an air pump will force the

ambient filtered air (radon decay products removed) within a short period of time (approx. 1 min) and flush the chamber. Foreseen electronics employs low power consumption microprocessor circuits enabling continuous operation for 2-3 months after the rechargeable battery is fully charged. The measuring results are displayed on a digital indicator of the gauge, and are transmitted to the laptop computer by serial port. The gauge will have the form of a cylinder, 8 cm in diameter, and approx. 40 cm in length placed in a hole in the rock.

References

[1]. Tsivoglou E.C., Ayer H.E., Holaday D.A.. Occurrence of nonequilibrium atmospheric mixtures of radon and its daughters. Nucleonics, **11**, 9, 40 (1953).

[2]. Thomas J.W.: Measurement of radon daughters in air. Health Phys., 23, 783 (1972).

[3]. Markov K.P., Ryabov N.W., Stas K.N.: A rapid method for estimating the radiation hazard associated with the presence of radon daughter products in air (in Russian). Atomnaja Energia, **12**, 4, 315-319 (1962).

[4]. Nazaroff W.W.: Optimizing the total alpha three count technique for measuring concentration of radon progeny in residences. Health Phys., 46, 395-405 (1984).

[5]. Scott A.G.: A field method for measurement of radon daughters in air. Health Phys., 41, 403-405 (1981).

[6]. Kartathov N.P.: A rapid method for determination of aerosol RaA and of potential energy in the air (in Russian). Atomnaja Energia, **20**, 5, 444-448 (1966).

[7]. Domański T., Chruścielewski W.: Measuring method of low concentration alpha potential energy of Rn-222 decay products in mines air (in Polish). Medycyna Pracy, **XXVII**, 1, 29-37 (1976).

[8]. Radiation monitoring in the mining and milling of radioactive ores. 1989. IAEA Safety Series no. 95.

[9]. The atomic nucleus. Ed. R.D. Evans. McGraw-Hill Book Company, 1970.

[10]. Radon and its decay products in indoor air. Eds. W.W. Nazaroff, A.V. Nero. John Willey & Sons, 1988.

A MATLAB PROGRAM FOR NONLINEAR PARTIAL LEAST SQUARES REGRESSION

P. Urbański

The linear biased regression methods such as partial least squares (PLS) and principal components regression (PCR) are widely used in multivariate calibration [1]. However, nonlinear relationship between the (y) and (x) variables often observed in practice prevents the use of these methods in routine applications [2]. There are many developed nonlinear regression methods, e.g. [2-7], but from the point of view of application in X-ray spectrometry the nonlinear PLS regression was chosen, since it is particularily well suited for underdetermined, highly collinear data [3]. An algorithm for the PLS regression with nonlinear inner relation is based on the known NIPALS procedure [1, 7-8]. If **X** and **Y** are the data matrices, **T** and **U** scores (latent variables) matrices, **P** and **C** are loadings, then the linear PLS model can be expressed by the follwing set of equations:

$$\mathbf{X} = \mathbf{TP'} + \mathbf{E_x}$$
$$\mathbf{Y} = \mathbf{UC'} + \mathbf{E_y}$$
$$\mathbf{U} = \mathbf{T} + \mathbf{E_u}$$
$$\mathbf{Y} = \mathbf{TC'} + \mathbf{E_{y*}}$$

where the matrices **E** contain residuals [7]. In the linear PLS model each column $\mathbf{u}_i$ of the matrix **X** is related to the corresponding column $\mathbf{t}_i$ of the matrix T. The concept of the nonlinear PLS model is to modify this relation for each dimension with a functional transformation

$$\mathbf{u}_i = \mathbf{f}_i(\mathbf{t}_i) + \mathbf{e}_i$$

where $\mathbf{e}_i$ - a vector of residuals.

The program for computing nonlinear PLS model is based on the described algorithm with the polynomial spline used as the inner relation $\mathbf{f}_i$. It is written in the MATLAB language as the M - file *spl-pls2.m* [9] and can compute various models depending on the three input parameters: *my* - number of dependent variables, *k* - number of knots in the polynomial spline function, *l* - degree of the polynomial. The models which can be computed by the program are listed in the Table.

Table. PLS models computed by the MATLAB spl_pls2.m program.

Input parameters			Model
my	k	l	
1	0	0	Linear PLS for one dependent variable
> 1	0	0	Linear PLS for my dependent variables
1	0	> 1	Nonlinear PLS for one dependent variable Inner realation - polynom of l-degree
>1	0	> 1	Nonlinear PLS for my dependent variables Inner realation - polynom of l-degree
1	> 1	> 1	Nonlinear PLS for one dependent variable Inner realation - regression spline
> 1	> 1	> 1	Nonlinear PLS for my dependent variable Inner realation - regression spline

The developed program will be used to study nonlinear calibration models of the radiometric gauges. This study should be continued, since according to the opinion expressed by some researches [3], "the nonlinear PLS algorithms are still in a research phase, they have not proved themselves in many applications".

References

[1]. Martens H., Naes T.: Multivariate Calibration. Wiley & Sons, Chichester 1991.

[2]. Gemperline P.: J. Chemometrics Intell. Lab. Syst., **15**, 115 (1992).

[3]. Frank I.E.: Chemometrics Intell. Lab. Syst., **27**, 1 (1995).

[4]. Hoskuldsson A.: J. Chemometrics, **9**, 91 (1995).

[5]. Hoskuldsson A.: J. Chemometrics, **6**, 307 (1992).

[6]. Taavitsainen V-M.: Chemometrics Intell. Lab. Syst., **14**, 185 (1992).

[7]. Wold S.: Chemometrics Intell. Lab. Syst., **14**, 71 (1992).

[8]. Geladi P., Kowalski B.: Anal. Chem., **185**, 1 (1986).

[9]. Urbański P.: Raport IChTJ. Seria B. Warszawa 1996 (in print).

ANALYSIS OF LEAD AND TIN IN GALVANIC BATH BY XRF AND MULTIVARIATE CALIBRATION

E. Kowalska, P. Urbański

Modern technologies often require strict and fast control of the composition of galvanic bath used for the deposition of Sn-Pb layers on printed boards. An XRF instrument developed for such purposes consists of a single measuring head with an Am-241 source, proportional counter, pulse amplifier and a personnal computer [1]. But the most important feature of the instrument lies in its multivariate calibration methodology, based on the partial least square regressions (PLS) [2].

The general goal of the PLS technique applied in this case is to express the information contained in the data matrix (counts collected in each of m channels of the measured X-rays spectrum) $X=\{x_1, x_2, ..., x_m\}$ by a lower number of latent variables $T = \{t_1, t_2, ..., t_a\}$ called the components or scores and the loadings $P=\{p_1, p_2, ..., p_a\}$. The number of components a used in the model is determined from the analysis of the mean square errors of crossvalidation (MSECV) [2-4].

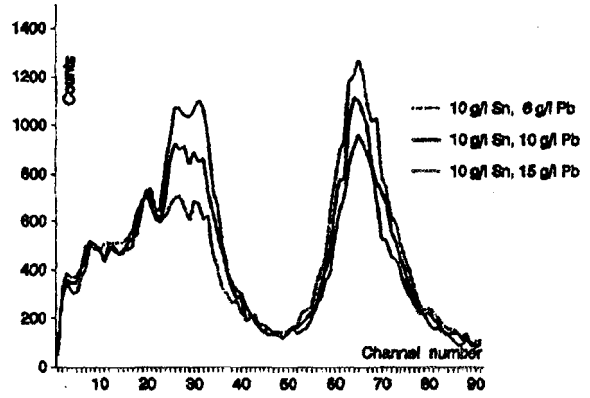

Fig.1. Spectrum of the X-ray excited by an Am-241 source in liquid samples of galvanic bath.

Fig.1 shows the spectrum of X-rays excited by the source of Am-241 in a liquid sample of galvanic bath with a constant tin content (10 g/l) and a variable concentration of lead (6-15 g/l). It can be seen that variations of the lead content in the bath strongly influence the intensity of the tin peak. This, so called the interelement effect is often observed in the XRF analysis. It was found that application of the partial least squares (PLS) method for calibration allows to correct this effect. Fig.2 shows the plot of the loading vectors p_1 and p_2 vs. channel number. It is seen, that the vector p_1 which represent the loadings corresponding to the latent variable t_1 responsible for tin content, contains some information from the channels of the lead peak area. Similar behaviour is observed in the case of the vector p_2 which corresponds to the lead content: its value is also dependent on the intensity of the Sn K peak. The scatter plot of the first two latent variables (scores) is shown in Fig.3. It is seen that in the new coordinates Pb vs. Sn content the lines

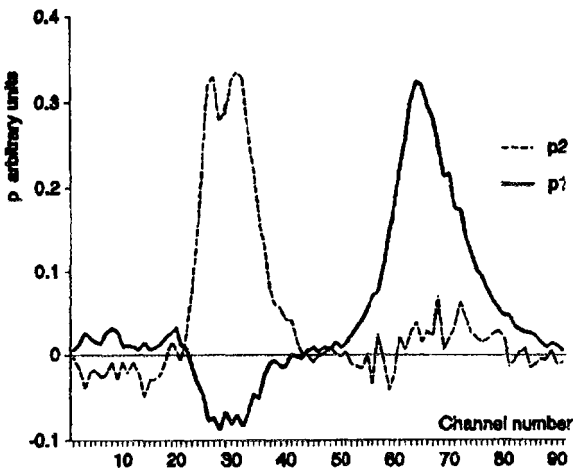

Fig.2. Plot of the loading vector p_1 and p_2 vs. channel number.

corresponding to the constant Pb and Sn concentrations are parallel to the new axes. This means that the Sn and Pb contents are independent of each other, hence the interelement effect was fully corrected. Fig.3 remains the nomograms construct-

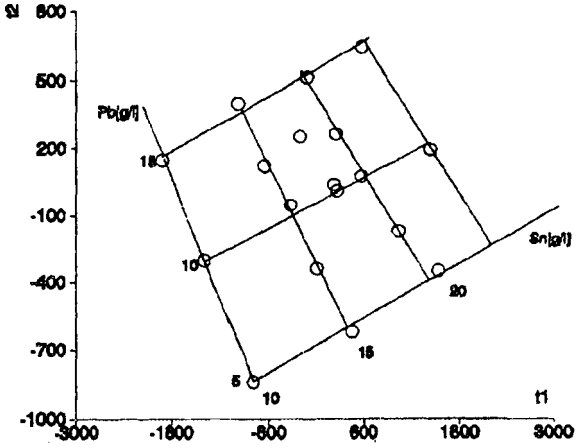

Fig.3. Scatter plot of the first two latent variable t_1 and t_2.

ed to correct matrix effects in the XRF analysis often used in the early days of the application of this method [5].

The evaluation of the established model shows that for the Pb concentration ranging from 6 to 15 g/l the root mean square error of crossvalidation (RMSECV) was 0.5 g/l whereas for the Sn content ranging from 10 to 25 g/l RMSECV it was 0.8 g/l. Obtained results have proved that implementation of the multivariate calibration in low-resolution XRF analysis can result not only in improvement in accuracy, but also may expand the range of application of this methodology.

References

[1]. Urbański P., Kowalska E.: Nukleonika, 40, 61 (1995).

[2]. Martens H., Naes T.: Multivariate Calibration. Wiley & Sons, Chichester 1991.

[3]. Geladi P., Kowalski B.: Anal. Chim. Acta, **185**, 1 (1986).
[4]. Haaland D., Thomas E.: Anal. Chem., **60**, 1193 (1988).
[5]. Dziunikowski B.: Energy Dispersive X-Ray Fluorescence Analysis. PWN, Warszawa 1989.

SMOOTHING OF X-RAYS SPECTRA USING REGRESSION SPLINES AND FOURIER ANALYSIS

W. Antoniak, P. Urbański

PL9700850

The real data obtained by physical measurements can be expressed as a sum of the two components: the noise component and the signal component [1]

$$y_r = y + s \quad (1)$$

where: y_r is the raw data vector, y - the signal vector and s - the noise vector. The noise vector can be considered here as a sample of the random distribution with the mean of zero. The assumption that the noise and signal components are additive and uncorrelated seems to be reasonable [1], also in the case of X-ray spectra. In the considered case, y_r is vector of the measured spectrum, y - an "ideal" spectrum. Two smoothing methods were tested: regression splines and Fourier analysis.

The first method is based on the approximation of the raw spectrum by y_r the polynomial piecewise regression splines y_w^s [2-3]:

$$y_w^s = b_0 + b_1 k + b_2 k^2 + b_3 k^3 + \sum_{j=1}^{l} b_{j+l}(k - kw_j)_+ \quad (2)$$

where: $(k-kw_j)_+ = k-kw_j$ for $k > kw_j$, $(k-kw_j)_+ = 0$ for $k \leq kw_j$; k - channel number; kw_j - knots position; l - knots number.

Coefficients b are computed by the least squares regressions. An example of the X-ray spectrum smoothed by means of regression splines is shown in Fig.1.

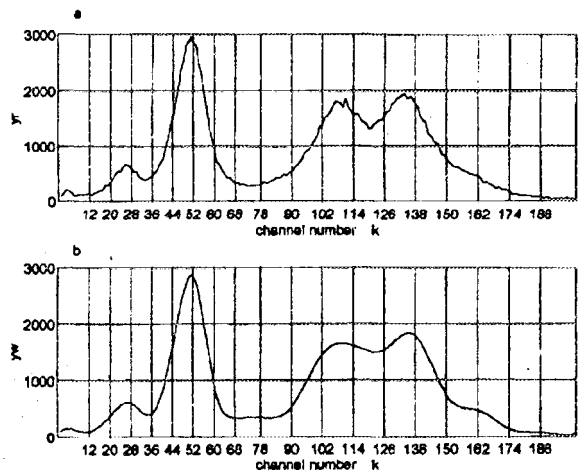

Fig.1. Spectrum of the X-rays excited in a sample of black coal by ^{109}Cd source: a - without smoothing, b - after smoothing using regression splines; knots position marked by the bars.

The second smoothing method utilizes the fact that Fourier transform $FFT(y_r)$ of equation (1) allows to perform the analysis of data in the frequency domain [4].

$$FFT(y_r) = y_r(\omega) = y(\omega) + s(\omega) \quad (3)$$

where: $y_r(\omega)$, $y(\omega)$, $s(\omega)$ - Fourier transforms of y_r, y and s to the frequency (ω) domain.

In the frequency domain $y(\omega)$ and $s(\omega)$ have a very different behaviour. Information about ideal spectral distribution (y) is concentrated at the low frequencies, whereas the noise is distributed in the higher band. The aim of the smoothing is to cut-off this part in which the noise is dominant from the frequency spectrum. Fig.2 shows an X-ray spectrum, its transform into frequency domain and

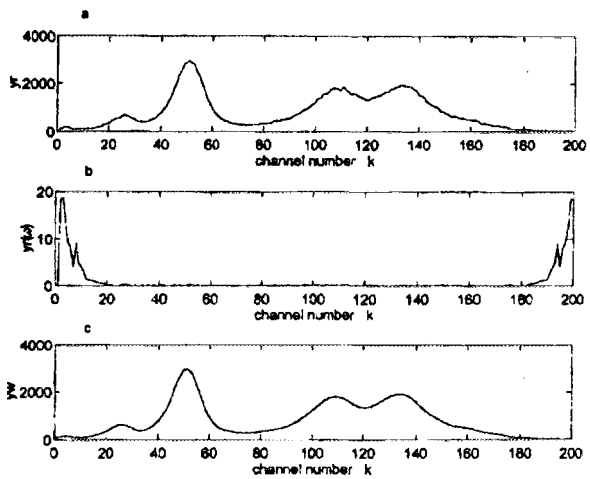

Fig.2. Spectrum smoothing using Fast Fourier Transform: a - before smoothing (the same as in Fig.1a), b - Fourier Transform of the spectrum, c - smoothed spectrum using cut-off window of 20 channels.

smoothed spectrum. The part of the frequency spectrum being cut-off contains all the channels from 21 to 179 (Fig.2b).

To obtain properly smoothed spectra in the case of regression splines, the optimal knots position and its numbers should be chosen. The same should

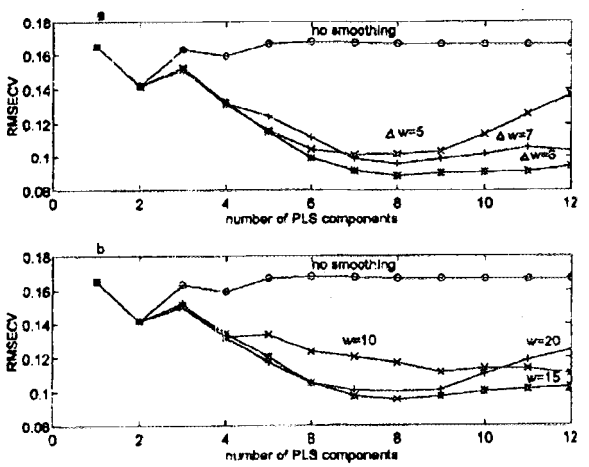

Fig.3. Influence of the smoothing on the crossvalidation error (RMSECV) of the PLS model: a - spline smoothing, (Δw - distance between knots), b - FFT smoothing (w - cut-off window).

PL9700851

be done with the cut-off window width in the case of FFT. The smoothing optimization criteria are discussed in [5]

The smoothed spectra were used in calculation of the multivariate calibration models using the PLS regression method. An example of their application for the XRF determination of sulphur in black coal [6] is shown in Fig.3. It should be noted, that application of the smoothed spectra can improve root mean square error of crossvalidation (RMSECV) by about 50%. However, in some other cases of the multivariate calibration very small or no improvement in the model performance was observed. Hence, further research is to be performed to explain when and why smoothing of the raw data can improve performance of the multivariate calibration model.

References

[1]. Larivee R.J., Brown S.D.: Anal. Chem., 64, 2057 (1992).

[2]. Wold S.: Technometrics, 16, 1 (1974).

[3]. Wegman J., Wright I.: IASA, 78, 351 (1983).

[4]. Garcia-Toraff o E.: Appl. Radiat. Isot., 43, 229 (1992).

[5]. Antoniak W. Urbański P.: Raporty IChTJ. Seria B. Warszawa 1996 (w druku).

[6]. Urbański P., Kowalska E.: X-ray Spectrometry, 24, 70 (1995).

DIRECT DETERMINATION OF ABSORBER THICKNESS FROM MÖSSBAUER SPECTRUM

W. Starosta

The shape of Mössbauer spectrum in transmission geometry is given by the expression:

$$n(E_s)=\frac{2f_s}{\Gamma_s\pi}\int_{-\infty}^{+\infty}\frac{\left(\frac{\Gamma_s}{2}\right)^2 dE}{(E-E_s)^2+\left(\frac{\Gamma_s}{2}\right)^2}\prod_{i=1}^{n}\exp\left(-t_i\frac{\left(\frac{\Gamma_s}{2}\right)^2}{(E-E_i)^2+\left(\frac{\Gamma_a}{2}\right)^2}\right) \quad (1)$$

which is also called the transmission integral (TI). In this expresssion Γ_s, Γ_a are energy line halfwidths of source and absorber, respectively, E_i, $t_i=f_i\, n_i\, \sigma_i$ - peak positions and effective thicknesses of the i-th line of absorber and $E_s=E_o(1+v/c)$ - energy of source quanta. Due to difficulties connected with obtaining a compact expression for TI, several methods for determining the shape of spectrum of absorber are applied, e.g. numerical integrations of TI, Fourier or Voigt based deconvolution method, approximation of exponent by Lorentz terms with width and amplitude depending on absorber thickness, or at last approximation by Lorentz function with the condition of "thin absorber". Each of these approaches have some disadvantages. Numerical integration is time consuming, especially if such a method is to be incorporated into the best parameters fitting routine. Fourier transform generally needs a knowledge of the halfwidth of source line. Two other methods need some calibrations if contents of Mössbauer nuclei are to be determined from the spectrum. Besides of that the conception of "thin absorber" requires some definition which can be drawn only on the basis of knowledge of spectrum distortion introduced by finite absorber thickness. All these problems could be avoided when a new formula recently obtained by the author is applied. Using it a direct determination of effective absorber thicknesses is possible.

The formula has been obtained using the following representation for Lorentz terms

$$\frac{t_k\left(\frac{\Gamma_a}{a}\right)^2}{(E-E_a)^2+\left(\frac{\Gamma_a}{2}\right)^2}=-\frac{t_k}{2}+\frac{t_k}{4}\left(\frac{E-E_k-i\frac{\Gamma}{2}}{E-E_k+i\frac{\Gamma}{2}}+\frac{E-E_k+i\frac{\Gamma}{2}}{E-E_k-i\frac{\Gamma}{2}}\right) \quad (2)$$

here $i=\sqrt{-1}$, and using the expansion of exponent containing the Lorentz terms in the form:

$$\exp\left(\frac{t_k}{2}\left(a_k+\frac{1}{a_k}\right)\right)=I_0\left(\frac{t_k}{2}\right)+\sum_{m=1}^{\infty}I_m\left(\frac{t_k}{2}\right)\left(a_k^m+\frac{1}{a_k^m}\right) \quad (3)$$

here I_m - Bessel modified function of m-th order.

Applying the known theorem concerning calculation of an integral in complex plane by the residuals method, the TI can be expressed as a sum of residuals in poles in upper half-plane. Finally, the TI is given by infinite series in the form:

$$n(E_s)=1.0+\left(\prod_{k=1}^{n}\exp\left(-\frac{t_i}{2}\right)\right)\sum_{k=1}^{n}\left(L_k(E_s)+L_k^*(E_s)\right) \quad (4)$$

where:

$$L_k(E_s)=\sum_{p=1}^{\infty}A_{kp}(a_{ks}^*-1.0),$$

$$a_{ks}=\frac{E_s-E_k+\frac{i}{2}(\Gamma_s-\Gamma_a)}{E_s-E_k+\frac{i}{2}(\Gamma_s+\Gamma_a)}.$$

Formula (4) can be easily calculated using a personal computer if the calculations on complex type data are involved.

In order to check the validity of the formula, calculations of the effective thickness of Armco absorber have been performed for 6 μm iron ARMCO foil supplied by Amersham for the calibrations of spectrometer. In the calculations, the halfwidth of the absorber line was assumed to be constant and equal to table value of iron ^{57}Fe nuclide halfwidth. The value of 2.76 has been obtained for the effective thickness of absorber in fair agreement with 2.80 as calculated for our Armco foil using the table nuclear data for iron ^{57}Fe. For the halfwidth of source line the value of 0.134 mm/s has been obtained. A larger value of halfwidth for the source line can be explained as due to self absorption of Mössbauer resonant radiation.

The obtained results show that the direct determination of the absorber effective thickness can be done using our exact formula for TI and the nuclear

data for iron ^{57}Fe nuclide. At present, the validity of the formula is under study as applied to the contents determination of iron containing minerals (pyrite, clay minerals) in coals and for alumino-silicates. It is expected that the application of this formula will be helpful in removing thickness distortion effects in the Mössbauer spectrum and for more accurate determination of physical parameters of the absorber, particularly in the case when spectra lines are overlapping.

THE INCT PUBLICATIONS IN 1995

1. **Ambroż H.B., Przybytniak G.K.**
   Different forms of triplet states of aryl cations.
   28th Annual International Meeting on ESR Spectroscopy of Radicals in Organic and Bio-Organic Systems. University of Surrey, England, 27-31.03.1995, pp. P1.

2. **Ambroż H.B., Przybytniak G.**
   Nietypowe własności spektroskopowe kationów arylowych (Some specific spectroscopic properties of aryl cations).
   X Krajowy Zjazd Polskiego Towarzystwa Badań Radiacyjnych im. Marii Skłodowskiej-Curie. Streszczenia referatów. Warszawa, Poland, 06-07.04.1995, p. 14.

3. **Ambroż H.B., Przybytniak G.K.**
   Radiation induced oxidation of organic sulphides in acidic glasses.
   Tenth International Congress of Radiation Research. Würzburg, Germany, 27.08.-01.09.1995, p. P09 4.

4. **Ambroż H.B., Przybytniak G.K.**
   Radiation induced radicals of organosulphur compounds.
   Electron Spin Resonance in Electron Transfer and Organic Solids. Abstract. Dresden, Germany, 22-25.11.1995, p. P-1.

5. **Ambroż H.B., Przybytniak G.K.**
   Unique properties of ground state aryl cations.
   16th Conference on Radio- and Microwave Spectroscopy. Poznań, Poland, 25-27.04.1995, pp. P-40.

6. **Ambroż H.B., Przybytniak G.K., Wrońska T.**
   EPR and NMR studies of intermediates of organosulphur compounds.
   17th Conference and Workshop on Magnetic Resonance and the Structure of Matter. Book of Abstracts. Gosen, Germany, 28-30.09.1995.

7. **Bartak J., Machaj B.**
   Instrumentalny pomiar produktów rozpadu radonu-222 w powietrzu (Instrumental measurement of Rn-222 decay products concentration in air).
   Krajowe Sympozjum "Technika Jądrowa w Przemyśle, Medycynie, Rolnictwie i Ochronie Środowiska". Referaty. Warszawa, Poland, 24-27.04.1995, pp. 268-272.

8. **Bartoś B., Bilewicz A.**
   Separation of In^{3+} from Cd^{2+} on crystalline antimonic acid. ^{115}Cd-^{115m}In generator.
   Journal of Radioanalytical and Nuclear Chemistry, Letters, 201, 2, 89-96 (1995).

9. **Bażela W., Guillot M., Leciejewicz J., Małetka K., Szytuła Z., Tomkowicz Z.**
   Magnetic properties of RAgSn (R=Nd, Tb, Ho) compounds.
   Journal of Magnetism an Magnetic Materials, 140-144, 1137-1138 (1995).

10. **Bażela W., Kolenda M., Leciejewicz J., Stuesser N., Szytuła A., Zygmunt A.**
    Magnetic structure of RPtSn (R=Ce, Tb, Ho).
    Journal of Magnetism and Magnetic Materials, 140-144, 881-882 (1995).

11. **Bażela W., Leciejewicz J., Szytuła A.**
    Neutron diffraction studies of RAgSn and RPtSn compounds.
    Selected Problems of Solid-State Physics. Anniversary issue. Vol. 1, no. 1. Kraków 1995, pp. 9-24.

12. **Bielik M., Dźwigalski Z.**
    Fiber-optic control system for an electron gun.
    2nd National Symposium PLASMA'95 "Research and applications of plasmas". Vol. 1. Contributed papers. Warszawa, Poland, 26-28.06.1995, pp. 279-282.

13. **Bieliński J., Głuszewski W., Stokarski W., Przyłuski J.**
Außenstromlos abgeschiedene Nickel-Korund-Dispersionsschichten-Abscheidungs- und Korrosionsverhalten.
Galvanotechnik, 86, 1, 81-86 (1995).

14. **Bilewicz A.**
Separation of ^{90}Y from ^{90}Sr on crystallione antimonic (V) acid.
Radiochimica Acta, 69, 137-140 (1995).

15. **Bilewicz A.**
Własności chemiczne najcięższych pierwiastków (Chemical properties of the heaviest elements).
Postępy Techniki Jądrowej, 38, 1, 35-42 (1995).

16. **Bilewicz A., Narbutt J.**
Specific and nonspecific interactions of amine complexes of silver, zinc and cadmium with ion exchangers.
Solvent Extraction and Ion Exchange, 13, 6, 1083-1096 (1995).

17. **Bobrowski K., Pogocki D., Schöneich C.**
Mechanizm utleniania kwasów zawierających grupę tioeterową generowanymi radiacyjnie rodnikami OH (OH induced oxydation mechanism of carboxylic acids containing thioether group).
X Krajowy Zjazd Polskiego Towarzystwa Badań Radiacyjnych im. Marii Skłodowskiej-Curie. Streszczenia referatów. Warszawa, Poland, 06-07.04.1995, p. 19.

18. **Bobrowski K., Pogocki D., Schöneich C.**
Mechanizm utleniania kwasów zawierających grupę tioeterową generowanymi radiacyjnie rodnikami OH (OH induced oxydation mechanism of carboxylic acids containing thioether group).
Zjazd Naukowy Polskiego Towarzystwa Chemicznego i Stowarzyszenia Inżynierów i Techników Przemysłu Chemicznego. Lublin, Poland, 25-28.09.1995, S-1 P-7.

19. **Bobrowski K., Schöneich C.**
Intermediates during OH-induced oxidation of methionine-containing peptides.
Polish-American Workshop on Reactive Intermediates. Zakopane, Poland, 13-18.08.1995, p. L21.

20. **Bojarski J., Zimek Z.**
Polipropylen odporny radiacyjnie (Radiation resistant polypropylene).
III Jesienna Szkoła Sterylizacji Radiacyjnej Sprzętu Medycznego i Przeszczepów. Warszawa, Poland, 05-06.10.1995, pp. 117-121.

21. **Bojarski J., Bułhak Z., Burlińska G., Kałuska I., Zimek Z., Szwojnicka D.**
Medical quality of the radiation resistant polypropylene.
Radiation Physics and Chemistry, 46, 4-6, 801-804 (1995).

22. **Bojarski J., Burlińska G., Zimek Z.**
Polipropylen w zastosowaniu do wyrobów medycznych sterylizowanych radiacyjnie (Radiation resistant polypropylene for medical devices).
Krajowe Sympozjum "Technika Jądrowa w Przemyśle, Medycynie, Rolnictwie i Ochronie Środowiska". Referaty. Warszawa, Poland, 24-27.04.1995, pp. 99-102.

23. **Bojarski J., Burlińska G., Zimek Z.**
Procesy radiacyjne w polipropylenie i jego odmianach. Rodniki pierwotne i nadtlenkowe (Radiation processes in polypropylene and its modification: Study of primary and peroxide radicals).
X Krajowy Zjazd Polskiego Towarzystwa Badań Radiacyjnych im. Marii Skłodowskiej-Curie. Streszczenia referatów. Warszawa, Poland, 06-07.04.1995, p. 20.

24. **Bojarski J., Burlińska G., Zimek Z.**
Radiacyjna modyfikacja polipropylenu (Radiation modification of polypropylene).
XII Konferencja Naukowa "Modyfikacja polimerów". Kudowa Zdrój, Poland, 11-15.09.1995, pp. 313-316.

25. **Borucki J., Pszonicki L.**
The seasonal geochemical variations in the active stream sediment of the tributaries of Lubatówka and Jasiołka by Rogi, near Krosno (Carpathians).
Geological Quarterly, 39, 1, 145-164 (1995).

26. **Bouzyk E.**
Opóźnienie mitotyczne indukowane przez promieniowanie jonizujące (Mitotic delay induced by ionizing radiation).
Postępy Techniki Jądrowej, 38, 1, 2-7 (1995).

27. **Bryl-Sandelewska T., Zimek Z.**
Obróbka radiacyjna leków, surowców farmaceutycznych i kosmetycznych oraz kosmetyków (Radiation treatment of drugs, pharmaceutical raw materials and cosmetics).
III Jesienna Szkoła Sterylizacji Radiacyjnej Sprzętu Medycznego i Przeszczepów. Warszawa, Poland, 05-06.10.1995, pp. 49-54.

28. **Buczkowski M., Fiderkiewicz A., Starosta W.**
Biomedyczne zastosowania trekowych membran filtracyjnych (Biomedical applications of particle track membranes).
III Jesienna Szkoła Sterylizacji Radiacyjnej Sprzętu Medycznego i Przeszczepów. Warszawa, Poland, 05-06.10.1995, pp. 122-134.

29. **Buczkowski M., Starosta W., Fiderkiewicz A., Kiełkiewicz J., Meinhardt E.**
Zastosowanie membran trekowych w charakterze bariery mikrobiologicznej (Application of particle track membranes as microbiological barrier).
Krajowe Sympozjum "Technika Jądrowa w Przemyśle, Medycynie, Rolnictwie i Ochronie Środowiska". Referaty. Warszawa, Poland, 24-27.04.1995, pp. 158-162.

30. **Bukowski A., Pańczyk E., Chajęcki T., Waliś L.**
Oznaczanie zanieczyszczeń w krzemie o czystości półprzewodnikowej metodą instrumentalnej reaktorowej neutronowej analizy aktywacyjnej (Determination of impurities in semiconductor grade purity silicon waters by means of instrumental reactor neutron activation analysis).
Krajowe Sympozjum "Technika Jądrowa w Przemyśle, Medycynie, Rolnictwie i Ochronie Środowiska". Referaty. Warszawa, Poland, 24-27.04.1995, pp. 381-385.

31. **Burlińska G., Bobrowski K., Holcman J.**
On the reaction of the hydrated electron with methionine-containing oligopeptides.
Symposium on Physical Organic Photochemistry. Book of Abstracts. Poznań, Poland, 23-27.07.1995, p. IP-14.

32. **Burlińska G., Bobrowski K., Michalik J.**
ESR study of solid methionine-containing peptides.
Electron Spin Resonance in Electron Transfer and Organic Solids. Abstracts. Dresden, Germany, 22-25.11.1995, p. P-29.

33. **Burlińska G., Bobrowski K., Michalik J.**
ESR study of solid oligopeptides.
17th Conference and Workshop on Magnetic Resonance and Their Structure of Matter. Book of Abstracts. Gosen, Germany, 28-30.09.1995.

34. **Burlińska G., Bobrowski K., Michalik J.**
Radical processes in methionine-containing oligopeptides. ESR study.
19th Miller Conference Radiation Chemistry. Programme & Abstracts. Cervia/Milano Marittima, Italy, 16-21.09.1995, p. 37.

35. **Burlińska G., Bobrowski K., Wąsowicz T.**
Procesy rodnikowe w polikrystalicznych peptydach metioninowych (Radicals processes in polycrystalline peptides containing methionine).
X Krajowy Zjazd Polskiego Towarzystwa Badań Radiacyjnych im. Marii Skłodowskiej-Curie. Streszczenia referatów. Warszawa, Poland, 06-07.04.1995, p. 21.

36. **Chmielewski A.G.**
Electron beam gaseous pollutants treatment.
IEEE International Conference on Plasma Science. Madison, Wisconsin, USA, 5-8.06.1995, p. 269.

37. **Chmielewski A.G.**
Inżynieria procesowa w technologiach jądrowych (Process engineering in nuclear technologies).

XV Ogólnopolska Konferencja Naukowa Inżynierii Chemicznej i Procesowej. Materiały Konferencyjne. T. IV. Gdańsk, Poland, 12-15.09.1995, pp. 214-217.

38. **Chmielewski A.G.**
Rozwój technologii zaawansowanych (High-Tech) na przykładzie technik radiacyjnych (High-tech development exemplified by radiation technologies).
Krajowe Sympozjum "Technika Jądrowa w Przemyśle, Medycynie, Rolnictwie i Ochronie Środowiska". Referaty. Warszawa, Poland, 24-27.04.1995, pp. 19-26.

39. **Chmielewski A.G.**
Techniki jądrowe i radiacyjne - stan obecny oraz kierunki rozwoju (Nuclear and radiation techniques - present state and directions of development).
III Walny Zjazd Polskiego Towarzystwa Nukleonicznego. Materiały Sesji Seminaryjnej. Raport IAE-10/A. Instytut Energii Atomowej, Otwock-Świerk 1995, pp. 39-48.

40. **Chmielewski A.G.**
Technological development of eb flue gas treatment based on physics and chemistry of the process.
Radiation Physics and Chemistry, 46, 4-6, 1057-1062 (1995).

41. **Chmielewski A.G., Harasimowicz M.**
Application of ultrafiltration and complexation to the treatment of low-level radioactive effluents.
Separation Science and Technology, 30, 7-9, 1779-1789 (1995).

42. **Chmielewski A.G., Harasimowicz M., Zakrzewska-Trznadel G.**
Applications of membrane processes in purification of radioactive wastes.
Towards Hybrid Membrane and Biotechnology Solutions for Polish Environmental Problems. Szklarska Poręba, Poland, 12-15.01.1995, pp. 227-233.

43. **Chmielewski A.G., Harasimowicz M., Zakrzewska-Trznadel G.**
Purification of radioactive wastes by membrane distillation.
IX Symposium on Separation Science and Technology for Energy Applications. Gatlinburg, USA, 22-26.10.1995, pp. 50-51.

44. **Chmielewski A.G., Iller E., Tymiński B., Licki J., Zimek Z.**
Technologia usuwania SO_2 i NO_x z gazów spalinowych przy pomocy wiązki elektronów (Electron and beam technology of removal SO_2 and NO_x from flue gases).
Krajowe Sympozjum "Technika Jądrowa w Przemyśle, Medycynie, Rolnictwie i Ochronie Środowiska". Referaty. Warszawa, Poland, 24-27.04.1995, pp. 67-75.

45. **Chmielewski A.G., Iller E., Tymiński B., Zimek Z., Licki J.**
Electron beam flue gas treatment process upscaling.
International Chemical Congress of Pacific Basin Societes. Book of Abstracts. Honolulu, Hawaii, 17-22.12.1995, p. ENVR-6(317).

46. **Chmielewski A.G., Iller E., Zimek Z., Romanowski M., Koperski K.**
Industrial demonstration plant for electron beam flue gas treatment.
Radiation Physics and Chemistry, 46, 4-6, 1063-1066 (1995).

47. **Chmielewski A.G., Licki J., Dobrowolski A., Tymiński B., Iller E., Zimek Z.**
Optimization of energy consumption for NO_x removal in multistage gas irradiation process.
Radiation Physics and Chemistry, 45, 6, 1077-1079 (1995).

48. **Chmielewski A.G., Palige J., Dobrowolski A.**
Nowe rozwiązanie uśredniacza ścieków - wynik badań radioznacznikowych (New design of equalization-settle tank - results of radiotracer studies).
Krajowe Sympozjum "Technika Jądrowa w Przemyśle, Medycynie, Rolnictwie i Ochronie Środowiska". Referaty. Warszawa, Poland, 24-27.04.1995, pp. 193-197.

49. **Chmielewski A.G., Palige J., Owczarczyk A., Dobrowolski A.**
Nowy typ wysokoefektywnego uśredniacza składu ścieków (A new type of highly efficient equalization-settle tank).
XV Ogólnopolska Konferencja Naukowa Inżynierii Chemicznej i Procesowej. Materiały Konferencyjne. T. IV. Gdańsk, Poland, 12-15.09.1995, pp. 218-221.

50. **Chmielewski A.G., Tymiński B., Licki J., Iller E., Zimek Z., Radzio B.**
Pilot plant for flue gas treatment - continuous operation tests.
Radiation Physics and Chemistry, 46, 4-6, 1067-1070 (1995).

51. **Chmielewski A.G., Waliś L.**
Technologie radiacyjne oraz techniki jądrowe przyjazne dla człowieka i środowiska naturalnego (Radiation technologies and nuclear technics friendly for human beings and natural environment).
III Jesienna Szkoła Sterylizacji Radiacyjnej Sprzętu Medycznego i Przeszczepów. Warszawa, Poland, 05-06.10.1995, pp. 135-141.

52. **Chmielewski A.G., Zakrzewska-Trznadel G.**
Efekty izotopowe wodoru i tlenu w procesie permeacji wody przez membrany polimerowe (Hydrogen and oxygen isotope effects in water permeation process through polymer membranes).
Prace Wydziału Inżynierii Chemicznej i Procesowej Politechniki Warszawskiej, 22, 1-2, 23-31 (1995).

53. **Chmielewski A.G., Zakrzewska-Trznadel G., Miljević N.R., Van Hook W.A.**
Membrane distillation employed for separation of water isotopic compounds.
Separation Science and Technology, 30, 7-9, 1653-1667 (1995).

54. **Chmielewski A.G., Zakrzewska-Trznadel G., Miljević N.R., Van Hook W.A.**
Multistage process of deuterium and heavy oxygen enrichment by membrane distillation.
IX Symposium on Separation Science and Technology for Energy Applications. Gatlinburg, USA, 22-26.10.1995. Program and Abstracts, p. 47.

55. **Chmielewski A.G., Zimek Z., Bryl-Sandelewska T., Kosmal W., Kalisz L., Kaźmierczuk M.**
Disinfection of municipal sewage sludges in installation equipped with electron accelerator.
Radiation Physics and Chemistry, 46, 4-6, 1071-1074 (1995).

56. **Chmielewski A.G., Zimek Z., Bryl-Sandelewska T., Kosmal W., Kalisz L., Kaźmierczuk M., Kubera A.**
Higienizacja osadów ściekowych przy użyciu wiązki elektronów (Sewage sludge hygienisation with electron beam).
Inżynieria i Aparatura Chemiczna, 4, 26-28, (1995).

57. **Chmielewski A.G., Zimek Z., Bryl-Sandelewska T., Kosmal W., Kalisz L., Kaźmierczuk M., Kubera A.**
Higienizacja osadów ściekowych przy użyciu wiązki elektronów (Sewage sludge hygienisation with electron beam).
X Krajowy Zjazd Polskiego Towarzystwa Badań Radiacyjnych im. Marii Skłodowskiej-Curie. Streszczenia referatów. Warszawa, Poland, 06-07.04.1995, p. 25.

58. **Chmielewski A.G., Zimek Z., Panta P., Drabik W.**
The double window for electron beam injection into the flue gas process vessel.
Radiation Physics and Chemistry, 45, 6, 1029-1033 (1995).

59. **Chudziak A., Trojanowicz M.**
Reversed-phase HPLC of phenols with preconcentration by solid-phase extraction.
Chemia Analityczna, 40, 39-52 (1995).

60. **Chwastowska J., Żmijewska W., Sterlińska E.**
Determination of antimony (III, V) in natural waters by separation and preconcentration on a thionalide loaded resin followed by neutron activation analysis.
Journal of Radioanalytical and Nuclear Chemistry, Articles, 196, 1, 3-9 (1995).

61. **Chwastowska J., Żmijewska W., Sterlińska E.**
Zastosowanie sorbentu chelatującego z tionalidem osadzonym na żywicy Bio-Beads SM-7 do wydzielania i wzbogacania śladów metali (Application of a thionalide loaded resin to the separation and preconcentration of traces of metals).
Piąta Polska Konferencja Chemii Analitycznej "Analityka w służbie człowieka i środowiska". Gdańsk, Poland, 03-09.10.1995. Materiały konferencyjne. T. 1, p. 206.

62. **Chwastowska J., Żmijewska W., Sterlińska E., Gołębiewska W.**
Group separation and preconcentration of some heavy metals by sorption on a thionalide loaded resin. Application to water analysis.
Chemia Analityczna, 40, 879-885, (1995).

63. **Cieśla K.**
Zastosowanie analizy termicznej w badaniach napromieniowanych białek (Application of thermal analysis to investigation of irradiated proteins).
Krajowe Sympozjum "Technika Jądrowa w Przemyśle, Medycynie, Rolnictwie i Ochronie Środowiska". Referaty. Warszawa, Poland, 24-27.04.1995, pp. 148-152.

64. **Cieśla K., Starosta W.**
Heavy ions track structure in a PETP.
Nuclear Instruments and Methods in Physics Research B, 105, 115-119 (1995).

65. **Cieśla K., Trautmant Ch., Vansant E.F.**
DSC examinations of heavy ion irradiated thin polymer foils.
Nukleonika, 40, 3, 141-152 (1995).

66. **Ciurapiński A., Przybylski K., Potoczek M.**
Autoradiograficzne badania kierunków dyfuzji pierwiastków w procesach wysokotemperaturowego siarkowania wolframu i molibdenu (Autoradiographic studies of directions of elements diffusion in high temperature sulphurization processes of tungsten and molybdenum).
Krajowe Sympozjum "Technika Jądrowa w Przemyśle, Medycynie, Rolnictwie i Ochronie Środowiska". Referaty. Warszawa, Poland, 24-27.04.1995, pp. 345-351.

67. **Danko B., Dybczyński R.**
Oznaczanie śladowych zawartości uranu w materiałach biologicznych za pomocą neutronowej analizy aktywacyjnej (NAA) (Determination of trace amount of uranium in biological materials by neutron activation analysis (NAA)).
Piąta Polska Konferencja Chemii Analitycznej "Analityka w służbie człowieka i środowiska". Gdańsk, Poland, 03-09.09.1995. Materiały konferencyjne. T. 1, p. 210.

68. **Danko B., Dybczyński R.**
Radiochemical scheme for the determination of molybdenum and uranium in biological materials by NAA.
Journal of Radioanalytical and Nuclear Chemistry, Articles, 192, 1, 117-129 (1995).

69. **Degueldre C., Bilewicz A., Alder H.P.**
Behavior and removal of radionuclides generated in the cooling water of a proton accelerator.
Nuclear Science and Engineering, 120, 65-71 (1995).

70. **Dembiński W., Mioduski T.**
Europium isotope separation in the HCl/HDEHP extraction system.
Journal of Radioanalytical and Nuclear Chemistry, Letters, 195, 2, 159-171 (1995).

71. **Deptuła A., Carewska M., Olczak T., Łada W., Bartolomeo A. di**
Sintering of ZrO_2-CaO, ZrO_2-Y_2O_3 and ZrO_2-CeO_2 spherical powders prepared by water extraction variant of sol-gel process.
European Ceramic Society Fourth Conference "Basic science - developments in processing of advanced ceramics". Part II. Riccione, Italy, 02-06.10.1995, pp. 301-307.

72. **Deptuła A., Łada W., Olczak T., Chmielewski A.G.**
Some comments on the production of medium sized spherical particles by anion and water extraction variant of sol-gel process.
Material Research Society Symposium. Proceedings. Vol. 372, pp.83-88.

73. **Desrosiers M.F., Burlińska G., Kuppusamy P., Zweier J., Yaczko D.M., Auteri F.P., McClelland M.R., Dick C.E., McLaughlin W.L.**
Research and development activities in electron paramagnetic resonance dosimetry.
Radiation Physics and Chemistry, 46, 4-6, 1181-1184 (1995).

74. **Dudek J., Pszonicki L.**
Zachowanie się arsenu w obecności różnych modyfikatorów oraz chlorków przy oznaczaniu go techniką ASA w kuwecie grafitowej (Behaviour of arsenic in the presence of various modifiers and chlorides at its determination by the graphite tube AAS).
Piąta Polska Konferencja Chemii Analitycznej "Analityka w służbie człowieka i środowiska". Gdańsk, Poland, 03-09.09.1995. Materiały konferencyjne. T. 1, p. 148.

75. **Dybczyński R.**
The contribution of various analytical techniques to the certification of reference materials.
Fresenius' Journal of Analytical Chemistry, 352, 120-124 (1995).

76. **Dziewoński Z., Kalicki A., Kielak W., Kraś J., Myczkowski S., Waliś L.**
Detektory nadążne do kontroli szczelności i lokalizacji miejsc nieszczelnych w rurociągach podziemnych metodą znaczników promieniotwórczych (Follow-up detectors for leak proof control and leak localization in underground pipelines by the radiotracer method).
Krajowe Sympozjum "Technika Jądrowa w Przemyśle, Medycynie, Rolnictwie i Ochronie Środowiska". Referaty. Warszawa, Poland, 24-27.04.1995, pp. 315-320.

77. **Escudero Berzal M., Marcos Crespo M.J., Świderska-Kowalczyk M., Martin Espigares M., López-Jiménez J.**
Nuclear science and technology. State-of-the-art review on fission products aerosol pool scrubbing under severe accident conditions.
Final report EUR 16241 EN. European Commission Madrid, 1995, 183+15 p.

78. **Fiderkiewicz A., Buczkowski M., Żółtowski T., Zhitariuk N., Orelovich O., Kovalev G.**
Odporność radiacyjna trekowych membran filtracyjnych (Radiation resistance of particle track membranes).
Krajowe Sympozjum "Technika Jądrowa w Przemyśle, Medycynie, Rolnictwie i Ochronie Środowiska". Referaty. Warszawa, Poland, 24-27.04.1995, pp. 103-109.

79. **Fiszer W., Migdał W.**
Progress of food irradiation in Poland.
XXV Annual Meeting European Society for New Methods in Agricultural Research. Abstract. Castelnuovo Fogliani, Italy, 15-19.09.1995, p. 15.

80. **Fiszer W., Migdał W.**
Stan obecny i perspektywy stosowania metody radiacyjnej do utrwalania żywności w różnych krajach świata oraz w Polsce (Present status of food irradiation in the world and in Poland).
Krajowe Sympozjum "Technika Jądrowa w Przemyśle, Medycynie, Rolnictwie i Ochronie Środowiska". Referaty. Warszawa, Poland, 24-27.04.1995, pp. 117-118.

81. **Fuks L., Kulyako Y., Malikov D.A**
Stability constans of acetylacetonate complexes of tetravalent berkelium.
Mendeleev Communication, 74-76 (1995).

82. **Fuks L., Narbutt J.**
Termodynamiczne funkcje podziału tetrakis-acetylo-acetonianów metali(IV) w układzie woda-heptan (Thermodynamic functions of partition of tetrakis-acetylacetonates of various metals(IV) in the system water-heptane).
Zjazd Naukowy Polskiego Towarzystwa Chemicznego i Stowarzyszenia Inżynierów i Techników Przemysłu Chemicznego. Lublin, Poland, 25-28.09.1995, p. S-6, P-44.

83. **Gil A., Leciejewicz J., Szytuła A., Tomkowicz Z., Zygmunt A.**
Magnetic properties of the $Tb_{1-x}R_xNiX_2$ systems ($x \leq 0.5$) where R = Pr, Nd and X = Si, Ge.
Journal of Magnetism and Magnetic Materials, 140-144, 927-928 (1995).

84. **Głuszewski W., Bieliński J.**
Badania korozyjne bezprądowych warstw dyspersyjnych NiP-Al_2O_3, NiP-SiC (Corrosion studies on Ni-P-Al_2O_3 and Ni-P-SiC electroless alloys in H_2SO_4 and NaCl electrolytes).
Zjazd Naukowy Polskiego Towarzystwa Chemicznego i Stowarzyszenia Inżynierów i Techników Przemysłu Chemicznego. Lublin, Poland, 25-28.09.1995, p. S-8 P-17.

85. **Gniazdowska E.**
Wykorzystanie analiz wykonywanych metodą GC do wyznaczania wysokich współczynników podziału cząsteczek organicznych w układzie woda/rozpuszczalnik organiczny (The application of GC method to determine high partition coefficients of organic compounds in water/organic solvent system).
II Ogólnopolskie Seminarium Chromatograficzne "Nowoczesne Metody Analityczne w Kontroli i Monitoringu Środowiska". Streszczenia referatów (P - 4/II). Toruń, Poland, 20-21.09.1995, p. 42.

86. **Grądzka I., Szumiel I., Afanasjew G.G., Kapiszewska M.**
Działanie kamptotecyny na komórki dwóch podlinii L5178Y napromienione promieniowaniem X (Action of camptothecin on two cell sublines L5178Y irradiated with X-rays).
X Krajowy Zjazd Polskiego Towarzystwa Badań Radiacyjnych im. Marii Skłodowskiej-Curie. Streszczenia referatów. Warszawa, Poland, 06-07.04.1995, p. 67.

87. **Grądzka I., Szumiel I., Squires S.**
Cellular factors determining differential sensitivity to camptothecin in two murine lymphoma L5178Y sublines.
5th International Symposium on Molecular Aspects of Chemotherapy. Abstracts. Gdańsk, Poland, 21-24.08.1995, p. 1.

88. **Grądzka I., Szumiel I., Squires S.**
Szybkość naprawy uszkodzeń DNA wywołanych przez kamptotecynę a przeżywalność komórek w dwóch podliniach białaczki mysiej L5178Y (Rate of DNA repair after camptothecin action and survival in two sublines of mouse lymphoma L5178Y cells).
XXXI Zjazd Polskiego Towarzystwa Biochemicznego. Streszczenia.Warszawa, Poland, 6-8.09.1995, p. 10.

89. **Grigoriew H., Jachimowicz M.**
Study of the mechanical nanocrystallization process of amorphous $Fe_{78}B_{13}Si_9$ aloy using the pair function method.
Journal of Applied Physics, 78, 1, 132-136 (1995).

90. **Hug G.L., Marciniak B., Bobrowski K.**
Sensitized photooxidation of sulfur-containing amino acids and peptides in aqueous solution.
Symposium on Physical Organic Photochemistry. Book of Abstracts. Poznań, Poland 23-27.07.1995, p. L-6.

91. **Hulewicz Z.Z., Chmielewski A.G.**
Filtracja zanieczyszczeń aerozolowych za pomocą filtrów ziarnistych (An aerosols contaminants by means of grain filters).
Metodyki Badań Odpadów Przemysłowych. Wojskowy Instytut Chemii i Radiometrii, Warszawa 1995, pp. 81-109.

92. **Hulewicz Z.Z., Chmielewski A.G.**
On dry granular bed filtration of aerosols induced by irradiation.
Radiation Physics and Chemistry, 45, 6, 1039-1047 (1995).

93. **Jackowski Z., Chmielewski A.G., Zimek Z.**
Optimization of irradiation chamber for electron beam flue gas treatment in application for large steam boilers.
International Chemical Congress of Pacific Basin Societes. Book of Abstracts. Honolulu, Hawaii, 17-22.12.1995, p. ENVR-6(316).

94. **Kalicki A., Pańczyk E., Kulczycki A., Banasik Z.**
Zastosowanie metod jądrowych do badania skuteczności środków obniżających zużycie (Applications of nuclear methods to the examination of the effectiveness of preparation for wear reduction).
Krajowe Sympozjum "Technika Jądrowa w Przemyśle, Medycynie, Rolnictwie i Ochronie Środowiska". Referaty. Warszawa, Poland, 24-27.04.1995, pp. 247-252.

95. **Kałuska I.**
Aktualne przepisy międzynarodowe dotyczące sterylizacji radiacyjnej (International requirements and guidelines concerning radiation sterilization).
III Jesienna Szkoła Sterylizacji Radiacyjnej Sprzętu Medycznego i Przeszczepów. Warszawa, Poland, 05-06.10.1995, pp. 55-60.

96. **Kałuska I.**
Polipropylen odporny radiacyjnie (Radiation resistant polypropylene).
Seminarium "Polimery 2000". Płock, Poland, 02.06.1995, p. 149.

97. **Kałuska I.**
Technologia sieciowania radiacyjnego polietylenu w zastosowaniu do otrzymywania wyrobów termokurczliwych (Radiation crosslinking processing of polyethylene applied for obtaining heat-shrinkable material).

Krajowe Sympozjum "Technika Jądrowa w Przemyśle, Medycynie, Rolnictwie i Ochronie Środowiska". Referaty. Warszawa, Poland, 24-27.04.1995, pp. 97-98.

98. **Kałuska I.**
Wyroby termokurczliwe (Heat-shrinkable materials).
Seminarium "POLIMERY 2000". Płock, Poland, 02.06.1995, pp. 147-148.

99. **Kałuska I., Mirkowski K.**
Radiacyjna degradacja polipropylenu (Radiation degradation of polypropylene).
Zjazd Naukowy Polskiego Towarzystwa Chemicznego i Stowarzyszenia Inżynierów i Techników Przemysłu Chemicznego. Lublin, Poland, 25-28.09.1995, p. S-10 P-46.

100. **Kierzek J., Kierzek A., Małożewska-Bućko B.**
Neural networks based calibration in x-ray fluorescence analysis of polymetallic ores.
Nukleonika, 40, 3, 133-140 (1995).

101. **Kierzek J., Małożewska-Bućko B., Bukowski P., Zaraś S., Kunach B., Wiland K.**
Badanie własności ekologicznych węgli i popiołów przy pomocy spektrometrii X i gamma (Investigation of ecological characteristics of coals and ashes by X-rays and gamma-spectrometry).
Krajowe Sympozjum "Technika Jądrowa w Przemyśle, Medycynie, Rolnictwie i Ochronie Środowiska". Referaty. Warszawa, Poland, 24-27.04.1995, pp. 398-404.

102. **Kapiszewska M., Grądzka I., Szumiel I., Afanasjev G.G.**
Modulation of camptothecin effects in X-irradiated L5178Y cells.
Tenth International Congress of Radiation Research. Würzburg, Germany, 27.08.-01.09.1995. Radiation Research 1895-1995. Vol. 1. Congress Abstracts, p. 237.

103. **Kleczkowska H.E., Althaus F.R., Szumiel I.**
Poly(ADP-ribose) metabolism in L5178Y cells exposed to ionizing radiation.
27th Annual Meeting of the USGEB/USSBE. Fribourg, Switzeland, 30-31.03.1995, p. 1.

104. **Kleczkowska H.E., Althaus F.R., Szumiel I.**
Poly(ADP-ribose) metabolism in X-irradiated L5178Y-R and L5178Y-S sublines.
Tenth International Congress of Radiation Research. Würzburg, Germany, 27.08.-01.09.1995. Radiation Research 1895-1995. Vol. 1. Congress Abstracts, p. 301.

105. **Kleczkowska H.E., Malanga M., Szumiel I., Althaus F.R.**
Poly(ADP-ribosyl)ation and radiation sensitivity of two mouse lymphoma cell sublines.
Symposium Genetic Predisposition to Cancer. Zürich, Switzerland, 15-17.03.1995, p. 1-3.

106. **Kleczkowska H.E., Szumiel I., Althaus F.R.**
Low dose ionizing radiation activates poly(ADP-ribose)-binding proteins.
Workshop: Biological Effects after Small Radiation Doses, Würzburg, Germany, 02.09.1995, p. 12/95.

107. **Kolenda M., Leciejewicz J., Stuesser N., Szytuła A., Zygmunt A.**
Incommensurate magnetic ordering in CePtSn and TbPtSn.
Journal of Magnetism and Magnetic Materials, 145, 85-92 (1995).

108. **Kraś A.B., Pańczyk E., Waliś L., Sartowska B.**
Application of track autoradiography in diagnostics of special closed radiation sources.
Radiation Measurements, 25, 1-4, 363-366 (1995).

109. **Kraś A.B., Pańczyk E., Waliś L., Sartowska B.**
Diagnozowanie zamkniętych źródeł promieniowania wykorzystywanych w czujkach dymu (Application of track autoradiography in diagnosis of special closed radiation sources).
Krajowe Sympozjum "Technika Jądrowa w Przemyśle, Medycynie, Rolnictwie i Ochronie Środowiska". Referaty. Warszawa, Poland, 24-27.04.1995, pp. 454-457.

110. **Kraś J., Waliś L., Kielak W.**
Szczelność instalacji technologicznych i rurociągów przesyłowych jako element ochrony środowiska naturalnego (Tightness of technological installations and industrial pipelines as an element of environmental protection).

Krajowe Sympozjum "Technika Jądrowa w Przemyśle, Medycynie, Rolnictwie i Ochronie Środowiska". Referaty. Warszawa, Poland, 24-27.04.1995, pp. 212-216.

111. **Krejzler J., Siekierski S.**
Specific and non-specific interaction of hydropseudohalic acids with water and organic solvents.
Journal of Solution Chemistry, 24, 3, 253-266 (1995).

112. **Kruszewski M.**
Indukcja i naprawa uszkodzeń DNA w komórkach L5178Y o zróżnicowanej wrażliwości na promieniowanie X i nadtlenek wodoru (DNA damage and its repair in L5178Z cell lines differing in sensitivity to X-rays and H_2O_2).
X Krajowy Zjazd Polskiego Towarzystwa Badań Radiacyjnych im. Marii Skłodowskiej-Curie. Streszczenia referatów. Warszawa, Poland, 06-07.04.1995, p. 75.

113. **Kruszewski M., Green M.H.L., Lowe J.E., Szumiel I.**
Comparison of effects of iron an calcium chelators on the response of L5178Y sublines to X-rays and H_2O_2.
Mutation Research, 326, 155-163 (1995).

114. **Kruszewski M., Szumiel I., Iwaneńko T., Kapiszewska M.**
Indukcja uszkodzeń labilnych w pH 9 w komórkach o zróżnicowanej wrażliwości na promieniowanie X i H_2O_2 (pH9-labile DNA damage in L5178Y cell lines differing in sensitivity to X-rays and H_2O_2).
XXXI Zjazd Polskiego Towarzystwa Biochemicznego. Streszczenia. Warszawa, Poland, 06-08.09.1995, p. 10.

115. **Kruszewski M., Szumiel I., Kapiszewska M., Iwaneńko T.**
Stosunek zawartości miedzi do żelaza oraz indukcja uszkodzeń labilnych w pH 9 w komórkach o zróżnicowanej wrażliwości na promieniowanie X i nadtlenek wodoru (Cu and Fe content and pH9-labile DNA damage in L5178Y cell lines differing in sensitivity to X-rays and H_2O_2).
X Krajowy Zjazd Polskiego Towarzystwa Badań Radiacyjnych im. Marii Skłodowskiej-Curie. Streszczenia referatów. Warszawa, Poland, 06-07.04.1995, p. 77.

116. **Krynicki J., Warchoł S., Rzewuski H., Groetzschel R.**
Damage production in As implanted $GaAs_{1-x}P_x$ (Proceedings of the XXIII International School of Semiconducting Compounds, Jaszowiec 1994).
Acta Physica Polonica A, 87, 1, 249-252 (1995).

117. **Kulisa K., Polkowska-Motrenko H., Dybczyński R.**
Jednoczesne oznaczanie za pomocą chromatografii jonów SO_3^{2-} i SO_4^{2-} oraz innych anionów (NO_2^-, NO_3^-, F^-, Cl^-) w roztworach wodnych uzyskanych w wyniku absorpcji gazów spalinowych z instalacji odsiarczania w Elektrociepłowni Kawęczyn (The use of ion chromatography for the sinultaneous determination of SO_3^{2-} and SO_4^{2-} anions along with other anions (NO_2^-, NO_3^-, F^-, Cl^-) in water solutions obtained as a result of absorption of combustion flue gases from Electron Beam Flue Gases Treatment Installation at Kawęczyn Electric Power Plant).
IV Poznańskie Konwersatorium Analityczne "Nowoczesne metody przygotowania próbek i oznaczania śladowych zawartości pierwiastków. Poznań, Poland, 27-28.04.1995. Materiały Konwersatorium, p. 19.

118. **Kulisa K., Polkowska-Motrenko H., Dybczyński R.**
Oznaczanie zawartości SO_2, SO_3 i NO_x w gazach odlotowych i aerozolach metodą chromatografii jonowej (Determination of SO_2, SO_3 and NO_x in combustion flue gases and aerosols by ion chormatography).
V Polska Konferencja Chemii Analitycznej "Analityka w służbie człowieka i środowiska". Gdańsk, Poland, 03-09.09.1995. Materiały konferencyjne, p. 550.

119. **Leciejewicz J., Alcock N.W., Kemp T.J.**
Carboxylato complexes of the uranyl ion: Effects of ligand size and coordination geometry upon molecular and crystal structure.
Structure and Bonding. **82** Springer-Verlag 1995, pp. 43-84.

120. **Leciejewicz J., Stuesser N., Szytuła A., Zygmunt A.**
Antiferromagnetic ordering in Ce_2RhSi_3.
Journal of Magnetism and Magnetic Materials, 147, 45-48 (1995).

121. **Lehmann A.R., Walicka M., Griffiths D.J.F., Murray J.M., Watts F.Z., McCready S., Carr A.M.**
The rad18 gene of schizosaccharomyces pombe defines a new subgroup of the SMC superfamily involved in DNA repair.
Molecular and Cellular Biology, 15, 12, 7067-7080 (1995).

122. **Lewandowska-Szumieł M., Kałuska I.**
Zastosowanie techniki radiacyjnej do otrzymywania i modyfikacji biopolimerów. Praca poglądowa (Application of radiation processing for obtaining and modification biopolimers. Overview).
Polimery w Medycynie, XXV, 1-2, 57-67 (1995).

123. **Licki J., Chmielewski A.G., Radzio B.**
Off-line system for measurement of nitrous oxide concentration in gases leaving the irradiation chamber.
Radiation Physics and Chemistry, 45, 6, 1035-1038 (1995).

124. **Licki J., Chmielewski A.G., Radzio B.**
Przemysłowe manualne i instrumentalne metody analizy składu spalin na wylocie z elektrowni (Industrial, manual and instrumental methods of analysis of flue gases composition at the outlet of EPS).
VIII Giełda "Nowoczesna Technika w Energetyce". Materiały sympozjalne II. Nowoczesne rozwiązania w dziedzinie wytwarzania energii elektrycznej i cieplnej; Nowe kierunki w technice informacyjno-sterowniczej i pomiarowej w energetyce. Bielsko-Biała, Poland, 26-28.09.1995, pp. 22/1-22/13.

125. **Łomot D., Juszczyk W., Pielaszek J., Kaszkur Z., Bakuleva T.N., Karpiński Z., Wąsowicz T., Michalik J.**
Structure and reactivity of supported palladium catalysts. I. Pd/SiO_2 prepared from $PdCl_2$.
New Journal of Chemistry, 19, 3, 263-273 (1995).

126. **Łukasiewicz J., Bartak J.**
Nowe techniki akwizycji danych z pomiarów radiometrycznych (New acquisition data technique of radiometric measurements).
Krajowe Sympozjum "Technika Jądrowa w Przemyśle, Medycynie, Rolnictwie i Ochronie Środowiska". Referaty. Warszawa, Poland, 24-27.04.1995, pp. 327-329.

127. **Machaj B., Krawczyńska B., Strzałkowski J.**
Ocena parametrów radioizotopowego miernika zapylenia powietrza (Assessment of parameters of airborne radioisotope dust monitor).
Krajowe Sympozjum "Technika Jądrowa w Przemyśle, Medycynie, Rolnictwie i Ochronie Środowiska". Referaty. Warszawa, Poland, 24-27.04.1995, pp. 261-267.

128. **Malec-Czechowska K., Dancewicz A.M., Szot Z.**
Metoda termoluminescencji w identyfikacji napromienionej żywności (Thermoluminescence method in identification of irradiated foodstuffs).
Krajowe Sympozjum "Technika Jądrowa w Przemyśle, Medycynie, Rolnictwie i Ochronie Środowiska". Referaty. Warszawa, Poland, 24-27.04.1995, pp. 131-136.

129. **Marciniak B., Hug G.L., Bobrowski K., Kozubek H.**
Mechanism of 4-carboxybenzophenone-sensitized photooxidation of methionine-containing dipeptides and tripeptides in aqueous solution.
Journal of Physical Chemistry, 99, 36, 13560-13568 (1995).

130. **Marciniak B., Hug G.L., Bobrowski K., Kozubek H.**
Photoinduced electron transfer between sulfur-containing simple peptides and the 4-carboxybenzophenone triplet state in aqueous solution.
Symposium on Physical Organic Photochemistry. Book of Abstracts. Poznań, Poland, 23-27.07.1995, p. IIP-2.

131. **Marciniak B., Hug G.L., Rozwadowski J., Bobrowski K.**
Excited triplet state of N-(9-methylpurin-6-yl)pyridinum cation as an efficient photosensitizer in the oxidation of sulfur-containing amino acids. Laser flash and steady-state photolysis studies.
Journal of the American Chemical Society, 117, 1, 127-134 (1995).

132. **Michalik J., Azuma N., Sadło J., Kevan L.**
Silver agglomeration in SAPO-5 and SAPO-11 molecular sieves.
Journal of Physical Chemistry, 99, 4679-4686 (1995).

133. **Michalik J., Azuma N., Sadło J., Kevan L.**
Tetrameric silver clusters in RHO zeolite stable above room temperature characterized by electron magnetic resonance.
VII International Symposium on Magnetic Resonance in Colloid and Interface Science. Conference Abstracts. Madrid, Spain, 11-15.09.1995, p. 122.

134. **Michalik A., Bartnik W., Owczarczyk A., Wierzchnicki R.**
Radioizotopowe metody pomiarów transportu materiału dennego w rzekach górskich (Radiotracer method of measurement of bed-load transport in sub-mountains rivers).
Krajowe Sympozjum "Technika Jądrowa w Przemyśle, Medycynie, Rolnictwie i Ochronie Środowiska". Referaty. Warszawa, Poland, 24-27.04.1995, pp. 231-236.

135. **Michalik J., Sadło J., Azuma N., Kevan L.**
Aglomeracja srebra w sitach molekularnych SAPO-5 i SAPO-11 (Silver agglomeration in SAPO-5 and SAPO-11 in molecular sieves).
X Krajowy Zjazd Polskiego Towarzystwa Badań Radiacyjnych im. Marii Skłodowskiej-Curie. Streszczenia referatów. Warszawa, Poland, 06-07.04.1995, p. 26.

136. **Michalik J., Sadło J., Kevan L.**
Small silver clusters in RHO zeolites.
17th Conference and Workshop on Magnetic Resonance and the Structure of Matter. Book of Abstracts. Gosen, Germany, 28-30.09.1995.

137. **Michalik J., Sadło J., Kevan L.**
Tetrameric silver clusters in RHO zeolite stable above room temperature.
19th Miller Conference Radiation Chemistry. Programme & Abstracts. Cervia/Milano Marittima, Italy, 16-21.09.1995, p. 33.

138. **Michalik J., Sadło J., Pol A. van der**
EPR and ESEM studies on organosilver radicals in zeolites.
16th Conference on Radio- and Microwave Spectroscopy. Poznań, Poland, 25-27.04.1995, p. P-47.

139. **Michalik J., Yamada H., Wąsowicz T., Kevan L.**
Pulsed electron spin resonance studies of silver atoms and clusters in smectite clays.
Science and Technology 48th Conference Proceedings. Springfield Virginia, USA, 1995, pp. 309-311.

140. **Migdał W.**
Napromieniowanie żywności (Food irradiation).
Roczniki Państwowego Zakładu Higieny, 46, 4, 323-328 (1995).

141. **Migdał W., Maciszewski W., Gryzlov A.**
Application of "Elektronika 10-10" electron linac for food irradiation.
Radiation Physics and Chemistry, 46, 4-6, 749-752 (1995).

142. **Migdał W., Owczarczyk B., Malec-Czechowska K.**
Doświadczalna Stacja Radiacyjnego Utrwalania Płodów Rolnych (Pilot plant for food irradiation).
Krajowe Sympozjum "Technika Jądrowa w Przemyśle, Medycynie, Rolnictwie i Ochronie Środowiska". Referaty. Warszawa, Poland, 24-27.04.1995, pp. 119-121.

143. **Migdał W., Owczarczyk B., Malec-Czechowska K.**
The task of pilot plant in legislation and commercialization of food irradiation in Poland.
XXV Annual Meeting European Society for New Methods in Agricultural Research. Castelnuovo Fogliani, Italy, 15-19.09.1995. Abstract, p. 20.

144. **Mioduski T.**
Ekologia i energetyka a nukleofobia (Ecology and energetics versus nucleophobia).
Postępy Techniki Jądrowej, 38, 1, 19-32 (1995).

145. **Mirowicz J.**
Zastosowania przemysłowych radioizotopowych mierników stężenia kwasu siarkowego i oleum (Application of industrial radioisotope gauges of sulphuric acid and oleum concentration).

Krajowe Sympozjum "Technika Jądrowa w Przemyśle, Medycynie, Rolnictwie i Ochronie Środowiska". Referaty. Warszawa, Poland, 24-27.04.1995, pp. 297-300.

146. **Narbutt J.**
On the reliability of "Individual Distribution Constants" of consecutive metal complexes, determined by curve-fitting method.
Polish Journal of Chemistry, 69, 1589-1590 (1995).

147. **Narbutt J.**
Outer-sphere hydration of metal β-diketonates.
VI Meżdunarodnaja Konferencija "Problemy sol'vatacii i kompleksoobrazovanija v rastvorach. Ivanovo, Russia, 10-12.10.1995, p. P-12,P-13.

148. **Nichipor H., Radouk E., Chmielewski A.G., Zimek Z., Lysov G.W.**
SO_2 oxidation in humid air by electron beam and microwave energy simultaneous application.
Radiation Physics and Chemistry, 46, 4-6, 1115-1118 (1995).

149. **Owczarczyk A., Pruszak Z., Szpilowski S., Wierzchnicki R.**
Some velocities and bed load transport due to wave and current.
Eight International Conference Transport and Sedimentation. Prague, Czech Republic, 24-26.01.1995. Materiały konferencyjne, p. B-13.

150. **Owczarczyk A., Strzelecki M.**
Bilanse wodne i ściekowe w energetyce i ciepłownictwie (Water and waste water balance in power and heat industry).
VIII Giełda "Nowoczesna Technika w Energetyce". Bielsko-Biala, Poland, 26-28.09.1995. Materiały z Sympozjum, p. 33/1-33/8.

151. **Owczarczyk A., Szpilowski S., Więcław B.**
Rozwój radioznacznikowych metod badania szczelności zbiorników (Development of radiotracer methods for examination of tank tightness).
Krajowe Sympozjum "Technika Jądrowa w Przemyśle, Medycynie, Rolnictwie i Ochronie Środowiska". Referaty. Warszawa, Poland, 24-27.04.1995, pp. 206-211.

152. **Owczarczyk A., Wierzchnicki R., Pruszak Z.**
Radiotracer use for bed-load movement parameters and transport estimation in near-shore Baltic Sea zone.
International Symposium on Isotopes in Water Resources Management. Vienna, Austria, 20-24.03.1995, pp. 284-285.

153. **Owczarczyk A., Wierzchnicki R., Szpilowski S.**
Transport zanieczyszczeń w naturalnych odbiornikach wodnych. Badania znacznikowe (Transport of impurities in natural water receivers. Tracer studies).
Konferencja "Ocena i stan środowiska przyrodniczego Polski i innych krajów". Jachranka, Poland, 10-13.10.1995, p. 106.

154. **Owczarczyk B., Malec-Czechowska K., Migdał W.**
Radiacyjna mikrobiologiczna dekontaminacja suszonych warzyw (Radiation microbiological decontamination of dry vegetables).
Krajowe Sympozjum "Technika Jądrowa w Przemyśle, Medycynie, Rolnictwie i Ochronie Środowiska". Referaty. Warszawa, Poland, 24-27.04.1995, pp. 128-130.

155. **Owczarczyk B , Migdał W.**
Radiation treatment of dry vegetables, dry mushrooms and some spieces.
XXV Annual Meeting European Society for New Methods in Agricultural Research. Castelnuovo Fogliani, Italy, 15-19.09.1995. Abstract, p. 21.

156. **Palige J., Chmielewski A.G., Dziewoński Z.R., Rahimi H., Naimpour A., Amini A., Abedinzadeh A., Khalilipour E.**
Radiotracer glass furnaces investigations.
Nukleonika, 40, 1, 67-80 (1995).

157. **Palige J., Harasimowicz M.**
Radioznacznikowe badania wanien szklarskich (Radiotracer investigation of glass furnaces).

Krajowe Sympozjum "Technika Jądrowa w Przemyśle, Medycynie, Rolnictwie i Ochronie Środowiska". Referaty. Warszawa, Poland, 24-27.04.1995, pp. 165-170.

158. **Panta P.P.**

Kontrola procesu napromieniania i sterylizacji (Control of irradiation and sterilization processing).

III Jesienna Szkoła Sterylizacji Radiacyjnej Sprzętu Medycznego i Przeszczepów. Warszawa, Poland, 05-06.10.1995, pp. 61-65.

159. **Panta P.P., Chmielewski A.G., Zimek Z., Paduch M., Tomaszewski K.**

Application of nitrogen fluorescence for the dosimetry of electron beam.

Radiation Physics and Chemistry, 46, 4-6, 1259-1262 (1995).

160. **Panta P.P., Głuszewski W.**

Badania dozymetryczne przy wdrażaniu do sterylizacji radiacyjnej nowych wyrobów medycznych w Stacji Sterylizacji Sprzętu Medycznego i Przeszczepów (Dosimertric investigations for the implementation of radiosterilization of new medical products in the Accelerator Facility for Radiation Sterilization).

X Krajowy Zjazd Polskiego Towarzystwa Badań Radiacyjnych im. Marii Skłodowskiej-Curie. Streszczenia referatów. Warszawa, Poland, 6-7.04.1995, p. 38.

161. **Panta P.P., Głuszewski W.**

Radiosterylizacja masowego sprzętu medycznego - technika spełniająca wymagania ochrony środowiska naturalnego (Industrial sterilization of medical equipment - the technique compatible to protection of environment).

Krajowe Sympozjum "Technika Jądrowa w Przemyśle, Medycynie, Rolnictwie i Ochronie Środowiska". Referaty. Warszawa, Poland, 24-27.04.1995, pp. 139-141.

162. **Panta P.P., Głuszewski W.**

Zastosowanie dozymetrii radiacyjnej dla technik ochrony środowiska naturalnego (Application of radiation dosimetry for techniques of protection of environment).

Krajowe Sympozjum "Technika Jądrowa w Przemyśle, Medycynie, Rolnictwie i Ochronie Środowiska". Referaty. Warszawa, Poland, 24-27.04.1995, pp. 81-82.

163. **Panta P.P., Zimek Z., Kowalewski R., Głuszewski W.**

Zastosowanie dozymetrii radiacyjnej dla technik ochrony środowiska i sterylizacji masowego sprzętu medycznego (Applications of radiation dosimetry for protection of environment and industrial sterilization of medical products).

Zjazd Naukowy Polskiego Towarzystwa Chemicznego i Stowarzyszenia Inżynierów i Techników Przemysłu Chemicznego. Lublin, Poland, 25-28.09.1995, p. S-16 K-6.

164. **Pańczyk E., Ligęza M., Waliś L.**

Zastosowanie reaktorowej neutronowej analizy aktywacyjnej do identyfikacji obrazów szkoły małopolskiej (Application of instrumental reactor neutron activation analysis for the identification of paintings of Malopolska school).

Krajowe Sympozjum "Technika Jądrowa w Przemyśle, Medycynie, Rolnictwie i Ochronie Środowiska". Referaty. Warszawa, Poland, 24-27.04.1995, pp. 386-391.

165. **Pawlukojć A., Bobrowicz L., Natkaniec I., Łeciejewicz J.**

The IINS spectroscopy of amino acids: L- and DL-valine.

Spectrochimica Acta, 51A, 2, 303-308 (1995).

166. **Pogocki D., Bobrowski K.**

Mechanistic study of intramolecular proton transfer to hydroxy sulphuranyl radical in methionine and its derivatives.

19th Miller Conference Radiation Chemistry. Programme & Abstracts. Cervia/Milano Marittima, Italy, 16-21.09.1995, p. 27.

167. **Poli D.C.R., Zimek Z., Vieira J.M., Rivelli V.**

Electron beam removal of SO_2 and NO_x from combustion flue gases in Brasil - national and international cooperation.

Proceedings of the Symposium on Regional Integration in Nuclear Energy. Rio de Janeiro, Brasil, 02-06.06.1995.

168. **Poli D.C.R., Zimek Z., Vieira J.M., Rivelli V.**

Technical and economical feasibility study of the electron beam process for SO_2 and NO_x removal from combustion flue gases in Brazil.

Applications of Intelligent Software Systems in Power Plant, Process Plant and Structural Engineering. Proceedings. Sao Paulo, Brasil, 21-23.08.1995, p. 1-16.

169. **Przybytniak G., Ambroż H.**

Radiolityczne utlenianie atomu siarki i stabilizacja produktów przejściowych w sulfidach (Radiolytical sulphur oxydation and stabilization of transients in sulphides).

X Krajowy Zjazd Polskiego Towarzystwa Badań Radiacyjnych im. Marii Skłodowskiej-Curie. Streszczenia referatów. Warszawa, Poland, 06-07.04.1995, p. 42.

170. **Pszonicki L., Skwara W., Dudek J.**

Elimination of interference effects by standard addition and successive dilution method in the graphite furnace atomic absorption spectrometry.

Chemia Analityczna, 40, 351-360 (1995).

171. **Ptasiewicz-Bąk H., Leciejewicz J., Zachara J.**

X-ray structure analysis of diaquobis (2-pyrazinecarboxylato) manganese(II), cobalt(II), nickel(II), copper(II) and zinc(II) complexes.

Journal of Coordination Chemistry, 36, 317-326 (1995).

172. **Rafalski A., Zagórski Z.P.**

Dozymetr alaninowy z detekcją spektrofotometryczną jako alternatywa dla dozymetru z detekcją EPR (Alanine dosimeter with spectrophotometric detection as the alternative to the dosimeter with EPR detection).

X Krajowy Zjazd Polskiego Towarzystwa Badań Radiacyjnych im. Marii Skłodowskiej-Curie. Streszczenia referatów. Warszawa, Poland, 06-07.04.1995, p. 43.

173. **Rowińska L., Waliś L., Nowicki A.**

Zastosowanie znaczników promieniotwórczych do określania stopnia oczyszczenia indu i galu do czystości półprzewodnikowej w procesie przetapiania pod żużlami syntetycznymi (Application of radiotracer for evaluation of the efficiency of the processes of purification of indium and galium to semiconductor grade purity under the synthetic slags).

Krajowe Sympozjum "Technika Jądrowa w Przemyśle, Medycynie, Rolnictwie i Ochronie Środowiska". Referaty. Warszawa, Poland, 24-27.04.1995, pp. 253-258.

174. **Sadło J., Wąsowicz T., Michalik J.**

Radiation-induced silver agglomeration in molecular sieves: A comparison between A and X zeolites.

Radiation Physics and Chemistry, 45, 6, 909-915 (1995).

175. **Samczyński Z., Dybczyński R.**

Oznaczanie niskich zawartości kadmu w materiałach biologicznych za pomocą radiochemicznej wersji neutronowej analizy aktywacyjnej (Determination of small amounts of cadmium in biological materials by neutron activation analysis employing amphoteric ion exchange resin for radiochemical separation).

V Polska Konferencja Chemii Analitycznej "Analityka w służbie człowieka i środowiska". Gdańsk, Poland, 03-09.09.1995. Materiały konferencyjne, p. 264.

176. **Skwara W., Pszonicki L.**

Eliminacja wpływu jonów chlorkowych przy oznaczaniu selenu technika ASA w kuwecie grafitowej (Elimination of chloride ion effects on the selenium determination by the graphite tube AAS).

V Polska Konferencja Chemii Analitycznej "Analityka w służbie człowieka i środowiska". Gdańsk, Poland, 03-09.09.1995. Materiały konferencyjne, p. 186.

177. **Sochanowicz B., Kruszewski M., Szumiel I.**

X-ray and H_2O_2-stimulated synthesis of prostaglandins in L5178Y cells.

Tenth International Congress of Radiation Research. Würzburg, Germany, 27.08.-01.09.1995. Radiation Research 1895-1995. Abstract P18/19, p. 292.

178. **Sochanowicz B., Szumiel I.**

Metabolizm kwasu arachidonowego w komórkach o zróżnicowanej wrażliwości na promieniowanie X (Arachidonic acid metabolism in the cell sublines differing in radiation sensitivity).

X Krajowy Zjazd Polskiego Towarzystwa Badań Radiacyjnych im. Marii Skłodowskiej-Curie. Streszczenia referatów. Warszawa, Poland, 06-07.04.1995, p. 86.

179. **Sowiński M., Pławski T., Osowiecki M., Kobus M., Żak M., Chmielewski A.G., Licki J.**
Computer monitoring and control system (CMCS) for electron beam flue gas treatment.
Radiation Physics and Chemistry, 45, 6, 1049-1055 (1995).

180. **Stachowicz W.**
Dozymetria EPR promieniowania jonizującego oparta na hydroksyapatytach biologicznych i syntetycznych (EPR dosimetry of ionizing radiation based in biological and synthetic hydroxyapatites).
Krajowe Sympozjum "Technika Jądrowa w Przemyśle, Medycynie, Rolnictwie i Ochronie Środowiska". Referaty. Warszawa, Poland, 24-27.04.1995, pp. 110-114.

181. **Stachowicz W.**
Identyfikacja żywności utrwalanej radiacyjnie (Detection of foods preserved by radiation).
Roczniki Państwowego Zakładu Higieny, XLVI, 4, 329-339 (1995).

182. **Stachowicz W.**
Metody sterylizacji medycznej (Methods of medical sterilization).
III Jesienna Szkoła Sterylizacji Radiacyjnej Sprzętu Medycznego i Przeszczepów. Warszawa, Poland, 05-06.10.1995, pp. 71-80.

183. **Stachowicz W., Burlińska G., Michalik J.**
Wykorzystanie spektroskopii EPR do oceny dawki promieniowania w środowisku skażonym w wyniku awarii jądrowej (Application of EPR spectroscopy for estimation radiation dose in areas contaminated by nuclear accidents).
Krajowe Sympozjum "Technika Jądrowa w Przemyśle, Medycynie, Rolnictwie i Ochronie Środowiska". Referaty. Warszawa, Poland, 24-27.04.1995, pp. 76-80.

184. **Stachowicz W., Burlińska G., Michalik J., Dziedzic-Gocławska A., Ostrowski K.**
The EPR detection of foods preserved with the use of ionizing radiation.
Radiation Physics and Chemistry, 46, 4-6, 771-777 (1995).

185. **Stachowicz W., Burlińska G., Michalik J., Dziedzic-Gocławska A., Ostrowski K.**
Identyfikacja napromienionej żywności metodą spekrometrii elektronowego rezonansu paramagnetycznego (Detection of irradiated foods by EPR spectrometry method).
X Krajowy Zjazd Polskiego Towarzystwa Badań Radiacyjnych im. Marii Skłodowskiej-Curie. Streszczenia referatów. Warszawa, Poland, 06-07.04.1995, p. 45.

186. **Stachowicz W., Michalik J., Burlińska G., Sadło J., Dziedzic-Gocławska A., Ostrowski K.**
Detection limits of absorbed dose of ionizing radiation in molluscan shells as determined by epr spectroscopy.
Applied Radiation and Isotopes, 46, 10, 1047-1052 (1995).

187. **Staroń K., Kowalska-Loth B., Ząbek J., Czerwiński R.M., Nieznański K., Szumiel I.**
Topoisomerase I is differently phosphorylated in two sublines of L5178Y mouse lymphoma cells.
Biochimica et Biophysica Acta, 1260, 35-42 (1995).

188. **Stuglik Z.**
Efekty wtórne towarzyszące radiolizie cieczy wiązkami ciężkich cząstek naładowanych (Secondary effects in heavy particle radiolysis).
X Krajowy Zjazd Polskiego Towarzystwa Badań Radiacyjnych im. Marii Skłodowskiej-Curie. Streszczenia referatów. Warszawa, Poland, 06-07.04.1995, p. 46.

189. **Stuglik Z.**
Krytyczny przegląd metod dozymetrycznych stosowanych w technologiach radiacyjnych zorientowanych na ochronę zdrowia (A critical review of dosimetric method for health preservation oriented radiation technologies).
Krajowe Sympozjum "Technika Jądrowa w Przemyśle, Medycynie, Rolnictwie i Ochronie Środowiska". Referaty. Warszawa, Poland, 24-27.04.1995, pp. 153-157.

190. **Stuglik Z.**
Laboratorium dozymetryczne dla potrzeb sterylizacji radiacyjnej (Dosimetric laboratory for radiation sterilization needs).
III Jesienna Szkoła Sterylizacji Radiacyjnej Sprzętu Medycznego i Przeszczepów. Warszawa, Poland, 05-06.10.1995, pp. 66-70.

191. **Stuglik Z.**
On the "oxygen in heavy-ion tracks" hypothesis.
Radiation Research, 143, 343-348 (1995).

192. **Stuglik Z.**
Radiation facility at the JINR U-400 cyclotron checked by Fricke dosimeter measurements.
OIJaI, Dubna 1995, E12-95-109, 8 p.

193. **Stuglik Z.**
Some dosimetric techniques for ion beam radiation experiments.
The 10th Congress of the Polish Society of Medical Physics. Medical Physics. 100 Years after the Discovery of X-Rays. Kraków, Poland, 15-18.09.1995, p. RT-13.

194. **Stuglik Z., Sadło J.**
EPR-dosimetry. An amplitude or a double integral of first derivative as a measure of radiation effects?
4th International Symposium on ESR Dosimetry an Applications. München/Neuherberg, Germany, 15-19.05.1995, p. 251.

195. **Stuglik Z., Sadło J.**
Latent tracks generated in micro-crystalline α-L-alanine and standard bone powder by ^{59}Co ion beams as investigated by EPR-method.
Radiation Measurements, 25, 1-4, 95-98 (1995).

196. **Stuglik Z., Sadło J.**
A response of L-α-alanine and standard bone powder on intermediate energy ion beams.
4th International Symposium on ESR Dosimetry an Applications. München/Neuherberg, Germany, 15-19.05.1995, p. 59.

197. **Stuglik Z., Sadło J.**
Syntetyczne hydroxyapatyty i możliwość ich wykorzystania w dozymetrii EPR (Synthetic hydroxy-apatites as possible materials for EPR dosimetry).
Zjazd Naukowy Polskiego Towarzystwa Chemicznego i Stowarzyszenia Inżynierów i Techników Przemysłu Chemicznego. Lublin, Poland, 25-28.09.1995, p. S-5 P-24.

198. **Szumiel I.**
Cellular radiosensitivity: lessons from rodent mutants.
Tenth International Congress on Radiation Research. Würzburg, Germany, 27.08.-01.09.1995. Radiation Research 1895-1995. Congress Proceedings. Vol. 1. Abstracts, p. 8.

199. **Szumiel I., Buraczewska I., Grądzka I., Gasińska A.**
Effects of topoisomerase I-targeted drugs on radiation response of L5178Y sublines differentially radiation and drug sensitive.
International Journal of Radiation Biology, 67, 4, 441-448 (1995).

200. **Szumiel I., Kapiszewska M., Kruszewski M., Iwaneńko T., Lange C.S.**
Content of iron and copper in the nuclei and induction of pH 9-labile lesions in L5178Y sublines inversely cross-sensitive to H_2O_2 and X-rays.
Radiation Environmental Biophysics, 34, 113-119 (1995).

201. **Szytuła A., Kolenda M., Leciejewicz J., Stuesser N.**
Incommensurate magnetic structures in TbRhGe.
Journal of Magnetism and Magnetic Materials, 149, 265-268 (1995).

202. **Urbański P.**
Wczoraj i dziś radioizotopowej aparatury pomiarowej (Past and present of nucleonic control systems).

Krajowe Sympozjum "Technika Jądrowa w Przemyśle, Medycynie, Rolnictwie i Ochronie Środowiska". Referaty. Warszawa, Poland, 24-27.04.1995, pp. 51-62.

203. **Urbański P., Kowalska E.**
Application of partial least-squares calibration methods in low-resolution EDXRS.
X-ray Spectrometry, 24, 70-75 (1995).

204. **Urbański P., Kowalska E., Antoniak W.**
Determination of thickness and composition of thin Sn-Pb layers XRF technique and multivariate calibration procedure.
Nukleonika, 40, 1, 61-66 (1995).

205. **Urbański P., Kowalska E., Antoniak W.**
Możliwości wykorzystania wielowymiarowych procedur wzorcowania w radioizotopowej aparaturze przemysłowej (Application of multivariate calibration in nucleonic control systems).
Krajowe Sympozjum "Technika Jądrowa w Przemyśle, Medycynie, Rolnictwie i Ochronie Środowiska". Referaty. Warszawa, Poland, 24-27.04.1995, pp. 461-466.

206. **Urbański T.S.**
INIS - źródło informacji dla pracowników naukowych i technicznych w zakresie nukleoniki (INIS - source of information for scientific workers and engineers in the field of nucleonics).
Krajowe Sympozjum "Technika Jądrowa w Przemyśle, Medycynie, Rolnictwie i Ochronie Środowiska". Referaty. Warszawa, Poland, 24-27.04.1995, pp. 496-498.

207. **Villanueva L.M., Ahumada L., Chmielewski A.G., Zimek Z., Bułka S., Licki J.**
Electron beam oxidation of SO_2 in high concentrated off-gases.
International Chemical Congress of Pacific Basin Societes. Book of Abstracts. Honolulu, Hawaii, 17-22.12.1995, p. ENVR-6(315).

208. **Wasek M., Kulisa K., Dybczyński R.**
Metoda ilościowego oznaczania lantanowców w materiałach ważnych dla ochrony środowiska za pomocą NAA z wykorzystaniem techniki wymiany jonowej (NAA method of quantitative determination of lanthanides in environmental materials with the use of ion exchange preconcentration).
V Polska Konferencja Chemii Analitycznej "Analityka w służbie człowieka i środowiska". Gdańsk, Poland, 03-09.09.1995. Materiały konferencyjne. T. 1, p. 253.

209. **Wasek M., Kulisa K., Dybczyński R.**
Oznaczanie lantanowców metodą neutronowej analizy aktywacyjnej w materiałach geologicznych i środowiskowych z wykorzystaniem techniki wymiany jonowej dla wstępnego wydzielania frakcji pierwiastków ziem rzadkich (A method for the determination of lanthanides in environmental and geological materials by neutron activation analysis after ion exchange preconcentration).
IV Poznańskie Konserwatorium Analityczne "Nowoczesne metody przygotowania próbek i oznaczania śladowych zawartości pierwiastków". Poznań, Poland, 27-28.04.1995. Materiały Konwersatorium, p. 20.

210. **Wierzchnicki R., Pruszak Z., Owczarczyk A.**
Badanie transportu osadów dennych w morskiej strefie brzegowej metodą radioznacznikową (Study of bed-load transport on marine near-shore zone by means of radiotracer method).
Krajowe Sympozjum "Technika Jądrowa w Przemyśle, Medycynie, Rolnictwie i Ochronie Środowiska". Referaty. Warszawa, Poland, 24-27.04.1995, pp. 226-230.

211. **Wierzchowski K.L., Poznański J., Bobrowski K.**
Modelling of long range electron transfer between proline-bridged tryptophan and tyrosine aromatic side chains.
Symposium on Physical Organic Photochemistry. Book of Abstracts. Poznań, Poland, 23-27.07.1995, p. L-17.

212. **Wojewódzka M., Kruszewski M., Szumiel I., Wójcik A., Straffer C.**
Alarm signal transduction and DNA repair in the adaptive response in human lymphocytes.
2nd International Conference on Environmental Mutagens in Human Populations. Abstract Book. Prague, Czech Republic, 20-25.08.1995, p. Comet-19.

213. **Wojewódzka M., Kruszewski M., Szumiel I., Wójcik A., Streffer C., Gasińska A.**
Alarm signal transduction and DNA repair in the adaptive response induced by X-rays in human lymphocytes.
Nukleonika, 40, 3, 115-124 (1995).

214. **Wojewódzka M., Walicka M., Sochanowicz B., Kruszewski M., Szumiel I.**
Inhibitory przekazywania sygnałów wewnątrzkomórkowych modyfikują odpowiedź adaptacyjną limfocytów ludzkich (Inhibitors of intracellular signalling pathway modify adaptive response of human lymphocytes).
XXXI Zjazd Polskiego Towarzystwa Biochemicznego. Streszczenia. Warszawa, Poland, 06-08.09.1995, p. 127.

215. **Wojewódzka M., Walicka M., Sochanowicz B., Szumiel I.**
Odpowiedź adaptacyjna limfocytów ludzkich, modyfikacja inhibitorami przekazywania sygnałów wewnątrzkomórkowych (Adaptive response of human lymphocytes is modified by inhibitors of intracellular signalling pathway).
X Krajowy Zjazd Polskiego Towarzystwa Badań Radiacyjnych im. Marii Skłodowskiej-Curie. Streszczenia referatów. Warszawa, Poland, 06-07.04.1995, p. 88.

216. **Wojewódzka M., Wójcik A., Szumiel I., Streffer C.**
Faster DNA damage repair in adapted human lymphocytes.
Tenth International Congress of Radiation Research. Würzburg, Germany, 27.08.-01.09.1995. Radiation Research 1895-1995. Congress Proceedings. Vol. 1. Abstract P20/4, p. 207.

217. **Wojtyńska E., Głuszewski W.**
Badanie wpływu promieniowania jonizującego na właściwości samoprzylepnych klejów akrylowych (Investigations of the influence of ionizing radiation on the properties of polyacrylic adhesive).
III Jesienna Szkoła Sterylizacji Radiacyjnej Sprzętu Medycznego i Przeszczepów. Warszawa, Poland, 05-06.10.1995, pp. 142-146.

218. **Zagórski Z.P.**
ALA/DRS as the alternative to ALA/EPR dosimetry.
Radiation Physics and Chemistry, 46, 4-6, 1291-1294 (1995).

219. **Zagórski Z.P.**
Jonizacje wielokrotne jednej cząsteczki w fazie stałej (Multi-ionizations of one molecule in the solid state).
Zjazd Naukowy Polskiego Towarzystwa Chemicznego i Stowarzyszenia Inżynierów i Techników Przemysłu Chemicznego. Lublin, Poland, 25-28.09.1995, S-R-4.

220. **Zagórski Z.P.**
Limits of energy utilization in electron beam radiation processing.
Radiation Physics and Chemistry, 46, 4-6, 1391-1394 (1995).

221. **Zagórski Z.P.**
O oddziaływaniach jonizujących wspólnych wszelkim układom napromieniowanym (On ionization phenomena, common to all irradiated systems).
X Krajowy Zjazd Polskiego Towarzystwa Badań Radiacyjnych im. Marii Skłodowskiej-Curie. Streszczenia referatów. Warszawa, Poland, 06-07.04.1995, p. 55.

222. **Zagórski Z.P.**
Radon zły i dobry czyli, jedna z osobliwości końca XX wieku (Radon "bed" and "beneficial": One of the pecularities at the end of the 20th century).
Postępy Techniki Jądrowej, 38, 2, 44-49 (1995).

223. **Zagórski Z.P.**
Sterylizacja radiacyjna a inne metody sterylizacji sprzętu medycznego (Comparison of radiation sterilization with another sterilization methods).
III Jesienna Szkoła Sterylizacji Radiacyjnej Sprzętu Medycznego i Przeszczepów. Warszawa, Poland, 05-06.10.1995, pp. 1-10.

224. **Zagórski Z.P., Gładysz K.**
Pulse radiolysis studies of short-lived species in solid amino acids as precursors of radicals detected by ESR.
Radiation Physics and Chemistry, 45, 6, 847-851 (1995).

225. **Zagórski Z.P., Rafalski A.**
Diffuse reflectance spectrophotometry in polypropylene radiolysis.
International Chemical Congress of Pacific Basin Societes. Book of Abstracts. Honolulu, Hawaii, 17-22.12.1995, p. MACR-8(026).

226. **Zagórski Z.P., Rafalski A.**
Metoda spektrofotometrii światła rozproszonego w chemii radiacyjnej polimerów (Spectrophotometry of diffuse light in the radiation chemistry of polymers).
XII Konferencja Naukowa "Modyfikacja Polimerów". Kudowa Zdrój, Poland, 11-15.09.1995, pp. 171-174.

227. **Zagórski Z.P., Rafalski A.**
Nowy dozymetr chemiczny z ciała stałego dla obróbki radiacyjnej, oparty o pomiar spektrofotometryczny światła rozproszonego (DRS) (A new chemical solid state dosimeter for radiation processing, based on diffuse reflection spectrophotometry (DRS)).
Krajowe Sympozjum "Technika Jądrowa w Przemyśle, Medycynie, Rolnictwie i Ochronie Środowiska". Referaty. Warszawa, Poland, 24-27.04.1995, pp. 83-89.

228. **Zagórski Z.P., Rafalski A.**
A thin alanine - polyethylene film dosimetry system with diffuse reflection spectrophotometric evaluation.
Journal of Radioanalytical and Nuclear Chemistry, Articles, 1961, 97-105 (1995).

229. **Zakrzewska D., Machaj B.**
Wykorzystanie beta odbiciowych grubościomierzy powłok w kontroli jakości wyrobu (Use of beta backscatter coating thickness gauge for product quality control).
Krajowe Sympozjum "Technika Jądrowa w Przemyśle, Medycynie, Rolnictwie i Ochronie Środowiska". Referaty. Warszawa, Poland, 24-27.04.1995, pp. 304-309.

230. **Zakrzewska-Trznadel G., Chmielewski A.G., Miljević N.R.**
Wielostopniowy proces wzbogacania izotopów wodoru i tlenu metodą permeacji z przemianą fazową (Multistage process of hydrogen and oxygen isotopes enrichment by membrane permeation coupled with phase transition).
XV Ogólnopolska Konferencja Naukowa Inżynierii Chemicznej i Procesowej. Materiały Konferencyjne. T. IV. Gdańsk, Poland, 12-15.09.1995, pp. 101-104.

231. **Zdunek K., Grigoriew H.**
Nanoporosity of Al_2O_3 coatings obtained by impulse plasma deposition.
Journal of Material Science, 30, 4479-4482 (1995).

232. **Zimek Z.**
Akceleratory elektronów dla potrzeb sterylizacji radiacyjnej (Sources of ionizing radiation - accelerators).
III Jesienna Szkoła Sterylizacji Radiacyjnej Sprzętu Medycznego i Przeszczepów. Warszawa, Poland, 05-06.10.1995, pp. 81-86a.

233. **Zimek Z.**
High power electron accelerators for flue gas treatment.
Radiation Physics and Chemistry, 45, 6, 1013-1015 (1995).

234. **Zimek Z.**
Radiacyjna modyfikacja materiałów (Radiation modification of materials).
Krajowe Sympozjum "Technika jądrowa w przemyśle, medycynie, rolnictwie i ochronie środowiska". Warszawa, Poland, 24-27.04.1995. Streszczenia referatów, p. 25.

235. **Zimek Z.**
Zastosowania wiązki elektronów w ochronie środowiska (The application of electron beam in environment protection).
Krajowe Sympozjum "Technika jądrowa w przemyśle, medycynie, rolnictwie i ochronie środowiska". Warszawa, Poland, 24-27.04.1995. Streszczenia referatów, p. 17.

236. **Zimek Z., Chmielewski A.G.**
Advanced accelerator technology for environmental protection.
International Chemical Congress of Pacific Basin Societes. Book of Abstracts. Honolulu, Hawaii, 17-22.12.1995, p. ENVR-6(478).

237. **Zimek Z., Chmielewski A.G.**
Wykorzystanie wiązki elektronów i energii mikrofalowej w procesie usuwania zanieczyszczeń z gazów odlotowych (Simultaneous electron beam and microvawe energy application for removal pollutants from flue gases).

X Krajowy Zjazd Polskiego Towarzystwa Badań Radiacyjnych im. Marii Skłodowskiej-Curie. Streszczenia referatów. Warszawa, Poland, 06-07.04.1995, p. 56.

238. **Zimek Z., Chmielewski A.G., Bułka S., Lysov G.W., Artukh I.G., Frank N.W.**
Flue gases treatment by simultaneous use of electron beam and streams of microwave energy.
Radiation Physics and Chemistry, 46, 4-6, 1159-1162 (1995).

239. **Zimek Z., Rzewuski H., Migdał W.**
Electron accelerators installed at the Institute of Nuclear Chemistry and Technology.
Nukleonika, 40, 3, 93-114 (1995).

240. **Żernik-Kobak M., Szumiel I., Levine A.S., Dixon K.**
Analysis of mutagenesis in UV-sensitive mouse lymphoma L5178Y-R cells with a polyomavirus-based shuttle vector.
Mutation Research, 344, 31-39 (1995).

SUPPLEMENT LIST OF THE INCT PUBLICATIONS IN 1994

241. **Buraczewska I., Szumiel I., Zagórski S., Afanasjev G.G.**
Effects of 8-chloroadenosine-3',5'-monophosphate in combination with irradiation in L5178Y mouse lymphoblasts.
Acta Oncologica, 33, 6, 671-675 (1994).

242. **Chudzlak A., Trojanowicz M.**
HPLC determination of patulin in apple juice.
Chemia Analityczna, 39, 729-733 (1994).

243. **Dybczyński R., Danko B.**
Accurate determination of cobalt traces in several biological reference materials.
Biological Trace Element Research, 43-45, 615-625 (1994).

244. **Migdał W., Bogus W.**
Napromieniowywanie produktów rolno-spożywczych i urządzenia radiacyjne w Polsce (Food irradiation and radiation facility in Poland).
Konferencja informcyjno-promocyjna "Utrwalanie i Higienizacja Artykułów Rolno-Spożywczych Metodą Radiacyjną". Program i streszczenie referatów. Łódź, Poland, 22.04.1994, pp. 14-19.

245. **Szot Z.**
Zdrowotne aspekty napromieniania żywności (Wholesome aspects of irradiated food).
Konferencja informacyjno-promocyjna "Utrwalanie i Higienizacja Artykułów Rolno-Spożywczych Metodą Radiacyjną". Program i streszczenie referatów. Łódź, Poland, 22.04.1994, pp. 20-25.

THE INCT REPORTS IN 1995

1. Annual Report 1994.
   IChTJ, Warszawa 1995, 140 p.

2. Stuglik Z., Sadło J.
   A comparison of three materials used in ESR dosimetry: L-α-alanine, DL-α-alanine and standard bone powder. Response to Co-60 gamma radiation.
   IChTJ, Warszawa 1995. Raporty IChTJ. Seria A, nr 1/95.

3. Kowalska E., Urbański P.
   Pomiary stężeń niektórych metali w kąpielach galwanicznych (Concentration measurements of some metals in galvanic bath).
   IChTJ, Warszawa 1995. Raporty IChTJ. Seria B, nr 0/95.

NUKLEONIKA
THE INTERNATIONAL JOURNAL OF NUCLEAR RESEARCH

CONTENTS OF No. 1/95

CONTENTS OF No. 2/95

CONTENTS OF No. 3/95

CONTENTS OF No. 4/95

3. Dziewoński Z.R., Chmielewski A.G., Palige J.
   Computer systems for data acquisition and processing in industrial and field radiotracer experiments.
4. Hrynkiewicz A.Z., Kisiel A.
   Electron spectroscopy using synchrotron radiation.
5. Cebulska-Wasilewska A., Litwiniszyn M., Pałka B.
   RBE of 5.6 MeV neutrons assessed for the various biological endpoints in two mutable clones of *Tradescantia*.
6. Suplińska M.
   Plutonium in sediments of the Baltic sea in the period of 1991-1993.
7. Szymczyk W.M.
   Automatic analysis of samples in "KSAF" and "SRDE" EDXRF systems.

Information and subscription

INSTITUTE OF NUCLEAR CHEMISTRY AND TECHNOLOGY
NUKLEONIKA
Dorodna 16, 03-195 Warszawa, Poland
phone: (48-22) 11-06-56 or 11-30-21 int. 14-91; tlx 813027; fax: (48-22) 11-15-32;
e-mail: jlachows@orange.ichtj.waw.pl

THE INCT PATENTS GRANTED IN 1995

1. Electron beam converter.
   Z. Zimek, A. Woźniak
   Polish Patent 168057

2. Method of preparation 3-amino-1,2,4-triazole complexes with transient metals.
   A. Łukasiewicz, Z. Bazaniak, L. Waliś, I. Woźniak
   Polish Patent 168745

3. The method of removal of acid gas pollutants such as SO_2 and NO_x and organic pollutants such as dioxine from industrial flue gases.
   A.G. Chmielewski, E. Iller, Z. Zimek, A. Janowski, L. Karpiński, Z. Kurzyński
   Polish Patent 167481

4. The method of natural water enrichment in oxygen-18.
   A.G. Chmielewski, G. Zakrzewska-Trznadel, A. Van Hook, N. Miljević
   Polish Patent 168152

5. Preparation of high temperatures superconductors.
   A. Deptuła, T. Olczak, W. Łada
   Polish Patent 168176

6. Process for removal of SO_2 and NO_x from combustion flue gases and an apparatus used therefor.
   Z. Zimek, A.G. Chmielewski, I. Artiuch, G. Łysow, N. Frank
   USA Patent 5,397,444

THE INCT PATENT APPLICATIONS IN 1995

1. Method for preparing radionuclides of yttrium and indium.
   A. Bilewicz, J. Narbutt
   P. 308860

2. Method of preparation of hollow spherical ceramic and metallic materials.
   A. Deptuła, A.G. Chmielewski, T. Olczak, W. Łada
   P. 310741

3. The method of radioactive wastes purification.
   A.G. Chmielewski, G. Zakrzewska-Trznadel, M. Harasimowicz, A. Van Hook
   P. 310865

CONFERENCES ORGANIZED BY THE INCT IN 1995

1. SEMINAR "THE MICROBIOLOGICAL DECONTAMINATION OF THE SPICES AND THE METHODS IMPROVING THEIR HYGIENIC QUALITY", 14 MARCH 1995, WARSZAWA, POLAND

- "Mikrobiologiczna jakość przypraw i problemy z tym związane" (The microbiological quality of the spices)
  B. Nowakowska (Institute of Biotechnology of the Agricultural and Food Industry, Warszawa, Poland)
- "Metody sterylizacji przypraw" (Methods of decontamination of spices)
  E. Kostrzewa (Institute of Biotechnology of the Agricultural and Food Industry, Warszawa, Poland)
- "Radiacyjna metoda higienizacji artykułów rolno-spożywczych" (The hygienization of the agricultural commodities by irradiation)
  W. Migdał (Institute of Nuclear Chemistry and Technology, Warszawa, Poland)
- "Wpływ metody radiacyjnej na zanieczyszczenia mikrobiologiczne badanych przypraw i ich wartość użytkową" (The effect of irradiation on the microbiological decontamination of some spices and their useful values)
  B. Owczarczyk (Institute of Nuclear Chemistry and Technology, Warszawa, Poland), E. Kostrzewa, S. Skąpska (Institute of Biotechnology of the Agricultural and Food Industry, Warszawa, Poland)
- "Argumenty za i przeciw napromienianiu żywności" (The arguments for and against food irradiation)
  W. Fiszer (Academy of Agriculture, Poznań, Poland)
- "Zdrowotne aspekty napromienionej żywności" (The wholesomeness of irradiated food)
  Z. Szot (Institute of Nuclear Chemistry and Technology, Warszawa, Poland)

2. NATIONAL SYMPOSIUM "NUCLEAR TECHNIQUE IN INDUSTRY, MEDICINE, AGRICULTURE AND ENVIRONMENTAL PROTECTION", 24-27 APRIL 1995, WARSZAWA, POLAND

Plenary lectures

- "Zastosowanie technik izotopowych" (Application of nuclear techniques)
  T. Florkowski (Stanisław Staszic Academy of Mining and Metallurgy, Kraków, Poland)
- "Rozwój technologii zaawansowanych (high-tech) na przykładzie technik radiacyjnych" (Development of high-tech as exemplified by radiation techniques)
  A.G. Chmielewski (Institute of Nuclear Chemistry and Technology, Warszawa, Poland)
- "Rozwój metody atomów znaczonych w zastosowaniach przemysłowych" (Development of tracer methods in industrial applications)
  K. Przewłocki (Stanisław Staszic Academy of Mining and Metallurgy, Kraków, Poland)
- "Podstawy fizykochemiczne procesów radiacyjnych" (Physico-chemical bases of radiation processes)
  J.M. Rosiak (Łódź Technical University, Poland)
- "Techniki jądrowe w geologii" (Nuclear techniques in geology)
  A. Kreft (Stanisław Staszic Academy of Mining and Metallurgy, Kraków, Poland)
- "Wczoraj i dziś radioizotopowej aparatury pomiarowej" (Past and present of radioisotope measuring instruments)
  P. Urbański (Institute of Nuclear Chemistry and Technology, Warszawa, Poland)

Radiation technologies in environmental protection

- "Technologia usuwania SO_2 i NO_x z gazów spalinowych przy pomocy wiązki elektronów" (Technology for the removal of SO_2 and NO_x from flue gases by means of electron beam)

  A.G. Chmielewski, E. Iller, B. Tymiński (Institute of Nuclear Chemistry and Technology, Warszawa, Poland), J. Licki (Institute of Atomic Energy, Otwock-Świerk, Poland), Z. Zimek (Institute of Nuclear Chemistry and Technology, Warszawa, Poland)

- "Wykorzystanie spektroskopii epr do oceny dawki promieniowania w środowisku skażonym w wyniku awarii jądrowej" (Use of EPR spectroscopy for the evaluation of radiation dose in the environment contaminated by nuclear accidents)

  W. Stachowicz, G. Burlińska, J. Michalik (Institute of Nuclear Chemistry and Technology, Warszawa, Poland)

- "Zastosowanie dozymetrii radiacyjnej dla technik ochrony środowiska naturalnego" (Application of radiation dosimetry in techniques for the protection of natural environment)

  P.P. Panta, W. Głuszewski (Institute of Nuclear Chemistry and Technology, Warszawa, Poland)

- "Nowy dozymetr chemiczny z ciała stałego dla obróbki radiacyjnej, oparty o pomiar spektrofotometryczny światła rozproszonego (DRS)" (A new chemical solid state dosimeter for radiation processing, based on diffuse reflection spectrophotometry (DRS))

  Z.P. Zagórski, A. Rafalski (Institute of Nuclear Chemistry and Technology, Warszawa, Poland)

Radiation technologies in material engineering

- "Utwardzalna radiacyjnie żywica poliestrowa do wykonywania dużych odlewów" (Use of radiation cured polyester resin to produce large castings)

  M. Pietrzak (Łódź Technical University, Poland)

- "Technologia sieciowania radiacyjnego polietylenu w zastosowaniu do otrzymywania wyrobów termokurczliwych" (Technology of radiation cross-linking of polyethylene as applied to produce thermo-shrinkable products)

  I. Kałuska (Institute of Nuclear Chemistry and Technology, Warszawa, Poland)

- "Polipropylen w zastosowaniu do wyrobów medycznych sterylizowanych radiacyjnie" (Application of polypropylene to medical appliances sterilized by radiation)

  J. Bojarski, G. Burlińska, Z. Zimek (Institute of Nuclear Chemistry and Technology, Warszawa, Poland)

- "Odporność radiacyjna trekowych membran filtracyjnych" (Radiation resistance of track filtration membranes)

  A. Fiderkiewicz, M. Buczkowski, T. Żółtowski (Institute of Nuclear Chemistry and Technology, Warszawa, Poland), N. Zhitariuk, O. Orelovich (Joint Institute for Nuclear Research FLNR, Dubna, Russia), G. Kovalev (Research Institute for Medical Polymers, Moscow, Russia)

- "Dozymetria epr promieniowania jonizującego oparta na hydroksyapatytach biologicznych i syntetycznych" (EPR dosimetry of ionizing radiation, based on biological and synthetic hydroxyapatites)

  W. Stachowicz (Institute of Nuclear Chemistry and Technology, Warszawa, Poland)

Food preservation by radiation

- "Stan obecny i perspektywy stosowania metody radiacyjnej do utrwalania żywności w różnych krajach świata oraz w Polsce" (Present status and prospects of application of the radiation method for food preservation in various countries and in Poland)

  W. Fiszer (Academy of Agriculture, Poznań, Poland), W. Migdał (Institute of Nuclear Chemistry and Technology, Warszawa, Poland)

- "Doświadczalna stacja radiacyjnego utrwalania płodów rolnych" (Experimental plant for radiation preservation of crops)

  W. Migdał, B. Owczarczyk, K. Malec-Czechowska (Institute of Nuclear Chemistry and Technology, Warszawa, Poland)

- "Zastosowanie promieniowania jonizującego w ochronie produktów rolniczych przed szkodnikami" (Application of ionizing radiation to protect agricultural products against pests)
  S. Ignatowicz (Agricultural University of Warsaw, Poland)
- "Radiacyjna mikrobiologiczna dekontaminacja suszonych warzyw" (Radiation microbiological decontamination of dried vegetables)
  B. Owczarczyk, K. Malec-Czechowska, W. Migdał (Institute of Nuclear Chemistry and Technology, Warszawa, Poland)
- "Metoda termoluminescencji w identyfikacji napromienionej żywności" (Thermoluminescence method for identification of irradiated food)
  K. Malec-Czechowska, A.M. Dancewicz, Z. Szot (Institute of Nuclear Chemistry and Technology, Warszawa, Poland)

Radiation technologies in medicine

- "Radiosterylizacja masowego sprzętu medycznego - technika spełniająca wymagania ochrony środowiska naturalnego" (Radiosterilization of mass medical utensiles - technique fulfilling ecological norms)
  P.P. Panta, W. Głuszewski (Institute of Nuclear Chemistry and Technology, Warszawa, Poland)
- "Kinetyka i mechanizm reakcji zachodzących podczas radiacyjnego tworzenia biomateriałów hydrożelowych" (Kinetics and mechanism of reactions occurring during radiational formation of hydrogel biomaterials)
  A. Rzeźnicki, J. Olejniczak, P. Ulański, J.M. Rosiak (Łódź Technical University, Poland)
- "Zastosowanie analizy termicznej w badaniach napromieniowanych białek" (Application of thermal analysis to study irradiated proteins)
  K. Cieśla (Institute of Nuclear Chemistry and Technology, Warszawa, Poland)
- "Krytyczny przegląd metod dozymetrycznych stosowanych w technologiach radiacyjnych zorientowanych na ochronę zdrowia" (Critical review of dosimetric methods used in radiation technologies directed towards health protection)
  Z. Stuglik (Institute of Nuclear Chemistry and Technology, Warszawa, Poland)
- "Zastosowanie membran trekowych w charakterze bariery mikrobiologicznej" (Application of track membranes as a microbiological barrier)
  M. Buczkowski, W. Starosta, A. Fiderkiewicz (Institute of Nuclear Chemistry and Technology, Warszawa, Poland), J. Kiełkiewicz (Warsaw University of Technology, Poland), E. Meinhardt (Central Mining Institute, Katowice, Poland)

Radiotracers in industrial investigations

- "Radioznacznikowe badania wanien szklarskich" (Radiotracer investigations of glass furnaces)
  J. Palige, M. Harasimowicz (Institute of Nuclear Chemistry and Technology, Warszawa, Poland)
- "Identyfikacja procesu odwadniania koncentratu rud miedzi metodą radioznacznikową" (Identification of dehydration process of copper ore concentrate using radiotracers)
  Z. Stęgowski, B. Tora (Stanisław Staszic Academy of Mining and Metallurgy, Kraków, Poland)
- "Badania kinetyki procesu flotacji rudy miedzi w maszynach typu PM-17 I OK-50" (Studies of kinetics of flotation process of copper ore in installations of PM-17 I OK-50 type)
  Z. Stęgowski, K. Przewłocki, L. Furman, L. Petryka (Stanisław Staszic Academy of Mining and Metallurgy, Kraków, Poland)
- "Radioizotopowe badania wpływu czynników technologicznych na homogeniczność mieszanek gumowych" (Studies of influence of technological parameters on homogeneity of rubber mixtures using radiotracers)
  E. Koczorowska, W. Gorączko (Poznań Technical University, Poland)

Radiotracers in water-sewage disposal and in studies of leak tightness

- "Nowe rozwiązanie uśredniacza ścieków - wynik badań radioznacznikowych" (A new solution for the sewage equalization tank - results of studies with radiotracers)

A.G. Chmielewski, J. Palige, A. Dobrowolski (Institute of Nuclear Chemistry and Technology, Warszawa, Poland)

- "Charakterystyki pracy dla aeratora stożkowego z łopatkami wewnętrznymi" (Functioning characteristics for a conical aerator with inner blades)

  A. Sierzputowski (Warsaw University of Technology, Poland)

- "Rozwój radioznacznikowych metod badania szczelności zbiorników" (Development of radiotracer methods for examination of tank tightness)

  A. Owczarczyk, S. Szpilowski, B. Więcław (Institute of Nuclear Chemistry and Technology, Warszawa, Poland)

- "Szczelność instalacji technologicznych i rurociągów przesyłowych jako element ochrony środowiska naturalnego" (Tightness of technological installations and transmitting pipelines as element of environmental protection)

  J. Kraś, L. Waliś, W. Kielak (Institute of Nuclear Chemistry and Technology, Warszawa, Poland)

Radiotracers in hydrology

- "Zastosowanie metod izotopów naturalnych (tryt, radiowęgiel, izotopy trwałe) w problematyce wód podziemnych i powierzchniowych w Polsce" (Application of tritium, radiocarbon and stable isotopes in studies of surface and underground waters)

  M. Duliński, T. Florkowski, J. Grabczak (Stanisław Staszic Academy of Mining and Metallurgy, Kraków, Poland), A. Zuber (Institute of Nuclear Physics, Kraków, Poland)

- "Badanie transportu osadów dennych w morskiej strefie brzegowej metodą radioznacznikową" (Studies of bed-load transport near-shore marine zone using radiotracer method)

  R. Wierzchnicki (Institute of Nuclear Chemistry and Technology, Warszawa, Poland), Z. Pruszak (Polish Academy of Sciences, Institute of Hydroengineering, Gdańsk, Poland), A. Owczarczyk (Institute of Nuclear Chemistry and Technology, Warszawa, Poland)

- "Radioizotopowe metody pomiarów transportu materiału dennego w rzekach górskich" (Radiotracer methods for measurements of bed-load transport in mountain rivers)

  A. Michalik, W. Bartnik (Hugo Kołłątaja Academy of Agriculture, Kraków, Poland), A. Owczarczyk, R. Wierzchnicki (Institute of Nuclear Chemistry and Technology, Warszawa, Poland)

- "Próba zastosowania ^{210}Pb do datowania osadów jezior Gościąż i Morskie Oko" (Test to apply ^{210}Pb for dating sediments of the Gościąż and Morskie Oko lakes)

  P. Wachniew (Stanisław Staszic Academy of Mining and Metallurgy, Kraków, Poland)

- "Badanie procesu erozji gleby w Australii" (Studies on erosion process of soil in Australia)

  W. Gorączko (Poznań Technical University, Poland), G. Elliott, K. Western (Australian Nuclear Science and Technology Organisation, Lucas Heights Research Laboratories, Australia)

Radiotracers in material engineering studies

- "Zastosowanie metod jądrowych do badania skuteczności środków obniżających zużycie" (Application of nuclear methods to study of effectivness of wear reducing agents)

  A. Kalicki, E. Pańczyk (Institute of Nuclear Chemistry and Technology, Warszawa, Poland), A. Kulczycki (Institute of Petroleum Processing, Kraków, Poland), Z. Banasik (Institute of Nuclear Chemistry and Technology, Warszawa, Poland)

- "Zastosowanie znaczników promieniotwórczych do określania stopnia oczyszczenia indu i galu do czystości półprzewodnikowej w procesie przetapiania pod żużlami syntetycznymi" (Use of radiotracers for determining purification degree of indium and gallium to semiconductor purity in the process of smelting under synthetic slags)

  L. Rowińska, L. Waliś, A. Nowicki (Institute of Nuclear Chemistry and Technology, Warszawa, Poland)

Apparatus for environmental protection

- "Ocena parametrów radioizotopowego miernika zapylenia powietrza" (Estimation of parameters of a radioisotope gauge for air dustiness)

B. Machaj, B. Krawczyńska, J. Strzałkowski (Institute of Nuclear Chemistry and Technology, Warszawa, Poland)

- "Instrumentalny pomiar produktów rozpadu radonu-222 w powietrzu" (Instumental measurement of decay products of ^{222}Rn in the air)

  J. Bartak, B. Machaj (Institute of Nuclear Chemistry and Technology, Warszawa, Poland)

- "Analizatory zanieczyszczeń mediów sypkich i płynnych izotopami naturalnymi" (Analyzers of impurities of loose and liquid media using natural nuclides)

  W. Michałowski (Nuclear Technique Enterprise POLON-IZOT, Warszawa, Poland)

- "Bezkalibracyjne ilościowe oznaczanie stężenia związków chlorowcowych detektorem wychwytu elektronów" (Quantitative determination of concentration of halogen compounds by a detector of electron capture without calibration)

  J. Lasa, I. Śliwka (Institute of Nuclear Physics, Kraków, Poland)

- "System pomiarów, monitoringu i kontroli zanieczyszczeń gazów odlotowych" (System of measurements, monitoring and controlling of impurities in flue gases)

  M. Sowiński (Sołtan Institute for Nuclear Studies, Otwock-Świerk, Poland)

Radioisotope industrial apparatus

- "Izotopowe mierniki grubości" (Isotope thickness gauges)

  E. Kowalewski (Nuclear Technique Enterprise POLON-IZOT, Warszawa, Poland)

- "Zastosowania przemysłowych radioizotopowych mierników stężenia kwasu siarkowego i oleum" (Application of radioisotope gauges for concentration of sulphuric acid and oleum)

  J. Mirowicz (Institute of Nuclear Chemistry and Technology, Warszawa, Poland)

- "Izotopowe mierniki gęstości i wagi taśmociągowe" (Isotope gauges for density and belt conveyer flight balance)

  R. Jabłoński (Nuclear Technique Enterprise POLON-IZOT, Warszawa, Poland)

- "Wykorzystanie beta odbiciowych grubościomierzy powłok w kontroli jakości wyrobu" (Use of beta-scattered thickness gauges of coatings in control of product quality)

  D. Zakrzewska, B. Machaj (Institute of Nuclear Chemistry and Technology, Warszawa, Poland)

- "Spektrometria fluorescencyjna w zastosowaniach laboratoryjnych i przemysłowych" (Fluorescence spectrometry in laboratory and industrial use)

  T. Dudek (Nuclear Technique Enterprise POLON-IZOT, Warszawa, Poland)

Diagnostic and measuring apparatus

- "Detektory nadążne do kontroli szczelności i lokalizacji miejsc nieszczelnych w rurociągach podziemnych metodą znaczników promieniotwórczych" (Follow-up detectors to control leak tightness and localization of leakages in underground pipelines with the radiotracer method)

  Z. Dziewoński, A. Kalicki, W. Kielak, J. Kraś, S. Myczkowski, L. Waliś (Institute of Nuclear Chemistry and Technology, Warszawa, Poland)

- "Aparatura do profilowania jądrowego płytkich otworów wiertniczych" (Apparatus for nuclear logging of shallow bore-holes)

  K.W. Pałka, T. Zorski (Stanisław Staszic Academy of Mining and Metallurgy, Kraków, Poland)

- "Nowe techniki akwizycji danych z pomiarów radiometrycznych" (Novel techniques of data acquisition from radiometric measurements)

  J. Łukasiewicz, J. Bartak (Institute of Nuclear Chemistry and Technology, Warszawa, Poland)

Application of nuclear techniques in material engineering studies

- "Pomiary makroskopowych parametrów neutronowych materiałów oraz ich zastosowania" (Measurements of macroscopic neutron parameters of materials and their applications)

A. Kreft, A. Bolewski Jr., M. Ciechanowski (Stanisław Staszic Academy of Mining and Metallurgy, Kraków, Poland)

- "Pomiar dyspersji ciała stałego" (Measurement of dispersion of solid state)

  M. Lech (Wrocław Technical University, Poland), E. Polednia, A. Werszler (Institute of Mineral Building Bond Materials, Opole, Poland)

- "Autoradiograficzne badania kierunków dyfuzji pierwiastków w procesach wysokotemperaturowego siarkowania wolframu i molibdenu" (Autoradiographic investigation of directions of diffusion of elements in high-temperature sulphurization of tungsten and molybdenum)

  A. Ciurapiński (Institute of Nuclear Chemistry and Technology, Warszawa, Poland), K. Przybylski, M. Potoczek (Stanisław Staszic Academy of Mining and Metallurgy, Kraków, Poland)

- "Probabilistyczna interpretacja autoradiogramów struktury stopów metali" (Probabilistic interpretation of autoradiograms of structure of metal alloys)

  K. Gibas (Poznań Technical University, Poland)

Application of nuclear techniques in geology and hydrogeology

- "Wybrane jądrowe metody badania węgla kamiennego w próbkach i w odwiertach" (Selected nuclear methods to study hard-coal in samples and bore-holes)

  E. Chruściel, Nguyen Dinh Chau, J. Niewodniczański, K.W. Pałka (Stanisław Staszic Academy of Mining and Metallurgy, Kraków, Poland)

- "Monitorowanie jakości węgla metodą rozpraszania neutronów" (Monitoring of coal quality by the scattered neutron method)

  T. Cywicka-Jakiel, J. Łoskiewicz, G. Tracz (Institute of Nuclear Physics, Kraków, Poland)

- "Oznaczanie izotopów radu w wodach w oparciu o pomiar aktywności alfa i beta z zastosowaniem ciekłych scyntylatorów lub spektrometru półprzewodnikowego" (Determination of radium isotopes in waters based on measurement of alpha and beta activity using liquid scintillations or a semiconductor spectrometer)

  Nguyen Dinh Chau, E. Chruściel, A. Ochoński (Stanisław Staszic Academy of Mining and Metallurgy, Kraków, Poland)

- "Czynniki wpływające na dokładność oznaczania izotopów radu metodą niespektrometryczną z zastosowaniem ciekłego scyntylatora" (Factors influencing accuracy of determination of radium isotopes by nonspectrometric method with a liquid scintillator)

  I. Tomza, E. Chruściel, Nguyen Dinh Chau, A. Ochoński (Stanisław Staszic Academy of Mining and Metallurgy, Kraków, Poland)

Radioanalytical methods

- "Oznaczanie zanieczyszczeń w krzemie o czystości półprzewodnikowej metodą instrumentalnej reaktorowej neutronowej analizy aktywacyjnej" (Determination of impurities in silicon of semiconductor purity by instrumental reactor neutron activation analysis)

  A. Bukowski (Institute of Electronic Materials Technology, Warszawa, Poland), E. Pańczyk, T. Chajęcki, L. Waliś (Institute of Nuclear Chemistry and Technology, Warszawa, Poland)

- "Zastosowanie reaktorowej neutronowej analizy aktywacyjnej do identyfikacji obrazów szkoły małopolskiej" (Application of reactor neutron activation analysis to the identification of paintings of the Little Poland School)

  E. Pańczyk (Institute of Nuclear Chemistry and Technology, Warszawa, Poland), M. Ligęza (Academy of Fine Arts, Kraków, Poland), L. Waliś (Institute of Nuclear Chemistry and Technology, Warszawa, Poland)

- "Badanie technik i materiałów stosowanych w malarstwie metodami jądrowymi" (Studies on techniques and materials used in painting applying nuclear methods)

  M. Ligęza (Academy of Fine Arts, Kraków, Poland)

- "Badanie własności ekologicznych węgli i popiołów przy pomocy spektrometrii X i gamma" (Studies on ecological properties of coals and ashes by means of X-rays and γ-spectrometry)

J. Kierzek, B. Małożewska-Bućko, P. Bukowski (Institute of Nuclear Chemistry and Technology, Warszawa, Poland), S. Zaraś, B. Kunach, K. Wiland (Electropower SIEKIERKI, Warszawa, Poland)

- "Oznaczanie jonów niklu za pomocą substechiometrycznego rozcieńczenia izotopowego z wykorzystaniem wybranych hydrofobizowanych ekstrahentów oksymowych" (Determination of nickel ions by means of substoichiometric isotope dilution using selected hydrophobic oxime extractants)

  Z. Górski (Poznań Technical University, Poland)

Detectors of radiation

- "Potencjalne możliwości detektorów z krzemu amorficznego w obrazowaniu rozkładów megawoltowych pól promieniowania" (Potential possibilities of detectors made of amorphous silicon to picture megavolt distributions of radiation fields)

  W.M. Szymczyk (Sołtan Institute for Nuclear Studies. Otwock-Świerk, Poland)

- "Zastosowanie liczników proporcjonalnych promieniowania X i miękkiego γ w przemyśle polskim" (Application of proportional counters of X-rays and soft γ-radiation in the Polish industry)

  B. Bednarek, K. Jeleń, T.Z. Kowalski, E. Rulikowska-Zarębska (Stanisław Staszic Academy of Mining and Metallurgy, Kraków, Poland), T. Sikora (Mining Automatization Centre EMAG, Katowice, Poland), J. Nocuń (Cement Plant RUDNIKI, Rudniki, Poland), A. Lorek (Mining Plant TRZEBIONKA, Trzebinia, Poland)

- "Elektroniczny dawkomierz personalny z detektorem krzemowym" (Electronic personal dosimeter with a silicon detector)

  M. Słapa, M. Traczyk (Sołtan Institute for Nuclear Studies, Otwock-Świerk, Poland)

- "Kolimacje wiązki w układzie radiometrycznym" (Collimations of beam in radiometric systems)

  M. Lech (Wrocław Technical University, Poland)

Measurements of radiation

- "Wieloparametryczny system określania aktywności dla wytwarzania wzorców radionuklidów" (Multiparametric system of radioactivity determination to produce standards of radionuclides)

  A. Chyliński, T. Radoszewski (Radioisotope Centre POLATOM, Otwock-Świerk, Poland)

- "Pomiar makroskopowego przekroju czynnego absorpcji neutronów termicznych na małych próbkach materiału przy użyciu impulsowego generatora neutronów" (Measurement of macroscopic absorption cross-section of thermal neutrons using small samples of material and a pulse generator of neutrons)

  J.A. Czubek, K. Drozdowicz, B. Gabańska, A. Igielski, E. Krynicka, U. Woźnicka (Institute of Nuclear Physics, Kraków, Poland)

- "Diagnozowanie zamkniętych źródeł promieniowania wykorzystywanych w czujkach dymu" (Diagnostics of sealed radiation sources used in smoke gauges)

  A.B. Kraś, E. Pańczyk, L. Waliś, B. Sartowska (Institute of Nuclear Chemistry and Technology, Warszawa, Poland)

Processing of data from radiometric experiments

- "Możliwości wykorzystania wielowymiarowych procedur wzorcowania w radioizotopowej aparaturze przemysłowej" (Possibilities of usage of multidimentional procedures of standarization in radioisotope industrial apparatus)

  P. Urbański, E. Kowalska, W. Antoniak (Institute of Nuclear Chemistry and Technology, Warszawa, Poland)

- "Zastosowanie filtracji adaptacyjnej do obróbki danych z eksperymentu radioznacznikowego" (Application of adaption filtration to process data from a radiotracer experiment)

  L. Furman (Stanisław Staszic Academy of Mining and Metallurgy, Kraków, Poland)

- "Zastosowanie detektora wychwytu elektronów w pomiarach znacznikowych" (Application of a detector of cuptured electrons in radiotracer measurements)

  J. Lasa, I. Śliwka (Institute of Nuclear Physics, Kraków, Poland)

Accelerators. Production of isotopes. Literature date baše (INIS)

- "Mobilny akcelerator radiograficzny - LILIPUT" (Mobile radiographic accelerator - LILIPUT)
  J. Bigolas, S. Kuliński, M. Pachan, J. Pracz, A. Sałaga (Sołtan Institute for Nuclear Studies, Otwock-Świerk, Poland)
- "Różne zastosowania źródeł promieniowania jonizującego w Polsce w ujęciu statystycznym" (Statistics of various applications of sources of ionizing radiation in Poland)
  R. Tańczyk (Central Laboratory for Radiological Protection, Warszawa, Poland)
- "Komputerowe forum dyskusyjne propozycją wykorzystania internetu do prezentacji problemów polskiej atomistyki" (A computer discussion forum as a proposal to use the internet for presentating problems of Polish atomistics)
  R. Frydryk (Technical University of Gdańsk, Poland)
- "INIS - źródło informacji dla pracowników naukowych i technicznych w zakresie nukleoniki" (INIS - a source of information for scientific and technical workers in the field of nucleonics)
  T. Urbański (Institute of Nuclear Chemistry and Technology, Warszawa, Poland)

3. SCHOOL "RADIATION STERILIZATION IN POLAND - POSSIBILITIES AND PERSPECTIVES", 5-6 OCTOBER 1995, WARSZAWA, POLAND

Reports

- "Comparison of radiation sterilization with another sterilization methods"
  Z.P. Zagórski (Institute of Nuclear Chemistry and Technology, Warszawa, Poland)
- "Hydrogel medical materials obtained in radiation processing"
  J. Rosiak (Technical University of Łódź, Poland)
- "Artificial implantation materials"
  M. Lewandowska-Szumieł (School of Medicine, Warszawa, Poland)
- "Microbiological aspects of radiation sterilization"
  E. Czerniawski (Technical University of Łódź, Poland)
- "Radiation treatments of drugs, pharmaceutical raw materials and cosmetics"
  T. Bryl-Sandelewska, Z. Zimek (Institute of Nuclear Chemistry and Technology, Warszawa, Poland)
- "International requirements and guidelines concerning radiation sterilization"
  I. Kałuska (Institute of Nuclear Chemistry and Technology, Warszawa, Poland)
- "Control of irradiation and sterilization processing"
  P.P. Panta (Institute of Nuclear Chemistry and Technology, Warszawa, Poland)
- "Dosimetric laboratory for radiation sterilization needs"
  Z. Stuglik (Institute of Nuclear Chemistry and Technology, Warszawa, Poland)
- "Investigations of the influence of ionizing radiation on the properties of polyacrylic adhesive"
  E. Wojtyńska (Institute of Industrial Chemistry, Warszawa, Poland), W. Głuszewski (Institute of Nuclear Chemistry and Technology, Warszawa, Poland)
- "Methods of medical sterilization"
  W. Stachowicz (Institute of Nuclear Chemistry and Technology, Warszawa, Poland)
- "Sources of ionizing radiation - accelerators"
  Z. Zimek (Institute of Nuclear Chemistry and Technology, Warszawa, Poland)
- "Isotope sources used for radiation sterilization"
  W. Bogus (Technical University of Łódź, Poland)
- "Rules of admittance radiation sterilized medical supplies for use in medicine"
  T. Achmatowicz (Institute for Drugs, Warszawa, Poland)

- "Packaging materials for radiation sterilization"
  H. Kubera (Polish Packing Research and Development Center, Warszawa, Poland)
- "Radiation sterilization in practice of bank tissue"
  J. Komender (School of Medicine, Warszawa, Poland)
- "Polypropylene radiation resistant"
  J. Bojarski (Institute of Nuclear Chemistry and Technology, Warszawa, Poland)
- "Biological applications of particle track membranes"
  M. Buczkowski (Institute of Nuclear Chemistry and Technology, Warszawa, Poland)
- "Radiation technologies and nuclear technics friendly for human beings and natural environment"
  A.G. Chmielewski (Institute of Nuclear Chemistry and Technology, Warszawa, Poland)

4. SEMINAR "PRO-ECOLOGICAL WORKS PERFORMED IN THE INCT" PRESENTED AT THE INTERNATIONAL POZNAŃ FAIR "POLEKO'95", 23 NOVEMBER 1995, POZNAŃ, POLAND

- "Badania własności ekologicznych węgli i popiołów" (Studies on ecological properties of coals and ashes)
  J. Kierzek (Institute of Nuclear Chemistry and Technology, Warszawa, Poland)
- "Wielopierwiastkowa analiza popiołów lotnych metodą neutronowej analizy aktywacyjnej. Badanie wymywalności i dynamiki procesu wymywania pierwiastków śladowych z popiołów lotnych pod wpływem kwaśnych deszczów" (Multielemental analysis of volatile ashes by neutron activation analysis. Studies of washing out and dynamics of elution of trace elements from volatile ashes under the influence of acid rains)
  H. Polkowska-Motrenko (Institute of Nuclear Chemistry and Technology, Warszawa, Poland)
- "Miernik produktów rozpadu radonu w powietrzu" (A gauge for decay products of radon in the air)
  B. Machaj (Institute of Nuclear Chemistry and Technology, Warszawa, Poland)
- "Automatyczny miernik zapylenia powietrza" (An automatic gauge for dustiness of the air)
  B. Machaj (Institute of Nuclear Chemistry and Technology, Warszawa, Poland)
- "Usuwanie SO_2 i NO_x z gazów spalinowych elektrowni przy użyciu wiązki elektronów" (Removal of SO_2 and NO_x from flue gases of power station by the use of electron beam)
  E. Iller (Institute of Nuclear Chemistry and Technology, Warszawa, Poland)
- "Higienizacja osadów ściekowych przy użyciu wiązki elektronów" (Hygienization of sludges by the use of electron beam)
  Z. Zimek (Institute of Nuclear Chemistry and Technology, Warszawa, Poland)
- "Kontrola jakości kompostów z utylizacji odpadów komunalnych. Oznaczanie metali ciężkich" (Verification of compost quality from municipal wastes. Determination of heavy elements)
  J. Chwastowska (Institute of Nuclear Chemistry and Technology, Warszawa, Poland)
- "Badania oczyszczalni ścieków, bilanse wodno-ściekowe, badanie szczelności sieci ściekowych oraz zbiorników" (Studies on: sewage-treatment plant, water-sewage balance, leak tightness of sewer system and tanks)
  J. Palige (Institute of Nuclear Chemistry and Technology, Warszawa, Poland)
- "Uśredniacz-odstojnik ścieków nowej konstrukcji" (Averaging-settler of sewage of new construction)
  J. Palige (Institute of Nuclear Chemistry and Technology, Warszawa, Poland)
- "Oznaczanie anionów w wodach metodą chromatografii jonów" (Determination of anions in waters by chromatography of ions)
  H. Polkowska-Motrenko (Institute of Nuclear Chemistry and Technology, Warszawa, Poland)

PhD THESES

Marian Harasimowicz, M.Sc.

Zastosowanie ultrafiltracji i hiperfiltracji w procesach zatężania ciekłych odpadów promieniotwórczych (Application of the ultrafiltration and reverse osmosis for liquid radioactive waste concentration).

supervisor: Prof. Andrzej G. Chmielewski, Ph.D., D.Sc.

Stanisław Staszic Academy of Mining and Metallurgy, Institute of Physics and Nuclear Techniques, 24.11.1995.

DOCTOR OF CHEMISTRY DEGREE PROGRAMME

The Institute of Nuclear Chemistry and Technology offers the four years Ph.D. degree programme to graduates of chemical, physical and biological departments of universities, engineers in chemical technology and material science and graduates of medical universities. The main areas of the programme are:

- chemistry of radioactive elements and isotope effects,
- coordination chemistry,
- chemistry of separation and analytical methods,
- radiation chemistry and biochemistry,
- chemistry of fast processes,
- application of nuclear methods in chemical and environmental research and in material science.

Besides of the employment for candidates accepted for the forementioned programme, the Institute offers an opportunity of application for supplemental doctorial scholarship.

During the programme each participant participates in 45 h course of lectures of fundamental physical chemistry, 30 h specialization course and is obliged to give an annual seminar on a topic of his/her dissertation area. The final requirements for the Ph.D. programme graduates, consistent with the Ministry of the National Education rules, are:

- submission of a formal dissertation, summarizing original research contributions suitable for publication;
- final examination and public defense of the dissertation theses.

Applicants for the Ph.D. degree programme are accepted all around the year. Detailed information can be obtained from Admission Secretary, Dr. Jadwiga Krejzler (phone: 11-27-35), or from the Scientific Information Department of the Institute (phone: 11-25-78).

RESEARCH PROJECTS AND CONTRACTS

RESEARCH PROJECTS GRANTED BY THE STATE COMMITTEE FOR SCIENTIFIC RESEARCH IN 1995 AND IN PREVIOUS YEARS

1. **New XRF methods and devices for coating thickness gauging and analysis.**
   supervisor: Assoc.Prof. Piotr Urbański, Ph.D., D.Sc.
2. **Dosimetric studies in processes of radiation cleaning up of the flue gases.**
   supervisor: Przemysław Panta, Ph.D.
3. **Using of bremstrahlung in radiation technology.**
   supervisor: Wojciech Migdał, Ph.D.
4. **New materials from polymetallic complexes of aminotriazole with transition metals.**
   supervisor: Prof. Andrzej Łukasiewicz, Ph.D., D.Sc.
5. **Application of various speciation techniques for investigation of the utility of composts.**
   supervisor: Assoc.Prof. Jadwiga Chwastowska, Ph.D., D.Sc.
6. **Studies on radionuclide adsorption on selective inorganic ion exchangers.**
   supervisor: Aleksander Bilewicz, Ph.D.
7. **The detection of irradiated food by means of electron paramagnetic resonanse spectrometry (EPR, ESR), thermoluminescence and differential calorimetry.**
   supervisor: Wacław Stachowicz, Ph.D.
8. **Investigation of homogeneity of reference materials intended for microanalysis by means of neutron activation analysis method.**
   supervisor: Prof. Rajmund Dybczyński, Ph.D., D.Sc.
9. **The computer spectra simulation in high resolution gamma-ray spectrometry as a tool enabling optimization of the costs, labour and time in instrumental neutron activation analysis.**
   supervisor: Zygmunt Szopa, M.Sc.
10. **Concentration of radioactive wastes using the membrane distillation (MD) process.**
    supervisor: Prof. Andrzej G. Chmielewski, Ph.D., D.Sc.
11. **Application of the ultrafiltration (UF) and hyperfiltration (HF) to the concentration of liquid radioactive wastes.**
    supervisor: Prof. Andrzej G. Chmielewski, Ph.D., D.Sc.
12. **Isotope effects of deuterium and oxygen-18 in the permeation process with phase transition.**
    supervisor: Prof. Andrzej G. Chmielewski, Ph.D., D.Sc.
13. **Examination of activation of the nuclear transcription factor NF_KB in two sublines of L5178Y cells damaged with X-rays or hydrogen peroxide.**
    supervisor: Prof. Irena Szumiel, Ph.D., D.Sc.
14. **Identification of irradiated food by use of single cell electrophoresis (comet assay).**
    supervisor: Prof. Zbigniew Szot, Ph.D., D.Sc.
15. **Investigations of new generation of particle track membranes and their applications.**
    supervisor: Assoc.Prof. Tadeusz Żółtowski, Ph.D., D.Sc.
16. **The influence of the even-odd nucleus number and other factors on the isotope effect accompanying the extraction of the f-electron elements.**
    supervisor: Wojciech Dembiński, Ph.D.

17. **High coordination number of metal ions in chelate complexes.**
supervisor: Assoc.Prof. Jerzy Narbutt, Ph.D., D.Sc.

18. **Investigations of radical processes induced by hydroxyl radicals in amino acids and peptides containing thioether group.**
supervisor: Assoc.Prof. Krzysztof Bobrowski, Ph.D., D.Sc.

19. **EPR studies of radiation induced radical processes in polycrystalline amino acids and peptides containing sulfur.**
supervisor: Assoc.Prof. Jacek Michalik, Ph.D., D.Sc.

20. **Optical spectra of free radicals in polypropylene at room temperature.**
supervisor: Prof. Zbigniew P. Zagórski, Ph.D., D.Sc.

21. **Optimization of radiation removal process of SO_2 and NO_x from flue gases containing high concentration of SO_2.** (supervision of IEA PhD fellow)
supervisor: Prof. Andrzej G. Chmielewski, Ph.D., D.Sc.

IMPLEMENTATION PROJECTS GRANTED BY THE STATE COMMITTEE FOR SCIENTIFIC RESEARCH IN 1995

1. **Absorptiometer for analysis of dosimetric films.**
8 8749 95 C/2294

2. **Graft copolymerization of polymers induced by radiation.**
7 748 093 C/1512

3. **Family of microprocessor radon radiometers.**
904/C S4-8/94

RESEARCH PROJECTS OF MARIA SKŁODOWSKA-CURIE JOINT FUND II IN 1995

1. **Reactivity of silver clusters in zeolites.**
PAA/NSF-92-91
principal investigator: Assoc.Prof. Jacek Michalik, Ph.D., D.Sc.

2. **Accurate method for the determination of molybdenum, uranium traces in biological materials.**
PAA/NIST-93-154
principal investigator: Prof. Rajmund Dybczyński, Ph.D., D.Sc.

IAEA RESEARCH CONTRACTS IN 1995

1. **Complexation and distribution of ecologically important metals in heterogenous systems.**
POL/7377/RB
principal investigator: Assoc.Prof. Jerzy Narbutt, Ph.D., D.Sc.

2. **Synthesis and studies of new selective absorbents for beryllium, strontium and radium radionuclides.**
POL/7216/RB
principal investigator: Aleksander Bilewicz, Ph.D.

3. **Examination of the adaptive response in human lymphocytes induced by hydrogen peroxide.**
POL/6655/RB
principal investigator: Prof. Irena Szumiel, Ph.D., D.Sc.

4. **Preparation and certification of the new certified reference material VIRGINIA TOBACCO LEAVES and development of neutron activation analysis (NAA) methods for checking the homogeneity.**
7192/R2/RB
principal investigator: Prof. Rajmund Dybczyński, Ph.D., D.Sc.

5. **To provide a pc implementation of the agency's analytical quality control service (AQCS) inter comparison program.**
   7741/RB/TC
   principal investigator: Zygmunt Szopa, M.Sc.

6. **Materials for in-situ monitoring of light water reactor (LWR) water chemistry by optical methods.**
   8426/RB
   principal investigator: Leon Fuks, Ph.D.

7. **Thin layer alanine dosimeter with optical spectrophotometric evaluation.**
   8533/RB
   principal investigator: Prof. Zbigniew P. Zagórski, Ph.D., D.Sc.

8. **Electron beam flue gas treatment.**
   POL/8/013
   principal investigator: Prof. Andrzej G. Chmielewski, Ph.D., D.Sc.

EUROPEAN COMMISSION RESEARCH PROJECTS IN 1995

1. **The comet assay: application in gentoxicity testing and as a screening method for assessing the exposure of human populations to genotoxins.**
   CIPA-CT94-0129
   supervisor: Marcin Kruszewski, Ph.D.

2. **Decontamination of aqueous waste streams.**
   CIPA-CT93-0224
   supervisor: Assoc.Prof. Jerzy Narbutt, Ph.D., D.Sc.

3. **Examination of homological recombination in mammalian cell mutants defective in DNA double strand break repair.**
   ERB CIPD CT-930417
   supervisor: Prof. Irena Szumiel, Ph.D., D.Sc.

4. **Establishment of an Eastern European Network of Laboratories for Identification of Irradiated Foodstuffs.**

a) ERB CIPA CT 940134-2
   supervisors: Wacław Stachowicz, Ph.D.

b) ERB CIPA CT 940134-3
   upervisors: Wojciech Migdał, Ph.D.

OTHER FOREIGN CONTRACTS IN 1995

1. **Preparation of cathodic materials precursors for fabrication of rechargeable Li batteries (Li manganates, $LiCoO_2$, $LiNi_{0.5}Co_{0.5}O_2$) by sol-gel process.**
   2526-ERG/TEA
   Contract with ENEA, Italy
   principal investigator: Andrzej Deptuła, Ph.D.

2. **Adaptation of the ABSR-3 detector including an additional power supply unit.**
   IRA/8/009/007C
   UN Development Programme Teheran (Iran)
   principal investigator: Janusz Kraś, M.Sc.

INSTITUTE OF NUCLEAR CHEMISTRY AND TECHNOLOGY
Dorodna 16, 03-195 Warszawa, Poland
Phone: (+48)-(22) 11-06-56
Fax: (+48)-(22) 11-15-32
Telex: 813027 ichtj pl
E-mail: sekdyrn@orange.ichtj.waw.pl